Averages of b-hadron Properties at the End of 2005

Heavy Flavor Averaging Group (HFAG)*

November 28, 2021

Abstract

This article reports world averages for measurements on b-hadron properties obtained by the Heavy Flavor Averaging Group (HFAG) using the available results as of at the end of 2005. In the averaging, the input parameters used in the various analyses are adjusted (rescaled) to common values, and all known correlations are taken into account. The averages include lifetimes, neutral meson mixing parameters, parameters of semileptonic decays, branching fractions of B decays to final states with open charm, charmonium and no charm, and measurements related to CP asymmetries.

*The HFAG members involved in producing the averages for the end of 2005 update are: E. Barberio, I. Bizjak, S. Blyth, G. Cavoto, P. Chang, J. Dingfelder, S. Eidelman, T. Gershon, R. Godang, R. Harr, A. Höcker, T. Iijima, R. Kowalewski, F. Lehner, A. Limosani, C.-J. Lin, O. Long, V. Luth, M. Morii, S. Prell, O. Schneider, J. Smith, A. Stocchi, S. Tosi, K. Trabelsi, R. Van Kooten, C. Voena, and C. Weiser.

Contents

1 Introduction **4**

2 Methodology **5**

3 b-hadron production fractions, lifetimes and mixing parameters **11**
3.1 b-hadron production fractions . . . 11
3.1.1 b-hadron production fractions in $\Upsilon(4S)$ decays . . . 11
3.1.2 b-hadron production fractions at high energy . . . 13
3.2 b-hadron lifetimes . . . 15
3.2.1 Lifetime measurements, uncertainties and correlations . . . 16
3.2.2 Inclusive b-hadron lifetimes . . . 18
3.2.3 B^0 and B^+ lifetimes and their ratio . . . 19
3.2.4 B_s^0 lifetime . . . 22
3.2.5 B_c^+ lifetime . . . 24
3.2.6 Λ_b^0 and b-baryon lifetimes . . . 25
3.2.7 Summary and comparison with theoretical predictions . . . 26
3.3 Neutral B-meson mixing . . . 27
3.3.1 B^0 mixing parameters . . . 28
3.3.2 B_s^0 mixing parameters . . . 34

4 Measurements related to Unitarity Triangle angles **43**
4.1 Introduction . . . 43
4.2 Notations . . . 45
4.2.1 CP asymmetries . . . 45
4.2.2 Time-dependent CP asymmetries in decays to CP eigenstates . . . 45
4.2.3 Time-dependent CP asymmetries in decays to vector-vector final states . . . 46
4.2.4 Time-dependent asymmetries in decays to multiparticle final states . . . 47
4.2.5 Time-dependent CP asymmetries in decays to non-CP eigenstates . . . 47
4.2.6 Asymmetries in $B \to D^{(*)}K^{(*)}$ decays . . . 51
4.3 Common inputs and error treatment . . . 53
4.4 Time-dependent CP asymmetries in $b \to c\bar{c}s$ transitions . . . 54
4.5 Time-dependent transversity analysis of $B^0 \to J/\psi K^{*0}$ . . . 55
4.6 Time-dependent CP asymmetries in colour-suppressed $b \to c\bar{u}d$ transitions . . . 57
4.7 Time-dependent CP asymmetries in charmless $b \to q\bar{q}s$ transitions . . . 58
4.8 Time-dependent CP asymmetries in $b \to c\bar{c}d$ transitions . . . 61
4.9 Time-dependent asymmetries in $b \to s\gamma$ transitions . . . 62
4.10 Time-dependent CP asymmetries in $b \to u\bar{u}d$ transitions . . . 64
4.11 Time-dependent CP asymmetries in $b \to c\bar{u}d/u\bar{c}d$ transitions . . . 68
4.12 Rates and asymmetries in $B^{\mp} \to D^{(*)}K^{(*)\mp}$ decays . . . 69

5 Semileptonic B decays **75**
5.1 Methodology . . . 75
5.2 Exclusive Cabibbo-favored decays . . . 76
5.3 Inclusive Cabibbo-favored decays . . . 76
5.4 Exclusive Cabibbo-suppressed decays . . . 77

5.5 Inclusive Cabibbo-suppressed decays 80

6 Charmless B-decay branching fractions and their asymmetries 83
6.1 Mesonic charmless decays 83
6.2 Radiative and leptonic decays 86
6.3 $B \to s\gamma$ 88
6.4 Baryonic decays 89
6.5 B_s decays 91
6.6 Charge asymmetries 91
6.7 Polarization measurements 94

7 B Decays to open charm and charmonium final states 96

8 Summary 117

1 Introduction

Flavor dynamics is an important element in understanding the nature of particle physics. The accurate knowledge of properties of heavy flavor hadrons, especially b hadrons, plays an essential role for determination of the Cabbibo-Kobayashi-Maskawa (CKM) matrix [1]. Since asymmetric-energy e^+e^- B factories started their operation, the size of available B meson samples has dramatically increased and the accuracies of measurements have been improved. Tevatron experiments also started to provide rich results on B hadron decays with increased Run-II data samples.

The Heavy Flavor Averaging Group (HFAG) has been formed in 2002, continuing the activities of LEP Heavy Flavor Steering group [2], to provide averages for measurements of b-flavor related quantities. The HFAG consists of representatives and contact persons from the experimental groups: *BABAR*, Belle, CDF, CLEO, DØ, and LEP.

The HFAG is currently organized into five subgroups:

- the "Lifetime and Mixing" group provides averages for b-hadron lifetimes, b-hadron fractions in $\Upsilon(4S)$ decay and high energy collisions, and various parameters in B^0 and B_s^0 oscillation (mixing);
- the "Semileptonic B Decays" group provides averages for inclusive and exclusive B-decay branching fractions, and estimates of the CKM matrix elements $|V_{cb}|$ and $|V_{ub}|$;
- the "$CP(t)$ and Unitarity Triangle Angles" group provides averages for time-dependent CP asymmetry parameters and angles of the B unitarity triangle;
- the "Rare Decays" group provides averages of branching fractions and their asymmetries between B and $\overline{B}$ for charmless mesonic, radiative, leptonic, and baryonic B decays;
- the "B to Charm Decays" group provides averages of branching fractions for B decays to final states involving open charm mesons or charmonium.

The first two subgroups continue the activities from LEP working groups with some reorganization (merging four groups into two groups). The latter three groups have been newly formed to provide averages for results which are available from B factory experiments.

This article is an update of the Winter 2005 HFAG document [4], and we report the world averages using the available results as of the end of 2005. All results that are publicly available, including recent preliminary results, are used in the averages. We do not use preliminary results which remain unpublished for a long time or for which no publication is planned. Close contacts have been established between representatives from the experiments and members of different subgroups in charge of the averages, to ensure that the data are prepared in a form suitable for combinations.

We do not scale the error of an average (as is presently done by the Particle Data Group [5]) in case $\chi^2/\mathrm{dof} > 1$, where dof is the number of degrees of freedom in the average calculation. In such a case, we examine the systematics of each measurement and try to understand them. Unless we find possible systematic discrepancies between the measurements, we do not make any special treatment for the calculated error. We provide the confidence level of the fit as an indicator for the consistency of the measurements included in the average. We attach a warning message in case that some special treatment was necessary to calculate the average

or the approximation used in the average calculation may not be good enough (*e.g.*, Gaussian error is used in averaging although the likelihood indicates non-Gaussian behavior).

Section 2 describes the methodology for calculating averages for various quantities used by the HFAG. In the averaging, the input parameters used in the various analyses are adjusted (rescaled) to common values, and, where possible, known correlations are taken into account. The general philosophy and tools for calculations of averages are presented. Sections 3–7 describe the averaging of the quantities from each of the subgroups mentioned above. A brief summary of the averages described in this article is given in Sec. 8.

The complete listing of averages and plots described in this article are also available on the HFAG web page:

`http://www.slac.stanford.edu/xorg/hfag` and

`http://belle.kek.jp/mirror/hfag` (KEK mirror site).

2 Methodology

The general averaging problem that HFAG faces is to combine the information provided by different measurements of the same parameter, to obtain our best estimate of the parameter's value and uncertainty. The methodology described here focuses on the problems of combining measurements performed with different systematic assumptions and with potentially-correlated systematic uncertainties. Our methodology relies on the close involvement of the people performing the measurements in the averaging process.

Consider two hypothetical measurements of a parameter x, which might be summarized as

$$x = x_1 \pm \delta x_1 \pm \Delta x_{1,1} \pm \Delta x_{2,1} \ldots$$
$$x = x_2 \pm \delta x_2 \pm \Delta x_{1,2} \pm \Delta x_{2,2} \ldots \ ,$$

where the δx_k are statistical uncertainties, and the $\Delta x_{i,k}$ are contributions to the systematic uncertainty. One popular approach is to combine statistical and systematic uncertainties in quadrature

$$x = x_1 \pm (\delta x_1 \oplus \Delta x_{1,1} \oplus \Delta x_{2,1} \oplus \ldots)$$
$$x = x_2 \pm (\delta x_2 \oplus \Delta x_{1,2} \oplus \Delta x_{2,2} \oplus \ldots)$$

and then perform a weighted average of x_1 and x_2, using their combined uncertainties, as if they were independent. This approach suffers from two potential problems that we attempt to address. First, the values of the x_k may have been obtained using different systematic assumptions. For example, different values of the B^0 lifetime may have been assumed in separate measurements of the oscillation frequency Δm_d. The second potential problem is that some contributions of the systematic uncertainty may be correlated between experiments. For example, separate measurements of Δm_d may both depend on an assumed Monte-Carlo branching fraction used to model a common background.

The problems mentioned above are related since, ideally, any quantity y_i that x_k depends on has a corresponding contribution $\Delta x_{i,k}$ to the systematic error which reflects the uncertainty Δy_i on y_i itself. We assume that this is the case, and use the values of y_i and Δy_i assumed by each measurement explicitly in our averaging (we refer to these values as $y_{i,k}$ and $\Delta y_{i,k}$ below). Furthermore, since we do not lump all the systematics together, we require that each

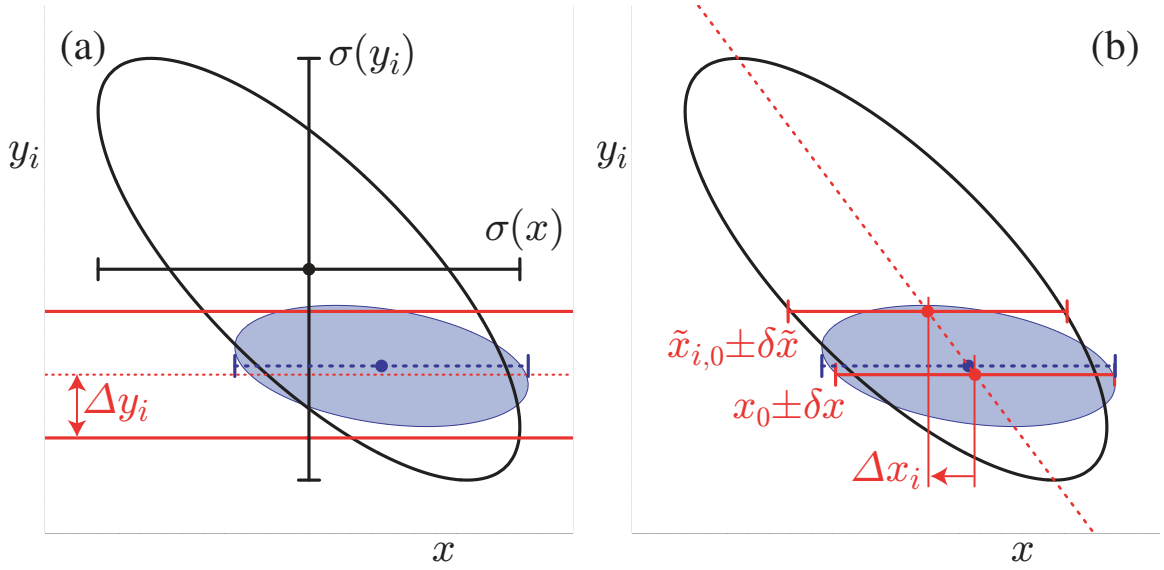

Figure 1: The left-hand plot, (a), compares the 68% confidence-level contours of a hypothetical measurement's unconstrained (large ellipse) and constrained (filled ellipse) likelihoods, using the Gaussian constraint on y_i represented by the horizontal band. The solid error bars represent the statistical uncertainties, $\sigma(x)$ and $\sigma(y_i)$, of the unconstrained likelihood. The dashed error bar shows the statistical error on x from a constrained simultaneous fit to x and y_i. The right-hand plot, (b), illustrates the method described in the text of performing fits to x only with y_i fixed at different values. The dashed diagonal line between these fit results has the slope $\rho(x, y_i)\sigma(y_i)/\sigma(x)$ in the limit of a parabolic unconstrained likelihood. The result of the constrained simultaneous fit from (a) is shown as a dashed error bar on x.

measurement used in an average have a consistent definition of the various contributions to the systematic uncertainty. Different analyses often use different decompositions of their systematic uncertainties, so achieving consistent definitions for any potentially correlated contributions requires close coordination between HFAG and the experiments. In some cases, a group of systematic uncertainties must be lumped to obtain a coarser description that is consistent between measurements. Systematic uncertainties that are uncorrelated with any other sources of uncertainty appearing in an average are lumped with the statistical error, so that the only systematic uncertainties treated explicitly are those that are correlated with at least one other measurement via a consistently-defined external parameter y_i. When asymmetric statistical or systematic uncertainties are quoted, we symmetrize them since our combination method implicitly assumes parabolic likelihoods for each measurement.

The fact that a measurement of x is sensitive to the value of y_i indicates that, in principle, the data used to measure x could equally-well be used for a simultaneous measurement of x and y_i, as illustrated by the large contour in Fig. 1(a) for a hypothetical measurement. However, we often have an external constraint Δy_i on the value of y_i (represented by the horizontal band in Fig. 1(a)) that is more precise than the constraint $\sigma(y_i)$ from our data alone. Ideally, in such cases we would perform a simultaneous fit to x and y_i, including the external constraint, obtaining the filled (x, y) contour and corresponding dashed one-dimensional estimate of x shown in Fig. 1(a). Throughout, we assume that the external constraint Δy_i on y_i is Gaussian.

In practice, the added technical complexity of a constrained fit with extra free parameters is not justified by the small increase in sensitivity, as long as the external constraints Δy_i are sufficiently precise when compared with the sensitivities $\sigma(y_i)$ to each y_i of the data alone. Instead, the usual procedure adopted by the experiments is to perform a baseline fit with all y_i fixed to nominal values $y_{i,0}$, obtaining $x = x_0 \pm \delta x$. This baseline fit neglects the uncertainty due to Δy_i, but this error can be mostly recovered by repeating the fit separately for each external parameter y_i with its value fixed at $y_i = y_{i,0} + \Delta y_i$ to obtain $x = \tilde{x}_{i,0} \pm \delta\tilde{x}$, as illustrated in Fig. 1(b). The absolute shift, $|\tilde{x}_{i,0} - x_0|$, in the central value of x is what the experiments usually quote as their systematic uncertainty Δx_i on x due to the unknown value of y_i. Our procedure requires that we know not only the magnitude of this shift but also its sign. In the limit that the unconstrained data is represented by a parabolic likelihood, the signed shift is given by

$$\Delta x_i = \rho(x, y_i) \frac{\sigma(x)}{\sigma(y_i)} \Delta y_i \ , \tag{1}$$

where $\sigma(x)$ and $\rho(x, y_i)$ are the statistical uncertainty on x and the correlation between x and y_i in the unconstrained data. While our procedure is not equivalent to the constrained fit with extra parameters, it yields (in the limit of a parabolic unconstrained likelihood) a central value x_0 that agrees to $\mathcal{O}(\Delta y_i/\sigma(y_i))^2$ and an uncertainty $\delta x \oplus \Delta x_i$ that agrees to $\mathcal{O}(\Delta y_i/\sigma(y_i))^4$.

In order to combine two or more measurements that share systematics due to the same external parameters y_i, we would ideally perform a constrained simultaneous fit of all data samples to obtain values of x and each y_i, being careful to only apply the constraint on each y_i once. This is not practical since we generally do not have sufficient information to reconstruct the unconstrained likelihoods corresponding to each measurement. Instead, we perform the two-step approximate procedure described below.

Figs. 2(a,b) illustrate two statistically-independent measurements, $x_1 \pm (\delta x_1 \oplus \Delta x_{i,1})$ and $x_2 \pm (\delta x_i \oplus \Delta x_{i,2})$, of the same hypothetical quantity x (for simplicity, we only show the contribution of a single correlated systematic due to an external parameter y_i). As our knowledge of the external parameters y_i evolves, it is natural that the different measurements of x will assume different nominal values and ranges for each y_i. The first step of our procedure is to adjust the values of each measurement to reflect the current best knowledge of the values y_i' and ranges $\Delta y_i'$ of the external parameters y_i, as illustrated in Figs. 2(c,b). We adjust the central values x_k and correlated systematic uncertainties $\Delta x_{i,k}$ linearly for each measurement (indexed by k) and each external parameter (indexed by i):

$$x_k' = x_k + \sum_i \frac{\Delta x_{i,k}}{\Delta y_{i,k}} (y_i' - y_{i,k}) \tag{2}$$

$$\Delta x_{i,k}' = \Delta x_{i,k} \cdot \frac{\Delta y_i'}{\Delta y_{i,k}} \ . \tag{3}$$

This procedure is exact in the limit that the unconstrained likelihoods of each measurement is parabolic.

The second step of our procedure is to combine the adjusted measurements, $x_k' \pm (\delta x_k \oplus \Delta x_{k,1}' \oplus \Delta x_{k,2}' \oplus \ldots)$ using the chi-square

$$\chi^2_{\rm comb}(x, y_1, y_2, \ldots) \equiv \sum_k \frac{1}{\delta x_k^2} \left[x_k' - \left(x + \sum_i (y_i - y_i') \frac{\Delta x_{i,k}'}{\Delta y_i'} \right) \right]^2 + \sum_i \left(\frac{y_i - y_i'}{\Delta y_i'} \right)^2 \ , \tag{4}$$

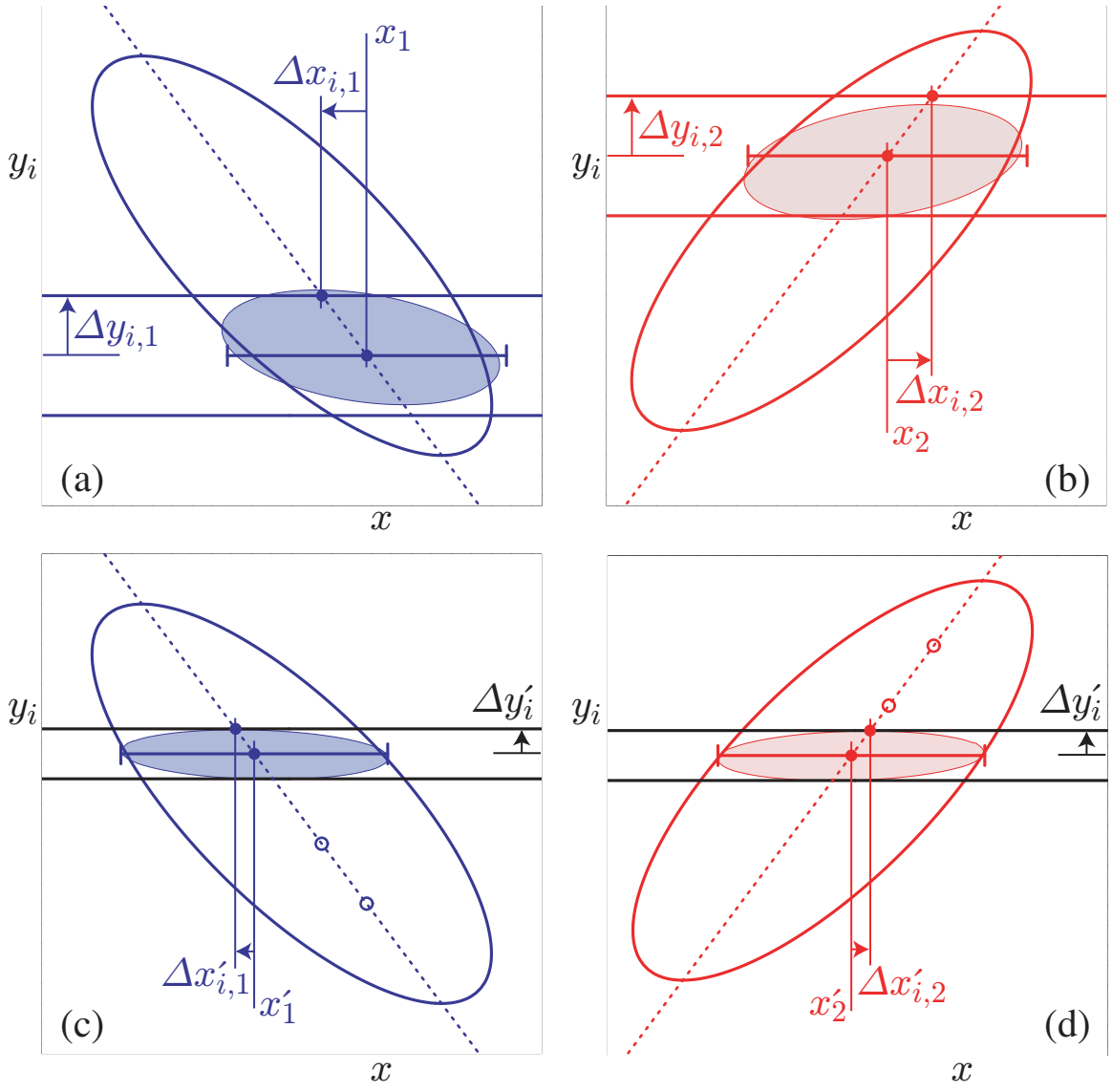

Figure 2: The upper plots, (a) and (b), show examples of two individual measurements to be combined. The large ellipses represent their unconstrained likelihoods, and the filled ellipses represent their constrained likelihoods. Horizontal bands indicate the different assumptions about the value and uncertainty of y_i used by each measurement. The error bars show the results of the approximate method described in the text for obtaining x by performing fits with y_i fixed to different values. The lower plots, (c) and (d), illustrate the adjustments to accommodate updated and consistent knowledge of y_i described in the text. Hollow circles mark the central values of the unadjusted fits to x with y fixed, which determine the dashed line used to obtain the adjusted values.

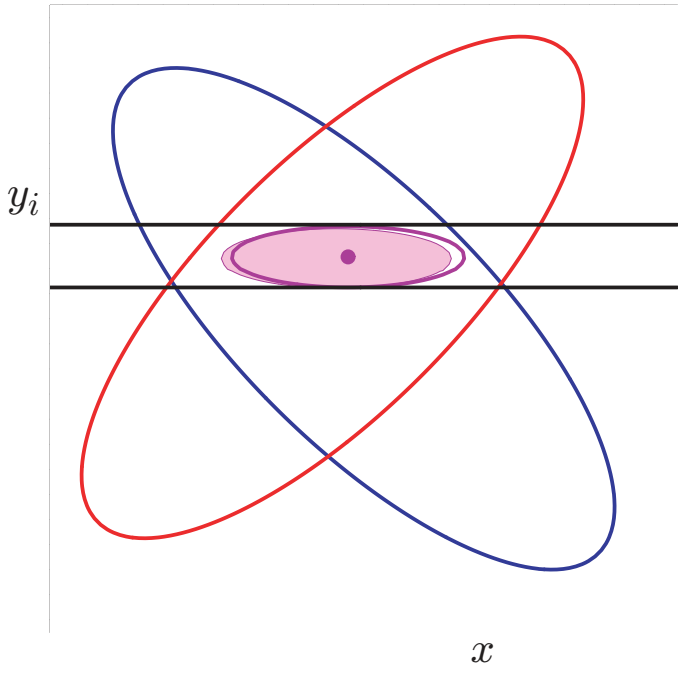

Figure 3: An illustration of the combination of two hypothetical measurements of x using the method described in the text. The ellipses represent the unconstrained likelihoods of each measurement and the horizontal band represents the latest knowledge about y_i that is used to adjust the individual measurements. The filled small ellipse shows the result of the exact method using $\mathcal{L}_{\rm comb}$ and the hollow small ellipse and dot show the result of the approximate method using $\chi^2_{\rm comb}$.

and then minimize this χ^2 to obtain the best values of x and y_i and their uncertainties, as illustrated in Fig. 3. Although this method determines new values for the y_i, we do not report them since the $\Delta x_{i,k}$ reported by each experiment are generally not intended for this purpose (for example, they may represent a conservative upper limit rather than a true reflection of a 68% confidence level).

For comparison, the exact method we would perform if we had the unconstrained likelihoods $\mathcal{L}_k(x, y_1, y_2, \ldots)$ available for each measurement is to minimize the simultaneous constrained likelihood

$$\mathcal{L}_{\rm comb}(x, y_1, y_2, \ldots) \equiv \prod_k \mathcal{L}_k(x, y_1, y_2, \ldots) \prod_i \mathcal{L}_i(y_i) \ , \tag{5}$$

with an independent Gaussian external constraint on each y_i

$$\mathcal{L}_i(y_i) \equiv \exp\left[-\frac{1}{2}\left(\frac{y_i - y_i'}{\Delta y_i'}\right)^2\right] \ . \tag{6}$$

The results of this exact method are illustrated by the filled ellipses in Figs. 3(a,b), and agree with our method in the limit that each $\mathcal{L}_k$ is parabolic and that each $\Delta y_i' \ll \sigma(y_i)$. In the case of a non-parabolic unconstrained likelihood, experiments would have to provide a description of $\mathcal{L}_k$ itself to allow an improved combination. In the case of some $\sigma(y_i) \simeq \Delta y_i'$, experiments

are advised to perform a simultaneous measurement of both x and y so that their data will improve the world knowledge about y.

The algorithm described above is used as a default in the averages reported in the following sections. For some cases, somewhat simplified or more complex algorithms are used and noted in the corresponding sections.

Following the prescription described above, the central values and errors are rescaled to a common set of input parameters in the averaging procedures, according to the dependency on any of these input parameters. We try to use the most up-to-date values for these common inputs and the same values among the HFAG subgroups. For the parameters whose averages are produced by the HFAG, we use the updated values in the current update cycle. For other external parameters, we use the most recent PDG values.

The parameters and values used in this update cycle are listed in each subgroup section.

3 b-hadron production fractions, lifetimes and mixing parameters

Quantities such as b-hadron production fractions, b-hadron lifetimes, and neutral B-meson oscillation frequencies have been measured for many years at high-energy colliders, namely at LEP and SLC (e^+e^- colliders at $\sqrt{s} = m_Z$) as well as at the first version of the Tevatron ($p\overline{p}$ collider at $\sqrt{s} = 1.8$ TeV). More recently, precise measurements of the B^0 and B^+ lifetimes, as well as of the B^0 oscillation frequency, have also been performed at the asymmetric B factories, KEKB and PEPII (e^+e^- colliders at $\sqrt{s} = m_{\Upsilon(4S)}$). In most cases, these basic quantities, although interesting by themselves, can now be seen as necessary ingredients for the more complicated and refined analyses being currently performed at the asymmetric B factories and at the upgraded Tevatron ($\sqrt{s} = 1.96$ TeV), in particular the time-dependent CP asymmetry measurements. It is therefore important that the best experimental values of these quantities continue to be kept up-to-date and improved.

In several cases, the averages presented in this chapter are indeed needed and used as input for the results given in the subsequent chapters. However, within this chapter, some averages need the knowledge of other averages in a circular way. This "coupling", which appears through the b-hadron fractions whenever inclusive or semi-exclusive measurements have to be considered, has been reduced significantly in the last years with increasingly precise exclusive measurements becoming available. To cope with this circularity, a rather involved averaging procedure had been developed, in the framework of the former LEP Heavy Flavour Steering Group. This is still in use now (details can be found in [2]), although simplifications can be envisaged in the future when even more precise exclusive measurements become available.

3.1 b-hadron production fractions

We consider here the relative fractions of the different b-hadron species found in an unbiased sample of weakly-decaying b hadrons produced under some specific conditions. The knowledge of these fractions is useful to characterize the signal composition in inclusive b-hadron analyses, or to predict the background composition in exclusive analyses. Many analyses in B physics need these fractions as input. We distinguish here the following two conditions: $\Upsilon(4S)$ decays and high-energy collisions.

3.1.1 b-hadron production fractions in $\Upsilon(4S)$ decays

Only pairs of the two lightest (charged and neutral) B mesons can be produced in $\Upsilon(4S)$ decays, and it is enough to determine the following branching fractions:

$$f^{+-} = \Gamma(\Upsilon(4S) \to B^+B^-)/\Gamma_{\rm tot}(\Upsilon(4S))\,, \tag{7}$$

$$f^{00} = \Gamma(\Upsilon(4S) \to B^0\overline{B}^0)/\Gamma_{\rm tot}(\Upsilon(4S))\,. \tag{8}$$

In practice, most analyses measure their ratio

$$R^{+-/00} = f^{+-}/f^{00} = \Gamma(\Upsilon(4S) \to B^+B^-)/\Gamma(\Upsilon(4S) \to B^0\overline{B}^0)\,, \tag{9}$$

which is easier to access experimentally. Since an inclusive (but separate) reconstruction of B^+ and B^0 is difficult, specific exclusive decay modes, $B^+ \to x^+$ and $B^0 \to x^0$, are usually

Table 1: Published measurements of the B^+/B^0 production ratio in $\Upsilon(4S)$ decays, together with their average (see text). Systematic uncertainties due to the imperfect knowledge of $\tau(B^+)/\tau(B^0)$ are included.

Experiment and year	Ref.	Decay modes or method	Published value of $R^{+-/00} = f^{+-}/f^{00}$	Assumed value of $\tau(B^+)/\tau(B^0)$
CLEO, 2001	[6]	$J/\psi K^{(*)}$	$1.04 \pm 0.07 \pm 0.04$	1.066 ± 0.024
BABAR, 2002	[7]	$(c\overline{c})K^{(*)}$	$1.10 \pm 0.06 \pm 0.05$	1.062 ± 0.029
CLEO, 2002	[8]	$D^*\ell\nu$	$1.058 \pm 0.084 \pm 0.136$	1.074 ± 0.028
Belle, 2003	[9]	dilepton events	$1.01 \pm 0.03 \pm 0.09$	1.083 ± 0.017
BABAR, 2004	[10]	$J/\psi K$	$1.006 \pm 0.036 \pm 0.031$	1.083 ± 0.017
Average			1.020 ± 0.034 (tot)	1.076 ± 0.008

considered to perform a measurement of $R^{+-/00}$, whenever they can be related by isospin symmetry (for example $B^+ \to J/\psi K^+$ and $B^0 \to J/\psi K^0$). Under the assumption that $\Gamma(B^+ \to x^+) = \Gamma(B^0 \to x^0)$, *i.e.* that isospin invariance holds in these B decays, the ratio of the number of reconstructed $B^+ \to x^+$ and $B^0 \to x^0$ mesons is proportional to

$$\frac{f^{+-}\,\mathcal{B}(B^+ \to x^+)}{f^{00}\,\mathcal{B}(B^0 \to x^0)} = \frac{f^{+-}\,\Gamma(B^+ \to x^+)\,\tau(B^+)}{f^{00}\,\Gamma(B^0 \to x^0)\,\tau(B^0)} = \frac{f^{+-}}{f^{00}}\,\frac{\tau(B^+)}{\tau(B^0)}\,, \tag{10}$$

where $\tau(B^+)$ and $\tau(B^0)$ are the B^+ and B^0 lifetimes respectively. Hence the primary quantity measured in these analyses is $R^{+-/00}\,\tau(B^+)/\tau(B^0)$, and the extraction of $R^{+-/00}$ with this method therefore requires the knowledge of the $\tau(B^+)/\tau(B^0)$ lifetime ratio.

The published measurements of $R^{+-/00}$ are listed in Table 1 together with the corresponding assumed values of $\tau(B^+)/\tau(B^0)$. All measurements are based on the above-mentioned method, except the one from Belle, which is a by-product of the B^0 mixing frequency analysis using dilepton events (but note that it also assumes isospin invariance, namely $\Gamma(B^+ \to \ell^+\mathrm{X}) = \Gamma(B^0 \to \ell^+\mathrm{X})$). The latter is therefore treated in a slightly different manner in the following procedure used to combine these measurements:

- each published value of $R^{+-/00}$ from CLEO and *BABAR* is first converted back to the original measurement of $R^{+-/00}\,\tau(B^+)/\tau(B^0)$, using the value of the lifetime ratio assumed in the corresponding analysis;

- a simple weighted average of these original measurements of $R^{+-/00}\,\tau(B^+)/\tau(B^0)$ from CLEO and *BABAR* (which do not depend on the assumed value of the lifetime ratio) is then computed, assuming no statistical or systematic correlations between them;

- the weighted average of $R^{+-/00}\,\tau(B^+)/\tau(B^0)$ is converted into a value of $R^{+-/00}$, using the latest average of the lifetime ratios, $\tau(B^+)/\tau(B^0) = 1.076 \pm 0.008$ (see Sec. 3.2.3);

- the Belle measurement of $R^{+-/00}$ is adjusted to the current values of $\tau(B^0) = 1.527 \pm 0.008$ ps and $\tau(B^+)/\tau(B^0) = 1.076 \pm 0.008$ (see Sec. 3.2.3), using the quoted systematic uncertainties due to these parameters;

- the combined value of $R^{+-/00}$ from CLEO and *BABAR* is averaged with the adjusted value of $R^{+-/00}$ from Belle, assuming a 100% correlation of the systematic uncertainty due to the limited knowledge on $\tau(B^+)/\tau(B^0)$; no other correlation is considered.

The resulting global average,

$$R^{+-/00} = \frac{f^{+-}}{f^{00}} = 1.020 \pm 0.034\,, \tag{11}$$

is consistent with an equal production of charged and neutral B mesons.

On the other hand, the *BABAR* collaboration has recently performed a direct measurement of the f^{00} fraction using a novel method, which does not rely on isospin symmetry nor requires the knowledge of $\tau(B^+)/\tau(B^0)$. Its analysis, based on a comparison between the number of events where a single $B^0 \to D^{*-}\ell^+\nu$ decay could be reconstructed and the number of events where two such decays could be reconstructed, yields [11]

$$f^{00} = 0.487 \pm 0.010\,(\text{stat}) \pm 0.008\,(\text{syst})\,. \tag{12}$$

The two results of Eqs. (11) and (12) are of very different natures and completely independent of each other. Their product is equal to $f^{+-} = 0.497 \pm 0.021$, while another combination of them gives $f^{+-} + f^{00} = 0.984 \pm 0.031$, compatible with unity. Assuming[1] $f^{+-} + f^{00} = 1$, also consistent with CLEO's observation that the fraction of $\Upsilon(4S)$ decays to $B\overline{B}$ pairs is larger than 0.96 at 95% CL [13], the results of Eqs. (11) and (12) can be averaged (first converting Eq. (11) into a value of $f^{00} = 1/(R^{+-/00} + 1)$) to yield the following more precise estimates:

$$f^{00} = 0.493 \pm 0.007\,, \quad f^{+-} = 1 - f^{00} = 0.507 \pm 0.007\,, \quad \frac{f^{+-}}{f^{00}} = 1.030 \pm 0.029\,. \tag{13}$$

3.1.2 *b*-hadron production fractions at high energy

At high energy, all species of weakly-decaying b hadrons can be produced, either directly or in strong and electromagnetic decays of excited b hadrons. We assume here that the fractions of these different species are the same in unbiased samples of high-$p_{\rm T}$ b jets originating from Z^0 decays or from $p\overline{p}$ collisions at the Tevatron. This hypothesis is plausible considering that, in both cases, the last step of the jet hadronization is a non-perturbative QCD process occurring at the scale of $\Lambda_{\rm QCD}$. On the other hand, there is no strong argument to claim that these fractions should be strictly equal, so this assumption should be checked experimentally. Although the available data is not sufficient at this time to perform a significant check, it is expected that the new data from Tevatron Run II may improve this situation and allow one to confirm or disprove this assumption with reasonable confidence. Meanwhile, the attitude adopted here is that these fractions are assumed to be equal at all high-energy colliders until demonstrated otherwise by experiment.[2]

[1] The first non-$B\overline{B}$ decay mode of the $\Upsilon(4S)$ has now been observed with a branching ratio of the order of 10^{-4} [12], corresponding to a partial width several times larger than that in the e^+e^- channel. However, this can still be neglected and the assumption $f^{+-} + f^{00} = 1$ remains valid in the present context of the determination of f^{+-} and f^{00}.

[2] It is not unlikely that the b-hadron fractions in low-$p_{\rm T}$ jets at a hadronic machine be different; in particular, beam-remnant effects may enhance the b-baryon production.

Contrary to what happens in the charm sector where the fractions of D^+ and D^0 are different, the relative amount of B^+ and B^0 is not affected by the electromagnetic decays of excited B^{+*} and B^{0*} states and strong decays of excited B^{+**} and B^{0**} states. Decays of the type $B_s^{0**} \to B^{(*)}K$ also contribute to the B^+ and B^0 rates, but with the same magnitude if mass effects can be neglected. We therefore assume equal production of B^+ and B^0. We also neglect the production of weakly-decaying states made of several heavy quarks (like B_c^+ and other heavy baryons) which is known to be very small. Hence, for the purpose of determining the b-hadron fractions, we use the constraints

$$f_u = f_d \quad \text{and} \quad f_u + f_d + f_s + f_{\rm baryon} = 1\,, \tag{14}$$

where f_u, f_d, f_s and $f_{\rm baryon}$ are the unbiased fractions of B^+, B^0, B_s^0 and b-baryons, respectively.

The LEP experiments have measured $f_s \times \mathcal{B}(B_s^0 \to D_s^- \ell^+ \nu_\ell X)$ [14], $\mathcal{B}(b \to \Lambda_b^0) \times \mathcal{B}(\Lambda_b^0 \to \Lambda_c^+ \ell^- \overline{\nu}_\ell X)$ [15, 16] and $\mathcal{B}(b \to \Xi_b^-) \times \mathcal{B}(\Xi_b^- \to \Xi^- \ell^- \overline{\nu}_\ell X)$ [17, 18] from partially reconstructed final states including a lepton, $f_{\rm baryon}$ from protons identified in b events [19], and the production rate of charged b hadrons [20]. The various b-hadron fractions have also been measured at CDF using electron-charm final states [21] and double semileptonic decays with $\phi\ell$ and $K^*\ell$ final states [22]. All these published results have been combined following the procedure and assumptions described in [2] to yield $f_u = f_d = 0.403 \pm 0.011$, $f_s = 0.089 \pm 0.021$ and $f_{\rm baryon} = 0.106 \pm 0.018$ under the constraints of Eq. (14). For this combination, other external inputs are used, *e.g.* the branching ratios of B mesons to final states with a D, D^* or D^{**} in semileptonic decays, which are needed to evaluate the fraction of semileptonic B_s^0 decays with a D_s^- in the final state.

Time-integrated mixing analyses performed with lepton pairs from $b\overline{b}$ events produced at high-energy colliders measure the quantity

$$\overline{\chi} = f'_d\,\chi_d + f'_s\,\chi_s\,, \tag{15}$$

where f'_d and f'_s are the fractions of B^0 and B_s^0 hadrons in a sample of semileptonic b-hadron decays, and where χ_d and χ_s are the B^0 and B_s^0 time-integrated mixing probabilities. Assuming that all b hadrons have the same semileptonic decay width implies $f'_i = f_i R_i$, where $R_i = \tau_i/\tau_b$ is the ratio of the lifetime τ_i of species i to the average b-hadron lifetime $\tau_b = \sum_i f_i \tau_i$. Hence measurements of the mixing probabilities $\overline{\chi}$, χ_d and χ_s can be used to improve our knowledge of f_u, f_d, f_s and $f_{\rm baryon}$. In practice, the above relations yield another determination of f_s obtained from $f_{\rm baryon}$ and mixing information,

$$f_s = \frac{1}{R_s}\frac{(1+r)\overline{\chi} - (1 - f_{\rm baryon}R_{\rm baryon})\chi_d}{(1+r)\chi_s - \chi_d}\,, \tag{16}$$

where $r = R_u/R_d = \tau(B^+)/\tau(B^0)$.

The published measurements of $\overline{\chi}$ performed by the LEP experiments have been combined by the LEP Electroweak Working Group to yield $\overline{\chi} = 0.1259 \pm 0.0042$ [23]. This can be compared with a recent measurement from CDF, $\overline{\chi} = 0.152 \pm 0.013$ [24], obtained from an analysis of the Run I data. The two estimates deviate from each other by $1.9\,\sigma$, and could be an indication that the production fractions of b hadrons at the Z peak or at the Tevatron are not the same. Although this discrepancy is not very significant it should be carefully monitored in the future. We choose to combine these two results in a simple weighted average, assuming

Table 2: Fractions of the different b-hadron species in an unbiased sample of weakly-decaying b hadrons produced at high energy, obtained from both direct and mixing measurements.

b-hadron species	Fraction	Correlation coefficients with $f_d = f_u$	and f_s
B^0, B^+	$f_d = f_u = 0.398 \pm 0.010$		
B_s^0	$f_s = 0.104 \pm 0.014$	-0.575	
b baryons	$f_{\rm baryon} = 0.099 \pm 0.017$	-0.720	-0.154

no correlations, and, following the PDG prescription, we multiply the combined uncertainty by 1.9 to account for the discrepancy. Our world average is then

$$\overline{\chi} = 0.1283 \pm 0.0076\,. \tag{17}$$

Introducing the latter result in Eq. (16), together with our world average $\chi_d = 0.188 \pm 0.002$ (see Eq. (45) of Sec. 3.3.1), the assumption $\chi_s = 1/2$ (justified by the large value of Δm_s, see Eq. (50) in Sec. 3.3.2), the best knowledge of the lifetimes (see Sec. 3.2) and the estimate of $f_{\rm baryon}$ given above, yields $f_s = 0.119 \pm 0.021$, an estimate dominated by the mixing information. Taking into account all known correlations (including the one introduced by $f_{\rm baryon}$), this result is then combined with the set of fractions obtained from direct measurements (given above), to yield the improved estimates of Table 2, still under the constraints of Eq. (14). As can be seen, our knowledge on the mixing parameters substantially reduces the uncertainty on f_s, despite the rather strong deweighting introduced in the computation of the world average of $\overline{\chi}$. It should be noted that the results are correlated, as indicated in Table 2.

3.2 *b*-hadron lifetimes

In the spectator model the decay of b-flavored hadrons H_b is governed entirely by the flavor changing $b \to Wq$ transition ($q = c, u$). For this very reason, lifetimes of all b-flavored hadrons are the same in the spectator approximation regardless of the (spectator) quark content of the H_b. In the early 1990's experiments became sophisticated enough to start seeing the differences of the lifetimes among various H_b species. The first theoretical calculations of the spectator quark effects on H_b lifetime emerged only few years earlier.

Currently, most of such calculations are performed in the framework of the Heavy Quark Expansion, HQE. In the HQE, under certain assumptions (most important of which is that of quark-hadron duality), the decay rate of an H_b to an inclusive final state f is expressed as the sum of a series of expectation values of operators of increasing dimension, multiplied by the correspondingly higher powers of $\Lambda_{\rm QCD}/m_b$:

$$\Gamma_{H_b \to f} = |CKM|^2 \sum_n c_n^{(f)} \Big(\frac{\Lambda_{\rm QCD}}{m_b}\Big)^n \langle H_b | O_n | H_b \rangle, \tag{18}$$

where $|CKM|^2$ is the relevant combination of the CKM matrix elements. Coefficients $c_n^{(f)}$ of this expansion, known as Operator Product Expansion [25], can be calculated perturbatively. Hence, the HQE predicts $\Gamma_{H_b \to f}$ in the form of an expansion in both $\Lambda_{\rm QCD}/m_b$ and $\alpha_s(m_b)$. The

precision of current experiments makes it mandatory to go to the next-to-leading order in QCD, *i.e.* to include correction of the order of $\alpha_s(m_b)$ to the $c_n^{(f)}$'s. All non-perturbative physics is shifted into the expectation values $\langle H_b|O_n|H_b\rangle$ of operators O_n. These can be calculated using lattice QCD or QCD sum rules, or can be related to other observables via the HQE [26]. One may reasonably expect that powers of $\Lambda_{\rm QCD}/m_b$ provide enough suppression that only the first few terms of the sum in Eq. (18) matter.

Theoretical predictions are usually made for the ratios of the lifetimes (with $\tau(B^0)$ chosen as the common denominator) rather than for the individual lifetimes, for this allows several uncertainties to cancel. The precision of the current HQE calculations (see Refs. [27–29] for the latest updates) is in some instances already surpassed by the measurements, *e.g.* in the case of $\tau(B^+)/\tau(B^0)$. Also, HQE calculations are not assumption-free. More accurate predictions are a matter of progress in the evaluation of the non-perturbative hadronic matrix elements and verifying the assumptions that the calculations are based upon. However, the HQE, even in its present shape, draws a number of important conclusions, which are in agreement with experimental observations:

- The heavier the mass of the heavy quark the smaller is the variation in the lifetimes among different hadrons containing this quark, which is to say that as $m_b \to \infty$ we retrieve the spectator picture in which the lifetimes of all H_b's are the same. This is well illustrated by the fact that lifetimes are rather similar in the b sector, while they differ by large factors in the c sector ($m_c < m_b$).

- The non-perturbative corrections arise only at the order of $\Lambda^2_{\rm QCD}/m_b^2$, which translates into differences among H_b lifetimes of only a few percent.

- It is only the difference between meson and baryon lifetimes that appears at the $\Lambda^2_{\rm QCD}/m_b^2$ level. The splitting of the meson lifetimes occurs at the $\Lambda^3_{\rm QCD}/m_b^3$ level, yet it is enhanced by a phase space factor $16\pi^2$ with respect to the leading free b decay.

To ensure that certain sources of systematic uncertainty cancel, lifetime analyses are sometimes designed to measure a ratio of lifetimes. However, because of the differences in decay topologies, abundance (or lack thereof) of decays of a certain kind, *etc.*, measurements of the individual lifetimes are more common. In the following section we review the most common types of the lifetime measurements. This discussion is followed by the presentation of the averaging of the various lifetime measurements, each with a brief description of its particularities.

3.2.1 Lifetime measurements, uncertainties and correlations

In most cases lifetime of an H_b is estimated from a flight distance and a $\beta\gamma$ factor which is used to convert the geometrical distance into the proper decay time. Methods of accessing lifetime information can roughly be divided in the following five categories:

1. ***Inclusive (flavor blind) measurements***. These measurements are aimed at extracting the lifetime from a mixture of b-hadron decays, without distinguishing the decaying species. Often the knowledge of the mixture composition is limited, which makes these measurements experiment-specific. Also, these measurements have to rely on Monte Carlo for estimating the $\beta\gamma$ factor, because the decaying hadrons are not fully reconstructed. On the bright side, these usually are the largest statistics b-hadron lifetime measurements

that are accessible to a given experiment, and can, therefore, serve as an important performance benchmark.

2. **Measurements in semileptonic decays of a specific H_b.** W from $b \to Wc$ produces $\ell\nu_l$ pair ($\ell = e, \mu$) in about 21% of the cases. Electron or muon from such decays is usually a well-detected signature, which provides for clean and efficient trigger. c quark from $b \to Wc$ transition and the other quark(s) making up the decaying H_b combine into a charm hadron, which is reconstructed in one or more exclusive decay channels. Knowing what this charmed hadron is allows one to separate, at least statistically, different H_b species. The advantage of these measurements is in statistics, which usually is superior to that of the exclusively reconstructed H_b decays. Some of the main disadvantages are related to the difficulty of estimating lepton+charm sample composition and Monte Carlo reliance for the $\beta\gamma$ factor estimate.

3. ***Measurements in exclusively reconstructed hadronic decays***. These have the advantage of complete reconstruction of decaying H_b, which allows one to infer the decaying species as well as to perform precise measurement of the $\beta\gamma$ factor. Both lead to generally smaller systematic uncertainties than in the above two categories. The downsides are smaller branching ratios, larger combinatoric backgrounds, especially in $H_b \to H_c\pi(\pi\pi)$ and multi-body H_c decays, or in a hadron collider environment with non-trivial underlying event. $H_b \to J/\psi H_s$ are relatively clean and easy to trigger on $J/\psi \to \ell^+\ell^-$, but their branching fraction is only about 1%.

4. ***Measurements at asymmetric B factories***. In the $\Upsilon(4S) \to B\overline{B}$ decay, the B mesons (B^+ or B^0) are essentially at rest in the $\Upsilon(4S)$ rest frame. This makes lifetime measurements impossible with experiments, such as CLEO, in which $\Upsilon(4S)$ produced at rest. At asymmetric B factories $\Upsilon(4S)$ is boosted resulting in B and $\overline{B}$ moving nearly parallel to each other. The lifetime is inferred from the distance Δz separating B and $\overline{B}$ decay vertices and $\Upsilon(4S)$ boost known from colliding beam energies. In order to determine the charge of the B mesons in each event, one of the them is fully reconstructed in semileptonic or fully hadronic decay modes. The other B is typically not fully reconstructed, only the position of its decay vertex is determined from the remaining tracks in the event. These measurements benefit from very large statistics, but suffer from poor Δz resolution.

5. ***Direct measurement of lifetime ratios***. This method has so far been only applied in the measurement of $\tau(B^+)/\tau(B^0)$. The ratio of the lifetimes is extracted from the dependence of the observed relative number of B^+ and B^0 candidates (both reconstructed in semileptonic decays) on the proper decay time.

In some of the latest analyses, measurements of two (*e.g.* $\tau(B^+)$ and $\tau(B^+)/\tau(B^0)$) or three (*e.g.* $\tau(B^+)$, $\tau(B^+)/\tau(B^0)$, and Δm_d) quantities are combined. This introduces correlations among measurements. Another source of correlations among the measurements are the systematic effects, which could be common to an experiment or to an analysis technique across the experiments. When calculating the averages, such correlations are taken into account per general procedure, described in Ref. [30].

Table 3: Measurements of average b-hadron lifetimes.

Experiment	Method	Data set	τ_b (ps)	Ref.
ALEPH	Dipole	91	$1.511 \pm 0.022 \pm 0.078$	[31]
DELPHI	All track i.p. (2D)	91–92	$1.542 \pm 0.021 \pm 0.045$	[32][a]
DELPHI	Sec. vtx	91–93	$1.582 \pm 0.011 \pm 0.027$	[33][a]
DELPHI	Sec. vtx	94–95	$1.570 \pm 0.005 \pm 0.008$	[34]
L3	Sec. vtx + i.p.	91–94	$1.556 \pm 0.010 \pm 0.017$	[35][b]
OPAL	Sec. vtx	91–94	$1.611 \pm 0.010 \pm 0.027$	[36]
SLD	Sec. vtx	93	$1.564 \pm 0.030 \pm 0.036$	[37]
Average set 1 (b vertex)			1.572 ± 0.009	
ALEPH	Lepton i.p. (3D)	91–93	$1.533 \pm 0.013 \pm 0.022$	[38]
L3	Lepton i.p. (2D)	91–94	$1.544 \pm 0.016 \pm 0.021$	[35][b]
OPAL	Lepton i.p. (2D)	90–91	$1.523 \pm 0.034 \pm 0.038$	[39]
Average set 2 ($b \to \ell$)			1.537 ± 0.020	
CDF1	J/ψ vtx	92–95	$1.533 \pm 0.015^{+0.035}_{-0.031}$	[40]
Average of all above			1.568 ± 0.009	

[a] The combined DELPHI result quoted in [33] is $1.575 \pm 0.010 \pm 0.026$ ps.
[b] The combined L3 result quoted in [35] is $1.549 \pm 0.009 \pm 0.015$ ps.

3.2.2 Inclusive *b*-hadron lifetimes

The inclusive b hadron lifetime is defined as $\tau_b = \sum_i f_i \tau_i$ where τ_i are the individual species lifetimes and f_i are the fractions of the various species present in an unbiased sample of weakly-decaying b hadrons produced at a high-energy collider.[3] This quantity is certainly less fundamental than the lifetimes of the individual species, the latter being much more useful in comparisons of the measurements with the theoretical predictions. Nonetheless, we perform the averaging of the inclusive lifetime measurements for completeness as well as for the reason that they might be of interest as "technical numbers."

In practice, an unbiased measurement of the inclusive lifetime is difficult to achieve, because it would imply an efficiency which is guaranteed to be the same across species. So most of the measurements are biased. In an attempt to group analyses which are expected to select the same mixture of b hadrons, the available results (given in Table 3) are divided into the following three sets:

1. measurements at LEP and SLD that accept any b-hadron decay, based on topological reconstruction (secondary vertex or track impact parameters);

2. measurements at LEP based on the identification of a lepton from a b decay; and

3. measurements at the Tevatron based on inclusive $H_b \to J/\psi X$ reconstruction, where the J/ψ is fully reconstructed.

[3] In principle such a quantity could be slightly different in Z decays and a the Tevatron, in case the fractions of b-hadron species are not exactly the same; see the discussion in Sec. 3.1.2.

The measurements of the first set are generally considered as estimates of τ_b, although the efficiency to reconstruct a secondary vertex most probably depends, in an analysis-specific way, on the number of tracks coming from the vertex, thereby depending on the type of the H_b. Even though these efficiency variations can in principle be accounted for using Monte Carlo simulations (which inevitably contain assumptions on branching fractions), the H_b mixture in that case can remain somewhat ill-defined and could be slightly different among analyses in this set.

On the contrary, the mixtures corresponding to the other two sets of measurements are better defined in the limit where the reconstruction and selection efficiency of a lepton or a J/ψ from an H_b does not depend on the decaying hadron type. These mixtures are given by the production fractions and the inclusive branching fractions for each H_b species to give a lepton or a J/ψ. In particular, under the assumption that all b hadrons have the same semileptonic decay width, the analyses of the second set should measure $\tau(b \to \ell) = (\sum_i f_i \tau_i^2)/(\sum_i f_i \tau_i)$ which is necessarily larger than τ_b if lifetime differences exist. Given the present knowledge on τ_i and f_i, $\tau(b \to \ell) - \tau_b$ is expected to be of the order of 0.01 ps.

Measurements by SLC and LEP experiments are subject to a number of common systematic uncertainties, such as those due to (lack of knowledge of) b and c fragmentation, b and c decay models, $\mathcal{B}(B \to \ell)$, $\mathcal{B}(B \to c \to \ell)$, $\mathcal{B}(c \to \ell)$, τ_c, and H_b decay multiplicity. In the averaging, these systematic uncertainties are assumed to be 100% correlated. The averages for the sets defined above (also given in Table 3) are

$$\tau(b \text{ vertex}) = 1.572 \pm 0.009 \text{ ps}, \quad (19)$$

$$\tau(b \to \ell) = 1.537 \pm 0.020 \text{ ps}, \quad (20)$$

$$\tau(b \to J/\psi) = 1.533^{+0.038}_{-0.034} \text{ ps}, \quad (21)$$

whereas an average of all measurements, ignoring mixture differences, yields 1.568 ± 0.009 ps.

3.2.3 B^0 and B^+ lifetimes and their ratio

After a number of years of dominating these averages the LEP experiments yielded the scene to the asymmetric B factories and the Tevatron experiments. The B factories have been very successful in utilizing their potential – in only a few years of running, *BABAR* and, to a greater extent, Belle, have struck a balance between the statistical and the systematic uncertainties, with both being close to (or even better than) the impressive 1%. In the meanwhile, CDF and DØ have emerged as significant contributors to the field as the Tevatron Run II data flowed in. Both appear to enjoy relatively small systematic effects, and while current statistical uncertainties of their measurements are factors of 2 to 4 larger than those of their B-factory counterparts, both Tevatron experiments stand to increase their samples by an order of magnitude.

At present time we are in an interesting position of having three sets of measurements (from LEP/SLC, B factories and the Tevatron) that originate from different environments, obtained using substantially different techniques and are precise enough for incisive comparison.

The averaging of $\tau(B^+)$, $\tau(B^0)$ and $\tau(B^+)/\tau(B^0)$ measurements is summarized in Tables 4, 5, and 6. For $\tau(B^+)/\tau(B^0)$ we averaged only the measurements of this quantity provided by experiments rather than using all available knowledge, which would have included, for example, $\tau(B^+)$ and $\tau(B^0)$ measurements which did not contribute to any of the ratio measurements.

The following sources of correlated (within experiment/machine) systematic uncertainties have been considered:

Table 4: Measurements of the B^0 lifetime.

Experiment	Method	Data set	$\tau(B^0)$ (ps)	Ref.
ALEPH	$D^{(*)}\ell$	91–95	$1.518 \pm 0.053 \pm 0.034$	[41]
ALEPH	Exclusive	91–94	$1.25^{+0.15}_{-0.13} \pm 0.05$	[42]
ALEPH	Partial rec. $\pi^+\pi^-$	91–94	$1.49^{+0.17+0.08}_{-0.15-0.06}$	[42]
DELPHI	$D^{(*)}\ell$	91–93	$1.61^{+0.14}_{-0.13} \pm 0.08$	[43]
DELPHI	Charge sec. vtx	91–93	$1.63 \pm 0.14 \pm 0.13$	[44]
DELPHI	Inclusive $D^*\ell$	91–93	$1.532 \pm 0.041 \pm 0.040$	[45]
DELPHI	Charge sec. vtx	94–95	$1.531 \pm 0.021 \pm 0.031$	[34]
L3	Charge sec. vtx	94–95	$1.52 \pm 0.06 \pm 0.04$	[46]
OPAL	$D^{(*)}\ell$	91–93	$1.53 \pm 0.12 \pm 0.08$	[47]
OPAL	Charge sec. vtx	93–95	$1.523 \pm 0.057 \pm 0.053$	[48]
OPAL	Inclusive $D^*\ell$	91–00	$1.541 \pm 0.028 \pm 0.023$	[49]
SLD	Charge sec. vtx ℓ	93–95	$1.56^{+0.14}_{-0.13} \pm 0.10$	[50][a]
SLD	Charge sec. vtx	93–95	$1.66 \pm 0.08 \pm 0.08$	[50][a]
CDF1	$D^{(*)}\ell$	92–95	$1.474 \pm 0.039^{+0.052}_{-0.051}$	[51]
CDF1	Excl. $J/\psi K^{*0}$	92–95	$1.497 \pm 0.073 \pm 0.032$	[52]
CDF2	Excl. $J/\psi K^{*0}$	02–04	$1.539 \pm 0.051 \pm 0.008$	[53][p]
CDF2	Incl. $D^{(*)}\ell$	02–04	$1.473 \pm 0.036 \pm 0.054$	[54][p]
CDF2	Excl. $D^-(3)\pi$	02–04	$1.511 \pm 0.023 \pm 0.013$	[55][p]
CDF2	Excl. $J/\psi K_S$	02–04	$1.503^{+0.050}_{-0.048} \pm 0.016$	[56][p]
DØ	Excl. $J/\psi K^{*0}$	02–05	$1.530 \pm 0.043 \pm 0.023$	[57, 58]
DØ	Excl. $J/\psi K_S$	02–04	$1.40^{+0.11}_{-0.10} \pm 0.03$	[59]
BABAR	Exclusive	99–00	$1.546 \pm 0.032 \pm 0.022$	[60]
BABAR	Inclusive $D^*\ell$	99–01	$1.529 \pm 0.012 \pm 0.029$	[61]
BABAR	Exclusive $D^*\ell$	99–02	$1.523^{+0.024}_{-0.023} \pm 0.022$	[62]
BABAR	Incl. $D^*\pi$, $D^*\rho$	99–01	$1.533 \pm 0.034 \pm 0.038$	[63]
BABAR	Inclusive $D^*\ell$	99–04	$1.504 \pm 0.013^{+0.018}_{-0.013}$	[64]
Belle	Exclusive	00–03	$1.534 \pm 0.008 \pm 0.010$	[65]
Average			1.527 ± 0.008	

[a] The combined SLD result quoted in [50] is $1.64 \pm 0.08 \pm 0.08$ ps.
[p] Preliminary.

Table 5: Measurements of the B^+ lifetime.

Experiment	Method	Data set	$\tau(B^+)$ (ps)	Ref.
ALEPH	$D^{(*)}\ell$	91–95	$1.648 \pm 0.049 \pm 0.035$	[41]
ALEPH	Exclusive	91–94	$1.58^{+0.21+0.04}_{-0.18-0.03}$	[42]
DELPHI	$D^{(*)}\ell$	91–93	$1.61 \pm 0.16 \pm 0.12$	[43][a]
DELPHI	Charge sec. vtx	91–93	$1.72 \pm 0.08 \pm 0.06$	[44][a]
DELPHI	Charge sec. vtx	94–95	$1.624 \pm 0.014 \pm 0.018$	[34]
L3	Charge sec. vtx	94–95	$1.66 \pm 0.06 \pm 0.03$	[46]
OPAL	$D^{(*)}\ell$	91–93	$1.52 \pm 0.14 \pm 0.09$	[47]
OPAL	Charge sec. vtx	93–95	$1.643 \pm 0.037 \pm 0.025$	[48]
SLD	Charge sec. vtx ℓ	93–95	$1.61^{+0.13}_{-0.12} \pm 0.07$	[50][b]
SLD	Charge sec. vtx	93–95	$1.67 \pm 0.07 \pm 0.06$	[50][b]
CDF1	$D^{(*)}\ell$	92–95	$1.637 \pm 0.058^{+0.045}_{-0.043}$	[51]
CDF1	Excl. $J/\psi K$	92–95	$1.636 \pm 0.058 \pm 0.025$	[52]
CDF2	Excl. $J/\psi K$	02–04	$1.662 \pm 0.033 \pm 0.008$	[53][p]
CDF2	Incl. $D^0\ell$	02–04	$1.653 \pm 0.029^{+0.033}_{-0.031}$	[54][p]
CDF2	Excl. $D^0\pi$	02–04	$1.661 \pm 0.027 \pm 0.013$	[55][p]
BABAR	Exclusive	99–00	$1.673 \pm 0.032 \pm 0.023$	[60]
Belle	Exclusive	00–03	$1.635 \pm 0.011 \pm 0.011$	[65]
Average			1.643 ± 0.010	

[a] The combined DELPHI result quoted in [44] is 1.70 ± 0.09 ps.
[b] The combined SLD result quoted in [50] is $1.66 \pm 0.06 \pm 0.05$ ps.
[p] Preliminary.

Table 6: Measurements of the ratio $\tau(B^+)/\tau(B^0)$.

Experiment	Method	Data set	Ratio $\tau(B^+)/\tau(B^0)$	Ref.
ALEPH	$D^{(*)}\ell$	91–95	$1.085 \pm 0.059 \pm 0.018$	[41]
ALEPH	Exclusive	91–94	$1.27^{+0.23+0.03}_{-0.19-0.02}$	[42]
DELPHI	$D^{(*)}\ell$	91–93	$1.00^{+0.17}_{-0.15} \pm 0.10$	[43]
DELPHI	Charge sec. vtx	91–93	$1.06^{+0.13}_{-0.11} \pm 0.10$	[44]
DELPHI	Charge sec. vtx	94–95	$1.060 \pm 0.021 \pm 0.024$	[34]
L3	Charge sec. vtx	94–95	$1.09 \pm 0.07 \pm 0.03$	[46]
OPAL	$D^{(*)}\ell$	91–93	$0.99 \pm 0.14^{+0.05}_{-0.04}$	[47]
OPAL	Charge sec. vtx	93–95	$1.079 \pm 0.064 \pm 0.041$	[48]
SLD	Charge sec. vtx ℓ	93–95	$1.03^{+0.16}_{-0.14} \pm 0.09$	[50][a]
SLD	Charge sec. vtx	93–95	$1.01^{+0.09}_{-0.08} \pm 0.05$	[50][a]
CDF1	$D^{(*)}\ell$	92–95	$1.110 \pm 0.056^{+0.033}_{-0.030}$	[51]
CDF1	Excl. $J/\psi K$	92–95	$1.093 \pm 0.066 \pm 0.028$	[52]
CDF2	Excl. $J/\psi K$	02–04	1.080 ± 0.042	[53][p]
CDF2	Incl. $D\ell$	02–04	$1.123 \pm 0.040^{+0.041}_{-0.039}$	[54][p]
CDF2	Excl. $D\pi$	02–04	$1.10 \pm 0.02 \pm 0.01$	[55][p]
DØ	$D^{*+}\mu$ $D^0\mu$ ratio	02–04	$1.080 \pm 0.016 \pm 0.014$	[66]
BABAR	Exclusive	99–00	$1.082 \pm 0.026 \pm 0.012$	[60]
Belle	Exclusive	00–03	$1.066 \pm 0.008 \pm 0.008$	[65]
Average			1.076 ± 0.008	

[a] The combined SLD result quoted in [50] is $1.01 \pm 0.07 \pm 0.06$.
[p] Preliminary.

- for SLC/LEP measurements – D^{**} branching ratio uncertainties [2], momentum estimation of b mesons from Z^0 decays (b-quark fragmentation parameter $\langle X_E \rangle = 0.702 \pm 0.008$ [2]), B_s^0 and b baryon lifetimes (see Secs. 3.2.4 and 3.2.6), and b hadron fractions at high energy (see Table 2).

- for *BABAR* measurements – alignment, z scale, PEP-II boost, sample composition (where applicable)

- for DØ and CDF Run II measurements – alignment (separately within each experiment)

The resultant averages are:

$$\tau(B^0) = 1.527 \pm 0.008 \text{ ps}, \quad (22)$$

$$\tau(B^+) = 1.643 \pm 0.010 \text{ ps}, \quad (23)$$

$$\tau(B^+)/\tau(B^0) = 1.076 \pm 0.008. \quad (24)$$

3.2.4 B_s^0 lifetime

Similar to the kaon system, neutral B mesons contain short- and long-lived components, since the light (L) and heavy (H) eigenstates, $B_{\rm L}$ and $B_{\rm H}$, differ not only in their masses, but also in

their widths with $\Delta\Gamma = \Gamma_{\rm L} - \Gamma_{\rm H}$. In the case of the B_s^0 system, $\Delta\Gamma_s$ can be particularly large. The current theoretical prediction in the Standard Model for the fractional width difference is $\Delta\Gamma_s/\Gamma_s = 0.12 \pm 0.05$ [67], where $\Gamma_s = (\Gamma_{\rm L} + \Gamma_{\rm H})/2$. Specific measurements of $\Delta\Gamma_s$ and Γ_s are explained in Sec. 3.3.2, but the result for Γ_s is quoted here.

Neglecting *CP* violation in $B_s^0 - \overline{B}_s^0$ mixing, which is expected to be small [67], the B_s^0 mass eigenstates are also *CP* eigenstates. In the Standard Model assuming no *CP* violation in the B_s^0 system, $\Gamma_{\rm L}$ is the width of the *CP*-even state and $\Gamma_{\rm H}$ the width of the *CP*-odd state. Final states can be decomposed into *CP*-even and *CP*-odd components, each with a different lifetime.

In view of a possibly substantial width difference, and the fact that various decay channels will have different proportions of the $B_{\rm L}$ and $B_{\rm H}$ eigenstates, the straight average of all available B_s^0 lifetime measurements is rather ill-defined. Therefore, the B_s^0 lifetime measurements are broken down into three categories and averaged separately.

- ***Flavor-specific decays***, such as semileptonic $B_s \to D_s \ell\nu$ or $B_s \to D_s\pi$, will have equal fractions of $B_{\rm L}$ and $B_{\rm H}$ at time zero, where $\tau_{\rm L} = 1/\Gamma_{\rm L}$ is expected to be the shorter-lived component and $\tau_{\rm H} = 1/\Gamma_{\rm H}$ expected to be the longer-lived component. A superposition of two exponentials thus results with decay widths $\Gamma_s \pm \Delta\Gamma_s/2$. Fitting to a single exponential one obtains a measure of the flavor-specific lifetime [68]:

$$\tau(B_s^0)_{\rm fs} = \frac{1}{\Gamma_s} \frac{1 + \left(\frac{\Delta\Gamma_s}{2\Gamma_s}\right)^2}{1 - \left(\frac{\Delta\Gamma_s}{2\Gamma_s}\right)^2}. \tag{25}$$

  As given in Table 7, the flavor-specific B_s^0 lifetime world average is:

$$\tau(B_s^0)_{\rm fs} = 1.454 \pm 0.040 \text{ ps}\,. \tag{26}$$

  This world average will be used later in Sec. 3.3.2 in combination with other measurements to find $\overline{\tau}(B_s^0) = 1/\Gamma_s$ and $\Delta\Gamma_s$.

  The following correlated systematic errors were considered: average B lifetime used in backgrounds, B_s^0 decay multiplicity, and branching ratios used to determine backgrounds (*e.g.* $\mathcal{B}(B \to D_s D)$). A knowledge of the multiplicity of B_s^0 decays is important for measurements that partially reconstruct the final state such as $B \to D_s X$ (where X is not a lepton). The boost deduced from Monte Carlo simulation depends on the multiplicity used. Since this is not well known, the multiplicity in the simulation is varied and this range of values observed is taken to be a systematic. Similarly not all the branching ratios for the potential background processes are measured. Where they are available, the PDG values are used for the error estimate. Where no measurements are available estimates can usually be made by using measured branching ratios of related processes and using some reasonable extrapolation.

- ***$B_s^0 \to D_s^+ X$ decays***. Included in Table 7 are measurements of lifetimes using samples of B_s^0 decays to D_s plus hadrons, and hence into a less known mixture of *CP*-states. A lifetime weighted this way can still be a useful input for analyses examining such an inclusive sample. These are separated in Table 7 and combined with the semileptonic lifetime to obtain:

$$\tau(B_s^0)_{D_s{\rm X}} = 1.461 \pm 0.040 \text{ ps}\,. \tag{27}$$

Table 7: Measurements of the B_s^0 lifetime.

Experiment	Method	Data set	$\tau(B_s^0)$ (ps)	Ref.
ALEPH	$D_s\ell$	91–95	$1.54^{+0.14}_{-0.13} \pm 0.04$	[69]
CDF1	$D_s\ell$	92–96	$1.36 \pm 0.09^{+0.06}_{-0.05}$	[70]
DELPHI	$D_s\ell$	91–95	$1.42^{+0.14}_{-0.13} \pm 0.03$	[71]
OPAL	$D_s\ell$	90–95	$1.50^{+0.16}_{-0.15} \pm 0.04$	[72]
DØ	$D_s\mu$	02–04	$1.420 \pm 0.043 \pm 0.057$	[73]^p
CDF2	$D_s\pi, D_s\pi\pi\pi$	02–04	$1.60 \pm 0.10 \pm 0.02$	[74]^p
CDF2	$D_s\ell$	02–04	$1.381 \pm 0.055^{+0.052}_{-0.046}$	[75]^p
Average of flavor-specific measurements			1.454 ± 0.040	
ALEPH	D_sh	91–95	$1.47 \pm 0.14 \pm 0.08$	[76]
DELPHI	D_sh	91–95	$1.53^{+0.16}_{-0.15} \pm 0.07$	[77]
OPAL	D_s incl.	90–95	$1.72^{+0.20+0.18}_{-0.19-0.17}$	[78]
Average of all above D_s measurements			1.461 ± 0.040	
CDF1	$J/\psi\phi$	92–95	$1.34^{+0.23}_{-0.19} \pm 0.05$	[40]
CDF2	$J/\psi\phi$	02–04	$1.369 \pm 0.100^{+0.008}_{-0.010}$	[53]^p
DØ	$J/\psi\phi$	02–04	$1.444^{+0.098}_{-0.090} \pm 0.02$	[58]
Average of $J/\psi\phi$ measurements			1.404 ± 0.066	

^{p} Preliminary.

- ***Fully exclusive $B_s^0 \to J/\psi\phi$ decays*** are expected to be dominated by the *CP*-even state and its lifetime. First measurements of the *CP* mix for this decay mode are outlined in Sec. 3.3.2. CDF and DØ measurements from this particular mode $B_s^0 \to J/\psi\phi$ are combined into an average given in Table 7. There are no correlations between the measurements for this fully exclusive channel, and the world average for this specific decay is:

$$\tau(B_s^0)_{J/\psi\phi} = 1.404 \pm 0.066 \text{ ps}\,. \tag{28}$$

  A caveat is that different experimental acceptances will likely lead to different admixtures of the *CP*-even and *CP*-odd states, and fits to a single exponential may result in inherently different measurements of these quantities.

Finally, as will be shown in Sec. 3.3.2, measurements of $\Delta\Gamma_s$, including separation into *CP*-even and *CP*-odd components, give

$$\overline{\tau}(B_s^0) = 1/\Gamma_s = 1.42^{+0.06}_{-0.07} \text{ ps}\,, \tag{29}$$

and when combined with the flavor-specific lifetime measurements:

$$\overline{\tau}(B_s^0) = 1/\Gamma_s = 1.396^{+0.044}_{-0.046} \text{ ps}\,. \tag{30}$$

3.2.5 B_c^+ lifetime

There are currently three measurements of the lifetime of the B_c^+ meson from CDF [79,80] and DØ [81] using the semileptonic decay mode $B_c^+ \to J/\psi\ell$ and fitting simultaneously to the mass

Table 8: Measurements of the B_c^+ lifetime.

Experiment	Method	Data set	$\tau(B_c^+)$ (ps)	Ref.
CDF1	$J/\psi\ell$	92–95	$0.46^{+0.18}_{-0.16} \pm 0.03$	[79]
CDF2	$J/\psi e$	02–04	$0.474^{+0.073}_{-0.066} \pm 0.033$	[80]^p
DØ	$J/\psi\mu$	02–04	$0.448^{+0.123}_{-0.096} \pm 0.121$	[81]^p
Average			0.469 ± 0.065	

^{p} Preliminary.

and lifetime using the vertex formed with the leptons from the decay of the J/ψ and the third lepton. Correction factors to estimate the boost due to the missing neutrino are used. Mass values of $6.40 \pm 0.39 \pm 0.13$ GeV/c^2 for the CDF Run 1 result [79] and $5.95^{+0.14}_{-0.13} \pm 0.34$ GeV/c^2 for the DØ Run 2 result [81] are found by fitting to the tri-lepton invariant mass spectrum. These mass measurements are consistent within uncertainties. In the CDF Run 2 result [80], the mass is fixed to 6.271 GeV/c^2, but then varied between 6.2 and 6.4 GeV/c^2 to assess the systematic error on the lifetime due to the B_c^+ mass value. Correlated systematic errors include the impact of the uncertainty of the B_c^+ p_T spectrum on the correction factors, the level of feed-down from $\psi(2S)$, MC modeling of the decay model varying from phase space to the ISGW model, and mass variations. Values of the B_c^+ lifetime are given in Table 8 and the world average is determined to be:

$$\tau(B_c^+) = 0.469 \pm 0.065 \text{ ps}\,. \tag{31}$$

3.2.6 Λ_b^0 and b-baryon lifetimes

The most precise measurements of the b-baryon lifetime originate from two classes of partially reconstructed decays. In the first class, decays with an exclusively reconstructed Λ_c^+ baryon and a lepton of opposite charge are used. These products are more likely to occur in the decay of Λ_b^0 baryons. In the second class, more inclusive final states with a baryon (p, $\overline{p}$, Λ, or $\overline{\Lambda}$) and a lepton have been used, and these final states can generally arise from any b baryon.

The following sources of correlated systematic uncertainties have been considered: experimental time resolution within a given experiment, b-quark fragmentation distribution into weakly decaying b baryons, Λ_b^0 polarization, decay model, and evaluation of the b-baryon purity in the selected event samples. In computing the averages the central values of the masses are scaled to $M(\Lambda_b^0) = 5624 \pm 9$ MeV/c^2 [82] and $M(b\text{-baryon}) = 5670 \pm 100$ MeV/c^2.

The meaning of decay model and the correlations are not always clear. Uncertainties related to the decay model are dominated by assumptions on the fraction of n-body decays. To be conservative it is assumed that it is correlated whenever given as an error. DELPHI varies the fraction of 4-body decays from 0.0 to 0.3. In computing the average, the DELPHI result is corrected for 0.2 ± 0.2.

Furthermore, in computing the average, the semileptonic decay results are corrected for a polarization of $-0.45^{+0.19}_{-0.17}$ [2] and a Λ_b^0 fragmentation parameter $\langle X_E \rangle = 0.70 \pm 0.03$ [83].

Inputs to the averages are given in Table 9. The world average lifetime of b baryons is then:

$$\langle \tau(b\text{-baryon}) \rangle = 1.242 \pm 0.046 \text{ ps}\,. \tag{32}$$

Table 9: Measurements of the b-baryon lifetimes.

Experiment	Method	Data set	Lifetime (ps)	Ref.
ALEPH	$\Lambda_c^+\ell$	91–95	$1.18^{+0.13}_{-0.12} \pm 0.03$	[16][a]
ALEPH	$\Lambda\ell^-\ell^+$	91–95	$1.30^{+0.26}_{-0.21} \pm 0.04$	[16][a]
CDF1	$\Lambda_c^+\ell$	91–95	$1.32 \pm 0.15 \pm 0.06$	[84]
CDF2	$J/\psi\Lambda$	02–04	$1.45^{+0.14}_{-0.13} \pm 0.02$	[56][p]
DØ	$J/\psi\Lambda$	02–04	$1.22^{+0.22}_{-0.18} \pm 0.04$	[59]
DELPHI	$\Lambda_c^+\ell$	91–94	$1.11^{+0.19}_{-0.18} \pm 0.05$	[85][b]
OPAL	$\Lambda_c^+\ell$, $\Lambda\ell^-\ell^+$	90–95	$1.29^{+0.24}_{-0.22} \pm 0.06$	[72]
Average of above 7 (Λ_b^0 lifetime)			1.288 ± 0.065	
ALEPH	$\Lambda\ell$	91–95	$1.20 \pm 0.08 \pm 0.06$	[16]
DELPHI	$\Lambda\ell\pi$ vtx	91–94	$1.16 \pm 0.20 \pm 0.08$	[85][b]
DELPHI	$\Lambda\mu$ i.p.	91–94	$1.10^{+0.19}_{-0.17} \pm 0.09$	[86][b]
DELPHI	$p\ell$	91–94	$1.19 \pm 0.14 \pm 0.07$	[85][b]
OPAL	$\Lambda\ell$ i.p.	90–94	$1.21^{+0.15}_{-0.13} \pm 0.10$	[87][c]
OPAL	$\Lambda\ell$ vtx	90–94	$1.15 \pm 0.12 \pm 0.06$	[87][c]
Average of above 13 (b-baryon lifetime)			1.242 ± 0.046	
ALEPH	$\Xi\ell$	90–95	$1.35^{+0.37+0.15}_{-0.28-0.17}$	[18]
DELPHI	$\Xi\ell$	91–93	$1.5^{+0.7}_{-0.4} \pm 0.3$	[17]
Average of above 2 (Ξ_b lifetime)			$1.39^{+0.34}_{-0.28}$	

[a] The combined ALEPH result quoted in [16] is 1.21 ± 0.11 ps.
[b] The combined DELPHI result quoted in [85] is $1.14 \pm 0.08 \pm 0.04$ ps.
[c] The combined OPAL result quoted in [87] is $1.16 \pm 0.11 \pm 0.06$ ps.
[p] Preliminary.

Keeping only $\Lambda_c^\pm\ell^\mp$, $\Lambda\ell^-\ell^+$, and fully exclusive final states, as representative of the Λ_b^0 baryon, the following lifetime is obtained:

$$\tau(\Lambda_b^0) = 1.288 \pm 0.065 \text{ ps}\,. \tag{33}$$

Averaging the measurements based on the $\Xi^\mp\ell^\mp$ final states [17, 18] gives a lifetime value for a sample of events containing Ξ_b^0 and Ξ_b^- baryons:

$$\langle\tau(\Xi_b)\rangle = 1.39^{+0.34}_{-0.28} \text{ ps}\,. \tag{34}$$

3.2.7 Summary and comparison with theoretical predictions

Averages of lifetimes of specific b-hadron species are collected in Table 10. As described in Sec. 3.2, Heavy Quark Effective Theory can be employed to explain the hierarchy of $\tau(B_c^+) \ll \tau(\Lambda_b^0) < \overline{\tau}(B_s^0) \approx \tau(B^0) < \tau(B^+)$, and used to predict the ratios between lifetimes. Typical predictions are compared to the measured lifetime ratios in Table 11.

A recent prediction of the ratio between the B^+ and B^0 lifetimes, is 1.06 ± 0.02 [28], in good agreement with experiment.

Table 10: Summary of lifetimes of different b-hadron species.

b-hadron species	Measured lifetime
B^+	1.643 ± 0.010 ps
B^0	1.527 ± 0.008 ps
B_s^0 ($\rightarrow$ flavor specific)	1.454 ± 0.040 ps
B_s^0 ($\rightarrow J/\psi\phi$)	1.404 ± 0.066 ps
B_s^0 ($1/\Gamma_s$)	$1.396^{+0.044}_{-0.046}$ ps
B_c^+	0.469 ± 0.065 ps
Λ_b^0	1.288 ± 0.065 ps
Ξ_b mixture	$1.39^{+0.34}_{-0.28}$ ps
b-baryon mixture	1.242 ± 0.046 ps
b-hadron mixture	1.568 ± 0.009 ps

Table 11: Measured ratios of b-hadron lifetimes relative to the B^0 lifetime and ranges predicted by theory [28, 29].

Lifetime ratio	Measured value	Predicted range
$\tau(B^+)/\tau(B^0)$	1.076 ± 0.008	1.04 – 1.08
$\overline{\tau}(B_s^0)/\tau(B^0)^a$	0.914 ± 0.030	0.99 – 1.01
$\tau(\Lambda_b^0)/\tau(B^0)$	0.844 ± 0.043	0.86 – 0.95
$\tau(b\text{-baryon})/\tau(B^0)$	0.813 ± 0.030	0.86 – 0.95

[a] Using $\overline{\tau}(B_s^0) = 1/\Gamma_s = 2/(\Gamma_{\rm L} + \Gamma_{\rm H})$.

The total widths of the B_s^0 and B^0 mesons are expected to be very close and differ by at most 1% [29, 88]. However, the experimental ratio $\overline{\tau}(B_s^0)/\tau(B^0)$, where $\overline{\tau}(B_s^0) = 1/\Gamma_s$ is obtained from $\Delta\Gamma_s$ and flavour-specific lifetime measurements, now appears to be smaller than 1 by $(8.6 \pm 3.0)\%$, at deviation with respect to the prediction.

The ratio $\tau(\Lambda_b^0)/\tau(B^0)$ has particularly been the source of theoretical scrutiny since earlier calculations [25, 89] predicted a value greater than 0.90, almost two sigma higher than the world average at the time. More recent calculations of this ratio that include higher-order effects predict a lower ratio between the Λ_b^0 and B^0 lifetimes [28, 29] and reduce this difference. References [28, 29] present probability density functions of their predictions with variation of theoretical inputs, and the indicated ranges in Table 11 are the RMS of the distributions from the most probable values.

3.3 Neutral B-meson mixing

The $B^0 - \overline{B}^0$ and $B_s^0 - \overline{B}_s^0$ systems both exhibit the phenomenon of particle-antiparticle mixing. For each of them, there are two mass eigenstates which are linear combinations of the two flavour states, B and $\overline{B}$. The heaviest (lightest) of the these mass states is denoted $B_{\rm H}$ ($B_{\rm L}$), with

mass $m_{\rm H}$ ($m_{\rm L}$) and total decay width $\Gamma_{\rm H}$ ($\Gamma_{\rm L}$). We define

$$\Delta m = m_{\rm H} - m_{\rm L}\,, \tag{35}$$
$$\Delta\Gamma = \Gamma_{\rm L} - \Gamma_{\rm H}\,, \tag{36}$$

where Δm is positive by definition, and $\Delta\Gamma$ is expected to be positive within the Standard Model.[4]

There are four different time-dependent probabilities describing the case of a neutral B meson produced as a flavour state and decaying to a flavour-specific final state. If CPT is conserved (which will be assumed throughout), they can be written as

$$\left\{\begin{array}{lcl} \mathcal{P}(B \to B) &=& \frac{e^{-\Gamma t}}{2}\left[\cosh\left(\frac{\Delta\Gamma}{2}t\right) + \cos(\Delta m t)\right] \\ \mathcal{P}(B \to \overline{B}) &=& \frac{e^{-\Gamma t}}{2}\left[\cosh\left(\frac{\Delta\Gamma}{2}t\right) - \cos(\Delta m t)\right] \left|\frac{q}{p}\right|^2 \\ \mathcal{P}(\overline{B} \to B) &=& \frac{e^{-\Gamma t}}{2}\left[\cosh\left(\frac{\Delta\Gamma}{2}t\right) - \cos(\Delta m t)\right] \left|\frac{p}{q}\right|^2 \\ \mathcal{P}(\overline{B} \to \overline{B}) &=& \frac{e^{-\Gamma t}}{2}\left[\cosh\left(\frac{\Delta\Gamma}{2}t\right) + \cos(\Delta m t)\right] \end{array}\right. , \tag{37}$$

where t is the proper time of the system (*i.e.* the time interval between the production and the decay in the rest frame of the B meson) and $\Gamma = (\Gamma_{\rm H} + \Gamma_{\rm L})/2 = 1/\overline{\tau}(B)$ is the average decay width. At the B factories, only the proper-time difference Δt between the decays of the two neutral B mesons from the $\Upsilon(4S)$ can be determined, but, because the two B mesons evolve coherently (keeping opposite flavours as long as none of them has decayed), the above formulae remain valid if t is replaced with Δt and the production flavour is replaced by the flavour at the time of the decay of the accompanying B meson in a flavour specific state. As can be seen in the above expressions, the mixing probabilities depend on three mixing observables: Δm, $\Delta\Gamma$, and $|q/p|^2$ which signals CP violation in the mixing if $|q/p|^2 \neq 1$.

In the next sections we review in turn the experimental knowledge on these three parameters, separately for the B^0 meson (Δm_d, $\Delta\Gamma_d$, $|q/p|_d$) and the B^0_s meson (Δm_s, $\Delta\Gamma_s$, $|q/p|_s$).

3.3.1 B^0 mixing parameters

CP violation parameter $|q/p|_d$

Evidence for CP violation in B^0 mixing has been searched for, both with flavor-specific and inclusive B^0 decays, in samples where the initial flavor state is tagged. In the case of semileptonic (or other flavor-specific) decays, where the final state tag is also available, the following asymmetry

$$\mathcal{A}_{\rm SL} = \frac{N(\overline{B}^0(t) \to \ell^+\nu_\ell X) - N(B^0(t) \to \ell^-\overline{\nu}_\ell X)}{N(\overline{B}^0(t) \to \ell^+\nu_\ell X) + N(B^0(t) \to \ell^-\overline{\nu}_\ell X)} = \frac{|p/q|_d^2 - |q/p|_d^2}{|p/q|_d^2 + |q/p|_d^2} \tag{38}$$

has been measured, either in time-integrated analyses at CLEO [90–92] and CDF [93], or in time-dependent analyses at OPAL [94], ALEPH [95], *BABAR* [96, 97] and Belle [98]. In the

[4]For reason of symmetry in Eqs. (35) and (36), $\Delta\Gamma$ is sometimes defined with the opposite sign. The definition adopted here, i.e. Eq. (36), is the one used by most experimentalists and many phenomenologists in B physics.

Table 12: Measurements of *CP* violation in B^0 mixing and their average in terms of both $\mathcal{A}_{\rm SL}$ and $|q/p|_d$. The individual results are listed as quoted in the original publications, or converted[5] to an $\mathcal{A}_{\rm SL}$ value. When two errors are quoted, the first one is statistical and the second one systematic.

Exp. & Ref.	Method	Measured $\mathcal{A}_{\rm SL}$	Measured $\lvert q/p\rvert_d$
CLEO [91]	partial hadronic rec.	$+0.017 \pm 0.070 \pm 0.014$	
CLEO [92]	dileptons	$+0.013 \pm 0.050 \pm 0.005$	
CLEO [92]	average of above two	$+0.014 \pm 0.041 \pm 0.006$	
OPAL [94]	leptons	$+0.008 \pm 0.028 \pm 0.012$	
OPAL [99]	inclusive (Eq. (39))	$+0.005 \pm 0.055 \pm 0.013$	
ALEPH [95]	leptons	$-0.037 \pm 0.032 \pm 0.007$	
ALEPH [95]	inclusive (Eq. (39))	$+0.016 \pm 0.034 \pm 0.009$	
ALEPH [95]	average of above two	-0.013 ± 0.026 (tot)	
BABAR [97]	dileptons	$+0.005 \pm 0.012 \pm 0.014$	$0.998 \pm 0.006 \pm 0.007$
BABAR [96]	full hadronic rec.		$1.029 \pm 0.013 \pm 0.011$
Belle [98]	dileptons	$-0.0011 \pm 0.0079 \pm 0.0070$	$1.0005 \pm 0.0040 \pm 0.0035$
	Average of all above	-0.0030 ± 0.0078 (tot)	1.0015 ± 0.0039 (tot)

inclusive case, also investigated and published at ALEPH [95] and OPAL [99], no final state tag is used, and the asymmetry [100]

$$\frac{N(B^0(t)\to \text{all}) - N(\overline{B}^0(t)\to \text{all})}{N(B^0(t)\to \text{all}) + N(\overline{B}^0(t)\to \text{all})} \simeq \mathcal{A}_{\rm SL}\left[\frac{\Delta m_d}{2\Gamma_d}\sin(\Delta m_d\, t) - \sin^2\left(\frac{\Delta m_d\, t}{2}\right)\right] \qquad (39)$$

must be measured as a function of the proper time to extract information on *CP* violation. In all cases asymmetries compatible with zero have been found, with a precision limited by the available statistics. A simple average of all published results for the B^0 meson [91, 92, 94–99] yields

$$\mathcal{A}_{\rm SL} = -0.0030 \pm 0.0078 \qquad (40)$$

or, equivalently through Eq. (38),

$$|q/p|_d = 1.0015 \pm 0.0039\,. \qquad (41)$$

This result[5], summarized in Table 12, is compatible with no *CP* violation in the mixing, an assumption we make for the rest of this section.

Mass and decay width differences Δm_d and $\Delta\Gamma_d$

Many time-dependent B^0–$\overline{B}^0$ oscillation analyses have been performed by the ALEPH, *BABAR*, Belle, CDF, DØ, DELPHI, L3 and OPAL collaborations. The corresponding measurements of Δm_d are summarized in Table 13, where only the most recent results are listed

[5]Early analyses and (perhaps hence) the PDG use the complex parameter $\epsilon_B = (p-q)/(p+q)$; if *CP* violation in the mixing in small, $\mathcal{A}_{\rm SL} \cong 4{\rm Re}(\epsilon_B)/(1+|\epsilon_B|^2)$ and our current world average is ${\rm Re}(\epsilon_B)/(1+|\epsilon_B|^2) = -0.0007 \pm 0.0020$.

Table 13: Time-dependent measurements included in the Δm_d average. The results obtained from multi-dimensional fits involving also the B^0 (and B^+) lifetimes as free parameter(s) [62, 64, 65] have been converted into one-dimensional measurements of Δm_d. All the measurements have then been adjusted to a common set of physics parameters before being combined. The CDF2 and DØ results are preliminary.

Experiment	Method		Δm_d in ps^{-1}	Δm_d in ps^{-1}
and Ref.	rec.	tag	before adjustment	after adjustment
ALEPH [101]	ℓ	$Q_{\rm jet}$	0.404±0.045±0.027	
ALEPH [101]	ℓ	ℓ	0.452±0.039±0.044	
ALEPH [101]	above two combined		0.422±0.032±0.026	$0.441\pm0.032\ ^{+0.021}_{-0.020}$
ALEPH [101]	D^*	$\ell, Q_{\rm jet}$	0.482±0.044±0.024	0.482±0.044±0.024
DELPHI [102]	ℓ	$Q_{\rm jet}$	0.493±0.042±0.027	0.504±0.042±0.024
DELPHI [102]	$\pi^*\ell$	$Q_{\rm jet}$	0.499±0.053±0.015	0.501±0.053±0.015
DELPHI [102]	ℓ	ℓ	0.480±0.040±0.051	$0.489\pm0.040\ ^{+0.049}_{-0.048}$
DELPHI [102]	D^*	$Q_{\rm jet}$	0.523±0.072±0.043	0.518±0.072±0.043
DELPHI [103]	vtx	comb	0.531±0.025±0.007	0.530±0.025±0.006
L3 [104]	ℓ	ℓ	0.458±0.046±0.032	0.470±0.046±0.029
L3 [104]	ℓ	$Q_{\rm jet}$	0.427±0.044±0.044	0.436±0.044±0.042
L3 [104]	ℓ	ℓ(IP)	0.462±0.063±0.053	0.481±0.063±0.047
OPAL [105]	ℓ	ℓ	$0.430\pm0.043\ ^{+0.028}_{-0.030}$	$0.462\pm0.043\ ^{+0.018}_{-0.017}$
OPAL [106]	ℓ	$Q_{\rm jet}$	$0.444\pm0.029\ ^{+0.020}_{-0.017}$	$0.467\pm0.029\ ^{+0.015}_{-0.014}$
OPAL [107]	$D^*\ell$	$Q_{\rm jet}$	0.539±0.060±0.024	0.544±0.060±0.023
OPAL [107]	D^*	ℓ	$0.567\pm0.089\ ^{+0.029}_{-0.023}$	$0.571\pm0.089\ ^{+0.028}_{-0.022}$
OPAL [108]	$\pi^*\ell$	$Q_{\rm jet}$	0.497±0.024±0.025	0.496±0.024±0.025
CDF1 [109]	$D\ell$	SST	$0.471\ ^{+0.078}_{-0.068}\ ^{+0.033}_{-0.034}$	$0.470\ ^{+0.078}_{-0.068}\ ^{+0.033}_{-0.034}$
CDF1 [110]	μ	μ	0.503±0.064±0.071	0.513±0.064±0.070
CDF1 [111]	ℓ	$\ell, Q_{\rm jet}$	0.500±0.052±0.043	0.537±0.052±0.036
CDF1 [112]	$D^*\ell$	ℓ	$0.516\pm0.099\ ^{+0.029}_{-0.035}$	$0.523\pm0.099\ ^{+0.028}_{-0.035}$
CDF2 [113]	$D^{(*)}\ell$	OST	0.511±0.020±0.014	0.511±0.020±0.014
CDF2 [114]	B^0	comb	0.536±0.028±0.006	0.536±0.028±0.006
DØ [115]	$D^{(*)}\mu$	OST	0.498±0.026±0.016	0.498±0.026±0.016
BABAR [116]	B^0	ℓ, K, NN	0.516±0.016±0.010	0.520±0.016±0.008
BABAR [117]	ℓ	ℓ	0.493±0.012±0.009	0.489±0.012±0.006
BABAR [64]	$D^*\ell\nu$(part)	ℓ	0.511±0.007±0.007	0.512±0.007±0.007
BABAR [62]	$D^*\ell\nu$	ℓ, K, NN	0.492±0.018±0.014	0.491±0.018±0.013
Belle [118]	$D^*\pi$(part)	ℓ	0.509±0.017±0.020	0.512±0.017±0.019
Belle [9]	ℓ	ℓ	0.503±0.008±0.010	0.506±0.008±0.009
Belle [65]	$B^0, D^*\ell\nu$	comb	0.511±0.005±0.006	0.512±0.005±0.006
World average (all above measurements included):				0.508±0.003±0.003
– ALEPH, DELPHI, L3, OPAL and CDF1 only:				0.496±0.010±0.009
– Above measurements of *BABAR* and Belle only:				0.508±0.003±0.003

(*i.e.* measurements superseded by more recent ones have been omitted). Although a variety of different techniques have been used, the individual Δm_d results obtained at high-energy colliders have remarkably similar precision. Their average is compatible with the recent and more precise measurements from the asymmetric B factories. The systematic uncertainties are not negligible; they are often dominated by sample composition, mistag probability, or b-hadron lifetime contributions. Before being combined, the measurements are adjusted on the basis of a common set of input values, including the averages of the b-hadron fractions and lifetimes given in this report (see Secs. 3.1 and 3.2). Some measurements are statistically correlated. Systematic correlations arise both from common physics sources (fractions, lifetimes, branching ratios of b hadrons), and from purely experimental or algorithmic effects (efficiency, resolution, flavour tagging, background description). Combining all published measurements listed in Table 13 and accounting for all identified correlations as described in [2] yields $\Delta m_d = 0.508 \pm 0.003 \pm 0.003$ ps^{-1}.

On the other hand, ARGUS and CLEO have published measurements of the time-integrated mixing probability χ_d [90,91,119], which average to $\chi_d = 0.182 \pm 0.015$. Following Ref. [91], the width difference $\Delta\Gamma_d$ could in principle be extracted from the measured value of $\Gamma_d = 1/\tau(B^0)$ and the above averages for Δm_d and χ_d (provided that $\Delta\Gamma_d$ has a negligible impact on the Δm_d $\tau(B^0)$ analyses that have assumed $\Delta\Gamma_d = 0$), using the relation

$$\chi_d = \frac{x_d^2 + y_d^2}{2(x_d^2+1)} \quad \text{with} \quad x_d = \frac{\Delta m_d}{\Gamma_d} \quad \text{and} \quad y_d = \frac{\Delta\Gamma_d}{2\Gamma_d}\,. \tag{42}$$

However, direct time-dependent studies provide much stronger constraints: $|\Delta\Gamma_d|/\Gamma_d < 18\%$ at 95% CL from DELPHI [103], and $-6.8\% < \mathrm{sign}(\mathrm{Re}\lambda_{CP})\Delta\Gamma_d/\Gamma_d < 8.4\%$ at 90% CL from BABAR [96], where $\lambda_{CP} = (q/p)_d(\overline{A}_{CP}/A_{CP})$ is defined for a CP-even final state (the sensitivity to the overall sign of $\mathrm{sign}(\mathrm{Re}\lambda_{CP})\Delta\Gamma_d/\Gamma_d$ comes from the use of B^0 decays to CP final states). Combining these two results after adjustment to $1/\Gamma_d = \tau(B^0) = 1.527 \pm 0.008$ ps yields

$$\mathrm{sign}(\mathrm{Re}\lambda_{CP})\Delta\Gamma_d/\Gamma_d = 0.009 \pm 0.037\,. \tag{43}$$

The sign of $\mathrm{Re}\lambda_{CP}$ is not measured, but expected to be positive from the global fits of the Unitarity Triangle within the Standard Model.

Assuming $\Delta\Gamma_d = 0$ and using $1/\Gamma_d = \tau(B^0) = 1.527 \pm 0.008$ ps, the Δm_d and χ_d results are combined through Eq. (42) to yield the world average

$$\Delta m_d = 0.507 \pm 0.004 \text{ ps}^{-1}\,, \tag{44}$$

or, equivalently,

$$x_d = 0.775 \pm 0.008 \quad \text{and} \quad \chi_d = 0.188 \pm 0.002\,. \tag{45}$$

Figure 4 compares the Δm_d values obtained by the different experiments.

The B^0 mixing averages given in Eqs. (44) and (45) and the b-hadron fractions of Table 2 have been obtained in a fully consistent way, taking into account the fact that the fractions are computed using the χ_d value of Eq. (45) and that many individual measurements of Δm_d at high energy depend on the assumed values for the b-hadron fractions. Furthermore, this set of averages is consistent with the lifetime averages of Sec. 3.2.

It should be noted that the most recent (and precise) analyses at the asymmetric B factories measure Δm_d as a result of a multi-dimensional fit. Two *BABAR* analyses [62, 64], based on

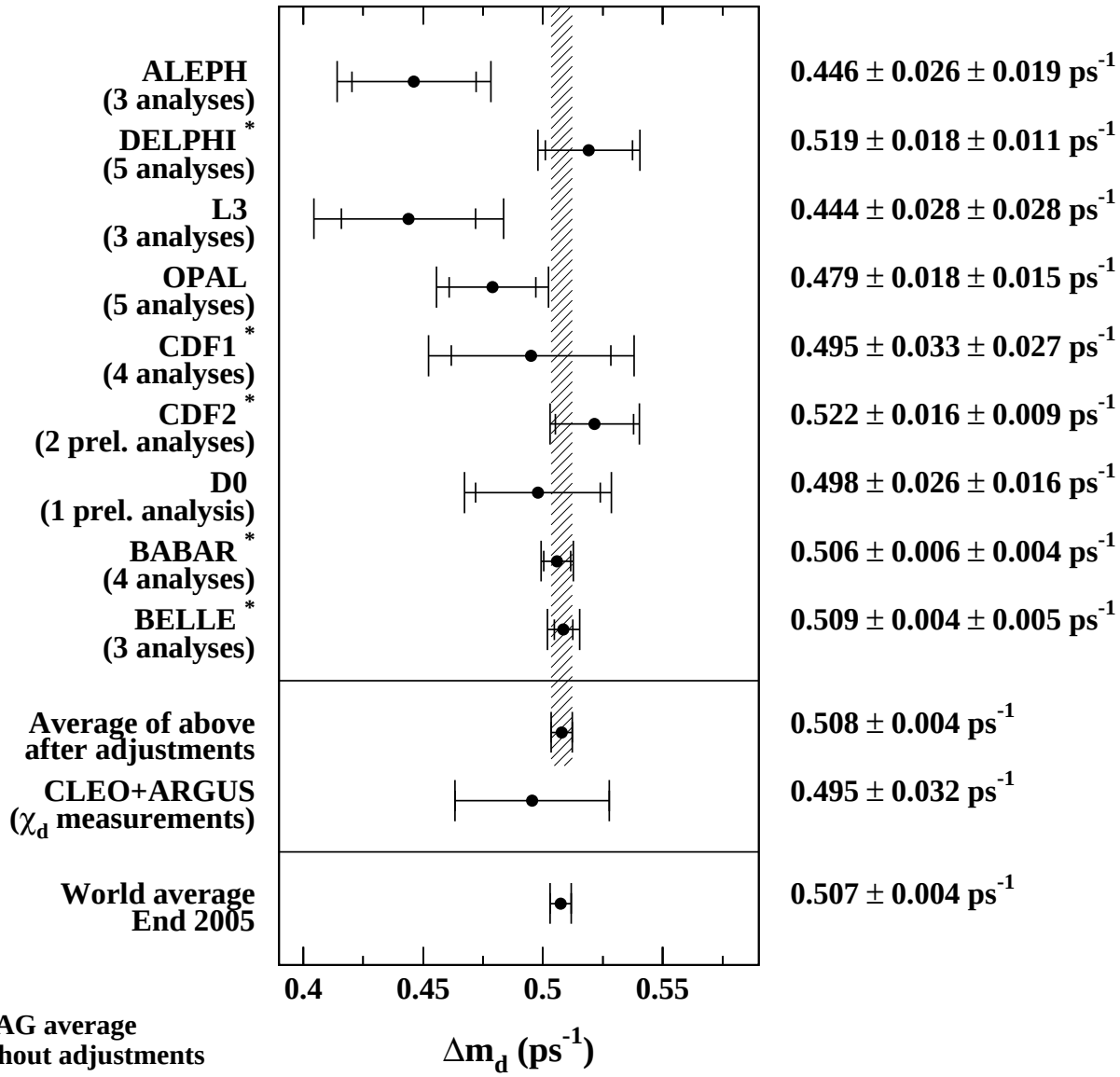

Figure 4: The B^0–$\overline{B}^0$ oscillation frequency Δm_d as measured by the different experiments. The averages quoted for ALEPH, L3 and OPAL are taken from the original publications, while the ones for DELPHI, CDF, *BABAR*, and Belle have been computed from the individual results listed in Table 13 without performing any adjustments. The time-integrated measurements of χ_d from the symmetric B factory experiments ARGUS and CLEO have been converted to a Δm_d value using $\tau(B^0) = 1.527 \pm 0.008$ ps. The two global averages have been obtained after adjustments of all the individual Δm_d results of Table 13 (see text).

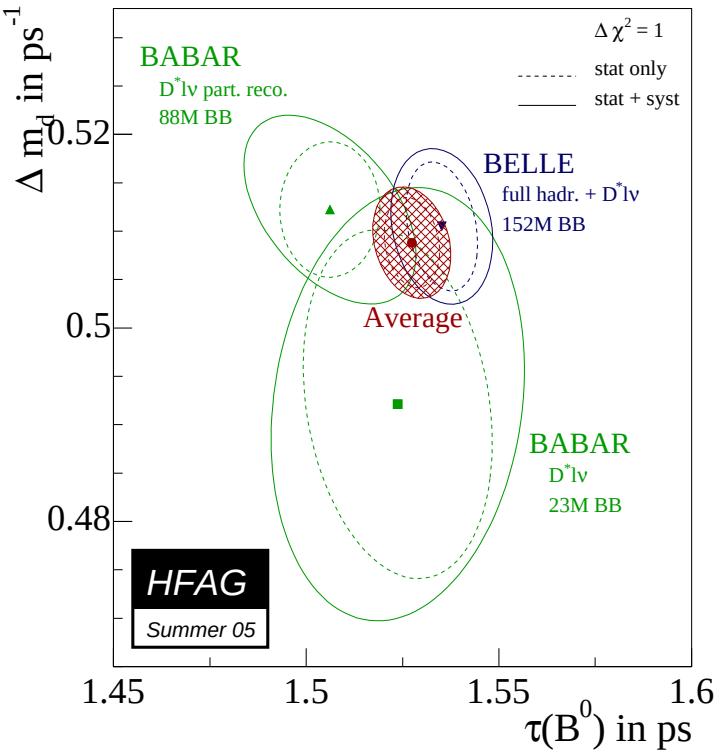

Figure 5: Simultaneous measurements of Δm_d and $\tau(B^0)$ [62, 64, 65], after adjustment to a common set of parameters (see text). Statistical and total uncertainties are represented as dashed and solid contours respectively. The average of the three measurements is indicated by a hatched ellipse.

Table 14: Simultaneous measurements of Δm_d and $\tau(B^0)$, and their average. The Belle analysis also measures $\tau(B^+)$ at the same time, but it is converted here into a two-dimensional measurement of Δm_d and $\tau(B^0)$, for an assumed value of $\tau(B^+)$. The first quoted error on the measurements is statistical and the second one systematic; in the case of adjusted measurements, the latter includes a contribution obtained from the variation of $\tau(B^+)$ or $\tau(B^+)/\tau(B^0)$ in the indicated range. Units are ps^{-1} for Δm_d and ps for lifetimes. The three different values of $\rho(\Delta m_d, \tau(B^0))$ correspond to the statistical, systematic and total correlation coefficients between the adjusted measurements of Δm_d and $\tau(B^0)$.

Exp. & Ref.	Measured Δm_d	Measured $\tau(B^0)$	Measured $\tau(B^+)$	Assumed $\tau(B^+)$
BABAR [62]	$0.492\pm0.018\pm0.013$	$1.523\pm0.024\pm0.022$	—	$(1.083\pm0.017)\tau(B^0)$
BABAR [64]	$0.511\pm0.007\ ^{+0.007}_{-0.006}$	$1.504\pm0.013\ ^{+0.018}_{-0.013}$	—	1.671 ± 0.018
Belle [65]	$0.511\pm0.005\pm0.006$	$1.534\pm0.008\pm0.010$	$1.635\pm0.011\pm0.011$	—
	Adjusted Δm_d	Adjusted $\tau(B^0)$	$\rho(\Delta m_d, B^0)$	
BABAR [62]	$0.492\pm0.018\pm0.013$	$1.524\pm0.025\pm0.022$	$-0.22\ +0.74\ +0.16$	$(1.076\pm0.008)\tau(B^0)$
BABAR [64]	$0.512\pm0.007\pm0.007$	$1.506\pm0.013\pm0.018$	$+0.01\ -0.85\ -0.48$	1.643 ± 0.010
Belle [65]	$0.510\pm0.007\pm0.005$	$1.535\pm0.009\pm0.009$	$-0.27\ -0.08\ -0.19$	1.643 ± 0.010
Average	$0.509\pm0.005\pm0.003$	$1.527\pm0.007\pm0.007$	$-0.19\ -0.29\ -0.23$	1.643 ± 0.010

fully and partially reconstructed $B^0 \to D^*\ell\nu$ decays respectively, extract simultaneously Δm_d and $\tau(B^0)$ while the latest Belle analysis [65], based on fully reconstructed hadronic B^0 decays and $B^0 \to D^*\ell\nu$ decays, extracts simultaneously Δm_d, $\tau(B^0)$ and $\tau(B^+)$. The measurements of Δm_d and $\tau(B^0)$ of these three analyses are displayed in Table 14 and in Fig. 5. Their two-dimensional average, taking into account all statistical and systematic correlations, and expressed at $\tau(B^+) = 1.643 \pm 0.010$ ps, is

$$\left.\begin{array}{r} \Delta m_d = 0.509 \pm 0.006\ \mathrm{ps}^{-1} \\ \tau(B^0) = 1.527 \pm 0.010\ \mathrm{ps} \end{array}\right\} \text{ with a total correlation of } -0.23. \tag{46}$$

3.3.2 B^0_s mixing parameters

CP violation parameter $|q/p|_s$

No measurement or experimental limit exists on $|q/p|_s$, except in the form of a relatively weak constraint from CDF on a combination of $|q/p|_d$ and $|q/p|_s$, $f'_d\,\chi_d(1-|q/p|^2_d) + f'_s\,\chi_s(1-|q/p|^2_s) = 0.006 \pm 0.017$ [93], using inclusive semileptonic decays of b hadrons. The result is compatible with no *CP* violation in the mixing, an assumption made in all results described below.

Mass difference Δm_s

The time-integrated measurements of $\overline{\chi}$ (see Sec. 3.1.2), when compared to our knowledge of χ_d and the b-hadron fractions, indicate that B^0_s mixing is large, with a value of χ_s close to its maximal possible value of 1/2. However, the time dependence of this mixing (called B^0_s

oscillations) has not been observed yet, mainly because the period of these oscillations turns out to be so small that it can't be resolved with the proper-time resolutions achieved so far.

The statistical significance $\mathcal{S}$ of a B_s^0 oscillation signal can be approximated as [120]

$$\mathcal{S} \approx \sqrt{\frac{N}{2}}\, f_{\rm sig}\,(1-2w)\,\exp\left(-\left(\Delta m_s \sigma_t\right)^2/2\right), \tag{47}$$

where N is the number of selected and tagged B_s^0 candidates, $f_{\rm sig}$ is the fraction of B_s^0 signal in the selected and tagged sample, w is the total mistag probability, and σ_t is the resolution on proper time. As can be seen, the quantity $\mathcal{S}$ decreases very quickly as Δm_s increases: this dependence is controlled by σ_t, which is therefore the most critical parameter for Δm_s analyses. The method widely used for B_s^0 oscillation searches consists of measuring a B_s^0 oscillation amplitude $\mathcal{A}$ at several different test values of Δm_s, using a maximum likelihood fit based on the functions of Eq. (37) where the cosine terms have been multiplied by $\mathcal{A}$. One expects $\mathcal{A} = 1$ at the true value of Δm_s and to $\mathcal{A} = 0$ at a test value of Δm_s (far) below the true value. To a good approximation, the statistical uncertainty on $\mathcal{A}$ is Gaussian and equal to $1/\mathcal{S}$ [120].

Figures 6 and 7 show the amplitude spectra obtained by ALEPH [121], CDF [122–124], D0 [125], DELPHI [77, 103, 126, 127], OPAL [128, 129] and SLD [130, 131].[6] In each analysis, a particular value of Δm_s can be excluded at 95% CL if $\mathcal{A} + 1.645\,\sigma_{\mathcal{A}} < 1$, where $\sigma_{\mathcal{A}}$ is the total uncertainty on $\mathcal{A}$. Because of the proper time resolution, the quantity $\sigma_{\mathcal{A}}(\Delta m_s)$ is an increasing function of Δm_s (see Eq. (47) which merely models $1/\sigma_{\mathcal{A}}(\Delta m_s)$ since all results are limited by the available statistics). Therefore, if the true value of Δm_s were infinitely large, one expects to be able to exclude all values of Δm_s up to $\Delta m_s^{\rm sens}$, where $\Delta m_s^{\rm sens}$, called here the sensitivity of the analysis, is defined by $1.645\,\sigma_{\mathcal{A}}(\Delta m_s^{\rm sens}) = 1$. At LEP times, the most sensitive analyses were the ones based on inclusive lepton samples, where reasonable statistics was available. Because of their better proper time resolution, the small data samples analyzed inclusively at SLD, as well as the few fully reconstructed B_s^0 decays at LEP, turned out to be also very useful to explore the high Δm_s region. New preliminary analyses are now available from CDF and DØ. These experiments presently are the only ones active in this area, and they are very soon going to reach sufficient statistics so that analyses of fully reconstructed hadronic modes can surpass the ones based on $D_s\ell\nu$X events.

These oscillation searches can easily be combined by averaging the measured amplitudes $\mathcal{A}$ at each test value of Δm_s. The combined amplitude spectra for the individual experiments are displayed in Fig. 8, and the world average spectrum is displayed in Fig. 9. The individual results have been adjusted to common physics inputs, and all known correlations have been accounted for; in the case of the inclusive analyses, the sensitivities (*i.e.* the statistical uncertainties on $\mathcal{A}$), which depend directly through Eq. (47) on the assumed fraction $f_{\rm sig} \sim f_s$ of B_s^0 mesons in an unbiased sample of weakly-decaying b hadrons, have also been rescaled to a common average of $f_s = 0.104 \pm 0.014$. The combined sensitivity for 95% CL exclusion of Δm_s values is found to be[7] 20.0 ps^{-1}. All values of Δm_s below 16.6 ps^{-1} are excluded at 95% CL, which we express

[6] An unpublished analysis from SLD [132], based on an inclusive reconstruction from a lepton and a topologically reconstructed D meson, is not included in the plots or combined results quoted in this section. However, nothing is known to be wrong about this analysis, and including it would increase the combined Δm_s limit of Eq. (48) by -0.0 ps^{-1} and the combined sensitivity by 0.1 ps^{-1}.

[7] As can be seen in Figs. 6, 7, and 8, as well as from the discontinuity of the dashed curve in Fig. 9, some experiments did not provide data above 20 ps^{-1}. The current combined sensitivity for 95% CL exclusion can now only be improved if new amplitude measurements are performed above 20 ps^{-1}.

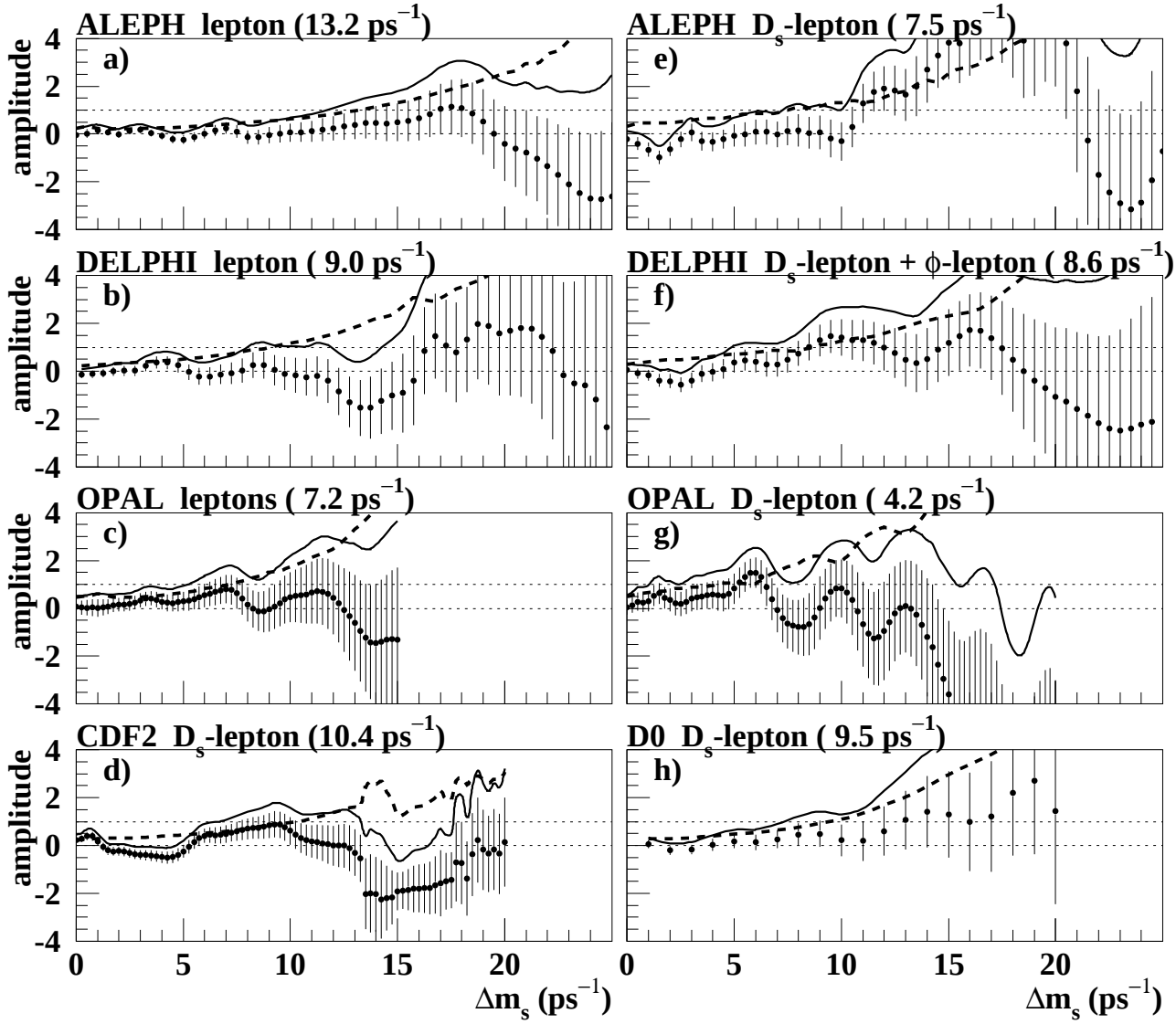

Figure 6: B_s^0-oscillation amplitude spectra, displayed separately for each B_s^0 oscillation analysis. The points and error bars represent the measurements of the amplitude $\mathcal{A}$ and their total uncertainties $\sigma_{\mathcal{A}}$, adjusted to a set of physics parameters common to all analyses (including $f_s = 0.104 \pm 0.014$). Values of Δm_s where the solid curve ($\mathcal{A} + 1.645\,\sigma_{\mathcal{A}}$) is below 1 are excluded at 95% CL. The dashed curve shows $1.645\,\sigma_{\mathcal{A}}$; the number in parenthesis indicates where this curve is equal to 1, and is a measure of the sensitivity of the analysis. a) ALEPH inclusive lepton [121], b) DELPHI inclusive lepton [127], c) OPAL inclusive lepton and dilepton [128], d) CDF2 D_s-ℓ (preliminary) [123], e) ALEPH D_s-ℓ [121], f) DELPHI D_s-ℓ [127] and ϕ-ℓ [126], g) OPAL D_s-ℓ [129], h) DØ D_s-μ (preliminary) [125]. Continuation on Fig. 7.

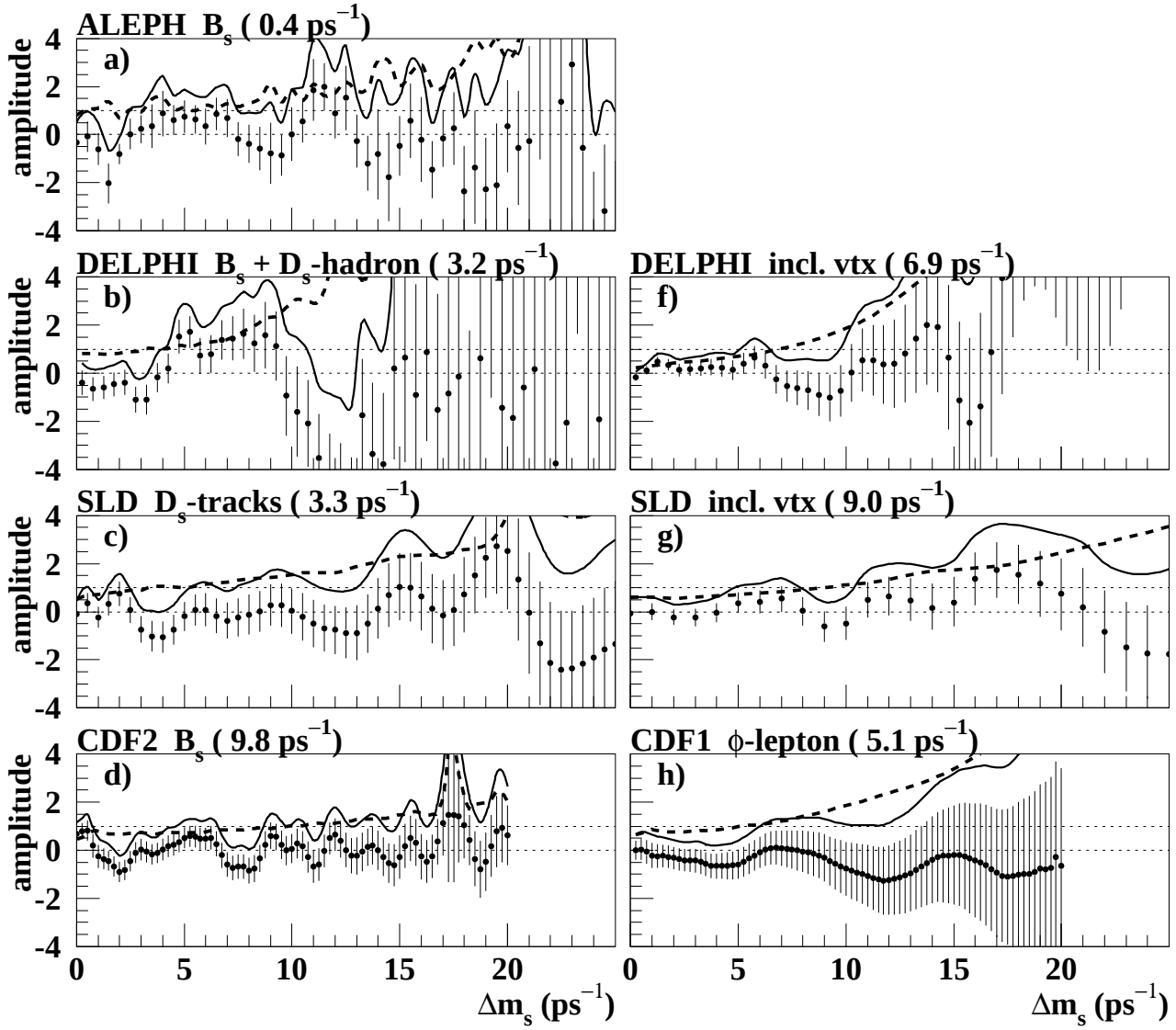

Figure 7: (continuation of Fig. 6) B_s^0-oscillation amplitude spectra, displayed separately for each B_s^0 oscillation analysis, in the same manner as in Fig. 6. a) ALEPH fully reconstructed B_s^0 [121], b) DELPHI fully reconstructed B_s^0 and D_s-hadron [77], c) SLD D_s +tracks [131], d) CDF2 fully reconstructed B_s^0 (preliminary) [124], f) DELPHI inclusive vertex [103], g) SLD inclusive vertex dipole [130], h) CDF1 ϕ-ℓ [122].

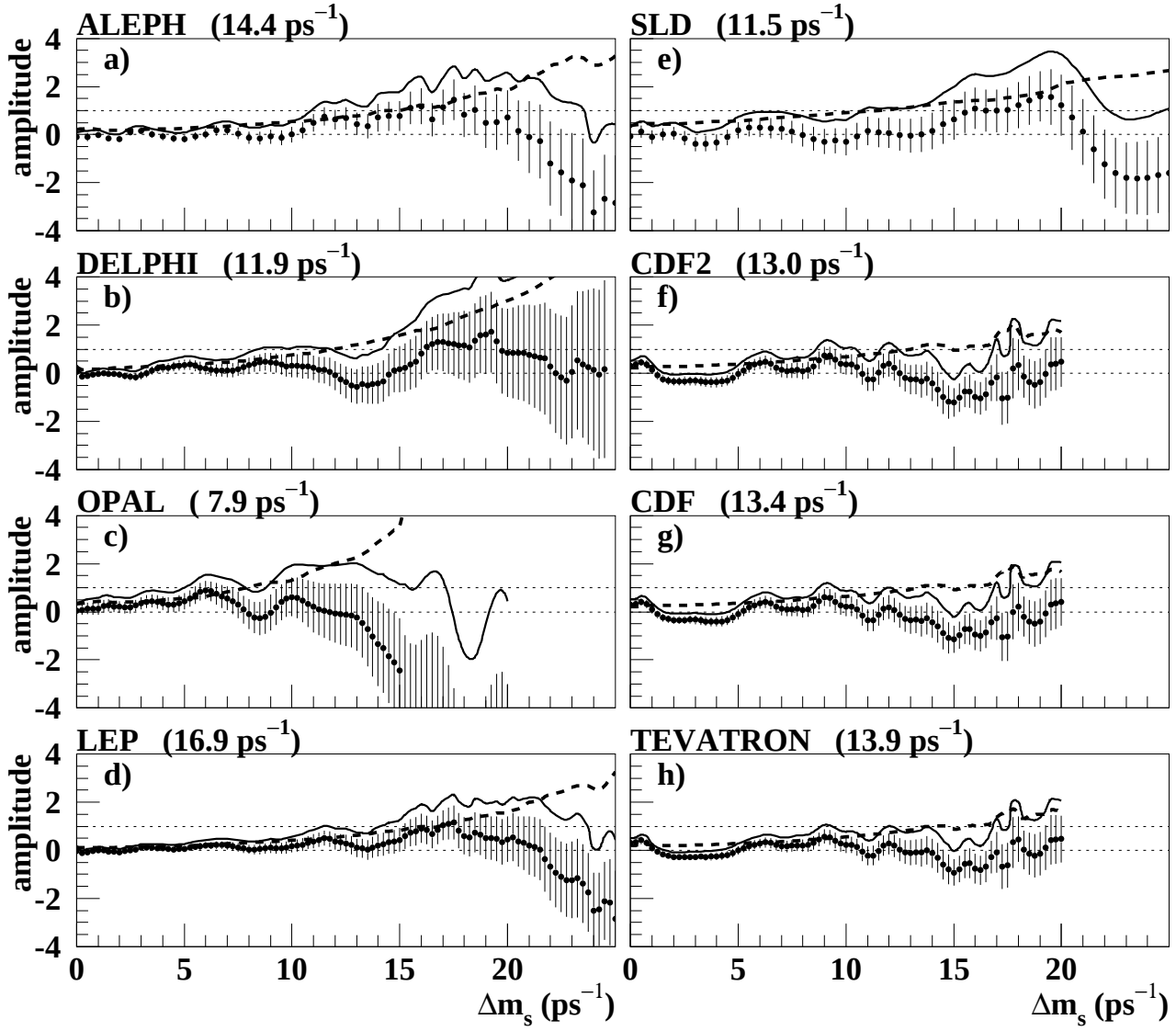

Figure 8: Combined B_s^0-oscillation amplitude spectra, displayed separately for each experiment and collider, in the same manner as in Fig. 6. a) ALEPH [121], b) DELPHI [77, 103, 126, 127], c) OPAL [128, 129], d) LEP [77, 103, 121, 126–129], e) SLD [130, 131], f) CDF2 [123, 124], g) CDF1 and CDF2 together [122–124], h) Tevatron [122–125]. See Fig. 7h) for CDF1 alone and Fig. 6h) for DØ alone.

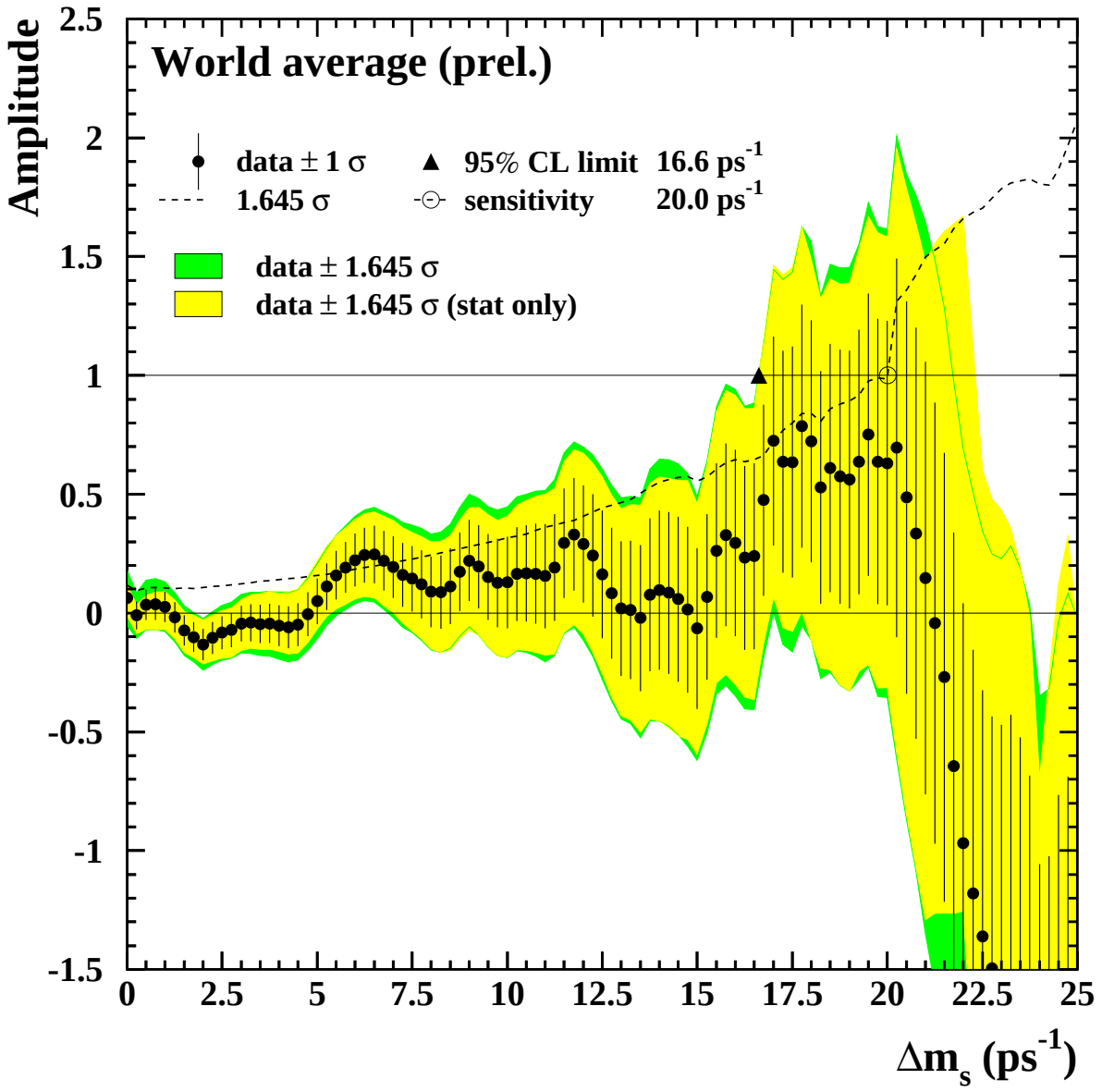

Figure 9: Combined measurements of the B_s^0 oscillation amplitude as a function of Δm_s, including all published results and preliminary results presented at the Summer and Fall 2005 conferences [77, 103, 121–131]. The measurements are dominated by statistical uncertainties. Neighboring points are statistically correlated.

as

$$\Delta m_s > 16.6 \text{ ps}^{-1} \text{ at } 95\% \text{ CL}\,. \tag{48}$$

The values between 16.6 ps^{-1} and 21.7 ps^{-1} cannot be excluded, because the data is compatible with a signal in this region. However, no deviation from $\mathcal{A} = 0$ is seen in Fig. 9 that would indicate the observation of a signal.

It should be noted that most Δm_s analyses assume no decay-width difference in the B_s^0 system. Due to the presence of the cosh terms in Eq. (37), a non-zero value of $\Delta\Gamma_s$ would reduce the oscillation amplitude with a small time-dependent factor that would be very difficult to distinguish from time resolution effects.

Convoluting the mean B_s^0 lifetime that will be obtained in Eq. (62), $1/\Gamma_s = 1.396^{+0.044}_{-0.046}$ ps, with the limit of Eq. (48) yields

$$x_s = \frac{\Delta m_s}{\Gamma_s} > 22.4 \text{ at } 95\% \text{ CL}\,. \tag{49}$$

Using $2y_s = \Delta\Gamma_s/\Gamma_s = +0.31^{+0.10}_{-0.11}$ (see Eq. (60)) and assuming no *CP* violation in the mixing, this corresponds to

$$\chi_s = \frac{x_s^2 + y_s^2}{2(x_s^2+1)} > 0.49904 \text{ at } 95\% \text{ CL}\,. \tag{50}$$

Decay width difference $\Delta\Gamma_s$

Definitions and an introduction to $\Delta\Gamma_s$ can also be found in Sec. 3.2.4. Neglecting *CP* violation, the mass eigenstates are also *CP* eigenstates, with the short-lived state being *CP*-even and the long-lived one being *CP*-odd. Information on $\Delta\Gamma_s$ can be obtained by studying the proper time distribution of untagged data samples enriched in B_s^0 mesons [68]. In the case of an inclusive B_s^0 selection [46] or a semileptonic B_s^0 decay selection [70,73,126], both the short- and long-lived components are present, and the proper time distribution is a superposition of two exponentials with decay constants $\Gamma_s \pm \Delta\Gamma_s/2$. In principle, this provides sensitivity to both Γ_s and $(\Delta\Gamma_s/\Gamma_s)^2$. Ignoring $\Delta\Gamma_s$ and fitting for a single exponential leads to an estimate of Γ_s with a relative bias proportional to $(\Delta\Gamma_s/\Gamma_s)^2$. An alternative approach, which is directly sensitive to first order in $\Delta\Gamma_s/\Gamma_s$, is to determine the lifetime of B_s^0 candidates decaying to *CP* eigenstates; measurements exist for $B_s^0 \to J/\psi\phi$ [40, 53, 58] and $B_s^0 \to D_s^{(*)+} D_s^{(*)-}$ [133], which are mostly *CP*-even states [134]. However, more recent time-dependent angular analyses of $B_s^0 \to J/\psi\phi$ allow the simultaneous extraction of $\Delta\Gamma_s/\Gamma_s$ and the *CP*-even and *CP*-odd amplitudes [57,135]. An estimate of $\Delta\Gamma_s/\Gamma_s$ has also been obtained directly from a measurement of the $B_s^0 \to D_s^{(*)+} D_s^{(*)-}$ branching ratio [133], under the assumption that these decays account for all the *CP*-even final states (however, no systematic uncertainty due to this assumption is given, so the average quoted below will not include this estimate).

Measurements quoting $\Delta\Gamma_s$ results are listed in Table 15. There is significant correlation between $\Delta\Gamma_s/\Gamma_s$ and $1/\Gamma_s$. In order to combine these measurements, the two-dimensional log-likelihood for each measurement in the $(1/\Gamma_s,\, \Delta\Gamma_s/\Gamma_s)$ plane is summed and the total normalized with respect to its minimum. The one-sigma contour (corresponding to 0.5 units of log-likelihood greater than the minimum) and 95% contour are found. Inputs as indicated in Table 15 were used in the combination, with the exception of the L3 [46] result since the likelihood for the results was not available, and the ALEPH [133] branching ratio result for the reason given above.

Table 15: Experimental constraints on $\Delta\Gamma_s/\Gamma_s$. The upper limits, which have been obtained by the working group, are quoted at the 95% CL.

Experiment	Method	$\Delta\Gamma_s/\Gamma_s$	Ref.
L3	lifetime of inclusive b-sample	< 0.67	[46]
DELPHI	$\overline{B}_s \to D_s^+ \ell^- \overline{\nu_\ell} X$, lifetime	< 0.46	[71]
ALEPH	$B_s^0 \to \phi\phi X$, $\mathcal{B}(B_s^0 \to D_s^{(*)+} D_s^{(*)-})$	$0.26^{+0.30}_{-0.15}$	[133]
ALEPH	$B_s^0 \to \phi\phi X$, lifetime	$0.45^{+0.80}_{-0.49}$	[133]
DELPHI	$\overline{B}_s \to D_s^+$ hadron, lifetime	< 0.69	[71]
CDF1	$B_s^0 \to J/\psi\phi$, lifetime	$0.33^{+0.45}_{-0.42}$	[40]
CDF2	$B_s^0 \to J/\psi\phi$, time-dependent angular analysis	$0.65^{+0.25}_{-0.33} \pm 0.01$	[135]
DØ	$B_s^0 \to J/\psi\phi$, time-dependent angular analysis	$0.24^{+0.28+0.03}_{-0.38-0.04}$	[57]

Results of the combination are shown as the one-sigma contour labelled "Direct" in both plots of Fig. 10. Transformation of variables from ($1/\Gamma_s$, $\Delta\Gamma_s/\Gamma_s$) space to other pairs of variables such as ($1/\Gamma_s$, $\Delta\Gamma_s$) and ($\tau_{\rm L} = 1/\Gamma_{\rm L}$, $\tau_{\rm H} = 1/\Gamma_{\rm H}$) are also made. The resulting one-sigma contour for the latter is shown in Fig. 10(b).

Numerical results of the combination of the described inputs of Table 15 are:

$$\Delta\Gamma_s/\Gamma_s \in [+0.01, +0.59] \text{ at } 95\% \text{ CL}\,, \tag{51}$$

$$\Delta\Gamma_s/\Gamma_s = +0.35^{+0.12}_{-0.16}\,, \tag{52}$$

$$\Delta\Gamma_s = +0.25^{+0.09}_{-0.11}\ \text{ps}^{-1}\,, \tag{53}$$

$$\overline{\tau}(B_s^0) = 1/\Gamma_s = 1.42^{+0.06}_{-0.07}\ \text{ps}\,, \tag{54}$$

$$\rho(\Delta\Gamma_s/\Gamma_s, 1/\Delta\Gamma_s) = +0.30\,, \tag{55}$$

$$1/\Gamma_{\rm L} = \tau_{\rm short} = 1.21^{+0.08}_{-0.09}\ \text{ps}\,, \tag{56}$$

$$1/\Gamma_{\rm H} = \tau_{\rm long} = 1.72 \pm 0.19\ \text{ps}\,. \tag{57}$$

Flavor-specific lifetime measurements are of an equal mix of *CP*-even and *CP*-odd states at time zero, and if a single exponential function is used in the likelihood lifetime fit of such a sample [68],

$$\tau(B_s^0)_{\rm fs} = \frac{1}{\Gamma_s} \frac{1 + \left(\frac{\Delta\Gamma_s}{2\Gamma_s}\right)^2}{1 - \left(\frac{\Delta\Gamma_s}{2\Gamma_s}\right)^2}. \tag{58}$$

Using the world average flavor-specific lifetime[8] of Sec. 3.2.4 the one-sigma blue bands shown in Fig. 10 are obtained. Higher-order corrections were checked to be negligible in the combination. When these flavor-specific measurements are combined with the measurements of Table 15, the

[8]The world average of all B_s^0 lifetime measurements using flavour-specific final states is 1.454 ± 0.040 ps; however, for the purpose of the $\Delta\Gamma_s$ extraction, we remove from this average one DELPHI analysis that is already included in the set of "direct measurements" and obtain 1.457 ± 0.042 ps, shown as the blue bands on the two plots of Fig. 10.

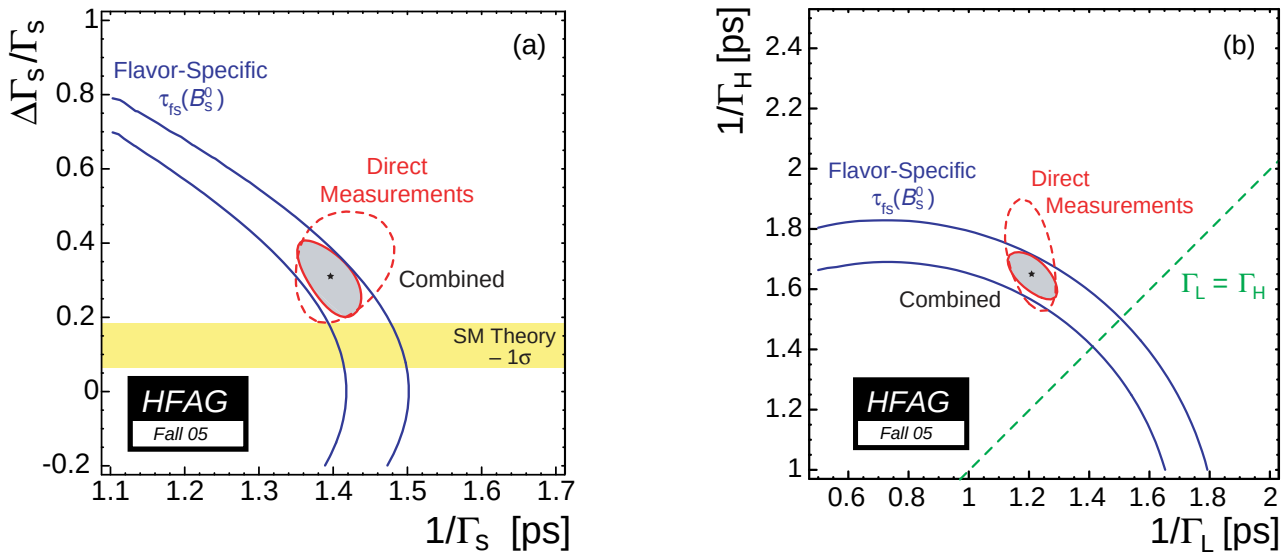

Figure 10: $\Delta\Gamma_s$ combination results with one-sigma contours ($\Delta \log \mathcal{L} = 0.5$) shown for (a) $\Delta\Gamma_s/\Gamma_s$ versus $\overline{\tau}(B_s^0) = 1/\Gamma_s$ and (b) $\tau_{\rm H} = 1/\Gamma_{\rm H}$ versus $\tau_{\rm L} = 1/\Gamma_{\rm L}$. Contours labelled "Direct" are the result of the combination of most measurements of Table 15, the blue bands are the one-sigma contours due to the world average of flavor-specific measurements, and the shaded region the combination of both. In (b), the diagonal dashed line indicates $\Gamma_{\rm L} = \Gamma_{\rm H}$, i.e., where $\Delta\Gamma_s = 0$.

shaded regions of Fig. 10 are obtained, with numerical results:

$$\Delta\Gamma_s/\Gamma_s \in [+0.01, +0.57] \text{ at } 95\% \text{ CL}\,, \tag{59}$$
$$\Delta\Gamma_s/\Gamma_s = +0.31^{+0.10}_{-0.11}\,, \tag{60}$$
$$\Delta\Gamma_s = +0.22 \pm 0.08 \text{ ps}^{-1}\,, \tag{61}$$
$$\overline{\tau}(B_s^0) = 1/\Gamma_s = 1.396^{+0.044}_{-0.046} \text{ ps}\,, \tag{62}$$
$$\rho(\Delta\Gamma_s/\Gamma_s, 1/\Delta\Gamma_s) = -0.74\,, \tag{63}$$
$$1/\Gamma_{\rm L} = \tau_{\rm short} = 1.21 \pm 0.08 \text{ ps}\,, \tag{64}$$
$$1/\Gamma_{\rm H} = \tau_{\rm long} = 1.65^{+0.07}_{-0.08} \text{ ps}\,. \tag{65}$$

These results can be compared with the theoretical prediction of $\Delta\Gamma_s/\Gamma_s = 0.12 \pm 0.05$ [67].

The *average* B_s^0 and B^0 lifetimes are predicted to be equal within 1% [29, 88] and in the past, an additional constraint applied by setting $\Gamma_s = \Gamma_d$, i.e., $1/\Gamma_s = \tau(B^0)$, where $\tau(B^0) = 1.527 \pm 0.008$ ps is the world average of experimental results, including a relative 1% theoretical uncertainty added in quadrature with the indicated experimental error. However, with the increased inconsistency of the measured values of $1/\Gamma_s = \overline{\tau}(B_s^0)$ and $\tau(B^0)$ at the level of $2.9\,\sigma$, this constraint is no longer applied.

4 Measurements related to Unitarity Triangle angles

The charge of the "$CP(t)$ and Unitarity Triangle angles" group is to provide averages of measurements related (mostly) to the angles of the Unitarity Triangle (UT). To date, most of the measurements that can be used to obtain model-independent information on the UT angles come from time-dependent CP asymmetry analyses. In cases where considerable theoretical input is required to extract the fundamental quantities, no attempt is made to do so at this stage. However, straightforward interpretations of the averages are given, where possible.

In Sec. 4.1 a brief introduction to the relevant phenomenology is given. In Sec. 4.2 an attempt is made to clarify the various different notations in use. In Sec. 4.3 the common inputs to which experimental results are rescaled in the averaging procedure are listed. We also briefly introduce the treatment of experimental errors. In the remainder of this section, the experimental results and their averages are given, divided into subsections based on the underlying quark-level decays.

4.1 Introduction

The Standard Model Cabibbo-Kobayashi-Maskawa (CKM) quark mixing matrix V must be unitary. A 3×3 unitary matrix has four free parameters,[9] and these are conventionally written by the product of three (complex) rotation matrices [136], where the rotations are characterized by the Euler angles θ_{12}, θ_{13} and θ_{23}, which are the mixing angles between the generations, and one overall phase δ,

$$V = \begin{pmatrix} V_{ud} & V_{us} & V_{ub} \\ V_{cd} & V_{cs} & V_{cb} \\ V_{td} & V_{ts} & V_{tb} \end{pmatrix} = \begin{pmatrix} c_{12}c_{13} & s_{12}c_{13} & s_{13}e^{-i\delta} \\ -s_{12}c_{23} - c_{12}s_{23}s_{13}e^{i\delta} & c_{12}c_{23} - s_{12}s_{23}s_{13}e^{i\delta} & s_{23}c_{13} \\ s_{12}s_{23} - c_{12}c_{23}s_{13}e^{i\delta} & -c_{12}s_{23} - s_{12}c_{23}s_{13}e^{i\delta} & c_{23}c_{13} \end{pmatrix} \quad (66)$$

where $c_{ij} = \cos\theta_{ij}$, $s_{ij} = \sin\theta_{ij}$ for $i < j = 1, 2, 3$.

Following the observation of a hierarchy between the different matrix elements, the Wolfenstein parameterization [137] is an expansion of V in terms of the four real parameters λ (the expansion parameter), A, ρ and η. Defining to all orders in λ [138]

$$\begin{aligned} s_{12} &\equiv \lambda, \\ s_{23} &\equiv A\lambda^2, \\ s_{13}e^{-i\delta} &\equiv A\lambda^3(\rho - i\eta), \end{aligned} \quad (67)$$

and inserting these into the representation of Eq. (66), unitarity of the CKM matrix is achieved to all orders. A Taylor expansion of V leads to the familiar approximation

$$V = \begin{pmatrix} 1 - \frac{1}{2}\lambda^2 & \lambda & A\lambda^3(\rho - i\eta) \\ -\lambda & 1 - \frac{1}{2}\lambda^2 & A\lambda^2 \\ A\lambda^3(1 - \rho - i\eta) & -A\lambda^2 & 1 \end{pmatrix} + \mathcal{O}\left(\lambda^4\right), \quad (68)$$

or, at order λ^5

$$V = \begin{pmatrix} 1 - \frac{1}{2}\lambda^2 - \frac{1}{8}\lambda^4 & \lambda & A\lambda^3(\rho - i\eta) \\ -\lambda + \frac{1}{2}A^2\lambda^5\left[1 - 2(\rho + i\eta)\right] & 1 - \frac{1}{2}\lambda^2 - \frac{1}{8}\lambda^4(1 + 4A^2) & A\lambda^2 \\ A\lambda^3\left[1 - (1 - \frac{1}{2}\lambda^2)(\rho + i\eta)\right] & -A\lambda^2 + \frac{1}{2}A\lambda^4\left[1 - 2(\rho + i\eta)\right] & 1 - \frac{1}{2}A^2\lambda^4 \end{pmatrix} + \mathcal{O}\left(\lambda^6\right). \quad (69)$$

[9] In the general case there are nine free parameters, but five of these are absorbed into unobservable quark phases.

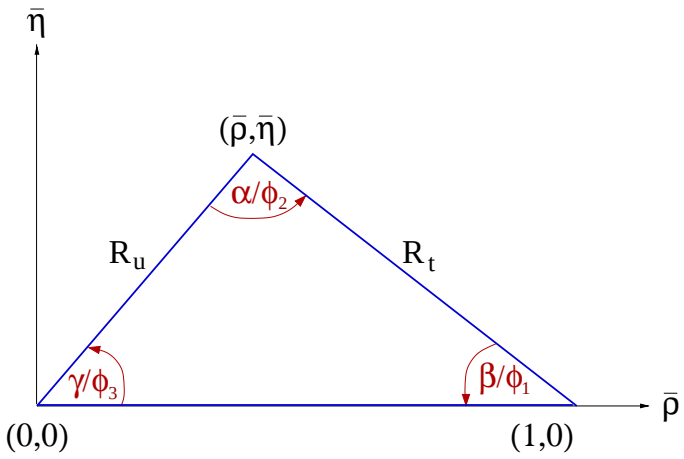

Figure 11: The Unitarity Triangle.

The non-zero imaginary part of the CKM matrix, which is the origin of *CP* violation in the Standard Model, is encapsulated in a non-zero value of η.

The unitarity relation $V^\dagger V = 1$ results in a total of nine expressions, that can be written as $\sum_{i=u,c,t} V_{ij}^* V_{ik} = \delta_{jk}$, where δ_{jk} is the Kronecker symbol. Of the off-diagonal expressions ($j \neq k$), three can be trivially transformed into the other three (under $j \leftrightarrow k$), leaving six relations, in which three complex numbers sum to zero, which therefore can be expressed as triangles in the complex plane.

One of these,

$$V_{ud}V_{ub}^* + V_{cd}V_{cb}^* + V_{td}V_{tb}^* = 0, \tag{70}$$

is specifically related to B decays. The three terms in Eq. (70) are of the same order ($\mathcal{O}(\lambda^3)$), and this relation is commonly known as the Unitarity Triangle. For presentational purposes, it is convenient to rescale the triangle by $(V_{cd}V_{cb}^*)^{-1}$, as shown in Fig. 11.

Two popular naming conventions for the UT angles exist in the literature:

$$\alpha \equiv \phi_2 = \arg\left[-\frac{V_{td}V_{tb}^*}{V_{ud}V_{ub}^*}\right], \quad \beta \equiv \phi_1 = \arg\left[-\frac{V_{cd}V_{cb}^*}{V_{td}V_{tb}^*}\right], \quad \gamma \equiv \phi_3 = \arg\left[-\frac{V_{ud}V_{ub}^*}{V_{cd}V_{cb}^*}\right].$$

In this document the (α, β, γ) set is used.

The apex of the Unitarity Triangle is written in terms of the parameters $(\overline{\rho}, \overline{\eta})$ [138]

$$\overline{\rho} + i\overline{\eta} \;\equiv\; -\frac{V_{ud}V_{ub}^*}{V_{cd}V_{cb}^*} = (\rho + i\eta)(1 - \frac{1}{2}\lambda^2) + \mathcal{O}(\lambda^4). \tag{71}$$

The exact (to all orders) relation between (ρ, η) and $(\overline{\rho}, \overline{\eta})$ is

$$\rho + i\eta \;=\; \frac{\sqrt{1 - A^2\lambda^4}(\overline{\rho} + i\overline{\eta})}{\sqrt{1 - \lambda^2}\,[1 - A^2\lambda^4(\overline{\rho} + i\overline{\eta})]}. \tag{72}$$

The sides R_u and R_t of the Unitarity Triangle (the third side being normalized to unity) are

given by

$$R_u = \left|\frac{V_{ud}V_{ub}^*}{V_{cd}V_{cb}^*}\right| = \sqrt{\overline{\rho}^2+\overline{\eta}^2}, \quad (73)$$

$$R_t = \left|\frac{V_{td}V_{tb}^*}{V_{cd}V_{cb}^*}\right| = \sqrt{(1-\overline{\rho})^2+\overline{\eta}^2}. \quad (74)$$

4.2 Notations

Several different notations for *CP* violation parameters are commonly used. This section reviews those found in the experimental literature, in the hope of reducing the potential for confusion, and to define the frame that is used for the averages.

In some cases, when B mesons decay into multibody final states via broad resonances (ρ, K^*, *etc.*), the experimental analyses ignore the effects of interference between the overlapping structures. This is referred to as the quasi-two-body (Q2B) approximation in the following.

4.2.1 *CP* asymmetries

The *CP* asymmetry is defined as the difference between the rate involving a b quark and that involving a $\overline{b}$ quark, divided by the sum. For example, the partial rate (or charge) asymmetry for a charged B decay would be given as

$$\mathcal{A}_f \equiv \frac{\Gamma(B^-\to f)-\Gamma(B^+\to \overline{f})}{\Gamma(B^-\to f)+\Gamma(B^+\to \overline{f})}. \quad (75)$$

4.2.2 Time-dependent *CP* asymmetries in decays to *CP* eigenstates

If the amplitudes for B^0 and $\overline{B}^0$ to decay to a final state f, which is a *CP* eigenstate with eigenvalue η_f, are given by A_f and $\overline{A}_f$, respectively, then the decay distributions for neutral B mesons, with known flavour at time $\Delta t = 0$, are given by

$$\Gamma_{\overline{B}^0\to f}(\Delta t) = \frac{e^{-|\Delta t|/\tau(B^0)}}{4\tau(B^0)}\left[1+\frac{2\,\mathrm{Im}(\lambda_f)}{1+|\lambda_f|^2}\sin(\Delta m\Delta t)-\frac{1-|\lambda_f|^2}{1+|\lambda_f|^2}\cos(\Delta m\Delta t)\right], \quad (76)$$

$$\Gamma_{B^0\to f}(\Delta t) = \frac{e^{-|\Delta t|/\tau(B^0)}}{4\tau(B^0)}\left[1-\frac{2\,\mathrm{Im}(\lambda_f)}{1+|\lambda_f|^2}\sin(\Delta m\Delta t)+\frac{1-|\lambda_f|^2}{1+|\lambda_f|^2}\cos(\Delta m\Delta t)\right]. \quad (77)$$

Here $\lambda_f = \frac{q}{p}\frac{\overline{A}_f}{A_f}$ contains terms related to B^0–$\overline{B}^0$ mixing and to the decay amplitude (the eigenstates of the effective Hamiltonian in the $B^0\overline{B}^0$ system are $|B_\pm\rangle = p\,|B^0\rangle \pm q\,|\overline{B}^0\rangle$). This formulation assumes *CPT* invariance, and neglects possible lifetime differences (between the eigenstates of the effective Hamiltonian; see Section 3.3 where the mass difference Δm is also defined) in the neutral B meson system. The time-dependent *CP* asymmetry, again defined as the difference between the rate involving a b quark and that involving a $\overline{b}$ quark, is then given by

$$\mathcal{A}_f(\Delta t) \equiv \frac{\Gamma_{\overline{B}^0\to f}(\Delta t)-\Gamma_{B^0\to f}(\Delta t)}{\Gamma_{\overline{B}^0\to f}(\Delta t)+\Gamma_{B^0\to f}(\Delta t)} = \frac{2\,\mathrm{Im}(\lambda_f)}{1+|\lambda_f|^2}\sin(\Delta m\Delta t)-\frac{1-|\lambda_f|^2}{1+|\lambda_f|^2}\cos(\Delta m\Delta t). \quad (78)$$

While the coefficient of the $\sin(\Delta m \Delta t)$ term in Eq. (78) is everywhere[10] denoted S_f:

$$S_f \equiv \frac{2\,\mathrm{Im}(\lambda_f)}{1+|\lambda_f|^2}, \tag{79}$$

different notations are in use for the coefficient of the $\cos(\Delta m \Delta t)$ term:

$$C_f \equiv -A_f \equiv \frac{1-|\lambda_f|^2}{1+|\lambda_f|^2}. \tag{80}$$

The C notation is used by the *BABAR* collaboration (see *e.g.* [148]), and also in this document. The A notation is used by the Belle collaboration (see *e.g.* [65]).

Neglecting effects due to *CP* violation in mixing (by taking $|q/p| = 1$), if the decay amplitude contains terms with a single weak (*i.e.*, *CP* violating) phase then $|\lambda_f| = 1$ and one finds $S_f = -\eta_f \sin(\phi_{\rm mix} + \phi_{\rm dec})$, $C_f = 0$, where $\phi_{\rm mix} = \arg(q/p)$ and $\phi_{\rm dec} = \arg(\overline{A}_f/A_f)$. Note that $\phi_{\rm mix} \approx 2\beta$ in the Standard Model (in the usual phase convention). If amplitudes with different weak phases contribute to the decay, no clean interpretation of S_f is possible. If the decay amplitudes have in addition different *CP* conserving strong phases, then $|\lambda_f| \neq 1$ and no clean interpretation is possible. The coefficient of the cosine term becomes non-zero, indicating direct *CP* violation. The sign of A_f as defined above is consistent with that of $\mathcal{A}_f$ in Eq. (75).

Frequently, we are interested in combining measurements governed by similar or identical short-distance physics, but with different final states (*e.g.*, $B^0 \to J/\psi\, K^0_S$ and $B^0 \to J/\psi\, K^0_L$). In this case, we remove the dependence on the *CP* eigenvalue of the final state by quoting $-\eta S_f$. In cases where the final state is not a *CP* eigenstate but has an effective *CP* (see below), the reported $-\eta S$ is corrected by the effective *CP*.

4.2.3 Time-dependent *CP* asymmetries in decays to vector-vector final states

Consider B decays to states consisting of two vector particles, such as $J/\psi\, K^{*0}(\to K^0_S\pi^0)$, $D^{*+}D^{*-}$ and $\rho^+\rho^-$, which are eigenstates of charge conjugation but not of parity.[11] In fact, for such a system, there are three possible final states; in the helicity basis these can be written h_{-1}, h_0, h_{+1}. The h_0 state is an eigenstate of parity, and hence of *CP*; however, *CP* transforms $h_{+1} \leftrightarrow h_{-1}$ (up to an unobservable phase). In the transversity basis, these states are transformed into $h_\parallel = (h_{+1}+h_{-1})/2$ and $h_\perp = (h_{+1}-h_{-1})/2$. In this basis all three states are *CP* eigenstates, and $h_\perp$ has the opposite *CP* to the others.

The amplitudes to these states are usually given by $A_{0,\perp,\parallel}$ (here we use a normalization such that $|A_0|^2 + |A_\perp|^2 + |A_\parallel|^2 = 1$). Then the effective *CP* of the vector-vector state is known if $|A_\perp|^2$ is measured. An alternative strategy is to measure just the longitudinally polarized component, $|A_0|^2$ (sometimes denoted by $f_{\rm long}$), which allows a limit to be set on the effective *CP* since $|A_\perp|^2 \leq |A_\perp|^2 + |A_\parallel|^2 = 1 - |A_0|^2$. The most complete treatment for neutral B decays to vector-vector final states is time-dependent angular analysis (also known as time-dependent transversity analysis). In such an analysis, the interference between the *CP* even and *CP* odd states provides additional sensitivity to the weak and strong phases involved.

[10] Occasionally one also finds Eq. (78) written as $\mathcal{A}_f\,(\Delta t) = \mathcal{A}_f^{\rm mix}\sin(\Delta m\Delta t) + \mathcal{A}_f^{\rm dir}\cos(\Delta m\Delta t)$, or similar.

[11] This is not true of all vector-vector final states, *e.g.*, $D^{*\pm}\rho^\mp$ is clearly not an eigenstate of charge conjugation.

4.2.4 Time-dependent asymmetries in decays to self-conjugate multiparticle final states

Amplitudes for neutral B decays into self-conjugate multiparticle final states such as $\pi^+\pi^-\pi^0$, $J/\psi\pi^+\pi^-$ or $D\pi^0$ with $D \to K^0_S\pi^+\pi^-$ may be written in terms of CP-even and CP-odd amplitudes. As above, the interference between these terms provides additional sensitivity to the weak and strong phases involved in the decay, and the time-dependence depends on both the sine and cosine of the weak phase difference. In order to perform unbinned maximum likelihood fits, and thereby extract as much information as possible from the distributions, it is necessary to select a model for the multiparticle decay, and therefore the results acquire some model dependence (binned, model independent methods are also possible, though are not as statistically powerful). The number of observables depends on the final state (and on the model used); the key feature is that as long as there are regions where both CP-even and CP-odd amplitudes contribute, the interference terms will be sensitive to the cosine of the weak phase difference. Therefore, these measurements allow distinction between multiple solutions for, *e.g.*, the four values of β from the measurement of $\sin(2\beta)$.

4.2.5 Time-dependent *CP* asymmetries in decays to non-*CP* eigenstates

Consider a non-CP eigenstate f, and its conjugate $\overline{f}$. For neutral B decays to these final states, there are four amplitudes to consider: those for B^0 to decay to f and $\overline{f}$ (A_f and $A_{\overline{f}}$, respectively), and the equivalents for $\overline{B}^0$ ($\overline{A}_f$ and $\overline{A}_{\overline{f}}$). If CP is conserved in the decay, then $A_f = \overline{A}_{\overline{f}}$ and $A_{\overline{f}} = \overline{A}_f$.

The time-dependent decay distributions can be written in many different ways. Here, we follow Sec. 4.2.2 and define $\lambda_f = \frac{q}{p}\frac{\overline{A}_f}{A_f}$ and $\lambda_{\overline{f}} = \frac{q}{p}\frac{\overline{A}_{\overline{f}}}{A_{\overline{f}}}$. The time-dependent CP asymmetries then follow Eq. (78):

$$\mathcal{A}_f(\Delta t) \equiv \frac{\Gamma_{\overline{B}^0\to f}(\Delta t) - \Gamma_{B^0\to f}(\Delta t)}{\Gamma_{\overline{B}^0\to f}(\Delta t) + \Gamma_{B^0\to f}(\Delta t)} = S_f \sin(\Delta m\Delta t) - C_f \cos(\Delta m\Delta t), \quad (81)$$

$$\mathcal{A}_{\overline{f}}(\Delta t) \equiv \frac{\Gamma_{\overline{B}^0\to \overline{f}}(\Delta t) - \Gamma_{B^0\to \overline{f}}(\Delta t)}{\Gamma_{\overline{B}^0\to \overline{f}}(\Delta t) + \Gamma_{B^0\to \overline{f}}(\Delta t)} = S_{\overline{f}} \sin(\Delta m\Delta t) - C_{\overline{f}} \cos(\Delta m\Delta t), \quad (82)$$

with the definitions of the parameters C_f, S_f, $C_{\overline{f}}$ and $S_{\overline{f}}$, following Eqs. (79) and (80).

The time-dependent decay rates are given by

$$\Gamma_{\overline{B}^0\to f}(\Delta t) = \frac{e^{-|\Delta t|/\tau(B^0)}}{8\tau(B^0)}(1 + \langle\mathcal{A}_{f\overline{f}}\rangle)\left\{1 + S_f \sin(\Delta m\Delta t) - C_f \cos(\Delta m\Delta t)\right\}, \quad (83)$$

$$\Gamma_{B^0\to f}(\Delta t) = \frac{e^{-|\Delta t|/\tau(B^0)}}{8\tau(B^0)}(1 + \langle\mathcal{A}_{f\overline{f}}\rangle)\left\{1 - S_f \sin(\Delta m\Delta t) + C_f \cos(\Delta m\Delta t)\right\}, \quad (84)$$

$$\Gamma_{\overline{B}^0\to \overline{f}}(\Delta t) = \frac{e^{-|\Delta t|/\tau(B^0)}}{8\tau(B^0)}(1 - \langle\mathcal{A}_{f\overline{f}}\rangle)\left\{1 + S_{\overline{f}} \sin(\Delta m\Delta t) - C_{\overline{f}} \cos(\Delta m\Delta t)\right\}, \quad (85)$$

$$\Gamma_{B^0\to \overline{f}}(\Delta t) = \frac{e^{-|\Delta t|/\tau(B^0)}}{8\tau(B^0)}(1 - \langle\mathcal{A}_{f\overline{f}}\rangle)\left\{1 - S_{\overline{f}} \sin(\Delta m\Delta t) + C_{\overline{f}} \cos(\Delta m\Delta t)\right\}, \quad (86)$$

where the time-independent parameter $\langle\mathcal{A}_{f\overline{f}}\rangle$ represents an overall asymmetry in the production

of the f and $\overline{f}$ final states,[12]

$$\langle \mathcal{A}_{f\overline{f}} \rangle = \frac{\left(|A_f|^2 + \left|\overline{A}_f\right|^2\right) - \left(\left|A_{\overline{f}}\right|^2 + \left|\overline{A}_{\overline{f}}\right|^2\right)}{\left(|A_f|^2 + \left|\overline{A}_f\right|^2\right) + \left(\left|A_{\overline{f}}\right|^2 + \left|\overline{A}_{\overline{f}}\right|^2\right)}. \tag{87}$$

Assuming $|q/p| = 1$, the parameters C_f and $C_{\overline{f}}$ can also be written in terms of the decay amplitudes as follows:

$$C_f = \frac{|A_f|^2 - \left|\overline{A}_f\right|^2}{|A_f|^2 + \left|\overline{A}_f\right|^2} \quad \text{and} \quad C_{\overline{f}} = \frac{\left|A_{\overline{f}}\right|^2 - \left|\overline{A}_{\overline{f}}\right|^2}{\left|A_{\overline{f}}\right|^2 + \left|\overline{A}_{\overline{f}}\right|^2}, \tag{88}$$

giving asymmetries in the decay amplitudes of B^0 and $\overline{B}^0$ to the final states f and $\overline{f}$ respectively. In this notation, the direct CP invariance conditions are $\langle \mathcal{A}_{f\overline{f}} \rangle = 0$ and $C_f = -C_{\overline{f}}$. Note that C_f and $C_{\overline{f}}$ are typically non-zero; *e.g.*, for a flavour-specific final state, $\overline{A}_f = A_{\overline{f}} = 0$ ($A_f = \overline{A}_{\overline{f}} = 0$), they take the values $C_f = -C_{\overline{f}} = 1$ ($C_f = -C_{\overline{f}} = -1$).

The coefficients of the sine terms contain information about the weak phase. In the case that each decay amplitude contains only a single weak phase (*i.e.*, no direct CP violation), these terms can be written

$$S_f = \frac{-2\,|A_f|\,\left|\overline{A}_f\right| \sin(\phi_{\rm mix} + \phi_{\rm dec} - \delta_f)}{|A_f|^2 + \left|\overline{A}_f\right|^2} \quad \text{and} \quad S_{\overline{f}} = \frac{-2\,\left|A_{\overline{f}}\right|\,\left|\overline{A}_{\overline{f}}\right| \sin(\phi_{\rm mix} + \phi_{\rm dec} + \delta_f)}{\left|A_{\overline{f}}\right|^2 + \left|\overline{A}_{\overline{f}}\right|^2}, \tag{89}$$

where δ_f is the strong phase difference between the decay amplitudes. If there is no CP violation, the condition $S_f = -S_{\overline{f}}$ holds. If decay amplitudes with different weak and strong phases contribute, no clean interpretation of S_f and $S_{\overline{f}}$ is possible.

Since two of the CP invariance conditions are $C_f = -C_{\overline{f}}$ and $S_f = -S_{\overline{f}}$, there is motivation for a rotation of the parameters:

$$S_{f\overline{f}} = \frac{S_f + S_{\overline{f}}}{2}, \quad \Delta S_{f\overline{f}} = \frac{S_f - S_{\overline{f}}}{2}, \quad C_{f\overline{f}} = \frac{C_f + C_{\overline{f}}}{2}, \quad \Delta C_{f\overline{f}} = \frac{C_f - C_{\overline{f}}}{2}. \tag{90}$$

With these parameters, the CP invariance conditions become $S_{f\overline{f}} = 0$ and $C_{f\overline{f}} = 0$. The parameter $\Delta C_{f\overline{f}}$ gives a measure of the "flavour-specificity" of the decay: $\Delta C_{f\overline{f}} = \pm 1$ corresponds to a completely flavour-specific decay, in which no interference between decays with and without mixing can occur, while $\Delta C_{f\overline{f}} = 0$ results in maximum sensitivity to mixing-induced CP violation. The parameter $\Delta S_{f\overline{f}}$ is related to the strong phase difference between the decay amplitudes of B^0 to f and to $\overline{f}$. We note that the observables of Eq. (90) exhibit experimental correlations (typically of $\sim 20\%$, depending on the tagging purity, and other effects) between $S_{f\overline{f}}$ and $\Delta S_{f\overline{f}}$, and between $C_{f\overline{f}}$ and $\Delta C_{f\overline{f}}$. On the other hand, the final state specific observables of Eq. (81) tend to have low correlations.

Alternatively, if we recall that the CP invariance conditions at the decay amplitude level are $A_f = \overline{A}_{\overline{f}}$ and $A_{\overline{f}} = \overline{A}_f$, we are led to consider the parameters [153]

$$\mathcal{A}_{f\overline{f}} = \frac{\left|\overline{A}_{\overline{f}}\right|^2 - |A_f|^2}{\left|\overline{A}_{\overline{f}}\right|^2 + |A_f|^2} \quad \text{and} \quad \mathcal{A}_{\overline{f}f} = \frac{\left|\overline{A}_f\right|^2 - \left|A_{\overline{f}}\right|^2}{\left|\overline{A}_f\right|^2 + \left|A_{\overline{f}}\right|^2}. \tag{91}$$

[12] This parameter is often denoted $\mathcal{A}_f$ (or $\mathcal{A}_{CP}$), but here we avoid this notation to prevent confusion with the time-dependent CP asymmetry.

These are sometimes considered more physically intuitive parameters since they characterize direct *CP* violation in decays with particular topologies. For example, in the case of $B^0 \to \rho^\pm\pi^\mp$ (choosing $f = \rho^+\pi^-$ and $\overline{f} = \rho^-\pi^+$), $\mathcal{A}_{f\overline{f}}$ (also denoted $\mathcal{A}_{\rho\pi}^{+-}$) parameterizes direct *CP* violation in decays in which the produced ρ meson does not contain the spectator quark, while $\mathcal{A}_{\overline{f}f}$ (also denoted $\mathcal{A}_{\rho\pi}^{-+}$) parameterizes direct *CP* violation in decays in which it does. Note that we have again followed the sign convention that the asymmetry is the difference between the rate involving a b quark and that involving a $\overline{b}$ quark, *cf.* Eq. (75). Of course, these parameters are not independent of the other sets of parameters given above, and can be written

$$\mathcal{A}_{f\overline{f}} = -\frac{\langle\mathcal{A}_{f\overline{f}}\rangle + C_{f\overline{f}} + \langle\mathcal{A}_{f\overline{f}}\rangle\Delta C_{f\overline{f}}}{1 + \Delta C_{f\overline{f}} + \langle\mathcal{A}_{f\overline{f}}\rangle C_{f\overline{f}}} \quad \text{and} \quad \mathcal{A}_{\overline{f}f} = \frac{-\langle\mathcal{A}_{f\overline{f}}\rangle + C_{f\overline{f}} + \langle\mathcal{A}_{f\overline{f}}\rangle\Delta C_{f\overline{f}}}{-1 + \Delta C_{f\overline{f}} + \langle\mathcal{A}_{f\overline{f}}\rangle C_{f\overline{f}}}. \tag{92}$$

They usually exhibit strong correlations.

We now consider the various notations which have been used in experimental studies of time-dependent *CP* asymmetries in decays to non-*CP* eigenstates.

$B^0 \to D^{*\pm}D^\mp$

The above set of parameters ($\langle\mathcal{A}_{f\overline{f}}\rangle$, C_f, S_f, $C_{\overline{f}}$, $S_{\overline{f}}$), has been used by both *BABAR* [174] and Belle [177] in the $D^{*\pm}D^\mp$ system ($f = D^{*+}D^-$, $\overline{f} = D^{*-}D^+$). However, slightly different names for the parameters are used: *BABAR* uses ($\mathcal{A}$, C_{+-}, S_{+-}, C_{-+}, S_{-+}); Belle uses ($\mathcal{A}$, C_+, S_+, C_-, S_-). In this document, we follow the notation used by *BABAR*.

$B^0 \to \rho^\pm\pi^\mp$

In the $\rho^\pm\pi^\mp$ system, the ($\langle\mathcal{A}_{f\overline{f}}\rangle$, $C_{f\overline{f}}$, $S_{f\overline{f}}$, $\Delta C_{f\overline{f}}$, $\Delta S_{f\overline{f}}$) set of parameters has been used originally by *BABAR* [185], and more recently by Belle [186], in the Q2B approximation; the exact names[13] used in this case are ($\mathcal{A}_{CP}^{\rho\pi}, C_{\rho\pi}, S_{\rho\pi}, \Delta C_{\rho\pi}, \Delta S_{\rho\pi}$), and these names are also used in this document.

Since $\rho^\pm\pi^\mp$ is reconstructed in the final state $\pi^+\pi^-\pi^0$, the interference between the ρ resonances can provide additional information about the phases (see Sec. 4.2.4). *BABAR* [187] has performed a time-dependent Dalitz plot analysis, from which the weak phase α is directly extracted. In such an analysis, the measured Q2B parameters are also naturally corrected for interference effects.

$B^0 \to D^\pm\pi^\mp, D^{*\pm}\pi^\mp, D^\pm\rho^\mp$

Time-dependent *CP* analyses have also been performed for the final states $D^\pm\pi^\mp$, $D^{*\pm}\pi^\mp$ and $D^\pm\rho^\mp$. In these theoretically clean cases, no penguin contributions are possible, so there is no direct *CP* violation. Furthermore, due to the smallness of the ratio of the magnitudes of the suppressed ($b \to u$) and favoured ($b \to c$) amplitudes (denoted R_f), to a very good approximation, $C_f = -C_{\overline{f}} = 1$ (using $f = D^{(*)-}h^+$, $\overline{f} = D^{(*)+}h^-$ $h = \pi, \rho$), and the coefficients of the sine terms are given by

$$S_f = -2R_f \sin(\phi_{\rm mix} + \phi_{\rm dec} - \delta_f) \quad \text{and} \quad S_{\overline{f}} = -2R_f \sin(\phi_{\rm mix} + \phi_{\rm dec} + \delta_f). \tag{93}$$

Thus weak phase information can be cleanly obtained from measurements of S_f and $S_{\overline{f}}$, although external information on at least one of R_f or δ_f is necessary. (Note that $\phi_{\rm mix} + \phi_{\rm dec} = 2\beta + \gamma$ for all the decay modes in question, while R_f and δ_f depend on the decay mode.)

[13] *BABAR* has used the notations $A_{CP}^{\rho\pi}$ [185] and $\mathcal{A}_{\rho\pi}$ [187] in place of $\mathcal{A}_{CP}^{\rho\pi}$.

Again, different notations have been used in the literature. *BABAR* [191, 193] defines the time-dependent probability function by

$$f^{\pm}(\eta, \Delta t) = \frac{e^{-|\Delta t|/\tau}}{4\tau} \left[1 \mp S_\zeta \sin(\Delta m \Delta t) \mp \eta C_\zeta \cos(\Delta m \Delta t)\right], \tag{94}$$

where the upper (lower) sign corresponds to the tagging meson being a B^0 ($\overline{B}^0$). [Note here that a tagging B^0 ($\overline{B}^0$) corresponds to $-S_\xi$ ($+S_\xi$).] The parameters η and ζ take the values $+1$ and $+$ (-1 and $-$) when the final state is, *e.g.*, $D^-\pi^+$ ($D^+\pi^-$). However, in the fit, the substitutions $C_\zeta = 1$ and $S_\zeta = a \mp \eta b_i - \eta c_i$ are made.[14] [Note that, neglecting b terms, $S_+ = a - c$ and $S_- = a + c$, so that $a = (S_+ + S_-)/2$, $c = (S_- - S_+)/2$, in analogy to the parameters of Eq. (90).] The subscript i denotes the tagging category. These are motivated by the possibility of *CP* violation on the tag side [195], which is absent for semileptonic B decays (mostly lepton tags). The parameter a is not affected by tag side *CP* violation. The parameter b only depends on tag side *CP* violation parameters and is not directly useful for determining UT angles. A clean interpretation of the c parameter is only possible for lepton-tagged events, so the *BABAR* measurements report c measured with those events only.

The parameters used by Belle in the analysis using partially reconstructed B decays [194], are similar to the S_ζ parameters defined above. However, in the Belle convention, a tagging B^0 corresponds to a $+$ sign in front of the sine coefficient; furthermore the correspondence between the super/subscript and the final state is opposite, so that $S_\pm$ (*BABAR*) $= -S^\mp$ (Belle). In this analysis, only lepton tags are used, so there is no effect from tag side *CP* violation. In the Belle analysis using fully reconstructed B decays [192], this effect is measured and taken into account using $D^* l\nu$ decays; in neither Belle analysis are the a, b and c parameters used. In the latter case, the measured parameters are $2R_{D^{(*)}\pi}\sin(2\phi_1 + \phi_3 \pm \delta_{D^{(*)}\pi})$; the definition is such that $S^\pm$ (Belle) $= -2R_{D^*\pi}\sin(2\phi_1 + \phi_3 \pm \delta_{D^*\pi})$. However, the definition includes an angular momentum factor $(-1)^L$ [196], and so for the results in the $D\pi$ system, there is an additional factor of -1 in the conversion.

Explicitly, the conversion then reads as given in Table 16, where we have neglected the b_i terms used by *BABAR* (which are zero in the absence of tag side *CP* violation). For the averages in this document, we use the a and c parameters, and give the explicit translations used in Table 17. It is to be fervently hoped that the experiments will converge on a common notation in future.

Time-dependent asymmetries in radiative B decays

As a special case of decays to non-*CP* eigenstates, let us consider radiative B decays. Here, the emitted photon has a distinct helicity, which is in principle observable, but in practice is not usually measured. Thus the measured time-dependent decay rates are given by [139, 140]

$$\begin{aligned}
\Gamma_{\overline{B}^0\to X\gamma}(\Delta t) &= \Gamma_{\overline{B}^0\to X\gamma_L}(\Delta t) + \Gamma_{\overline{B}^0\to X\gamma_R}(\Delta t) \qquad (95)\\
&= \frac{e^{-|\Delta t|/\tau(B^0)}}{4\tau(B^0)}\left\{1 + (S_L + S_R)\sin(\Delta m\Delta t) - (C_L + C_R)\cos(\Delta m\Delta t)\right\},\\
\Gamma_{B^0\to X\gamma}(\Delta t) &= \Gamma_{B^0\to X\gamma_L}(\Delta t) + \Gamma_{B^0\to X\gamma_R}(\Delta t) \qquad (96)\\
&= \frac{e^{-|\Delta t|/\tau(B^0)}}{4\tau(B^0)}\left\{1 - (S_L + S_R)\sin(\Delta m\Delta t) + (C_L + C_R)\cos(\Delta m\Delta t)\right\},
\end{aligned}$$

[14] The subscript i denotes tagging category.

Table 16: Conversion between the various notations used for *CP* violation parameters in the $D^{\pm}\pi^{\mp}$, $D^{*\pm}\pi^{\mp}$ and $D^{\pm}\rho^{\mp}$ systems. The b_i terms used by *BABAR* have been neglected. Recall that $(\alpha, \beta, \gamma) = (\phi_2, \phi_1, \phi_3)$.

	BABAR	Belle partial rec.	Belle full rec.
$S_{D^+\pi^-}$	$-S_- = -(a + c_i)$	N/A	$2R_{D\pi}\sin(2\phi_1 + \phi_3 + \delta_{D\pi})$
$S_{D^-\pi^+}$	$-S_+ = -(a - c_i)$	N/A	$2R_{D\pi}\sin(2\phi_1 + \phi_3 - \delta_{D\pi})$
$S_{D^{*+}\pi^-}$	$-S_- = -(a + c_i)$	S^+	$-2R_{D^*\pi}\sin(2\phi_1 + \phi_3 + \delta_{D^*\pi})$
$S_{D^{*-}\pi^+}$	$-S_+ = -(a - c_i)$	S^-	$-2R_{D^*\pi}\sin(2\phi_1 + \phi_3 - \delta_{D^*\pi})$
$S_{D^+\rho^-}$	$-S_- = -(a + c_i)$	N/A	N/A
$S_{D^-\rho^+}$	$-S_+ = -(a - c_i)$	N/A	N/A

Table 17: Translations used to convert the parameters measured by Belle to the parameters used for averaging in this document. The angular momentum factor L is -1 for $D^*\pi$ and $+1$ for $D\pi$. Recall that $(\alpha, \beta, \gamma) = (\phi_2, \phi_1, \phi_3)$.

	$D^*\pi$ partial rec.	$D^{(*)}\pi$ full rec.
a	$-(S^+ + S^-)$	$\frac{1}{2}(-1)^{L+1}\left(2R_{D^{(*)}\pi}\sin(2\phi_1 + \phi_3 + \delta_{D^{(*)}\pi}) + 2R_{D^{(*)}\pi}\sin(2\phi_1 + \phi_3 - \delta_{D^{(*)}\pi})\right)$
c	$-(S^+ - S^-)$	$\frac{1}{2}(-1)^{L+1}\left(2R_{D^{(*)}\pi}\sin(2\phi_1 + \phi_3 + \delta_{D^{(*)}\pi}) - 2R_{D^{(*)}\pi}\sin(2\phi_1 + \phi_3 - \delta_{D^{(*)}\pi})\right)$

where in place of the subscripts f and $\overline{f}$ we have used L and R to indicate the photon helicity. In order for interference between decays with and without B^0-$\overline{B}^0$ mixing to occur, the X system must not be flavour-specific, *e.g.*, in case of $B^0 \to K^{*0}\gamma$, the final state must be $K^0_S\pi^0\gamma$. The sign of the sine term depends on the C eigenvalue of the X system. The photons from $b \to q\gamma$ ($\overline{b} \to \overline{q}\gamma$) are predominantly left (right) polarized, with corrections of order of m_q/m_b, thus interference effects are suppressed. The predicted smallness of the S terms in the Standard Model results in sensitivity to new physics contributions.

4.2.6 Asymmetries in $B \to D^{(*)}K^{(*)}$ decays

CP asymmetries in $B \to D^{(*)}K^{(*)}$ decays are sensitive to γ. The neutral $D^{(*)}$ meson produced is an admixture of $D^{(*)0}$ (produced by a $b \to c$ transition) and $\overline{D}^{(*)0}$ (produced by a colour-suppressed $b \to u$ transition) states. If the final state is chosen so that both $D^{(*)0}$ and $\overline{D}^{(*)0}$ can contribute, the two amplitudes interfere, and the resulting observables are sensitive to γ, the relative weak phase between the two B decay amplitudes [141]. Various methods have been proposed to exploit this interference, including those where the neutral D meson is reconstructed as a *CP* eigenstate (GLW) [142], in a suppressed final state (ADS) [143], or in a self-conjugate three-body final state, such as $K^0_S\pi^+\pi^-$ (Dalitz) [144]. It should be emphasized that while each method differs in the choice of D decay, they are all sensitive to the same parameters of the B decay, and can be considered as variations of the same technique.

Consider the case of $B^{\mp} \to DK^{\mp}$, with D decaying to a final state f, which is accessible to both D^0 and $\overline{D}^0$. We can write the decay rates for B^- and B^+ ($\Gamma_{\mp}$), the charge averaged rate

$(\Gamma = (\Gamma_- + \Gamma_+)/2)$ and the charge asymmetry ($\mathcal{A} = (\Gamma_- - \Gamma_+)/(\Gamma_- + \Gamma_+)$, see Eq. (75)) as

$$\begin{aligned}
\Gamma_\mp &\propto r_B^2 + r_D^2 + 2r_B r_D \cos(\delta_B + \delta_D \mp \gamma), &(97)\\
\Gamma &\propto r_B^2 + r_D^2 + 2r_B r_D \cos(\delta_B + \delta_D)\cos(\gamma), &(98)\\
\mathcal{A} &= \frac{2r_B r_D \sin(\delta_B + \delta_D)\sin(\gamma)}{r_B^2 + r_D^2 + 2r_B r_D \cos(\delta_B + \delta_D)\cos(\gamma)}, &(99)
\end{aligned}$$

where the ratio of B decay amplitudes[15] is usually defined to be less than one,

$$r_B = \frac{\left|A\left(B^- \to \overline{D}^0 K^-\right)\right|}{\left|A\left(B^- \to D^0 K^-\right)\right|}, \tag{100}$$

and the ratio of D decay amplitudes is correspondingly defined by

$$r_D = \frac{\left|A\left(D^0 \to f\right)\right|}{\left|A\left(\overline{D}^0 \to f\right)\right|}. \tag{101}$$

The strong phase differences between the B and D decay amplitudes are given by δ_B and δ_D, respectively. The values of r_D and δ_D depend on the final state f: for the GLW analysis, $r_D = 1$ and δ_D is trivial (either zero or π), in the Dalitz plot analysis r_D and δ_D vary across the Dalitz plot, and depend on the D decay model used, for the ADS analysis, the values of r_D and δ_D are not trivial.

Note that, for given values of r_B and r_D, the maximum size of $\mathcal{A}$ (at $\sin(\delta_B + \delta_D) = 1$) is $2r_B r_D \sin(\gamma)/(r_B^2 + r_D^2)$. Thus even for D decay modes with small r_D, large asymmetries, and hence sensitivity to γ, may occur for B decay modes with similar values of r_B. For this reason, the ADS analysis of the decay $B^\mp \to D\pi^\mp$ is also of interest.

In the GLW analysis, the measured quantities are the partial rate asymmetry, and the charge averaged rate, which are measured both for *CP* even and *CP* odd D decays. For the latter, it is experimentally convenient to measure a double ratio,

$$R_{CP} = \frac{\Gamma\left(B^- \to D_{CP} K^-\right) / \Gamma\left(B^- \to D^0 K^-\right)}{\Gamma\left(B^- \to D_{CP} \pi^-\right) / \Gamma\left(B^- \to D^0 \pi^-\right)} \tag{102}$$

that is normalized both to the rate for the favoured $D^0 \to K^-\pi^+$ decay, and to the equivalent quantities for $B^- \to D\pi^-$ decays (charge conjugate modes are implicitly included in Eq. (102)). In this way the constant of proportionality drops out of Eq. (98).

For the ADS analysis, using a suppressed $D \to f$ decay, the measured quantities are again the partial rate asymmetry, and the charge averaged rate. In this case it is sufficient to measure the rate in a single ratio (normalized to the favoured $D \to \overline{f}$ decay) since detection systematics cancel naturally; the observed quantity is then

$$R_{\rm ADS} = \frac{\Gamma\left(B^- \to [f]_D K^-\right)}{\Gamma\left(B^- \to \left[\overline{f}\right]_D K^-\right)}. \tag{103}$$

[15]Note that here we use the notation r_B to denote the ratio of B decay amplitudes, whereas in Sec. 4.2.5 we used, *e.g.*, $R_{D\pi}$, for a rather similar quantity. The reason is that here we need to be concerned also with D decay amplitudes, and so it is convenient to use the subscript to denote the decaying particle. Hopefully, using r in place of R will help reduce potential confusion.

Table 18: Summary of relations between measured and physical parameters in GLW and ADS analyses of $B \to D^{(*)}K^{(*)}$.

GLW analysis	
$R_{CP\pm}$	$1 + r_B^2 \pm 2r_B \cos(\delta_B)\cos(\gamma)$
$A_{CP\pm}$	$\pm 2r_B \sin(\delta_B)\sin(\gamma)\,/R_{CP\pm}$
ADS analysis	
$R_{\rm ADS}$	$r_B^2 + r_D^2 + 2r_B r_D \cos(\delta_B+\delta_D)\cos(\gamma)$
$A_{\rm ADS}$	$2r_B r_D \sin(\delta_B+\delta_D)\sin(\gamma)\,/R_{\rm ADS}$
Dalitz analysis	
$x_\pm$	$r_B \cos(\delta_B \pm \gamma)$
$y_\pm$	$r_B \sin(\delta_B \pm \gamma)$

In the ADS analysis, there are an additional two unknowns (r_D and δ_D) compared to the GLW case. However, the value of r_D can be measured using decays of D mesons of known flavour.

In the Dalitz plot analysis, once a model is assumed for the D decay, which gives the values of r_D and δ_D across the Dalitz plot, it is possible to perform a simultaneous fit to the B^+ and B^- samples and directly extract γ, r_B and δ_B. However, the uncertainties on the phases depend inversely on r_B. Furthermore, r_B is positive definite (and small), and therefore tends to be overestimated, which can lead to an underestimation of the uncertainty. Some statistical treatment is necessary to correct for this bias. An alternative approach is to extract from the data the "Cartesian" variables

$$(x_\pm, y_\pm) = \left(\mathrm{Re}(r_B e^{i(\delta_B \pm \gamma)}), \mathrm{Im}(r_B e^{i(\delta_B \pm \gamma)})\right) = (r_B \cos(\delta_B \pm \gamma), r_B \sin(\delta_B \pm \gamma))\,. \qquad (104)$$

These are (a) approximately statistically uncorrelated and (b) almost Gaussian. Use of these variables makes the combination of results much simpler.

The relations between the measured quantities and the underlying parameters are summarized in Table 18. Note carefully that the hadronic factors r_B and δ_B are different, in general, for each B decay mode.

4.3 Common inputs and error treatment

The common inputs used for rescaling are listed in Table 19. The B^0 lifetime ($\tau(B^0)$) and mixing parameter (Δm_d) averages are provided by the HFAG Lifetimes and Oscillations subgroup (Sec. 3). The fraction of the perpendicularly polarized component ($|A_\perp|^2$) in $B \to J/\psi K^*(892)$ decays, which determines the *CP* composition, is averaged from results by *BABAR* [146] and Belle [147].

At present, we only rescale to a common set of input parameters for modes with reasonably small statistical errors ($b \to c\bar{c}s$ transitions). Correlated systematic errors are taken into account in these modes as well. For all other modes, the effect of such a procedure is currently negligible.

As explained in Sec. 1, we do not apply a rescaling factor on the error of an average that has $\chi^2/\mathrm{dof} > 1$ (unlike the procedure currently used by the PDG [5]). We provide a confidence level of the fit so that one can know the consistency of the measurements included in the average,

Table 19: Common inputs used in calculating the averages.

$\tau(B^0)$ (ps)	1.528 ± 0.009
Δm_d (ps^{-1})	0.509 ± 0.004
$\lvert A_\perp \rvert^2 (J/\psi K^*)$	0.217 ± 0.010

Table 20: $S_{b\to c\bar{c}s}$ and $C_{b\to c\bar{c}s}$.

Experiment		$-\eta S_{b\to c\bar{c}s}$	$C_{b\to c\bar{c}s}$
BABAR	[148]	$0.722 \pm 0.040 \pm 0.023$	$0.051 \pm 0.033 \pm 0.014$
Belle	[149]	$0.652 \pm 0.039 \pm 0.020$	$-0.010 \pm 0.026 \pm 0.036$
B factory average		0.685 ± 0.032	0.026 ± 0.041
Confidence level		0.27	0.31
ALEPH	[150]	$0.84\,^{+0.82}_{-1.04} \pm 0.16$	
OPAL	[151]	$3.2\,^{+1.8}_{-2.0} \pm 0.5$	
CDF	[152]	$0.79\,^{+0.41}_{-0.44}$	
Average		0.687 ± 0.032	0.026 ± 0.041

and attach comments in case some care needs to be taken in the interpretation. Note that, in general, results obtained from data samples with low statistics will exhibit some non-Gaussian behaviour. For measurements where one error is given, it represents the total error, where statistical and systematic uncertainties have been added in quadrature. If two errors are given, the first is statistical and the second systematic. If more than two errors are given, the origin of the additional uncertainty will be explained in the text.

Averages are computed by maximizing a log-likelihood function $\mathcal{L}$ assuming Gaussian statistical and systematic errors. When observables exhibit significant correlations (*e.g.*, sine and cosine coefficients in some time-dependent *CP* asymmetries), a combined minimization is performed, taking into account the correlations. Asymmetric errors are treated by defining an asymmetric log-likelihood function: $\mathcal{L}_i = (x - x_i)^2/(2\sigma_i^2)$, where $\sigma_i = \sigma_{i,+}$ ($\sigma_i = \sigma_{i,-}$) if $x > x_i$ ($x < x_i$), and where x_i is the ith measurement of the observable x that is averaged. This example assumes no correlations between observables. The correlated case is a straightforward extension to this.

4.4 Time-dependent *CP* asymmetries in $b \to c\bar{c}s$ transitions

In the Standard Model, the time-dependent parameters for $b \to c\bar{c}s$ transitions are predicted to be: $S_{b\to c\bar{c}s} = -\eta \sin(2\beta)$, $C_{b\to c\bar{c}s} = 0$ to very good accuracy. The averages for $-\eta S_{b\to c\bar{c}s}$ and $C_{b\to c\bar{c}s}$ are provided in Table 20. The averages for $-\eta S_{b\to c\bar{c}s}$ are shown in Fig. 12.

Both *BABAR* and Belle have used the $\eta = -1$ modes $J/\psi K^0_S$, $\psi(2S)K^0_S$, $\chi_{c1}K^0_S$ and $\eta_c K^0_S$, as well as $J/\psi K^0_L$, which has $\eta = +1$ and $J/\psi K^{*0}(892)$, which is found to have η close to $+1$ based on the measurement of $|A_\perp|$ (see Sec. 4.3). ALEPH, OPAL and CDF use only the $J/\psi K^0_S$ final state. In the latest result from Belle, only $J/\psi K^0_S$ and $J/\psi K^0_L$ are used. In future updates, it is hoped to perform separate averages for each charmonium-kaon final state.

It should be noted that, while the uncertainty in the average for $-\eta S_{b\to c\bar{c}s}$ is still limited

by statistics, that for $C_{b\to c\bar{c}s}$ is currently dominated by systematics. This occurs due to the possible effect of tag side interference on the $C_{b\to c\bar{c}s}$ measurement, an effect which is correlated between the different experiments. Understanding of this effect may improve in future, allowing the uncertainty to reduce.

From the average for $-\eta S_{b\to c\bar{c}s}$ above, we obtain the following solutions for β (in $[0,\pi]$):

$$\beta = \left(21.7\,^{+1.3}_{-1.2}\right)^\circ \quad \text{or} \quad \beta = \left(68.3\,^{+1.2}_{-1.3}\right)^\circ \tag{105}$$

This result gives a precise constraint on the $(\overline{\rho},\overline{\eta})$ plane, as shown in Fig. 12. The measurement is in remarkable agreement with other constraints from *CP* conserving quantities, and with *CP* violation in the kaon system, in the form of the parameter ϵ_K. Such comparisons have been performed by various phenomenological groups, such as CKMfitter [153] and UTFit [154]. Fig. 13 displays the constraints obtained from these two groups.

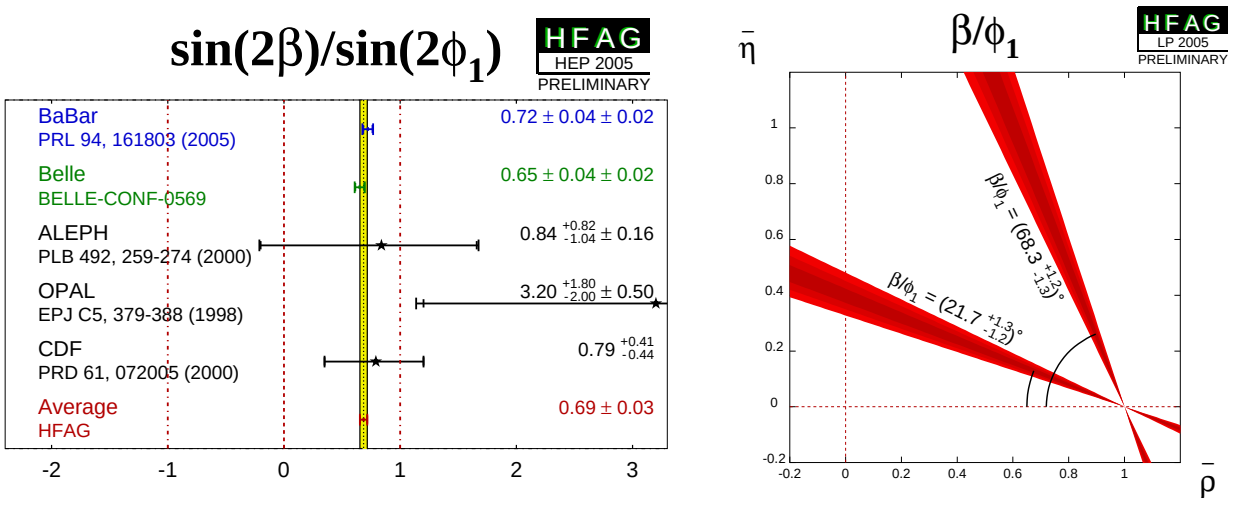

Figure 12: (Left) Average of measurements of $S_{b\to c\bar{c}s}$. (Right) Constraints on the $(\overline{\rho},\overline{\eta})$ plane, obtained from the average of $-\eta S_{b\to c\bar{c}s}$ and Eq. 105.

4.5 Time-dependent transversity analysis of $B^0 \to J/\psi K^{*0}$

B meson decays to the vector-vector final state $J/\psi K^{*0}$ are also mediated by the $b \to c\bar{c}s$ transition. When a final state which is not flavour-specific ($K^{*0} \to K^0_S\pi^0$) is used, a time-dependent transversity analysis can be performed allowing sensitivity to both $\sin(2\beta)$ and $\cos(2\beta)$ [155]. Such analyses have been performed by both B factory experiments. In principle, the strong phases between the transversity amplitudes are not uniquely determined by such an analysis, leading to a discrete ambiguity in the sign of $\cos(2\beta)$. The *BABAR* collaboration resolves this ambiguity using the known variation [156] of the P-wave phase (fast) relative to the S-wave phase (slow) with the invariant mass of the $K\pi$ system in the vicinity of the $K^*(892)$ resonance. The result is in agreement with the prediction from s quark helicity conservation, and corresponds to Solution II defined by Suzuki [157]. We use this phase convention for the averages given in Table 21.

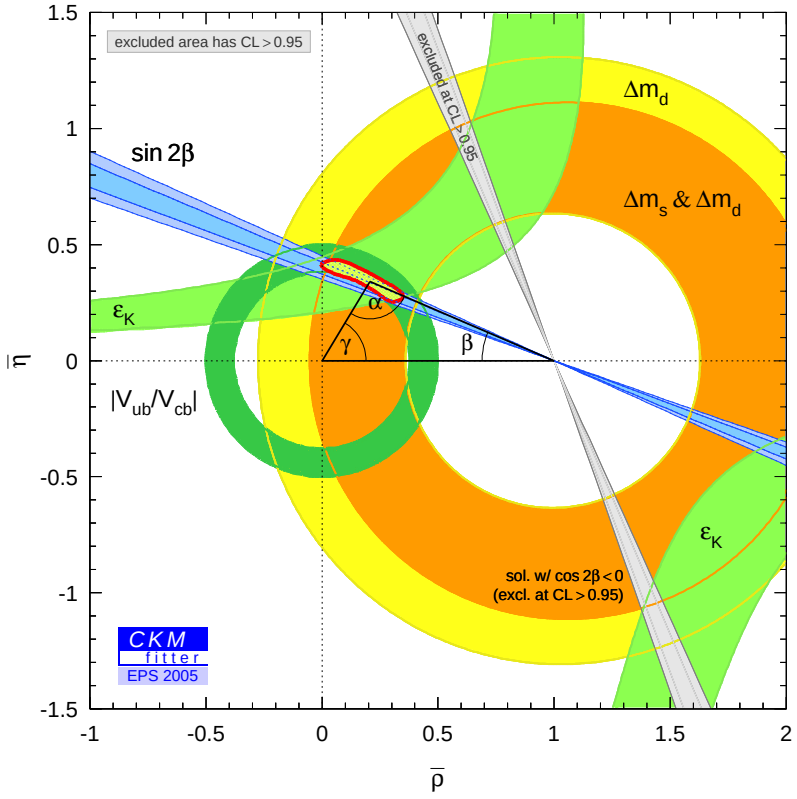

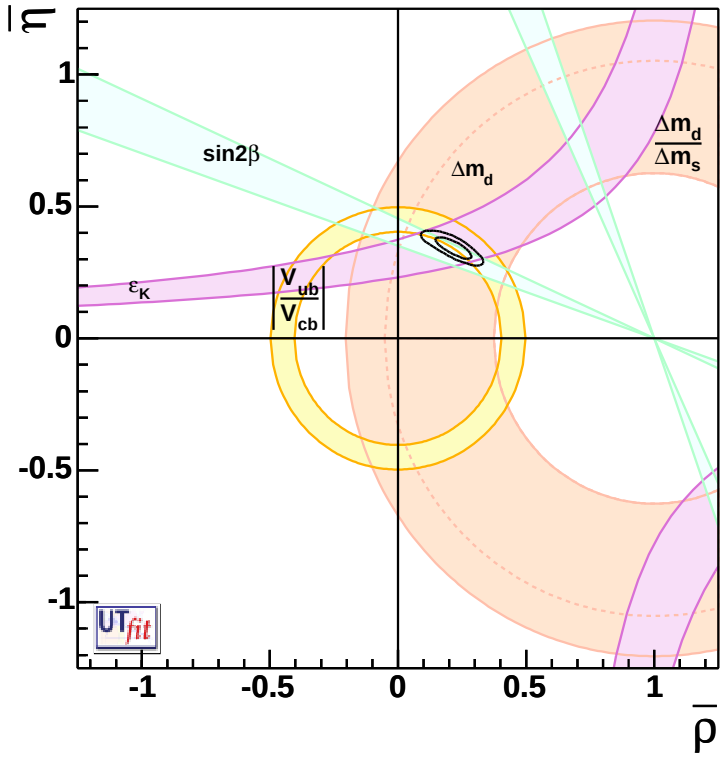

Figure 13: Typical Standard Model constraints on the $(\overline{\rho}, \overline{\eta})$ plane, from (top) [153] and (bottom) [154].

Table 21: Averages from $B^0 \to J/\psi K^{*0}$ transversity analyses.

Experiment		$\sin(2\beta)$	$\cos(2\beta)$	Correlation
BABAR	[146]	$-0.10 \pm 0.57 \pm 0.14$	$3.32\,^{+0.76}_{-0.96} \pm 0.27$	-0.37
Belle	[147]	$0.24 \pm 0.31 \pm 0.05$	$0.56 \pm 0.79 \pm 0.11$	$+0.22$
Average		In Preparation		

Table 22: Averages from $B^0 \to D^{(*)}h^0$ analyses.

Experiment		$\beta\,(^\circ)$
Belle	[161]	$16 \pm 21 \pm 12$

At present the results are dominated by large and non-Gaussian statistical errors. In addition, there are significant correlations which need to be taken into account. At present, we do not provide averages for the results in Table 21; nevertheless $\cos(2\beta) > 0$ is preferred by the experimental data in $J/\psi K^*$.

4.6 Time-dependent *CP* asymmetries in colour-suppressed $b \to c\overline{u}d$ transitions

Decays of B mesons to final states such as $D\pi^0$ are governed by $b \to c\overline{u}d$ transitions. If the final state is a CP eigenstate, *i.e.* $D_{CP}\pi^0$, the usual time-dependence formulae are recovered, with the sine coefficient sensitive to $\sin(2\beta)$. Since there is no penguin contribution to these decays, there is even less associated theoretical uncertainty than for $b \to c\overline{c}s$ decays like $B \to J/\psi\, K^0_S$. Such measurements therefore allow to test the Standard Model prediction that the CP violation parameters in $b \to c\overline{u}d$ transitions are the same as those in $b \to c\overline{c}s$ [158].

Note that there is an additional contribution from CKM suppressed $b \to u\overline{c}d$ decays. The effect of this contribution is small, and can be taken into account in the analysis [159].

When multibody D decays, such as $D \to K^0_S\pi^+\pi^-$ are used, a time-dependent analysis of the Dalitz plot of the neutral D decay allows a direct determination of the weak phase: 2β. (Equivalently, both $\sin(2\beta)$ and $\cos(2\beta)$ can be measured.) This information allows to resolve the ambiguity in the measurement of 2β from $\sin(2\beta)$ [160].

Results of such an analysis are available from Belle. The decays $B \to D\pi^0$, $B \to D\eta$, $B \to D\omega$, $B \to D^*\pi^0$ and $B \to D^*\eta$ are used. [This collection of states is denoted by $D^{(*)}h^0$.] The daughter decays are $D^* \to D\pi^0$ and $D \to K^0_S\pi^+\pi^-$. The results are shown in Table 22.

Again, it is clear that the data prefer $\cos(2\beta) > 0$. Taken in conjunction with the $J/\psi\, K^*$ results, $\cos(2\beta) < 0$ can be considered to be ruled out (at approximately 3σ).

4.7 Time-dependent *CP* asymmetries in charmless $b \to q\overline{q}s$ transitions

The flavour changing neutral current $b \to s$ penguin can be mediated by any up-type quark in the loop, and hence the amplitude can be written as

$$\begin{aligned} A_{b\to s} &= F_u V_{ub}V_{us}^* + F_c V_{cb}V_{cs}^* + F_t V_{tb}V_{ts}^* \\ &= (F_u - F_c)V_{ub}V_{us}^* + (F_t - F_c)V_{tb}V_{ts}^* \\ &= \mathcal{O}(\lambda^4) + \mathcal{O}(\lambda^2) \end{aligned} \tag{106}$$

using the unitarity of the CKM matrix. Therefore, in the Standard Model, this amplitude is dominated by $V_{tb}V_{ts}^*$, and to within a few degrees ($\delta\beta \lesssim 2^\circ$ for $\beta \approx 20^\circ$) the time-dependent parameters can be written[16] $S_{b\to q\overline{q}s} \approx -\eta \sin(2\beta)$, $C_{b\to q\overline{q}s} \approx 0$, assuming $b \to s$ penguin contributions only ($q = u, d, s$).

Due to the large virtual mass scales occurring in the penguin loops, additional diagrams from physics beyond the Standard Model, with heavy particles in the loops, may contribute. In general, these contributions will affect the values of $S_{b\to q\overline{q}s}$ and $C_{b\to q\overline{q}s}$. A discrepancy between the values of $S_{b\to c\overline{c}s}$ and $S_{b\to q\overline{q}s}$ can therefore provide a clean indication of new physics.

However, there is an additional consideration to take into account. The above argument assumes only the $b \to s$ penguin contributes to the $b \to q\overline{q}s$ transition. For $q = s$ this is a good assumption, which neglects only rescattering effects. However, for $q = u$ there is a colour-suppressed $b \to u$ tree diagram (of order $\mathcal{O}(\lambda^4)$), which has a different weak (and possibly strong) phase. In the case $q = d$, any light neutral meson that is formed from $d\overline{d}$ also has a $u\overline{u}$ component, and so again there is "tree pollution". The B^0 decays to $\pi^0 K_S^0$ and ωK_S^0 belong to this category. The mesons f_0 and η' are expected to have predominant $s\overline{s}$ parts, which reduces the possible tree pollution. If the inclusive decay $B^0 \to K^+K^-K^0$ (excluding ϕK^0) is dominated by a non-resonant three-body transition, an OZI-rule suppressed tree-level diagram can occur through insertion of an $s\overline{s}$ pair. The corresponding penguin-type transition proceeds via insertion of a $u\overline{u}$ pair, which is expected to be favored over the $s\overline{s}$ insertion by fragmentation models. Neglecting rescattering, the final state $K^0\overline{K}^0K^0$ (reconstructed as $K_S^0K_S^0K_S^0$) has no tree pollution. Various estimates, using different theoretical approaches, of the values of $\Delta S = S_{b\to q\overline{q}s} - S_{b\to c\overline{c}s}$ exist in the literature [162]. In general, there is agreement that the modes ϕK^0, $\eta' K^0$ and $K^0\overline{K}^0K^0$ are the cleanest, with values of $|\Delta S|$ at or below the few percent level (ΔS is usually positive).

The averages for $-\eta S_{b\to q\overline{q}s}$ and $C_{b\to q\overline{q}s}$ can be found in Table 23, and are shown in Fig. 14. Results from both *BABAR* and Belle are averaged for the modes ϕK^0, $\eta' K^0$ and $K^+K^-K^0$ (K^0 indicates that both K_S^0 and K_L^0 are used, although Belle do not use $K^+K^-K_L^0$), $f_0K_S^0$, $\pi^0K_S^0$, ωK_S^0 and $K_S^0K_S^0K_S^0$. *BABAR* also has results using $\pi^0\pi^0K_S^0$. Of these modes, ϕK_S^0, $\eta' K_S^0$, $\pi^0K_S^0$ and ωK_S^0 have *CP* eigenvalue $\eta = -1$, while ϕK_L^0, $\eta' K_L^0$, $f_0K_S^0$, $\pi^0\pi^0K_S^0$ and $K_S^0K_S^0K_S^0$ have $\eta = +1$.

The final state $K^+K^-K^0$ (contributions from ϕK^0 are implicitly excluded) is not a *CP* eigenstate. However, the *CP* composition can be determined using either an isospin argument (used by Belle to determine a *CP* even fraction of $0.93 \pm 0.09 \pm 0.05$ [164]) or a moments

[16] The presence of a small ($\mathcal{O}(\lambda^2)$) weak phase in the dominant amplitude of the s penguin decays introduces a phase shift given by $S_{b\to q\overline{q}s} = -\eta \sin(2\beta) \cdot (1 + \Delta)$. Using the CKMfitter results for the Wolfenstein parameters [153], one finds: $\Delta \simeq 0.033$, which corresponds to a shift of 2β of $+2.1$ degrees. Nonperturbative contributions can alter this result.

analysis (used by *BABAR* to find *CP* even fractions of $0.89 \pm 0.08 \pm 0.06$ in $K^+K^-K^0_S$ [163] and $0.92 \pm 0.07 \pm 0.06$ in $K^+K^-K^0_L$ [170]). The uncertainty in the *CP* even fraction leads to an asymmetric error on $S_{b\to q\bar{q}s}$, which is taken to be correlated among the experiments. To combine, we rescale the results to the average *CP* even fraction of 0.91 ± 0.07.

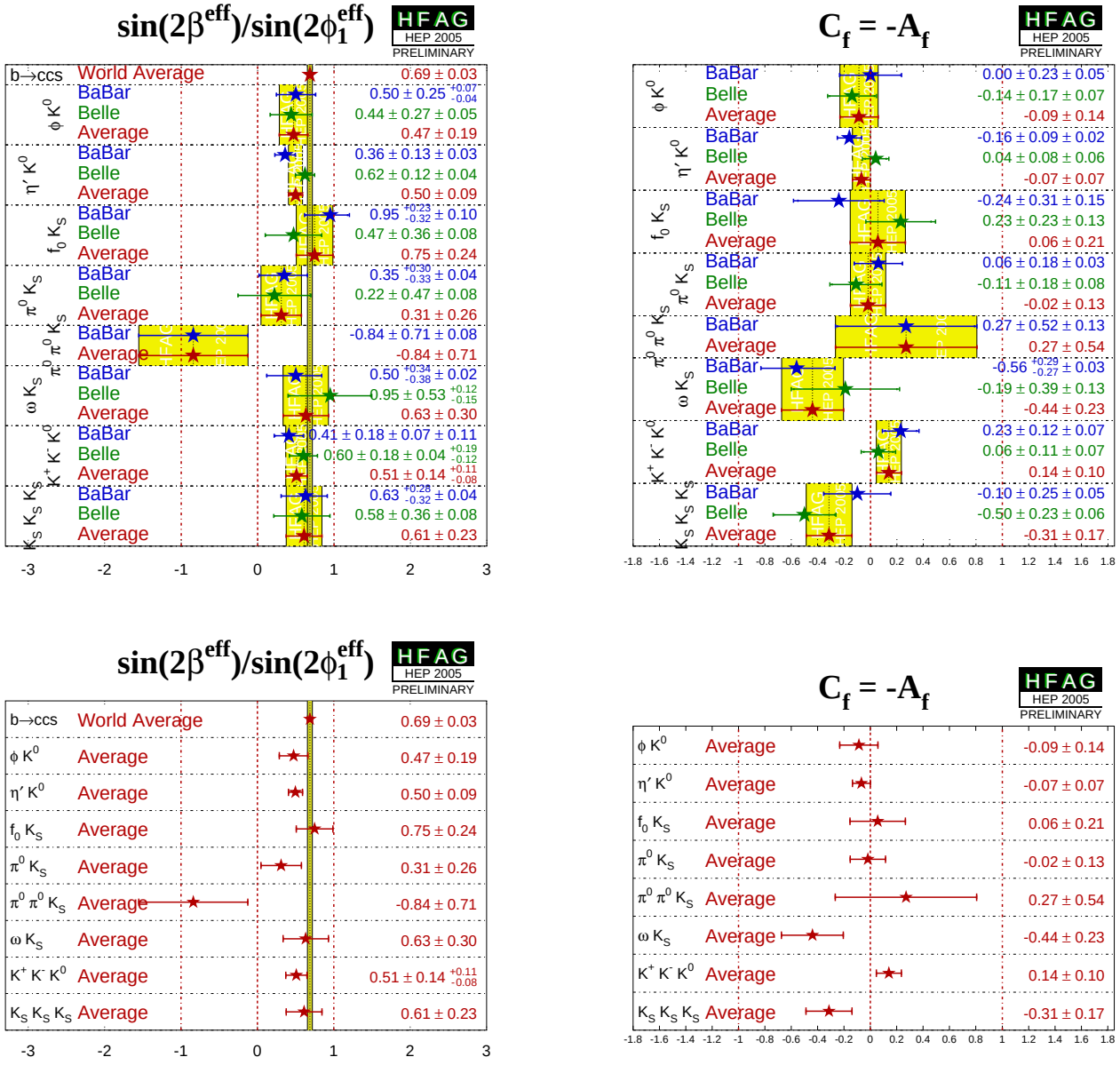

Figure 14: (Top) Averages of (left) $-\eta S_{b\to q\bar{q}s}$ and (right) $C_{b\to q\bar{q}s}$. The $-\eta S_{b\to q\bar{q}s}$ figure compares the results to the world average for $-\eta S_{b\to c\bar{c}s}$ (see Section 4.4). (Bottom) Same, but only averages for each mode are shown. More figures are available from the HFAG web pages.

As explained above, each of the modes listed in Table 23 has different uncertainties within the Standard Model, and so each may have a different value of $-\eta S_{b\to q\bar{q}s}$. Therefore, there is no strong motivation to make a combined average over the different modes. We refer to such an average as a "naïve s-penguin average." It is naïve not only because of the neglect of the theoretical uncertainty, but also since possible correlations of systematic effects between

Table 23: Averages of $-\eta S_{b\to q\overline{q}s}$ and $C_{b\to q\overline{q}s}$. Note that the averages are calculated without taking correlations into account.

Experiment		$-\eta S_{b\to q\overline{q}s}$	$C_{b\to q\overline{q}s}$
		ϕK^0	
BABAR	[163]	$0.50 \pm 0.25\,^{+0.07}_{-0.04}$	$0.00 \pm 0.23 \pm 0.05$
Belle	[164]	$0.44 \pm 0.27 \pm 0.05$	$-0.14 \pm 0.17 \pm 0.07$
Average		0.47 ± 0.19	-0.09 ± 0.14
Confidence level		0.87 (0.2σ)	0.64 (0.5σ)
		$\eta' K^0$	
BABAR	[165]	$0.36 \pm 0.13 \pm 0.03$	$-0.16 \pm 0.09 \pm 0.02$
Belle	[164]	$0.62 \pm 0.12 \pm 0.04$	$0.04 \pm 0.08 \pm 0.06$
Average		0.50 ± 0.09	-0.07 ± 0.07
Confidence level		0.16 (1.4σ)	0.14 (1.5σ)
		$f_0 K^0_S$	
BABAR	[166]	$0.95\,^{+0.23}_{-0.32} \pm 0.10$	$-0.24 \pm 0.31 \pm 0.15$
Belle	[164]	$0.47 \pm 0.36 \pm 0.08$	$0.23 \pm 0.23 \pm 0.13$
Average		0.75 ± 0.24	0.06 ± 0.21
Confidence level		0.32 (1.0σ)	0.28 (1.1σ)
		$\pi^0 K^0_S$	
BABAR	[167]	$0.35\,^{+0.30}_{-0.33} \pm 0.04$	$0.06 \pm 0.18 \pm 0.03$
Belle	[164]	$0.22 \pm 0.47 \pm 0.08$	$-0.11 \pm 0.18 \pm 0.08$
Average		0.31 ± 0.26	-0.02 ± 0.13
Confidence level		0.82 (0.2σ)	0.53 (0.6σ)
		$\pi^0\pi^0 K^0_S$	
BABAR	[168]	$-0.84 \pm 0.71 \pm 0.08$	$0.27 \pm 0.52 \pm 0.13$
Average		-0.84 ± 0.71	0.27 ± 0.54
		ωK^0_S	
BABAR	[169]	$0.50\,^{+0.34}_{-0.38} \pm 0.02$	$-0.56\,^{+0.29}_{-0.27} \pm 0.03$
Belle	[164]	$0.95 \pm 0.53\,^{+0.12}_{-0.15}$	$-0.19 \pm 0.39 \pm 0.13$
Average		0.63 ± 0.30	-0.44 ± 0.23
Confidence level		0.49 (0.7σ)	0.46 (0.7σ)
		$K^+K^-K^0$	
BABAR	[170]	$0.41 \pm 0.18 \pm 0.07 \pm 0.11$	0.23 ± 0.13
Belle	[164]	$0.60 \pm 0.18 \pm 0.04\,^{+0.19}_{-0.12}$	$0.06 \pm 0.11 \pm 0.07$
Average		$0.51 \pm 0.14\,^{+0.11}_{-0.08}$	0.15 ± 0.09
Confidence level		0.38 (0.9σ)	0.36 (0.9σ)
		$K^0_S K^0_S K^0_S$	
BABAR	[171]	$0.63\,^{+0.28}_{-0.32} \pm 0.04$	$-0.10 \pm 0.25 \pm 0.05$
Belle	[164]	$0.58 \pm 0.36 \pm 0.08$	$-0.50 \pm 0.23 \pm 0.06$
Average		0.61 ± 0.23	-0.31 ± 0.17
Confidence level		0.92 (0.1σ)	0.25 (1.1σ)

different modes are neglected. In spite of these caveats, there remains substantial interest in the value of this quantity, and therefore it is given here: $\langle -\eta S_{b\to q\overline{q}s}\rangle = 0.50 \pm 0.06$, with confidence level 0.79 (0.3σ). Again treating the uncertainties as Gaussian and neglecting correlations, this value is found to be 2.6σ below the average $-\eta S_{b\to c\overline{c}s}$ given in Sec. 4.4. (The average for $C_{b\to q\overline{q}s}$ is $\langle C_{b\to q\overline{q}s}\rangle = -0.04 \pm 0.04$ with confidence level 0.30 (1.0σ)). However, we do not advocate the use of these averages, and we emphasize that the values should be treated with *extreme caution*, if at all. What is unambiguous (although only qualitative) is that there is a trend that the values of $-\eta S_{b\to c\overline{c}s}$ in different modes are below the average for $-\eta S_{b\to c\overline{c}s}$.

From Table 23 it may be noted that the average for $-\eta S_{b\to c\overline{c}s}$ in $\eta' K^0$ (0.50 ± 0.09), is more than 5σ away from zero, so that *CP* violation in this mode may now be considered established. Among other modes, *CP* violation in both $f_0 K^0_S$ and $K^+K^-K^0$ is near the 3σ level, although due to possible non-Gaussian errors in these results it may be prudent to defer any strong conclusion on these modes. There is no evidence (above 2σ) for direct *CP* violation in any $b \to q\overline{q}s$ mode.

4.8 Time-dependent *CP* asymmetries in $b \to c\overline{c}d$ transitions

The transition $b \to c\overline{c}d$ can occur via either a $b \to c$ tree or a $b \to d$ penguin amplitude. Similarly to Eq. (106), the amplitude for the $b \to d$ penguin can be written

$$\begin{array}{rcccl} A_{b\to d} & = & F_u V_{ub}V^*_{ud} + F_c V_{cb}V^*_{cd} + F_t V_{tb}V^*_{td} & & \\ & = & (F_u - F_c)V_{ub}V^*_{ud} & + & (F_t - F_c)V_{tb}V^*_{td} \\ & = & \mathcal{O}(\lambda^3) & + & \mathcal{O}(\lambda^3). \end{array} \tag{107}$$

From this it can be seen that the $b \to d$ penguin amplitude contains terms with different weak phases at the same order of CKM suppression.

In the above, we have followed Eq. (106) by eliminating the F_c term using unitarity. However, we could equally well write

$$\begin{array}{rcccl} A_{b\to d} & = & (F_u - F_t)V_{ub}V^*_{ud} & + & (F_c - F_t)V_{cb}V^*_{cd}, \\ & = & (F_c - F_u)V_{cb}V^*_{cd} & + & (F_t - F_u)V_{tb}V^*_{td}. \end{array} \tag{108}$$

Since the $b \to c\overline{c}d$ tree amplitude has the weak phase of $V_{cb}V^*_{cd}$, either of the above expressions allow the penguin to be decomposed into parts with weak phases the same and different to the tree amplitude (the relative weak phase can be chosen to be either β or γ). However, if the tree amplitude dominates, there is little sensitivity to any phase other than that from B^0–$\overline{B}^0$ mixing.

The $b \to c\overline{c}d$ transitions can be investigated with studies of various different final states. Results are available from both *BABAR* and Belle using the final states $J/\psi\pi^0$, $D^{*+}D^{*-}$ and $D^{*\pm}D^{\mp}$, and *BABAR* have also used the final state D^+D^-; the averages of these results are given in Table 24. The results using the *CP* eigenstate ($\eta = +1$) $J/\psi\pi^0$ are shown in Fig. 15.

The vector-vector mode $D^{*+}D^{*-}$ is found to be dominated by the *CP* even longitudinally polarized component; *BABAR* measures a *CP* odd fraction of $0.125 \pm 0.044 \pm 0.007$ [175] while Belle measures a *CP* odd fraction of $0.19 \pm 0.08 \pm 0.01$ [176] (here we do not average these fractions and rescale the inputs, however the average is almost independent of the treatment). We treat the uncertainty due to the error in the *CP*-odd fractions (quoted as a third uncertainty) as a correlated systematic error. Results using $D^{*+}D^{*-}$ are shown in Fig. 16.

Table 24: Averages for $b \to c\overline{c}d$ modes. Note that the averages are calculated without taking correlations into account.

Experiment		$S_{b\to c\bar{c}d}$	$C_{b\to c\bar{c}d}$
		$J/\psi\pi^0$	
BABAR	[172]	$-0.68 \pm 0.30 \pm 0.04$	$-0.21 \pm 0.26 \pm 0.09$
Belle	[173]	$-0.72 \pm 0.42 \pm 0.09$	$0.01 \pm 0.29 \pm 0.03$
Average		-0.69 ± 0.25	-0.11 ± 0.20
Confidence level		0.94 (0.1σ)	0.58 (0.6σ))
		D^+D^-	
BABAR	[174]	$-0.29 \pm 0.63 \pm 0.06$	$0.11 \pm 0.35 \pm 0.06$
Average		-0.29 ± 0.63	0.11 ± 0.36
		$D^{*+}D^{*-}$	
BABAR	[175]	$-0.75 \pm 0.25 \pm 0.03$	$0.06 \pm 0.17 \pm 0.03$
Belle	[176]	$-0.75 \pm 0.56 \pm 0.10 \pm 0.06$	$0.26 \pm 0.26 \pm 0.05 \pm 0.01$
Average		-0.75 ± 0.23	0.12 ± 0.14
Confidence level		1.00 (0.0σ)	0.52 (0.6σ)

Experiment		S_{+-}	C_{+-}	S_{-+}	C_{-+}	A
				$D^{*\pm}D^{\mp}$		
BABAR	[174]	$-0.54 \pm 0.35 \pm 0.07$	$0.09 \pm 0.25 \pm 0.06$	$-0.29 \pm 0.33 \pm 0.07$	$0.17 \pm 0.24 \pm 0.04$	
Belle	[177]	$-0.55 \pm 0.39 \pm 0.12$	$-0.37 \pm 0.22 \pm 0.06$	$-0.96 \pm 0.43 \pm 0.12$	$0.23 \pm 0.25 \pm 0.06$	$0.07 \pm 0.08 \pm 0.04$
Average		-0.54 ± 0.27	-0.16 ± 0.17	-0.53 ± 0.27	0.20 ± 0.18	0.07 ± 0.09
Confidence level		0.99 (0.0σ)	0.18 (1.3σ)	0.23 (1.2σ)	0.87 (0.2σ)	

For the non-*CP* eigenstate mode $D^{*\pm}D^{\mp}$ *BABAR* uses fully reconstructed events while Belle combines both fully and partially reconstructed samples. The most recent results from *BABAR* do not include a measurement of the overall asymmetry A. At present we perform uncorrelated averages of the parameters in the $D^{*\pm}D^{\mp}$ system, using only the information from Belle on A.

In the absence of the penguin contribution (tree dominance), the time-dependent parameters would be given by $S_{b\to c\bar{c}d} = -\eta\sin(2\beta)$, $C_{b\to c\bar{c}d} = 0$, $S_{+-} = \sin(2\beta+\delta)$, $S_{-+} = \sin(2\beta-\delta)$, $C_{+-} = -C_{-+}$ and $A_{+-} = 0$, where δ is the strong phase difference between the $D^{*+}D^-$ and $D^{*-}D^+$ decay amplitudes. In the presence of the penguin contribution, there is no clean interpretation in terms of CKM parameters, however direct *CP* violation may be observed as any of $C_{b\to c\bar{c}d} \neq 0$, $C_{+-} \neq -C_{-+}$ or $A_{+-} \neq 0$.

The averages for the $b \to c\overline{c}d$ modes are shown in Fig. 17. All results are consistent with tree dominance, and with the Standard Model. The average of $S_{b\to c\bar{c}d}$ in the $D^{*+}D^{*-}$ final state is about 3σ from zero; however, due to the large uncertainty and possible non-Gaussian effects, any strong conclusion should be deferred.

4.9 Time-dependent asymmetries in $b \to s\gamma$ transitions

The radiative decays $b \to s\gamma$ produce photons which are highly polarized in the Standard Model. The decays $B^0 \to F\gamma$ and $\overline{B}^0 \to F\gamma$ produce photons with opposite helicities, and since the polarization is, in principle, observable, these final states cannot interfere. The finite mass of the s quark introduces small corrections to the limit of maximum polarization, but any

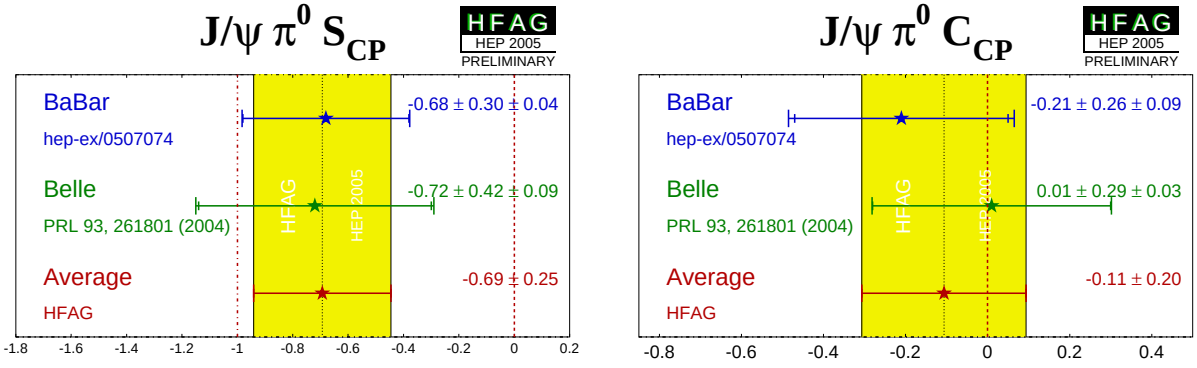

Figure 15: Averages of (left) $S_{b\to c\bar{c}d}$ and (right) $C_{b\to c\bar{c}d}$ for the mode $B^0 \to J/\psi\pi^0$.

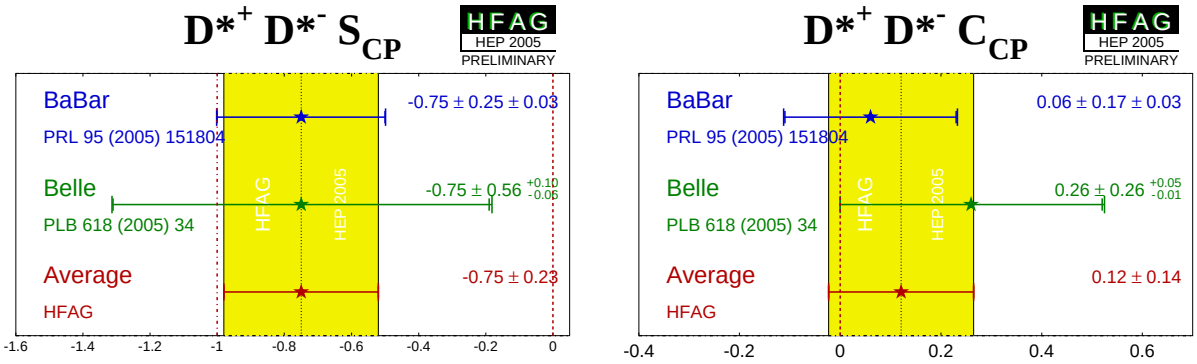

Figure 16: Averages of (left) $S_{b\to c\bar{c}d}$ and (right) $C_{b\to c\bar{c}d}$ for the mode $B^0 \to D^{*+}D^{*-}$.

large mixing induced *CP* violation would be a signal for new physics. Since a single weak phase dominates the $b \to s\gamma$ transition in the Standard Model, the cosine term is also expected to be small.

Atwood *et al.* [140] have shown that an inclusive analysis with respect to $K^0_S\pi^0\gamma$ can be performed, since the properties of the decay amplitudes are independent of the angular momentum of the $K^0_S\pi^0$ system. However, if non-dipole operators contribute significantly to the amplitudes, then the Standard Model mixing-induced *CP* violation could be larger than the naïve expectation $S \simeq -2(m_s/m_b)\sin(2\beta)$, and the *CP* parameters may vary over the $K^0_S\pi^0\gamma$ Dalitz plot, for example as a function of the $K^0_S\pi^0$ invariant mass.

With the above in mind, we quote two averages: one for $K^*(892)$ candidates only, and the other one for the inclusive $K^0_S\pi^0\gamma$ decay (including the $K^*(892)$). If the Standard Model dipole operator is dominant, both should give the same quantities (the latter naturally with smaller statistical error). If not, care needs to be taken in interpretation of the inclusive parameters, while the results on the $K^*(892)$ resonance remain relatively clean. Results from *BABAR* and Belle are used for both averages; both experiments use the invariant mass range $0.60\ \mathrm{GeV}/c^2 < M_{K^0_S\pi^0} < 1.80\ \mathrm{GeV}/c^2$ in the inclusive analysis.

The results are shown in Table 25, and in Fig. 18. No significant *CP* violation results are seen; the results are consistent with the Standard Model and with other measurements in the

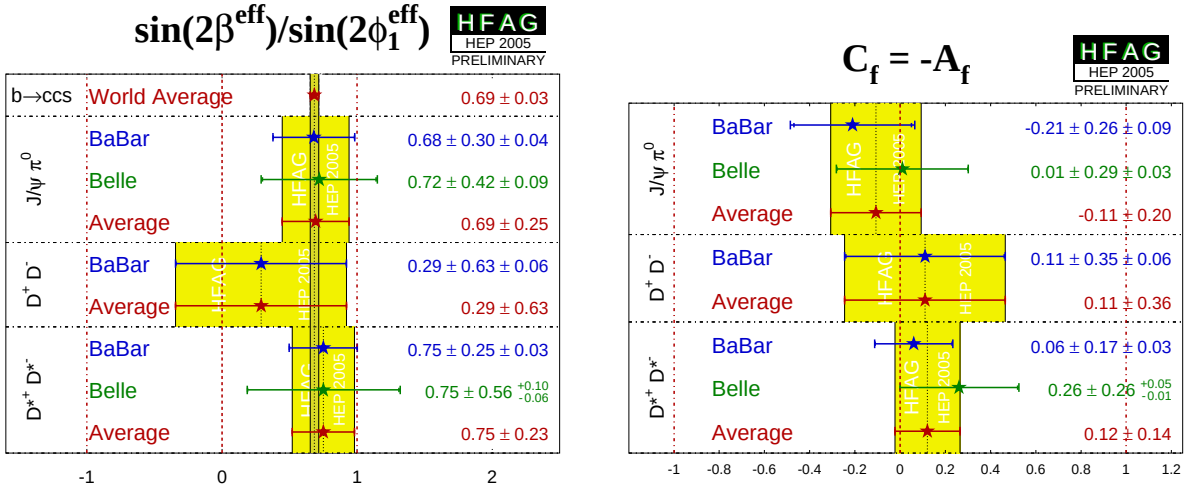

Figure 17: Averages of (left) $-\eta S_{b\to c\bar{c}d}$ and (right) $C_{b\to c\bar{c}d}$. The $-\eta S_{b\to q\bar{q}s}$ figure compares the results to the world average for $-\eta S_{b\to c\bar{c}s}$ (see Section 4.4).

Table 25: Averages for $b \to s\gamma$ modes. Note that the averages are calculated without taking correlations into account.

Experiment		$S_{b\to s\gamma}$	$C_{b\to s\gamma}$	Correlation
		$K^*(892)\gamma$		
BABAR	[178]	$-0.21 \pm 0.40 \pm 0.05$	$-0.40 \pm 0.23 \pm 0.04$	-0.064
Belle	[179]	$0.01 \pm 0.52 \pm 0.11$	$-0.11 \pm 0.33 \pm 0.09$	0.002
Average		-0.13 ± 0.32	-0.31 ± 0.19	
Confidence level		0.74 (0.3σ)	0.48 (0.7σ)	
		$K^0_S\pi^0\gamma$ (including $K^*(892)\gamma$)		
BABAR	[178]	-0.06 ± 0.37	-0.48 ± 0.22	
Belle	[179]	$0.08 \pm 0.41 \pm 0.10$	$-0.12 \pm 0.27 \pm 0.10$	0.004
Average		0.00 ± 0.28	-0.35 ± 0.17	
Confidence level		0.80 (0.3σ)	0.32 (1.0σ)	

$b \to s\gamma$ system (see Sec. 6).

4.10 Time-dependent *CP* asymmetries in $b \to u\bar{u}d$ transitions

The $b \to u\bar{u}d$ transition can be mediated by either a $b \to u$ tree amplitude or a $b \to d$ penguin amplitude. These transitions can be investigated using the time dependence of B^0 decays to final states containing light mesons. Results are available from both *BABAR* and Belle for the *CP* eigenstate ($\eta = +1$) $\pi^+\pi^-$ final state and for the vector-vector final state $\rho^+\rho^-$, which is found to be dominated by the *CP* even longitudinally polarized component (*BABAR* measure $f_{\rm long} = 0.978 \pm 0.014\,^{+0.021}_{-0.029}$ [183] while Belle measure $f_{\rm long} = 0.951\,^{+0.033}_{-0.039}\,^{+0.029}_{-0.031}$ [184]).

For the non-*CP* eigenstate $\rho^\pm\pi^\mp$, Belle has performed a quasi-two-body analysis, while *BABAR* performs a time-dependent Dalitz plot (DP) analysis of the $\pi^+\pi^-\pi^0$ final state [180];

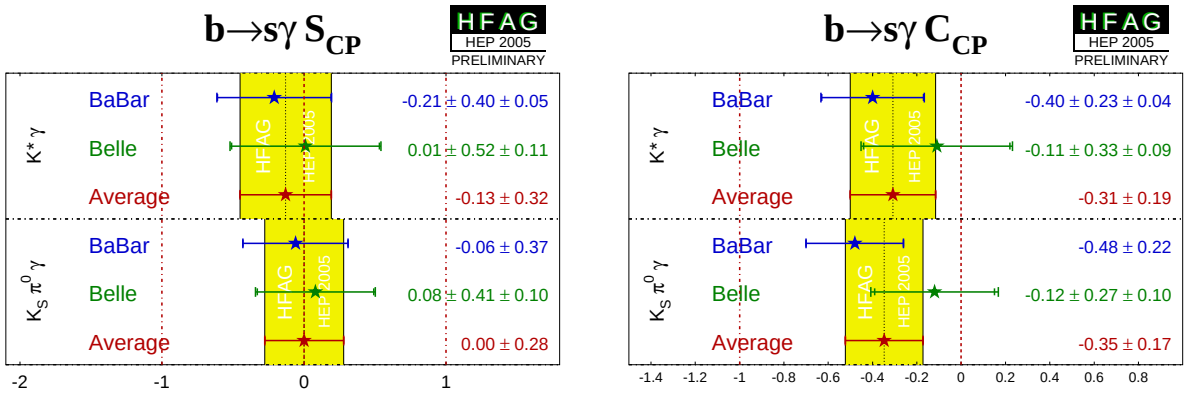

Figure 18: Averages of (left) $S_{b\to s\gamma}$ and (right) $C_{b\to s\gamma}$. Recall that the data for $K^*\gamma$ is a subset of that for $K^0_S\pi^0\gamma$.

such an analysis allows direct measurements of the phases. These results, and averages, are listed in Table 26. The averages for $\pi^+\pi^-$ are shown in Fig. 19.

If the penguin contribution is negligible, the time-dependent parameters for $B^0 \to \pi^+\pi^-$ and $B^0 \to \rho^+\rho^-$ are given by $S_{b\to u\overline{u}d} = \eta\sin(2\alpha)$ and $C_{b\to u\overline{u}d} = 0$. With the notation described in Sec. 4.2 (Eq. (90)), the time-dependent parameters for the Q2B $B^0 \to \rho^\pm\pi^\mp$ analysis are, neglecting penguin contributions, given by $S_{\rho\pi} = \sqrt{1-(\frac{\Delta C}{2})^2}\sin(2\alpha)\cos(\delta)$, $\Delta S_{\rho\pi} = \sqrt{1-(\frac{\Delta C}{2})^2}\cos(2\alpha)\sin(\delta)$ and $C_{\rho\pi} = \mathcal{A}^{\rho\pi}_{CP} = 0$, where $\delta = \arg(A_{-+}A^*_{+-})$ is the strong phase difference between the $\rho^-\pi^+$ and $\rho^+\pi^-$ decay amplitudes. In the presence of the penguin contribution, there is no straightforward interpretation of the Q2B observables in the $B^0 \to \rho^\pm\pi^\mp$ system in terms of CKM parameters. However direct CP violation may arise, resulting in either or both of $C_{\rho\pi} \neq 0$ and $\mathcal{A}^{\rho\pi}_{CP} \neq 0$. Equivalently, direct CP violation may be seen by either of the decay-type-specific observables $\mathcal{A}^{+-}_{\rho\pi}$ and $\mathcal{A}^{-+}_{\rho\pi}$, defined in Eq. (91), deviating from zero. Results and averages for these parameters are also given in Table 26. They exhibit a linear correlation coefficient of +0.59. The significance of observing direct CP violation computed from the difference of the χ^2 obtained in the nominal average, compared to setting $C_{\rho\pi} = \mathcal{A}^{\rho\pi}_{CP} = 0$ is found to be 3.4σ in this mode. The confidence level contours of $\mathcal{A}^{+-}_{\rho\pi}$ versus $\mathcal{A}^{-+}_{\rho\pi}$ are shown in Fig. 20.

Some difference is seen between the *BABAR* and Belle measurements in the $\pi^+\pi^-$ system. The confidence level of the average is 0.019, which corresponds to a 2.3σ discrepancy. Since there is no evidence of systematic problems in either analysis, we do not rescale the errors of the averages. The average for $S_{b\to u\overline{u}d}$ in $B^0 \to \pi^+\pi^-$ is more than 4σ away from zero, while that for $C_{b\to u\overline{u}d}$ is more than 3σ for zero. Due to the possible discrepancy mentioned above, only a cautious interpretation should be made. Nevertheless, the averages give (at least) a strong indication for CP violation in $B^0 \to \pi^+\pi^-$ (for which Belle has already claimed observation).

The precision of the measured CP violation parameters in $b \to u\overline{u}d$ transitions allows constraints to be set on the UT angle α. In addition to the value of α from the *BABAR* time-dependent DP analysis, given in Table 26, constraints have been obtained with various methods:

- Both *BABAR* [181] and Belle [182] have performed isospin analyses in the $\pi\pi$ system.

Table 26: Averages for $b \to u\overline{u}d$ modes.

Experiment		$S_{b\to u\overline{u}d}$	$C_{b\to u\overline{u}d}$	Correlation
		$\pi^+\pi^-$		
BABAR	[181]	$-0.30 \pm 0.17 \pm 0.03$	$-0.09 \pm 0.15 \pm 0.04$	-0.016
Belle	[182]	$-0.67 \pm 0.16 \pm 0.06$	$-0.56 \pm 0.12 \pm 0.06$	-0.09
Average		-0.50 ± 0.12	-0.37 ± 0.10	-0.056
Confidence level		combined average: 0.019 (2.3σ)		
		$\rho^+\rho^-$		
BABAR	[183]	$-0.33 \pm 0.24\,^{+0.08}_{-0.14}$	$-0.03 \pm 0.18 \pm 0.09$	-0.042
Belle	[184]	$0.09 \pm 0.42 \pm 0.08$	$0.00 \pm 0.30\,^{+0.09}_{-0.10}$	0.06
Average		-0.21 ± 0.22	-0.03 ± 0.17	0.01
Confidence level		combined average: xxx		

		$\rho^\pm\pi^\mp$ Q2B/DP analysis				
Experiment		$S_{\rho\pi}$	$C_{\rho\pi}$	$\Delta S_{\rho\pi}$	$\Delta C_{\rho\pi}$	$\mathcal{A}_{CP}^{\rho\pi}$
BABAR	[187]	$-0.10 \pm 0.14 \pm 0.04$	$0.34 \pm 0.11 \pm 0.05$	$0.22 \pm 0.15 \pm 0.03$	$0.15 \pm 0.11 \pm 0.03$	$-0.088 \pm 0.049 \pm 0.013$
Belle	[186]	$-0.28 \pm 0.23\,^{+0.10}_{-0.08}$	$0.25 \pm 0.17\,^{+0.02}_{-0.06}$	$-0.30 \pm 0.24 \pm 0.09$	$0.38 \pm 0.18\,^{+0.02}_{-0.04}$	$-0.16 \pm 0.10 \pm 0.02$
Average		-0.13 ± 0.13	0.31 ± 0.10	0.09 ± 0.13	0.22 ± 0.10	-0.102 ± 0.045
			$\mathcal{A}_{\rho\pi}^{+-}$		$\mathcal{A}_{\rho\pi}^{-+}$	
BABAR	[187]		$0.25 \pm 0.17\,^{+0.02}_{-0.06}$		$-0.47\,^{+0.14}_{-0.15} \pm 0.06$	
Belle	[186]		$-0.02 \pm 0.16\,^{+0.05}_{-0.02}$		$-0.53 \pm 0.29\,^{+0.09}_{-0.04}$	
Average			-0.15 ± 0.09		$-0.47\,^{+0.13}_{-0.14}$	

$\rho^\pm\pi^\mp$ DP analysis			
Experiment		α (°)	δ_{+-} (°)
BABAR	[187]	$113\,^{+27}_{-17} \pm 6$	$-67\,^{+28}_{-31} \pm 7$

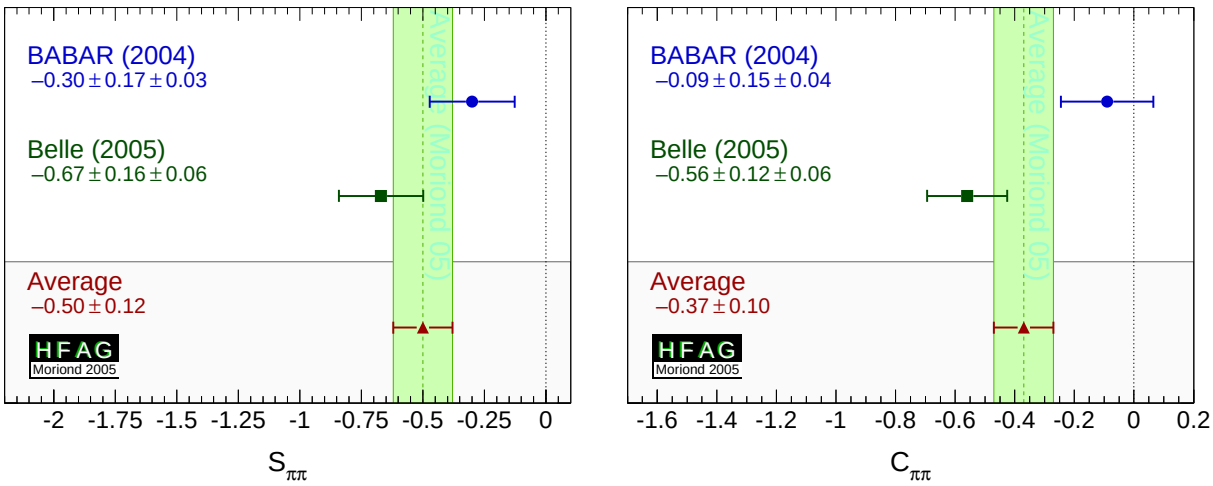

Figure 19: Averages of (left) $S_{b\to u\overline{u}d}$ and (right) $C_{b\to u\overline{u}d}$ for the mode $B^0 \to \pi^+\pi^-$.

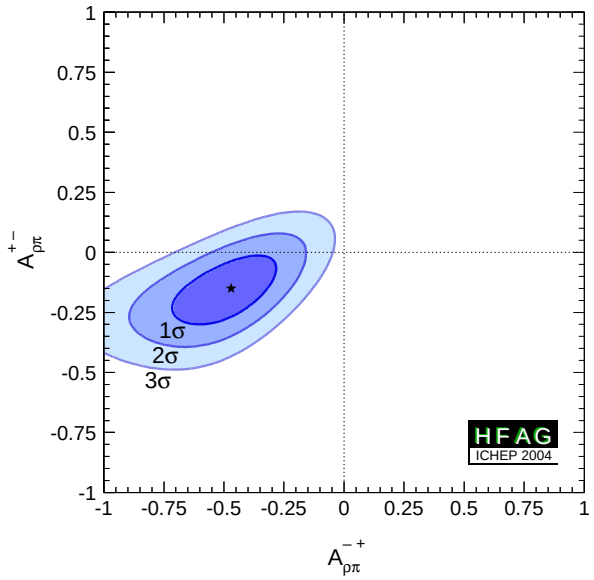

Figure 20: Direct *CP* violation in $B^0 \to \rho^\pm\pi^\mp$. The no-*CP* violation hypothesis is excluded at the 3.4σ level.

BABAR exclude $29° < \alpha < 61°$ at the 90% C.L. while Belle exclude $19° < \alpha < 71°$ at the 95.4% C.L. In both cases, only solutions in 0°–180° are considered.

- Both experiments have also performed isospin analyses in the $\rho\rho$ system. *BABAR* [183] obtain $\alpha = (100 \pm 13)°$, while Belle [184] obtain $\alpha = (87 \pm 17)°$. The largest contribution to the uncertainty is due to the possible penguin contribution, limited by the knowledge of the $B^0 \to \rho^0\rho^0$ branching fraction [189], and is correlated between the measurements.

- Each experiment has obtained a value of α from combining its results in the different $b \to u\overline{u}d$ modes (with some input also from HFAG). These values have appeared in talks, but not in publications, and are not listed here.

- The CKMfitter group [153] uses the measurements from Belle and *BABAR* given in Table 26, with other branching fractions and *CP* asymmetries in $B \to \pi\pi$, $\rho\pi$ and $\rho\rho$

Table 27: Averages for $b \to c\overline{u}d/u\overline{c}d$ modes.

Experiment		a	c
		$D^{*\pm}\pi^{\mp}$	
BABAR (full rec.)	[191]	$-0.043 \pm 0.023 \pm 0.010$	$0.047 \pm 0.042 \pm 0.015$
Belle (full rec.)	[192]	$0.060 \pm 0.040 \pm 0.019$	$0.049 \pm 0.040 \pm 0.019$
BABAR (partial rec.)	[193]	$-0.034 \pm 0.014 \pm 0.009$	$-0.019 \pm 0.022 \pm 0.013$
Belle (partial rec.)	[194]	$-0.030 \pm 0.028 \pm 0.018$	$-0.005 \pm 0.028 \pm 0.018$
Average		-0.028 ± 0.012	0.004 ± 0.017
Confidence level		0.22 (1.2σ)	0.42 (0.8σ)
		$D^{\pm}\pi^{\mp}$	
BABAR (full rec.)	[191]	$-0.013 \pm 0.022 \pm 0.007$	$-0.043 \pm 0.042 \pm 0.011$
Belle (full rec.)	[192]	$-0.062 \pm 0.037 \pm 0.018$	$-0.025 \pm 0.037 \pm 0.018$
Average		-0.025 ± 0.020	-0.034 ± 0.030
Confidence level		0.30 (1.0σ)	0.76 (0.3σ)
		$D^{\pm}\rho^{\mp}$	
BABAR (full rec.)	[191]	$-0.024 \pm 0.031 \pm 0.010$	$-0.098 \pm 0.055 \pm 0.019$
Average		-0.024 ± 0.033	-0.098 ± 0.058

modes, to perform isospin analyses for each system. They then combine the results to obtain $\alpha = (98.6\,^{+12.6}_{-8.1})^{\circ}$. A similar analysis is performed by the UTFit group [154].

Note that each method suffers from ambiguities in the solutions. The model assumption in the $B^0 \to \pi^+\pi^-\pi^0$ analysis allows to resolve some of the multiple solutions, and results in a single preferred value for α in $[0, \pi]$. All the above measurements correspond to the choice that is in agreement with the global CKM fit.

At present we make no attempt to provide an HFAG average for α. More details on procedures to calculate a best fit value for α can be found in Refs. [153, 154].

4.11 Time-dependent *CP* asymmetries in $b \to c\overline{u}d/u\overline{c}d$ transitions

Non-*CP* eigenstates such as $D^{\pm}\pi^{\mp}$, $D^{*\pm}\pi^{\mp}$ and $D^{\pm}\rho^{\mp}$ can be produced in decays of B^0 mesons either via Cabibbo favoured ($b \to c$) or doubly Cabibbo suppressed ($b \to u$) tree amplitudes. Since no penguin contribution is possible, these modes are theoretically clean. The ratio of the magnitudes of the suppressed and favoured amplitudes, R, is sufficiently small (predicted to be about 0.02), that terms of $\mathcal{O}(R^2)$ can be neglected, and the sine terms give sensitivity to the combination of UT angles $2\beta + \gamma$.

As described in Sec. 4.2.5, the averages are given in terms of parameters a and c. *CP* violation would appear as $a \neq 0$. Results are available from both *BABAR* and Belle in the modes $D^{\pm}\pi^{\mp}$ and $D^{*\pm}\pi^{\mp}$; for the latter mode both experiments have used both full and partial reconstruction techniques. Results are also available from *BABAR* using $D^{\pm}\rho^{\mp}$. These results, and their averages, are listed in Table 27, and are shown in Fig. 21. The constraints in c *vs.* a space for the $D\pi$ and $D^*\pi$ modes are shown in Fig. 22.

For each of $D\pi$, $D^*\pi$ and $D\rho$, there are two measurements (a and c, or S^+ and S^-) which depend on three unknowns (R, δ and $2\beta + \gamma$), of which two are different for each decay mode.

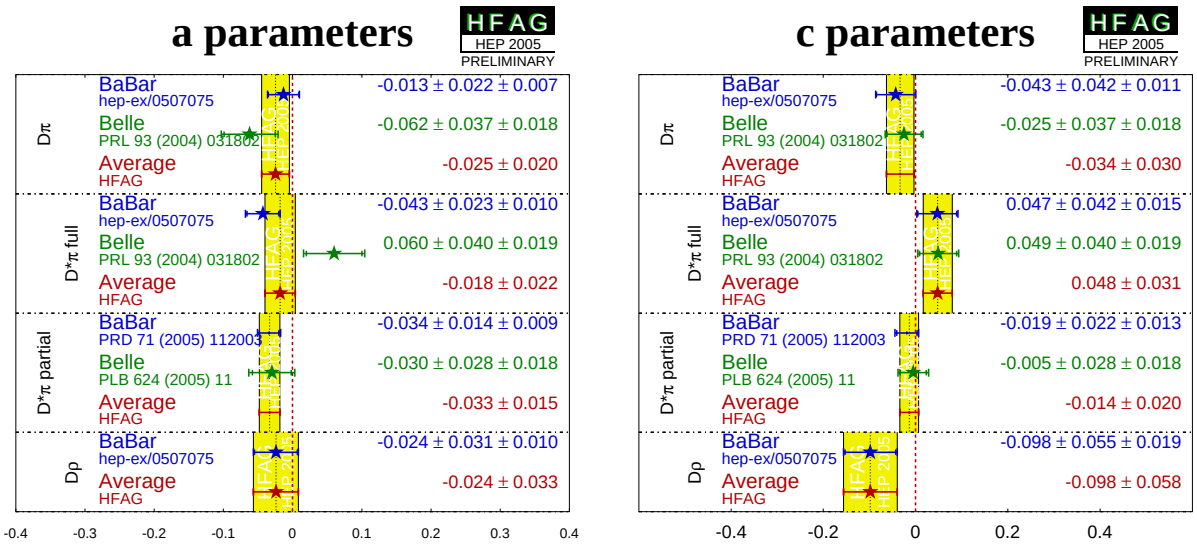

Figure 21: Averages for $b \to c\overline{u}d/u\overline{c}d$ modes.

Therefore, there is not enough information to solve directly for $2\beta + \gamma$. However, for each choice of R and $2\beta + \gamma$, one can find the value of δ that allows a and c to be closest to their measured values, and calculate the distance in terms of numbers of standard deviations. (We currently neglect experimental correlations in this analysis.) These values of $N(\sigma)_{\rm min}$ can then be plotted as a function of R and $2\beta + \gamma$ (and can trivially be converted to confidence levels). These plots are given for the $D\pi$ and $D^*\pi$ modes in Figure 22; the uncertainties in the $D\rho$ mode are currently too large to give any meaningful constraint.

The constraints can be tightened if one is willing to use theoretical input on the values of R and/or δ. One popular choice is the use of SU(3) symmetry to obtain R by relating the suppressed decay mode to B decays involving D_s mesons. More details can be found in Refs. [153, 154].

4.12 Rates and asymmetries in $B^\mp \to D^{(*)}K^{(*)\mp}$ decays

As explained in Sec. 4.2.6, rates and asymmetries in $B^\mp \to D^{(*)}K^{(*)\mp}$ decays are sensitive to γ. Various methods using different $D^{(*)}$ final states exist.

Results are available from both *BABAR* and Belle on GLW analyses in the decay modes $B^\mp \to DK^\mp$, $B^\mp \to D^*K^\mp$ and $B^\mp \to DK^{*\mp}$. Both experiments use the CP even D decay final states K^+K^- and $\pi^+\pi^-$ in all three modes; both experiments also use only the $D^* \to D\pi^0$ decay, which gives $CP(D^*) = CP(D)$. For CP odd D decay final states, Belle uses $K^0_S\pi^0$, $K^0_S\eta$ and $K^0_S\phi$ in all three analyses, and also use $K^0_S\omega$ in $DK^\mp$ and $D^*K^\mp$ analyses. *BABAR* uses $K^0_S\pi^0$ only for $DK^\mp$ analysis; for $DK^{*\mp}$ analysis they also use $K^0_S\phi$ and $K^0_S\omega$ (and assign an asymmetric systematic error due to CP even pollution in these CP odd channels [199]). The results and averages are given in Table 28 and shown in Fig. 23.

For ADS analysis, both *BABAR* and Belle have studied the mode $B^\mp \to DK^\mp$; Belle has also studied $B^\mp \to D\pi^\mp$ and *BABAR* has also analyzed the $B^\mp \to D^*K^\mp$ and $B^\mp \to DK^{*\mp}$ modes ($D^* \to D\pi^0$ and $D^* \to D\gamma$ are studied separately; $K^{*\mp}$ is reconstructed as $K^0_S\pi^\mp$). In

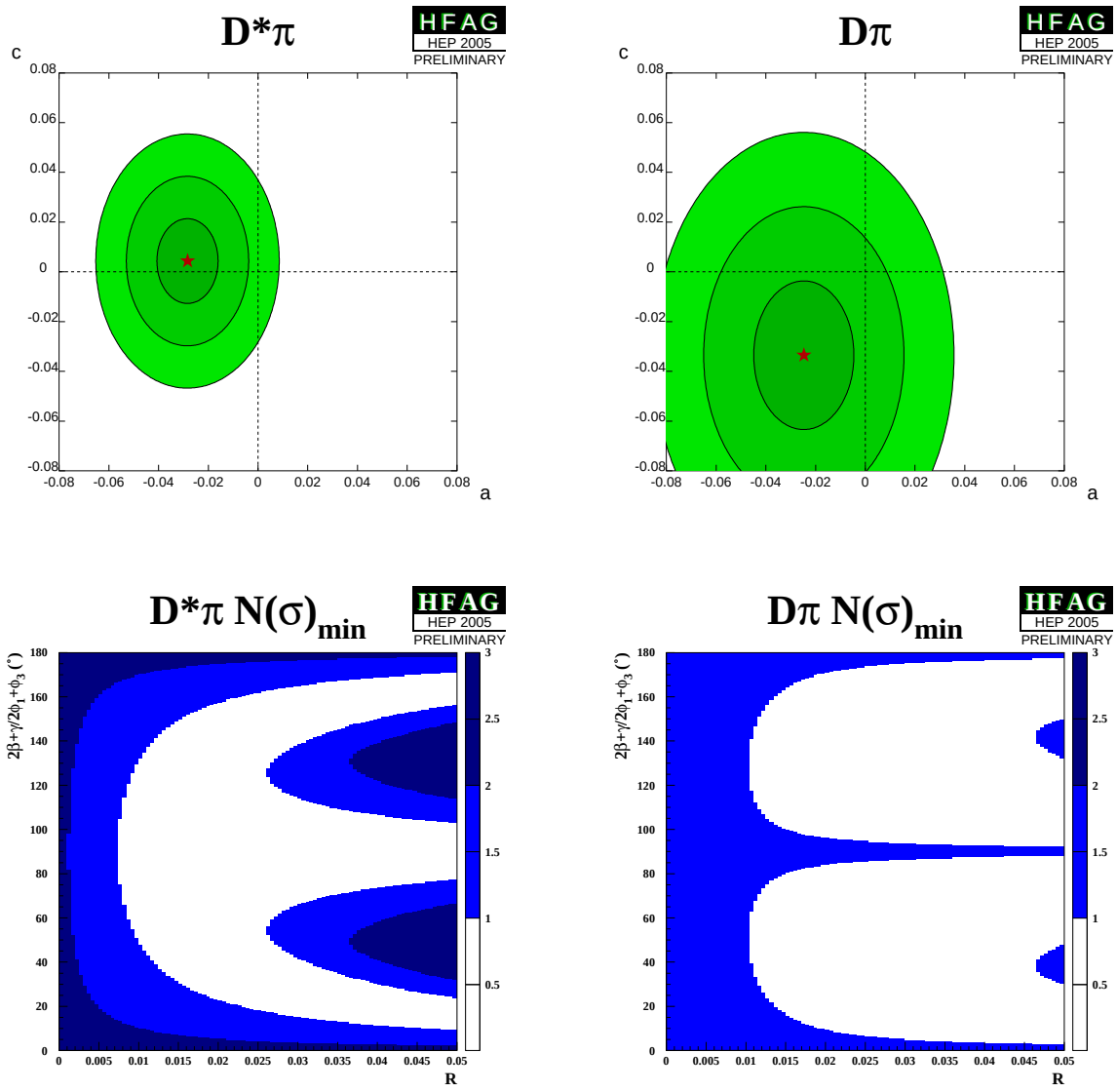

Figure 22: Results from $b \to c\bar{u}d/u\bar{c}d$ modes. (Top) Constraints in c *vs.* a space. (Bottom) Constraints in $2\beta + \gamma$ *vs.* R space. (Left) $D^*\pi$ and (right) $D\pi$ modes.

all cases the suppressed decay $D \to K^+\pi^-$ has been used. The results and averages are given in Table 29 and shown in Fig. 24. Note that although no clear signals for these modes have yet been seen, the central values are given. In $B^- \to D^*K^-$ decays there is an effective shift of π in the strong phase difference between the cases that the D^* is reconstructed as $D\pi^0$ and $D\gamma$ [145]. As a consequence, the different D^* decay modes are treated separately.

For the Dalitz plot analysis, both *BABAR* and Belle have studied the modes $B^\mp \to DK^\mp$, $B^\mp \to D^*K^\mp$ and $B^\mp \to DK^{*\mp}$. For $B^\mp \to D^*K^\mp$, Belle has used only $D^* \to D\pi^0$, while *BABAR* has used both D^* decay modes and taken the effective shift in the strong phase difference into account. In all cases the decay $D \to K^0_S\pi^+\pi^-$ has been used. Results are given in Table 30.

The parameters measured in the different analyses are explained in Sec. 4.2.6. Belle directly extract γ, r_B and δ_B for each decay mode and perform a frequentist statistical procedure to correct for bias originating from the positive definite nature of r_B. Results from $DK^\mp$ and

Table 28: Averages from GLW analyses of $b \to c\overline{u}s/u\overline{c}s$ modes.

Experiment	A_{CP+}	A_{CP-}	R_{CP+}	R_{CP-}
		$D_{CP}K^-$		
BABAR [197]	$0.35 \pm 0.13 \pm 0.04$	$0.06 \pm 0.13 \pm 0.04$	$0.90 \pm 0.12 \pm 0.04$	$0.86 \pm 0.10 \pm 0.05$
Belle [198]	$0.06 \pm 0.14 \pm 0.05$	$-0.12 \pm 0.14 \pm 0.05$	$1.13 \pm 0.16 \pm 0.08$	$1.17 \pm 0.14 \pm 0.14$
Average	0.22 ± 0.10	-0.09 ± 0.10	0.98 ± 0.10	0.94 ± 0.10
		$D^*_{CP}K^-$		
BABAR [199]	$-0.10 \pm 0.23\,^{+0.03}_{-0.04}$		$1.06 \pm 0.26\,^{+0.10}_{-0.09}$	
Belle [198]	$-0.20 \pm 0.22 \pm 0.04$	$0.13 \pm 0.30 \pm 0.08$	$1.41 \pm 0.25 \pm 0.06$	$1.15 \pm 0.31 \pm 0.12$
Average	-0.15 ± 0.16	0.13 ± 0.31	1.25 ± 0.19	1.15 ± 0.33
		$D_{CP}K^{*-}$		
BABAR [200]	$-0.08 \pm 0.19 \pm 0.08$	$-0.26 \pm 0.40 \pm 0.12$	$1.96 \pm 0.40 \pm 0.11$	$0.65 \pm 0.26 \pm 0.08$
Belle [201]	$-0.02 \pm 0.33 \pm 0.07$	$0.19 \pm 0.50 \pm 0.04$		
Average	-0.06 ± 0.18	-0.08 ± 0.32	1.96 ± 0.41	0.65 ± 0.27

Table 29: Averages from ADS analyses of $b \to c\overline{u}s/u\overline{c}s$ and $b \to c\overline{u}d/u\overline{c}d$ modes.

Experiment		$A_{\rm ADS}$	$R_{\rm ADS}$
		DK^-, $D \to K^+\pi^-$	
BABAR	[202]		$0.013\,^{+0.011}_{-0.009}$
Belle	[203]		$0.000 \pm 0.008 \pm 0.001$
Average			0.006 ± 0.006
		D^*K^-, $D^* \to D\pi^0$, $D \to K^+\pi^-$	
BABAR	[202]		$-0.002\,^{+0.010}_{-0.006}$
		D^*K^-, $D^* \to D\gamma$, $D \to K^+\pi^-$	
BABAR	[202]		$0.011\,^{+0.018}_{-0.013}$
		DK^{*-}, $D \to K^+\pi^-$, $K^{*-} \to K^0_S\pi^-$	
BABAR	[204]	$-0.22 \pm 0.61 \pm 0.17$	$0.046 \pm 0.031 \pm 0.008$
		$D\pi^-$, $D \to K^+\pi^-$	
Belle	[203]	$0.10 \pm 0.22 \pm 0.06$	$0.0035\,^{+0.0008}_{-0.0007} \pm 0.0003$

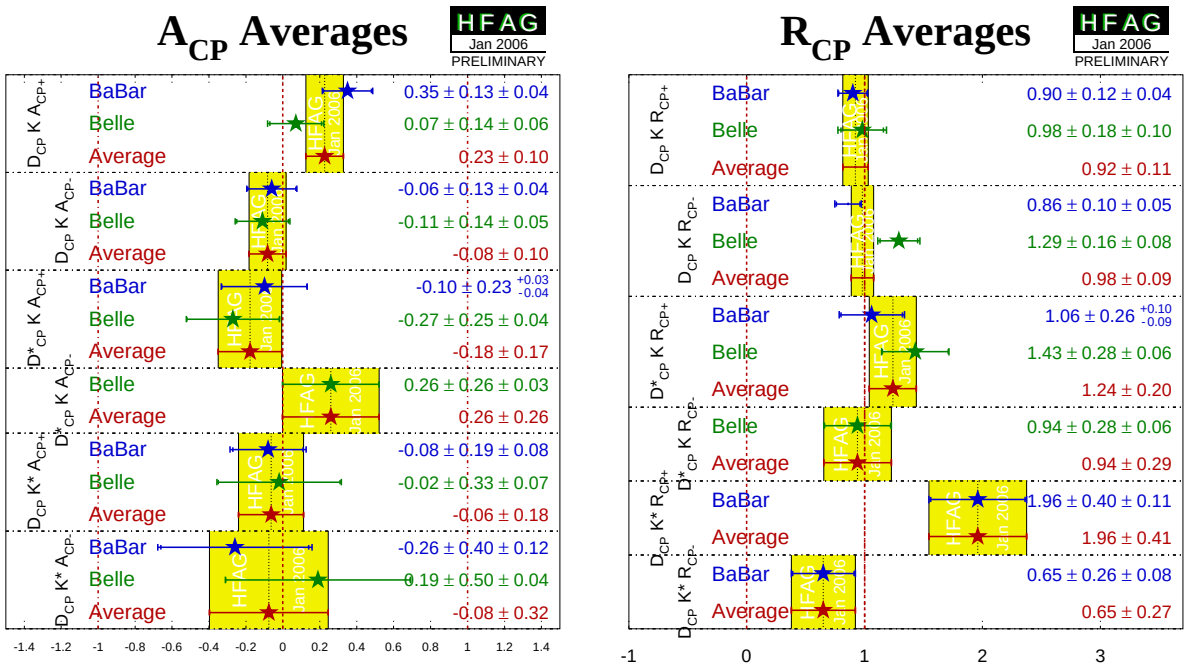

Figure 23: Averages of A_{CP} and R_{CP} from GLW analyses.

$D^*K^{\mp}$ are used to obtain a combined value of γ; results for $DK^{*\mp}$ are not currently included in this procedure. *BABAR* measure the $(x_{\pm}, y_{\pm})$ variables, and perform a frequentist statistical procedure, using all three B decay modes, to convert these into measurements of γ, r_B and δ_B.

Both experiments reconstruct $K^{*\mp}$ as $K^0_S\pi^{\mp}$, but the treatment of possible nonresonant $K^0_S\pi^{\mp}$ differs: Belle assign an additional model uncertainty, while *BABAR* use a reparametrization suggested by Gronau [205]. The parameters r_B and δ_B are replaced with effective parameters κr_s and δ_s; no attempt is made to extract the true hadronic parameters of the $B^{\mp} \to DK^{*\mp}$ decay.

At present, we make no attempt to average the results of the Dalitz plot analyses. Additionally, we have not attempted to combine the results of the GLW, ADS and Dalitz analyses in order to obtain the most precise determination of γ (and associated parameters, such as r_B). Such attempts have been made by the CKMfitter and UTFit groups; see Refs. [153, 154].

Table 30: Averages from Dalitz plot analyses of $b \to c\overline{u}s/u\overline{c}s$ modes.

Experiment	x_+	y_+	x_-	y_-
		DK^-, $D \to K^0_S\pi^+\pi^-$		
BABAR [206]		$0.02 \pm 0.08 \pm 0.02 \pm 0.02$		$0.06 \pm 0.09 \pm 0.04 \pm 0.04$
	$-0.13 \pm 0.07 \pm 0.03 \pm 0.03$		$0.08 \pm 0.07 \pm 0.03 \pm 0.02$	
		D^*K^-, $D^* \to D\pi^0$ & $D\gamma$, $D \to K^0_S\pi^+\pi^-$		
BABAR [206]		$0.01 \pm 0.12 \pm 0.04 \pm 0.06$		$-0.14 \pm 0.11 \pm 0.02 \pm 0.03$
	$0.14 \pm 0.09 \pm 0.03 \pm 0.03$		$-0.13 \pm 0.09 \pm 0.03 \pm 0.02$	
		DK^{*-}, $D \to K^0_S\pi^+\pi^-$, $K^{*-} \to K^0_S\pi^-$		
BABAR [206]		$-0.01 \pm 0.32 \pm 0.18 \pm 0.05$		$0.26 \pm 0.30 \pm 0.16 \pm 0.03$
	$-0.07 \pm 0.23 \pm 0.13 \pm 0.03$		$-0.20 \pm 0.20 \pm 0.11 \pm 0.03$	

Experiment	γ (°)	δ_B (°)	r_B
		DK^-, $D \to K^0_S\pi^+\pi^-$	
BABAR [206]		$104 \pm 45\,^{+17}_{-21}\,^{+16}_{-24}$	$0.12 \pm 0.08 \pm 0.03 \pm 0.04$
Belle [207]	$64 \pm 19 \pm 13 \pm 11$	$157 \pm 19 \pm 11 \pm 21$	$0.21 \pm 0.08 \pm 0.03 \pm 0.04$
Average		IN PREPARATION	
		D^*K^-, $D^* \to D\pi^0$ or $D\gamma$, $D \to K^0_S\pi^+\pi^-$	
BABAR [206]		$296 \pm 41\,^{+14}_{-12} \pm 15$	$0.17 \pm 0.10 \pm 0.03 \pm 0.03$
Belle [207]	$75 \pm 57 \pm 11 \pm 11$	$321 \pm 57 \pm 11 \pm 21$	$0.12\,^{+0.16}_{-0.11} \pm 0.02 \pm 0.04$
Average		IN PREPARATION	
		DK^{*-}, $D \to K^0_S\pi^+\pi^-$	
Belle [208]	$112 \pm 35 \pm 9 \pm 11 \pm 8$	$353 \pm 35 \pm 8 \pm 21 \pm 49$	$0.25 \pm 0.18 \pm 0.09 \pm 0.04 \pm 0.08$
		DK^- and D^*K^- combined	
Belle [207]	$68\,^{+14}_{-15} \pm 13 \pm 11$		
		DK^-, D^*K^- and DK^{*-} combined	
BABAR [206]	$67 \pm 28 \pm 13 \pm 11$		

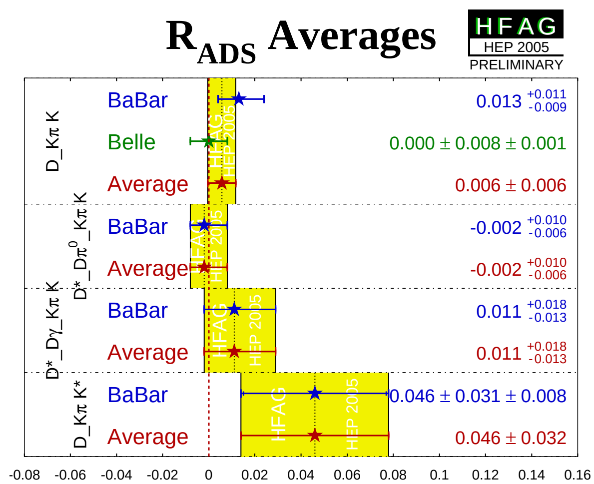

Figure 24: Averages of R_{ADS}.

5 Semileptonic B decays

Major updates of $|V_{ub}|$ in both inclusive and exclusive B decays have been made since the last HFAG document [4], and are described here in detail.

The determination of $|V_{ub}|$ from inclusive decays involves intense ongoing activity in both experiment and theory. HFAG subgroups have recently determined updated values for the heavy quark parameters m_b and μ_π^2 based on moments measured in inclusive $\overline{B} \to X_c \ell \overline{\nu}$ and $\overline{B} \to X_s \gamma$ decays. In addition, the theoretical tools have improved and have been incorporated by the experiments. A comprehensive determination of $|V_{ub}|$ from inclusive decays based on the results presented at the 2005 summer conferences is given below.

Several new measurements of the exclusive decay $\overline{B} \to \pi \ell \overline{\nu}$ were presented at the 2005 Summer conferences. Their precision is at a level that calls for improved calculations of the form factors and in particular their normalization. An average of these results and the subsequent determination of $|V_{ub}|$ is discussed below.

In the following, brief descriptions of all parameters and analyses (published or preliminary) relevant for the determination of the combined results are given. The description is based on the information available on the web page at

`http://www.slac.stanford.edu/xorg/hfag/semi/eps05/eps05.shtml`

The values for $|V_{ub}|$ from inclusive decays have been updated relative to the web page using the current HFAG value of the average B meson lifetime: $\langle \tau_B \rangle = 1.585 \pm 0.007$ ps.

5.1 Methodology

The method for extracting averages is described in section 2. In the following, the method has been extended to take into account the fact that measurement errors often depend on the measured value, i.e. are relative errors. Furthermore, an effort has been made to separate statistical, and different sources of systematic and theoretical errors.

For measurements with Gaussian errors, the usual estimator for the average of a set of measurements is obtained by minimizing the following χ^2:

$$\chi^2(t) = \sum_i^N \frac{(y_i - t)^2}{\sigma_i^2}, \tag{109}$$

where y_i is the measured value for input i and σ_i^2 is the variance of the distribution from which y_i was drawn. The value $\hat{t}$ of t at minimum χ^2 is our estimator for the average. (This discussion is given for independent measurements for the sake of simplicity; the generalization to correlated measurements is straightforward, and has been used when averaging results.) The true σ_i are unknown but typically the error as assigned by the experiment $\sigma_i^{\rm raw}$ is used as an estimator for it. Caution is advised, however, in the case where $\sigma_i^{\rm raw}$ depends on the value measured for y_i. Examples of this include an uncertainty in any multiplicative factor (like an acceptance) that enters the determination of y_i, i.e. the $\sqrt{N}$ dependence of Poisson statistics, where $y_i \propto N$ and $\sigma_i \propto \sqrt{N}$. Failing to account for this type of dependence when averaging leads to a biased average. Biases in the average can be avoided (or at least reduced) by minimizing the following χ^2:

$$\chi^2(t) = \sum_i^N \frac{(y_i - t)^2}{\sigma_i^2(\hat{t})}. \tag{110}$$

In the above $\sigma_i(\hat{t})$ is the uncertainty assigned to input i that includes the assumed dependence of the stated error on the value measured. As an example, consider a pure acceptance error, for which $\sigma_i(\hat{t}) = (\hat{t}/y_i) \times \sigma_i^{\rm raw}$. It is easily verified that solving Eq. 110 leads to the correct behavior, namely

$$\hat{t} = \frac{\sum_i^N y_i^3/(\sigma_i^{\rm raw})^2}{\sum_i^N y_i^2/(\sigma_i^{\rm raw})^2},$$

i.e. weighting by the inverse square of the fractional uncertainty, $\sigma_i^{\rm raw}/y_i$.

It is sometimes difficult to assess the dependence of $\sigma_i^{\rm raw}$ on $\hat{t}$ from the errors quoted by experiments. As a result, the sensitivity to different assumptions on these dependences has been studied for the averages given in this section.

Another issue that needs careful treatment is the question of correlation among different measurements, e.g. due to using the same theory for calculating acceptances. A common practice is to set the correlation coefficient to unity to indicate full correlation. However, this is not a "conservative" thing to do, and can in fact lead to a significantly underestimated uncertainty on the average. In the absence of better information, the most conservative choice of correlation coefficient between two measurements i and j is the one that maximizes the uncertainty on $\hat{t}$ due to that pair of measurements:

$$\sigma^2_{\hat{t}(i,j)} = \frac{\sigma_i^2\,\sigma_j^2\,(1-\rho_{ij}^2)}{\sigma_i^2+\sigma_j^2-2\,\rho_{ij}\,\sigma_i\,\sigma_j}, \tag{111}$$

namely

$$\rho_{ij} = \min\left(\frac{\sigma_i}{\sigma_j}, \frac{\sigma_j}{\sigma_i}\right), \tag{112}$$

which corresponds to setting $\sigma^2_{\hat{t}(i,j)} = \min(\sigma_i^2, \sigma_j^2)$. Setting $\rho_{ij} = 1$ when $\sigma_i \neq \sigma_j$ can lead to a significant underestimate of the uncertainty on $\hat{t}$, as can be seen from Eq. 111.

Finally, a note on the breakdown of the error sources contributing to the overall uncertainty on the average. The overall covariance matrix is constructed from a number of individual sources, e.g. $\mathbf{V} = \mathbf{V_{stat}} + \mathbf{V_{sys}} + \mathbf{V_{th}}$. The variance on the average $\hat{t}$ can be written

$$\sigma^2_{\hat{t}} \;=\; \frac{\sum_{i,j}\left(\mathbf{V^{-1}}\left[\mathbf{V_{stat}}+\mathbf{V_{sys}}+\mathbf{V_{th}}\right]\mathbf{V^{-1}}\right)_{ij}}{\left(\sum_{i,j} V_{ij}^{-1}\right)^2} = \sigma^2_{stat}+\sigma^2_{sys}+\sigma^2_{th}. \tag{113}$$

Written in this form, one can readily determine the contribution of each source of uncertainty to the overall uncertainty on the average. This breakdown of the uncertainties is used below.

5.2 Exclusive Cabibbo-favored decays

There were no major updates in this area; the reader is referred to the averages given in Ref. [4].

5.3 Inclusive Cabibbo-favored decays

Aspects of the theory and phenomenology of inclusive Cabibbo-favored B decays and their use in the determination of $|V_{cb}|$ in the context of the Heavy Quark Expansion (HQE), an Operator Product Expansion based on HQET, are described in many places [209].

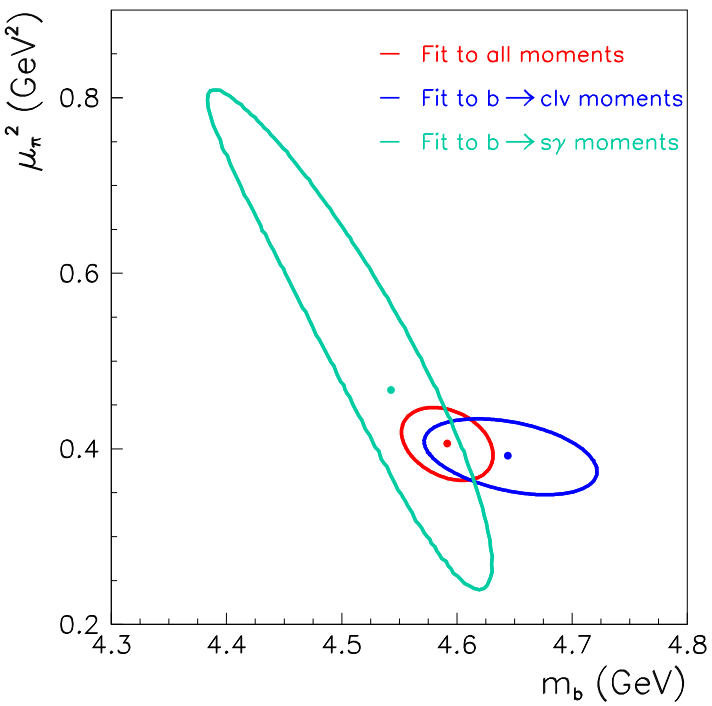

Figure 25: Results of HQE fits to moments in $\overline{B} \to X_s\gamma$ and $\overline{B} \to X_c\ell\overline{\nu}$ decays from Ref. [223]. The quantities shown are in the kinetic mass scheme.

Updated values for the parameters m_b and μ_π^2 are used below in the determination of $|V_{ub}|$ from inclusive decays. These are taken from a fit to energy and mass moments in $\overline{B} \to X_c\ell\overline{\nu}$ decays [210–218] and to photon energy moments in $\overline{B} \to X_s\gamma$ decays [219–222] in the "kinetic" mass scheme [223]. The fit results are shown in Fig. 25. These values are translated into the shape-function mass scheme [224, 225] for use in the extraction of $|V_{ub}|$, giving $m_b(\mathrm{SF}) = 4.60 \pm 0.04$ GeV and $\mu_\pi^2(\mathrm{SF}) = 0.20 \pm 0.04$ GeV^2 with correlation coefficient -0.26. Similar fits in other mass schemes, e.g. the "1S" scheme [226], have not yet been updated to include the latest measurements; that work is in progress. Once it is complete the full set of parameters (including $|V_{cb}|$ and the $\mathcal{B}(\overline{B} \to X\ell\overline{\nu})$) will be given. Previously published fits in this area can be found in Refs. [226–229]). For an average of the total semileptonic branching fraction the reader is referred to Ref. [4].

5.4 Exclusive Cabibbo-suppressed decays

Here we list results on exclusive semileptonic branching fractions and determinations of $|V_{ub}|$ based on $\overline{B} \to \pi\ell\overline{\nu}$ decays. The measurements are based on two different event selections: Tagged events, in which case the second B meson in the event is fully reconstructed in either a hadronic decay or in a Cabibbo-favored semileptonic decay; and Untagged events, in which case the selection infers the momentum of the undetected neutrino based on measurements of the total momentum sum of detected particles and knowledge of the initial state. The results for the full and partial branching fraction are given in Table 31 and shown in Fig. 26.

When averaging these results, systematic uncertainties due to external inputs, e.g. form factor shapes and background estimates from the modeling of $\overline{B} \to X_c \ell \overline{\nu}$ and $\overline{B} \to X_u \ell \overline{\nu}$ decays, are treated as fully correlated (in the sense of Eq. 112). Uncertainties due to experimental reconstruction effects are treated as fully correlated among measurements from a given experiment. Varying the assumed dependence of the quoted errors on the measured value (see Eq. 110) for error sources where the dependence was not obvious had no significant impact.

Table 31: Summary of exclusive determinations of $\mathcal{B}(\overline{B} \to \pi \ell \overline{\nu})$. The errors quoted correspond to statistical and systematic uncertainties, respectively. Measured branching fractions for $B \to \pi^0 l \nu$ have been multiplied by $2 \times \tau_{B^0}/\tau_{B^+}$ in accordance with isospin symmetry.

	$\mathcal{B}[10^{-4}]$	$\mathcal{B}(q^2 > 16\,\mathrm{GeV}^2/c^2)[10^{-4}]$
CLEO π^+, π^0 [230]	$1.32 \pm 0.18 \pm 0.13$	$0.25 \pm 0.09 \pm 0.05$
BABAR π^+, π^0 [231]	$1.38 \pm 0.10 \pm 0.18$	$0.49 \pm 0.05 \pm 0.06$
Average of untagged	$1.35 \pm 0.10 \pm 0.14$	$0.40 \pm 0.05 \pm 0.05$
BELLE SL π^+ [232]	$1.48 \pm 0.20 \pm 0.16$	$0.40 \pm 0.12 \pm 0.05$
BELLE SL π^0 [232]	$1.40 \pm 0.24 \pm 0.16$	$0.41 \pm 0.15 \pm 0.04$
BABAR SL π^+ [233]	$1.03 \pm 0.25 \pm 0.13$	$0.21 \pm 0.14 \pm 0.05$
BABAR SL π^0 [234]	$3.31 \pm 0.68 \pm 0.42$	n/a
BABAR had π^+ [235]	$1.14 \pm 0.27 \pm 0.17$	$0.70 \pm 0.22 \pm 0.11$
BABAR had π^0 [235]	$1.60 \pm 0.41 \pm 0.22$	$0.46 \pm 0.20 \pm 0.04$
Average of tagged	$1.34 \pm 0.11 \pm 0.09$	$0.38 \pm 0.07 \pm 0.04$
Average	$1.34 \pm 0.08 \pm 0.08$	$0.40 \pm 0.04 \pm 0.04$

The determination of $|V_{ub}|$ from the $\overline{B} \to \pi \ell \overline{\nu}$ decays is shown in Table 32 and uses our average for branching fraction given in Table 31. Two theoretical approaches are used: unquenched ($N_f = 2 + 1$) Lattice QCD and QCD sum rules. Lattice calculations of the FF are limited to small hadron momenta, i.e. large q^2, while calculations based on light cone sum rules are restricted to small q^2. More precise calculations of the FF, in particular their normalization, are needed to reduce the overall uncertainties.

Table 32: Determinations of $|V_{ub}|$ based on the average total and partial $\overline{B} \to \pi \ell \overline{\nu}$ decay branching fraction stated in Table 31.The first uncertainty is experimental, the second theoretical. The full or partial $\mathcal{B}$ are used as indicated.

Method	$\lvert V_{ub}\rvert[10^{-3}]$
LCSR, full q^2 [236]	$3.36 \pm 0.15^{+0.66}_{-0.41}$
LCSR, $q^2 < 16\,\mathrm{GeV}^2/c^2$ [236]	$3.25 \pm 0.17^{+0.54}_{-0.36}$
HPQCD, full q^2 [237]	$3.92 \pm 0.17^{+0.76}_{-0.48}$
HPQCD, $q^2 > 16\,\mathrm{GeV}^2/c^2$ [237]	$4.44 \pm 0.30^{+0.67}_{-0.46}$
FNAL, full q^2 [238]	$3.74 \pm 0.16^{+0.86}_{-0.51}$
FNAL, $q^2 > 16\,\mathrm{GeV}^2/c^2$ [238]	$3.76 \pm 0.25^{+0.65}_{-0.43}$

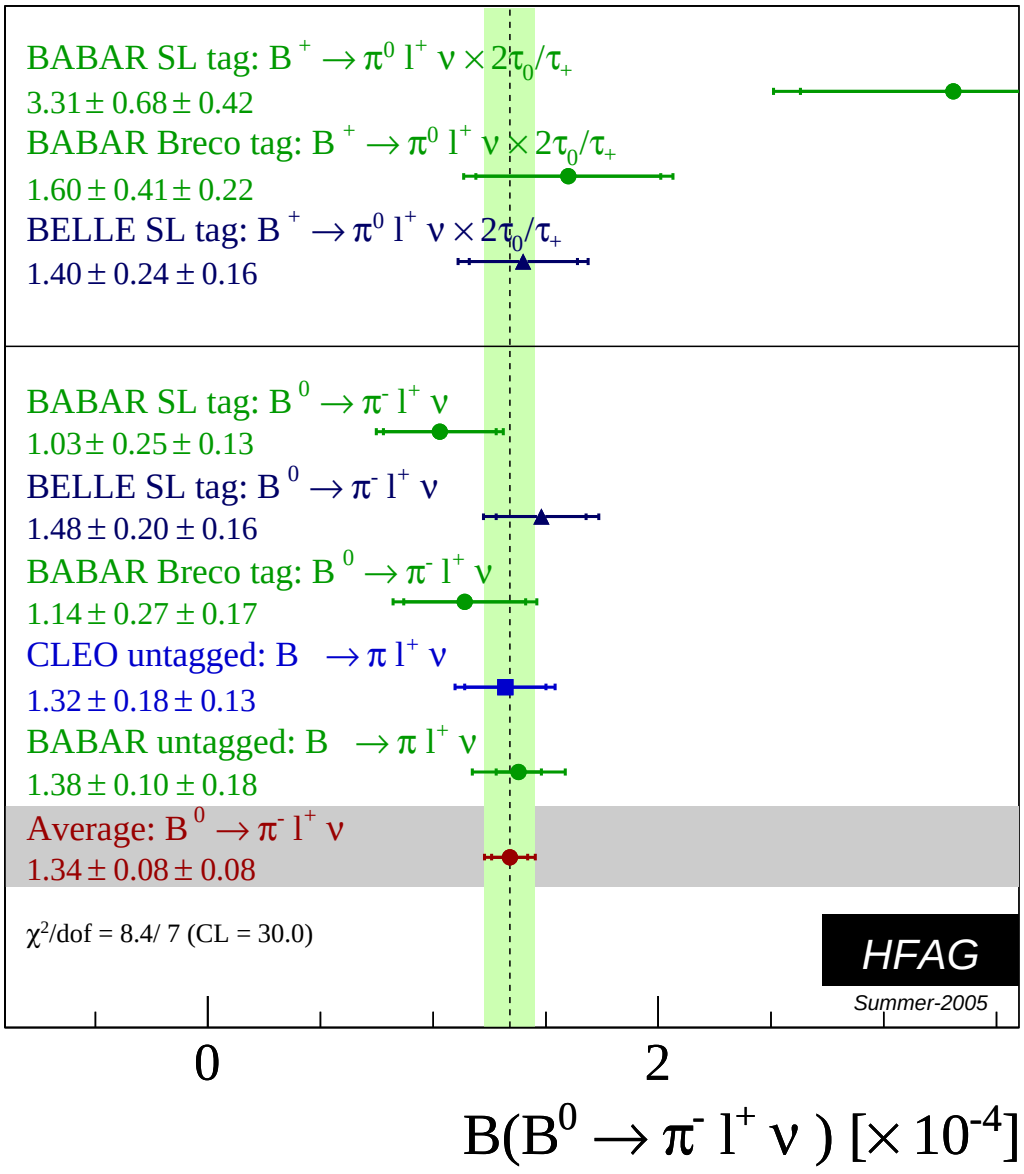

Figure 26: Measurements of $\mathcal{B}(\overline{B} \to \pi \ell \overline{\nu})$ and their average.

Branching fractions for other $\overline{B} \to X_u \ell \overline{\nu}$ decays are given in Table 33. At this time the determination of $|V_{ub}|$ from these other channels looks less promising than for $\overline{B} \to \pi \ell \overline{\nu}$.

Table 33: Summary of branching fractions to $\mathcal{B}(\overline{B} \to X \ell \overline{\nu})$ decays other than $\overline{B} \to \pi \ell \overline{\nu}$. The errors quoted correspond to statistical and systematic uncertainties, respectively. Where a third uncertainty is quoted it corresponds to uncertainties from form factor shapes.

Experiment	Mode	$\mathcal{B}[10^{-4}]$
CLEO [230]	$B^0 \to \rho^- \ell \overline{\nu}$	$2.17 \pm 0.34 \, ^{+\, 0.47}_{-\, 0.54} \pm 0.41$
CLEO [239]	$B^0 \to \rho^- \ell \overline{\nu}$	$2.69 \pm 0.41 \, ^{+\, 0.35}_{-\, 0.40} \pm 0.50$
BABAR [235]	$B^0 \to \rho^- \ell \overline{\nu}$	$2.57 \pm 0.52 \pm 0.59$
BABAR [240]	$B^0 \to \rho^- \ell \overline{\nu}$	$3.29 \pm 0.42 \pm 0.47 \pm 0.60$
BABAR [231]	$B^0 \to \rho^- \ell \overline{\nu}$	$2.14 \pm 0.21 \pm 0.51 \pm 0.28$
BELLE [232]	$B^0 \to \rho^- \ell \overline{\nu}$	$2.07 \pm 0.47 \pm 0.25 \pm 0.14$
CLEO [230]	$B^+ \to \eta \ell \overline{\nu}$	$0.84 \pm 0.31 \pm 0.16 \pm 0.09$
BELLE [232]	$B^+ \to \rho^0 \ell \overline{\nu}$	$1.39 \pm 0.23 \pm 0.16 \pm 0.02$
BELLE [241]	$B^+ \to \omega \ell \overline{\nu}$	$1.3 \pm 0.4 \pm 0.2 \pm 0.3$

5.5 Inclusive Cabibbo-suppressed decays

The large background from $\overline{B} \to X_c \ell \overline{\nu}$ decays is the chief experimental limitation in determinations of $|V_{ub}|$. Cuts designed to reject this background limit the acceptance for $\overline{B} \to X_u \ell \overline{\nu}$ decays. The calculation of partial rates for these restricted acceptances is more complicated and requires the resummation of an infinite number of terms into non-perturbative "shape functions" at each order in the $1/m_b$ expansion. The leading shape function is the same in semileptonic and radiative $\overline{B} \to X_s \gamma$ decays. Subleading shape functions differ between semileptonic and radiative decays, however. Theoretical uncertainties arise from the modeling of these subleading shape functions and from higher order perturbative and non-perturbative contributions, including weak annihilation [242]. The various extractions of $|V_{ub}|$ presented here are based on calculations by Bosch, Lange, Neubert and Paz (BLNP) [225, 243–246]. The dominant error remains the uncertainty of the b-quark mass, even though recent HQE fits to moments have significantly reduced this uncertainty. The results of such fits are shown in Fig. 25. The relative large uncertainty in μ_π^2 has a much smaller impact on the shape function error on $|V_{ub}|$.

Measurements of partial decay rates for $\overline{B} \to X_u \ell \overline{\nu}$ transitions from $\Upsilon(4S)$ decays are given in Table 34, along with extracted values for $|V_{ub}|$, which are also shown in Fig. 27. Earlier measurements from LEP [247–250] are less precise and cannot readily be used in a consistent framework with the $\Upsilon(4S)$ results. The recent measurements tend to include a larger fraction f_u of the total phase space for $\overline{B} \to X_u \ell \overline{\nu}$ decay than did earlier measurements.

The systematic errors associated with the modeling of $\overline{B} \to X_c \ell \overline{\nu}$ and $\overline{B} \to X_u \ell \overline{\nu}$ decays and the theoretical uncertainties are taken as fully correlated among all measurements in the sense of Eq. 112. Reconstruction-related uncertainties are taken as fully correlated within a given experiment. From the three results quoted in Ref. [258], only one is used in the average, as they are based on the same dataset and are highly correlated. The other experimental results have negligible statistical correlation. The assumed dependence of the quoted error on the measured

value was input for each source of error, as discussed in section 5.1. The average is given in Table 34. The breakdown of the uncertainties on the average (in percent) is ±2.1 (statistical), ±2.4 (experimental), ±1.9 ($b \to c\ell\overline{\nu}$ model), ±2.4 ($b \to u\ell\overline{\nu}$ model), ±4.7 (m_b and μ_π^2), ±3.5 (subleading shape functions), ±1.9 (weak annihilation). No uncertainty is assigned to the assumption of quark-hadron duality. The average $|V_{ub}|$ corresponds to an inclusive charmless semileptonic B decay average branching fraction $\mathcal{B}(B \to X_u l \nu_l) = (2.16 \pm 0.33) \times 10^{-3}$.

Table 34: Summary of inclusive determinations of partial branching fractions for $B \to X_u l\nu$ decays and $|V_{ub}|$. The errors quoted on $|V_{ub}|$ correspond to experimental and theoretical uncertainties, respectively. The $s_{\rm h}^{\rm max}$ variable is described in Ref. [253]

	accepted region	f_u	$\Delta\mathcal{B}[10^{-4}]$	$\lvert V_{ub}\rvert[10^{-3}]$
∗CLEO [251]	$E_e > 2.1\,\text{GeV}$	0.19	$3.3 \pm 0.2 \pm 0.7$	$4.05 \pm 0.47 \pm 0.36$
∗BABAR [252]	$E_e > 2.0\,\text{GeV}$, $s_{\rm h}^{\rm max} < 3.5\,\text{GeV}^2$	0.19	$3.5 \pm 0.3 \pm 0.3$	$4.06 \pm 0.27 \pm 0.36$
∗BABAR [254]	$E_e > 2.0\,\text{GeV}$	0.26	$5.3 \pm 0.3 \pm 0.5$	$4.25 \pm 0.30 \pm 0.31$
∗BELLE [255]	$E_e > 1.9\,\text{GeV}$	0.34	$8.5 \pm 0.4 \pm 1.5$	$4.85 \pm 0.45 \pm 0.31$
∗BABAR [256]	$M_X < 1.7\,\text{GeV}/c^2, q^2 > 8\,\text{GeV}^2/c^2$	0.34	$8.7 \pm 0.9 \pm 0.9$	$4.79 \pm 0.35 \pm 0.33$
∗BELLE [257]	$M_X < 1.7\,\text{GeV}/c^2, q^2 > 8\,\text{GeV}^2/c^2$	0.34	$7.4 \pm 0.9 \pm 1.3$	$4.41 \pm 0.46 \pm 0.30$
BELLE [258]	$M_X < 1.7\,\text{GeV}/c^2, q^2 > 8\,\text{GeV}^2/c^2$	0.34	$8.4 \pm 0.8 \pm 1.0$	$4.68 \pm 0.37 \pm 0.32$
BELLE [258]	$P_+ < 0.66\,\text{GeV}$	0.57	$11.0 \pm 1.0 \pm 1.6$	$4.14 \pm 0.35 \pm 0.29$
∗BELLE [258]	$M_X < 1.7\,\text{GeV}/c^2$	0.66	$12.4 \pm 1.1 \pm 1.2$	$4.10 \pm 0.27 \pm 0.25$
Average of ∗	$\chi^2 = 6.3/6$, CL=0.40			$4.39 \pm 0.19 \pm 0.27$

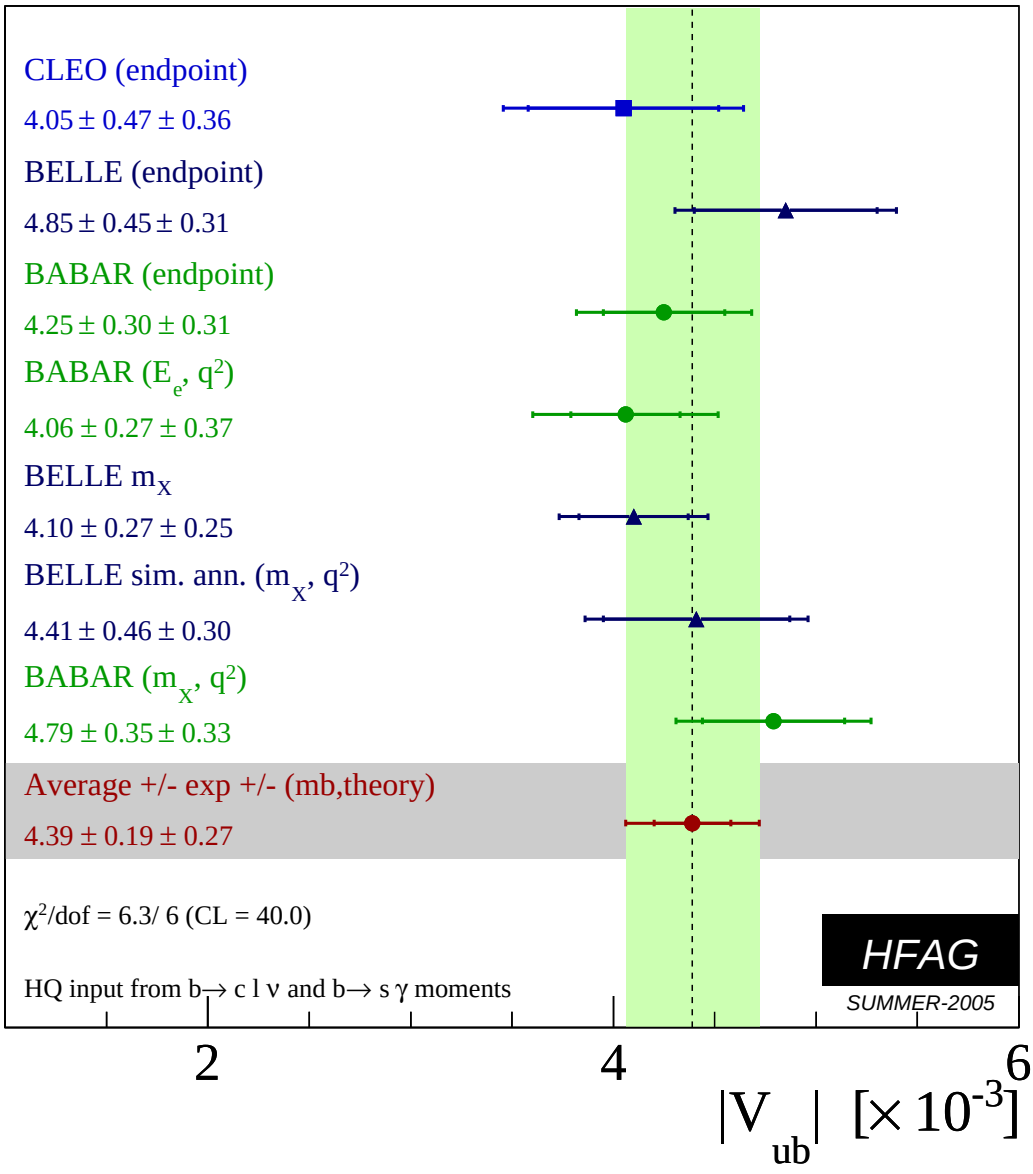

Figure 27: Measurements of $|V_{ub}|$ from inclusive semileptonic decays and their average.

6 Charmless B-decay branching fractions and their asymmetries

The aim of this section is to provide the branching fractions and the partial rate asymmetries (A_{CP}) of charmless B decays. The asymmetry is defined as $A_{CP} = \frac{N_{\overline{B}} - N_B}{N_{\overline{B}} + N_B}$, where $N_{\overline{B}}$ and N_B are respectively the number of $\overline{B}^0/B^-$ and B^0/B^+ decaying into a specific final state. Four different B decay categories are considered: charmless mesonic, baryonic, radiative and leptonic. Measurements supported with written documents are accepted in the averages; written documents could be journal papers, conference contributed papers, preprints or conference proceedings. Results from A_{CP} measurements obtained from time dependent analyses are listed and described in Sec. 4. Measurements of charmful baryonic B decays, which were included in our previous averages [3, 4], are now shown in Section 7, which deals with B decays to charm.

So far all branching fractions assume equal production of charged and neutral B pairs. The best measurements to date show that this is still a good approximation (see Sec. 3.1.1). For branching fractions, we provide either averages or the most stringent 90% confidence level upper limits. If one or more experiments have measurements with $>4\sigma$ significance for a decay channel, all available central values for that channel are used in the averaging. We also give central values and errors for cases where the significance of the average value is at least 3σ, even if no single measurement is above 4σ. Since some decay modes are sensitive to the contribution of new physics and the current experimental upper limits are not far from the Standard Model expectation, it's better to provide the combined upper limits or averages rather than to list the most stringent upper limits. For instance, $B^+ \to \tau^+\nu$ is one of these decays. In our update of Summer 2005, the combined averages are given for the decays $B^+ \to \tau^+\nu$ and $B^0 \to K^+K^-$ although no significant signals are observed. Their upper limits can be estimated assuming that the errors are Gaussian. For A_{CP} we provide averages in all cases.

Our averaging is performed by maximizing the likelihood, $\mathcal{L} = \prod_i \mathcal{P}_i(x)$, where $\mathcal{P}_i$ is the probability density function (PDF) of the ith measurement, and x is the branching fraction or A_{CP}. The PDF is modeled by an asymmetric Gaussian function with the measured central value as its mean and the quadratic sum of the statistical and systematic errors as the standard deviations. The experimental uncertainties are considered to be uncorrelated with each other when the averaging is performed. No error scaling is applied when the fit χ^2 is greater than 1 since we believe that tends to overestimate the errors except in cases of extreme disagreement (we have no such cases). One exception to consider the correlated systematic errors is the inclusive $b \to s\gamma$ mode, which is sensitive to physics beyond the Standard Model. We tried to include as many measurements as possible and take the common systematic errors into account when performing the average. The details are described in section 6.3.

At present, we have measurements of more than 250 decay modes, reported in more than 150 papers. Because the number of references is so large, we do not include them with the tables shown here but the full set of references is available quickly from active gifs at the "Summer 2005" link on the rare web page: `http://www.slac.stanford.edu/xorg/hfag/rare/index.html`

6.1 Mesonic charmless decays

Table 35: Branching fractions (BF) of charmless mesonic B^+ decays (in units of 10^{-6}). Upper limits are at 90% CL. Values in red (blue) are new published (preliminary) result since PDG2004 [as of July 15, 2005].

RPP#	Mode	PDG2004 Avg.	BABAR	Belle	CLEO	CDF	New Avg.
117	$K^0\pi^+$	18.8 ± 2.1	$26.0 \pm 1.3 \pm 1.0$	$22.0 \pm 1.9 \pm 1.1$	$18.8^{+3.7+2.1}_{-3.3-1.8}$		24.1 ± 1.3
118	$K^+\pi^0$	12.9 ± 1.2	$12.0 \pm 0.7 \pm 0.6$	$12.0 \pm 1.3^{+1.3}_{-0.9}$	$12.9^{+2.4+1.2}_{-2.2-1.1}$		12.1 ± 0.8
119	$\eta' K^+$	78 ± 5	$68.9 \pm 2.0 \pm 3.2$	$68.6 \pm 2.1 \pm 3.6$	$80^{+10}_{-9} \pm 7$		69.4 ± 2.7
120	$\eta' K^{*+}$	< 35	< 14	< 90	< 35		< 14
121	ηK^+	< 6.9	$3.3 \pm 0.6 \pm 0.3$	$2.2 \pm 0.4 \pm 0.1$	$2.2^{+2.8}_{-2.2}$		2.5 ± 0.3
122	ηK^{*+}	26^{+10}_{-9}	$25.6 \pm 4.0 \pm 2.4$	$22.8^{+3.7}_{-3.5} \pm 2.2$	$26.4^{+9.6}_{-8.2} \pm 3.3$		$24.3^{+3.0}_{-2.9}$
–	$a_0^0(980)K^+$ †	New	< 2.5				< 2.5
–	$a_0^+(980)K^0$ †	New	< 3.9				< 3.9
123	ωK^+	$9.2^{+2.8}_{-2.5}$	$4.8 \pm 0.8 \pm 0.4$	$8.1 \pm 0.6 \pm 0.5$	$3.2^{+2.4}_{-1.9} \pm 0.8$		6.5 ± 0.6
124	ωK^{*+}	< 87	< 7.4		< 87		< 7.4
125	$K^{*0}\pi^+$	19^{+6}_{-8}	$13.5 \pm 1.2^{+0.8}_{-0.9}$	$9.7 \pm 0.6^{+0.8}_{-0.9}$	$7.6^{+3.5}_{-3.0} \pm 1.6$		10.8 ± 0.8
126	$K^{*+}\pi^0$	< 31	$6.9 \pm 2.0 \pm 1.3$		$7.1^{+11.4}_{-7.1} \pm 1.0$		6.9 ± 2.3
127	$K^+\pi^+\pi^-$	57 ± 4	$64.1 \pm 2.4 \pm 4.0$	$48.8 \pm 1.1 \pm 3.6$			54.1 ± 3.1
128	$K^+\pi^+\pi^-(NR)$	< 28	$2.9 \pm 0.6^{+0.8}_{-0.5}$		< 28		$2.9^{+1.1}_{-0.9}$
129	$K^+ f_0(980)$ †	seen	$9.5 \pm 1.0^{+0.6}_{-0.9}$	$8.78 \pm 0.82^{+0.85}_{-1.76}$			$9.07^{+0.81}_{-1.06}$
130	$K^+\rho^0$	< 12	$5.1 \pm 0.8^{+0.5}_{-0.8}$	$3.89 \pm 0.47^{+0.43}_{-0.41}$	$8.4^{+4.0}_{-3.4} \pm 1.8$		$4.23^{+0.56}_{-0.57}$
–	$\rho^0(1450)K^+$	New	< 11.7				< 11.7
–	$f_2(1270)K^+$ †	New	< 8.9	$0.75 \pm 0.17^{+0.13}_{-0.19}$			$0.75^{+0.21}_{-0.26}$
–	$f_2(1370)K^+$ †	New	< 10.7				< 10.7
–	$f_0(1500)K^+$ †	New	< 4.4				< 4.4
–	$f_2'(1525)K^+$ †	New	< 3.4	< 4.9			< 3.4
–	$K_0^*(1430)^0\pi^+$	New	$37.0 \pm 1.8^{+4.6}_{-4.7}$	$45.0 \pm 2.9^{+15.0}_{-10.6}$‡			$38.2^{+4.6}_{-4.5}$
131	$K_2^*(1430)^0\pi^+$	< 680	< 23.1	< 6.9			< 2.3
–	$K^*(1680)^0\pi^+$	New	< 11.4	< 9.3			< 3.1
132	$K^-\pi^+\pi^+$	< 1.8	< 1.8	< 4.5			< 1.8
135	$K^0\pi^+\pi^0$	< 66			< 66		< 66
136	$K^0\rho^+$	< 48			< 48		< 48
–	$K^{*0}\rho^+$	New	$17.0 \pm 2.9^{+2.0}_{-2.8}$	$8.9 \pm 1.7 \pm 1.2$			10.6 ± 1.9
138	$K^{*+}\rho^0$	11 ± 4	$10.6^{+3.0}_{-2.6} \pm 2.4$		< 74		$10.6^{+3.8}_{-3.5}$
139	$K^{*+}\overline{K^{*0}}$	< 71			< 71		< 71
142	$K^+\overline{K^0}$	< 2.0	$1.5 \pm 0.5 \pm 0.1$	$1.0 \pm 0.4 \pm 0.1$	< 3.3		1.2 ± 0.3
143	$K^+\overline{K^0}\pi^0$	< 24			< 24		< 24
144	$K^+K_SK_S$	13.4 ± 2.4	$10.7 \pm 1.2 \pm 1.0$	$13.4 \pm 1.9 \pm 1.5$			11.5 ± 1.3
145	$K_SK_S\pi^+$	< 3.2		< 3.2			< 3.2
146	$K^+K^-\pi^+$	< 6.3	< 6.3	< 13			< 6.3
148	$K^+K^+\pi^-$	< 1.3	< 1.3	< 2.4			< 1.3
150	$\overline{K^{*0}}K^+$	< 5.3			< 5.3		< 5.3
152	$K^+K^-K^+$	30.8 ± 2.1	$29.6 \pm 2.1 \pm 1.6$	$30.6 \pm 1.2 \pm 2.3$			30.1 ± 1.9
153	ϕK^+	9.3 ± 1.0	$10.0^{+0.9}_{-0.8} \pm 0.5$	$9.60 \pm 0.92^{+1.05}_{-0.84}$	$5.5^{+2.1}_{-1.8} \pm 0.6$	$7.6 \pm 1.3 \pm 0.6$	$9.03^{+0.65}_{-0.63}$
–	a_2K^+†	New		< 1.1			< 1.1
–	$\phi(1680)K^+$†	New		< 0.8			< 0.8
156	ϕK^{*+}	9.6 ± 3.0	$12.7^{+2.2}_{-2.0} \pm 1.1$	$6.7^{+2.1+0.7}_{-1.9-1.0}$	$10.6^{+6.4+1.8}_{-4.9-1.6}$		9.7 ± 1.5
159	$\phi\phi K^+$ §	$2.6^{+1.1}_{-0.9}$		$2.6^{+1.1}_{-0.9} \pm 0.3$			$2.6^{+1.1}_{-0.9}$
173	$\pi^+\pi^0$	$5.6^{+0.9}_{-1.1}$	$5.8 \pm 0.6 \pm 0.4$	$5.0 \pm 1.2 \pm 0.5$	$4.6^{+1.8+0.6}_{-1.6-0.7}$		5.5 ± 0.6
174	$\pi^+\pi^-\pi^+$	11 ± 4	$16.2 \pm 1.2 \pm 0.9$				16.2 ± 1.5
175	$\rho^0\pi^+$	8.6 ± 2.0	$8.8 \pm 1.0^{+0.6}_{-0.9}$	$8.0^{+2.3}_{-2.0} \pm 0.7$	$10.4^{+3.3}_{-3.4} \pm 2.1$		$8.7^{+1.0}_{-1.1}$
–	$\rho^0(1450)\pi^+$	New	< 2.3				< 2.3
176	$f_0(980)\pi^+$ †	< 140	< 3.0				< 3.0
–	$f_0(600)\pi^+$	New	< 4.1				< 4.1
177	$f_2(1270)\pi^+$	< 240	< 3.5				< 3.5
–	$f_0(1370)\pi^+$	New	< 3.0				< 3.0
178	$\pi^+\pi^-\pi^+(NR)$	< 41	< 4.6				< 4.6
180	$\rho^+\pi^0$	< 43	$10.0 \pm 1.4 \pm 0.9$	$13.2 \pm 2.3^{+1.4}_{-1.9}$	< 43		$10.8^{+1.4}_{-1.5}$
182	$\rho^+\rho^0$	26 ± 6	$22.5^{+5.7}_{-5.4} \pm 5.8$	$31.7 \pm 7.1^{+3.8}_{-6.7}$			$26.4^{+6.1}_{-6.4}$
185	$\omega\pi^+$	$6.4^{+1.8}_{-1.6}$	$5.5 \pm 0.9 \pm 0.5$	$7.0 \pm 0.6 \pm 0.5$	$11.3^{+3.3}_{-2.9} \pm 1.4$		6.6 ± 0.6
186	$\omega\rho^+$	< 61	$12.6^{+3.7}_{-3.3} \pm 1.6$		< 61		$12.6^{+4.0}_{-3.7}$
187	$\eta\pi^+$	< 5.7	$5.1 \pm 0.6 \pm 0.3$	$3.9 \pm 0.5 \pm 0.2$	$1.2^{+2.8}_{-1.2}$		4.3 ± 0.4
188	$\eta'\pi^+$	< 7	$4.0 \pm 0.8 \pm 0.4$	$1.73^{+0.69}_{-0.63} \pm 0.10$	$1.0^{+5.8}_{-1.0}$		$2.53^{+0.59}_{-0.50}$
189	$\eta'\rho^+$	< 33	< 22		< 33		< 22
190	$\eta\rho^+$	< 15	$8.4 \pm 1.9 \pm 1.1$	$8.5^{+2.6}_{-2.4} \pm 1.0$	$4.8^{+5.2}_{-3.8}$		$8.1^{+1.7}_{-1.5}$
–	$a_0^0(980)\pi^+$ †	New	< 5.8				< 5.8
191	$\phi\pi^+$	< 0.41	< 0.41		< 5		< 0.41
192	$\phi\rho^+$	< 16			< 16		< 16

†Product BF - daughter BF taken to be 100%; ‡Larger of two solutions taken; §$M_{\phi\phi} < 2.85$ GeV/c^2

Table 36: Branching fractions of charmless mesonic B^0 decays (in units of 10^{-6}). Upper limits are at 90% CL. Values in red (blue) are new published (preliminary) result since PDG2004 [as of July 15, 2005].

RPP#	Mode	PDG2004 Avg.	BABAR	Belle	CLEO	CDF	New Avg.
123	$K^+\pi^-$	18.5 ± 1.1	$19.2 \pm 0.6 \pm 0.6$	$18.5 \pm 1.0 \pm 0.7$	$18.0^{+2.3+1.2}_{-2.1-0.9}$		18.9 ± 0.7
124	$K^0\pi^0$	$9.5^{+2.1}_{-1.9}$	$11.4 \pm 0.9 \pm 0.6$	$11.7 \pm 2.3^{+1.2}_{-1.3}$	$12.8^{+4.0+1.7}_{-3.3-1.4}$		11.5 ± 1.0
125	$\eta' K^0$	63 ± 7	$67.4 \pm 3.3 \pm 3.2$	$56.6 \pm 3.6 \pm 3.3$	$89^{+18}_{-16} \pm 9$		63.2 ± 3.3
126	$\eta' K^{*0}$	< 24	< 7.6	< 20	< 24		< 7.6
127	ηK^{*0}	14^{+6}_{-5}	$18.6 \pm 2.3 \pm 1.2$	$19.8^{+2.1}_{-2.0} \pm 1.4$	$13.8^{+5.5}_{-4.6} \pm 1.6$		18.7 ± 1.7
128	ηK^0	< 9.3	< 2.5	< 1.9	< 9.3		< 1.9
–	$\eta K^+\pi^-$	New		$31.7 \pm 1.9^{+2.2}_{-2.6}$			$31.7^{+2.9}_{-3.2}$
–	$a_0^-(980)K^+$ †	New	< 2.1	< 1.6			< 1.6
–	$a_0^0(980)K^0$ †	New	< 7.8				< 7.8
129	ωK^0	< 13	$5.9 \pm 1.0 \pm 0.4$	$3.9 \pm 0.7 \pm 0.4$	$10.0^{+5.4}_{-4.2} \pm 1.4$		4.7 ± 0.6
131	ωK^{*0}	< 23	< 6.0		< 23		< 6.0
132	K^+K^-	< 0.6	$0.04 \pm 0.15 \pm 0.08$	0.06 ± 0.10	< 0.8	< 3.1 ‡	$0.05^{+0.10}_{-0.09}$
133	$K^0\overline{K^0}$	< 3.3	$1.19^{+0.40}_{-0.35} \pm 0.13$	0.8 ± 0.3	< 3.3		$0.96^{+0.25}_{-0.24}$
134	$K_SK_SK_S$	$4.2^{+1.8}_{-1.5}$	$6.9^{+0.9}_{-0.8} \pm 0.6$	$4.2^{+1.6}_{-1.3} \pm 0.8$			6.2 ± 0.9
135	$K^+\pi^-\pi^0$	< 40	$34.9 \pm 2.1 \pm 3.9$	$36.6^{+4.2}_{-4.1} \pm 3.0$	< 40		$35.6^{+3.4}_{-3.3}$
136	$K^+\rho^-$	7.3 ± 1.8	$8.6 \pm 1.4 \pm 1.0$	$15.1^{+3.4+2.4}_{-3.3-2.6}$	$16^{+8}_{-6} \pm 3$		$9.9^{+1.6}_{-1.5}$
–	$K^+\rho(1450)^-$ †	New	< 3.2				< 3.2
–	$K^+\rho(1700)^-$ †	New	< 1.7				< 1.7
137	$K^0\pi^+\pi^-$	47 ± 7	$43.0 \pm 2.3 \pm 2.3$	$47.5 \pm 2.4 \pm 3.7$	$50^{+10}_{-9} \pm 7$		43.8 ± 2.9
–	$K^+\pi^-\pi^0(NR)$	New	< 4.6	< 9.4			< 4.6
–	$K_0^*(1430)^+\pi^-$	New	$36.1 \pm 4.8 \pm 11.3$	$49.7 \pm 3.8^{+4.0}_{-6.1}$			36.1 ± 12.3
–	$K_0^*(1430)^0\pi^0$	New	$25.5 \pm 4.8 \pm 8.7$				23.7 ± 10.0
138	$K^0\rho^0$	< 39	$5.1 \pm 1.0 \pm 1.2$	$6.1 \pm 1.0 \pm 1.1$	< 39		5.1 ± 1.6
139	$K^0 f_0(980)$ †	< 36	$5.5 \pm 0.7 \pm 0.7$	$7.6 \pm 1.7^{+0.8}_{-0.9}$			5.5 ± 1.0
140	$K^{*+}\pi^-$	16^{+6}_{-5}	$10.9 \pm 2.3 \pm 1.5$	$8.4 \pm 1.1^{+0.9}_{-0.8}$	$16^{+6}_{-5} \pm 2$		$11.7^{+1.5}_{-1.4}$
141	$K^{*0}\pi^0$	< 3.6	$3.0 \pm 0.9 \pm 0.5$	$0.4^{+1.9}_{-1.7} \pm 0.1$	$0.0^{+1.3+0.5}_{-0.0-0.0}$		1.7 ± 0.8
142	$K_2^*(1430)^+\pi^-$	< 18	< 13.2	< 6.3			< 13.2
–	$K_2^*(1430)^0\pi^0$	New	< 3.6				< 3.6
–	$K^*(1680)^+\pi^-$	New	< 19.4	< 10.1			< 10.1
–	$K^*(1680)^0\pi^0$	New	< 5.0				< 5.0
143	$K^+\overline{K^0}\pi^-$	< 21		< 18	< 21		< 18
144	$K^+K^-\pi^0$	< 19			< 19		< 19
145	$K^+K^-K^0$	28 ± 5	$23.8 \pm 2.0 \pm 1.6$	$28.3 \pm 3.3 \pm 4.0$			24.7 ± 2.3
146	ϕK^0	$8.6^{+1.3}_{-1.1}$	$8.4^{+1.5}_{-1.3} \pm 0.5$	$9.0^{+2.2}_{-1.8} \pm 0.7$	$5.4^{+3.7}_{-2.7} \pm 0.7$		$8.3^{+1.2}_{-1.0}$
149	$K^{*0}\rho^0$	< 34		< 2.6	< 34		< 2.6
–	$K^{*+}\rho^-$	New	< 24				< 24
154	ϕK^{*0}	10.7 ± 1.1	$9.2 \pm 0.9 \pm 0.5$	$10.0^{+1.6+0.7}_{-1.5-0.8}$	$11.5^{+4.5+1.8}_{-3.7-1.7}$		9.5 ± 0.9
155	$K^{*0}\overline{K^{*0}}$	< 22			< 22		< 22
157	$K^{*+}K^{*-}$	< 141			< 141		< 141
176	$\pi^+\pi^-$	4.8 ± 0.5	$5.5 \pm 0.4 \pm 0.3$	$4.4 \pm 0.6 \pm 0.3$	$4.5^{+1.4+0.5}_{-1.2-0.4}$	4.4 ± 1.3 ‡	5.0 ± 0.4
177	$\pi^0\pi^0$	1.9 ± 0.5	$1.17 \pm 0.32 \pm 0.10$	$2.3^{+0.4+0.2}_{-0.5-0.3}$	< 4.4		1.45 ± 0.29
178	$\eta\pi^0$	< 2.9	< 2.5	< 2.5	< 2.9		< 2.5
179	$\eta\eta$	< 18	< 2.8	< 2.0	< 18		< 2.0
180	$\eta'\pi^0$	< 5.7	< 3.7		< 5.7		< 3.7
181	$\eta'\eta'$	< 47	< 10		< 47		< 10
182	$\eta'\eta$	< 27	< 4.6		< 27		< 4.6
183	$\eta'\rho^0$	< 12	< 4.3	< 14	< 12		< 4.3
184	$\eta\rho^0$	< 10	< 1.5	< 5.5	< 10		< 1.5
–	$\eta\pi^+\pi^-$	New		$6.2^{+1.8+0.8}_{-1.6-0.6}$			$6.2^{+2.0}_{-1.7}$
–	$a_0^\mp(980)\pi^\pm$ †	New	< 5.1	< 2.8			< 2.8
185	$\omega\eta$	< 12	< 1.9		< 12		< 1.9
186	$\omega\eta'$	< 60	< 2.8		< 60		< 2.8
187	$\omega\rho^0$	< 11	< 3.3		< 11		< 3.3
189	$\phi\pi^0$	< 5	< 1.0		< 5		< 1.0
190	$\phi\eta$	< 9	< 1.0		< 9		< 1.0
191	$\phi\eta'$	< 31	< 4.5		< 31		< 4.5
192	$\phi\rho^0$	< 13			< 13		< 13
194	$\phi\phi$	< 12	< 1.5		< 12		< 1.5
196	$\rho^0\pi^0$	< 5.3	$1.4 \pm 0.6 \pm 0.3$	$3.12^{+0.88+0.60}_{-0.82-0.76}$	$1.6^{+2.0}_{-1.4} \pm 0.8$		$1.83^{+0.56}_{-0.55}$
197	$\rho^\mp\pi^\pm$	22.8 ± 2.5	$22.6 \pm 1.8 \pm 2.2$	$29.1^{+5.0}_{-4.9} \pm 4.0$	$27.6^{+8.4}_{-7.4} \pm 4.2$		24.0 ± 2.5
199	$\rho^0\rho^0$	< 2.1	< 1.1		< 18		< 1.1
200	$a_1^-\pi^+$	< 490	$40.2 \pm 3.9 \pm 3.8$	$48.6 \pm 4.1 \pm 3.9$			44.3 ± 4.0
203	$\rho^+\rho^-$	< 2200	$30 \pm 4 \pm 5$	$22.8 \pm 3.8^{+2.3}_{-2.6}$			$26.2^{+3.6}_{-3.7}$
205	$\omega\pi^0$	< 3	< 1.2	< 1.5	< 5.5		< 1.2

†Product BF - daughter BF taken to be 100%, ‡Relative BF converted to absolute BF

Table 37: Relative branching fractions of $B^0 \to K^+K^-, K^+\pi^-, \pi^+\pi^-$. Values in red (blue) are new published (preliminary) result since PDG2004 [as of July 15, 2005].

RPP#	Mode	PDG2004 Avg.	CDF	D0	New Avg.
132	$\mathcal{B}(B^0 \to K^+K^-)/\mathcal{B}(B^0 \to K^+\pi^-)$		< 0.17		< 0.17
176	$\mathcal{B}(B^0 \to \pi^+\pi^-)/\mathcal{B}(B^0 \to K^+\pi^-)$		$0.24 \pm 0.06 \pm 0.05$		0.24 ± 0.08

6.2 Radiative and leptonic decays

Table 38: Branchign fractions of semileptonic and radiative B^+ decays (in units of 10^{-6}). Upper limits are at 90% CL. Values in red (blue) are new published (preliminary) result since PDG2004 [as of July 15, 2005].

RPP#	Mode	PDG2004 Avg.	BABAR	Belle	CLEO	New Avg.
160	$K^*(892)^+\gamma$	38 ± 5	$38.7 \pm 2.8 \pm 2.6$	$42.5 \pm 3.1 \pm 2.4$	$37.6^{+8.9}_{-8.3} \pm 2.8$	40.3 ± 2.6
161	$K_1(1270)^+\gamma$	< 99		$43 \pm 9 \pm 9$		43 ± 12
162	$K^+\phi\gamma$	3.4 ± 1.0		$3.4 \pm 0.9 \pm 0.4$		3.4 ± 1.0
163	$K^+\pi^-\pi^+\gamma$ §	24^{+6}_{-5}	$29.5 \pm 1.3 \pm 1.9$	$25.0 \pm 1.8 \pm 2.2$		27.7 ± 1.8
–	$K^0\pi^+\pi^0\gamma$ §	New	$45.6 \pm 4.2 \pm 3.1$			45.6 ± 5.2
164	$K^{*0}\pi^+\gamma$ §	20^{+7}_{-6}		$20^{+7}_{-6} \pm 2$		20^{+7}_{-6}
165	$K^+\rho^0\gamma$ §	< 20		< 20		< 20
166	$K^+\pi^-\pi^+\gamma$ (N.R.) §	< 9.2		< 9.2		< 9.2
167	$K_1(1400)^+\gamma$	< 50		< 15		< 15
168	$K_2^*(1430)^+\gamma$	< 1400	$14.5 \pm 4.0 \pm 1.5$			14.5 ± 4.3
172	$\rho^+\gamma$	< 2.1	$0.9^{+0.6}_{-0.5} \pm 0.1$	$0.55^{+0.43+0.12}_{-0.37-0.11}$	< 13	$0.68^{+0.36}_{-0.31}$
–	$K^+\eta\gamma$	New		$8.4^{+1.5}_{-1.1} \pm 0.9$		$8.4^{+1.7}_{-1.4}$
207	$p\overline{\Lambda}\gamma$	New		$2.16^{+0.58}_{-0.53} \pm 0.20$		$2.16^{+0.61}_{-0.57}$
208	$p\overline{\Sigma^0}\gamma$	New		< 3.3		< 3.3
–	$\pi^+\nu\overline{\nu}$	New	< 100			< 100
226	$K^+e^+e^-$	$0.63^{+0.19}_{-0.17}$	$0.43^{+0.12}_{-0.11} \pm 0.03$	$0.640^{+0.150+0.029}_{-0.134-0.031}$	< 2.4	$0.522^{+0.094}_{-0.090}$
227	$K^+\mu^+\mu^-$	$0.45^{+0.14}_{-0.12}$	$0.31^{+0.15}_{-0.12} \pm 0.04$	$0.628^{+0.110}_{-0.108} \pm 0.033$	< 3.68	0.518 ± 0.092
228	$K^+l^+l^-$	$0.53^{+0.11}_{-0.10} \pm 0.3$		$0.632^{+0.092}_{-0.088} \pm 0.030$		$0.632^{+0.097}_{-0.093}$
229	$K^+\nu\overline{\nu}$	< 240	< 52	< 36	< 240	< 36
230	$K^*(892)^+e^+e^-$	< 4.6	$0.77^{+0.87}_{-0.70} \pm 0.60$ ‡	$1.60^{+1.04+0.14}_{-0.87-0.19}$ ‡		$1.22^{+0.73}_{-0.65}$
231	$K^*(892)^+\mu^+\mu^-$	< 2.2	$1.00^{+0.96}_{-0.71} \pm 0.16$ ‡	$1.63^{+0.64+0.10}_{-0.54-0.13}$ ‡		$1.44^{+0.54}_{-0.45}$
232	$K^*(892)^+l^+l^-$	< 2.2		$1.34^{+0.48+0.09}_{-0.40-0.10}$ ‡		$1.34^{+0.49}_{-0.41}$
238	$\pi^-e^+e^+$	< 1.6			< 1.6	< 1.6
239	$\pi^-\mu^+\mu^+$	< 1.4			< 1.4	< 1.4
240	$\pi^-e^+\mu^+$	< 1.3			< 1.3	< 1.3
241	$\rho^-e^+e^+$	< 2.6			< 2.6	< 2.6
242	$\rho^-\mu^+\mu^+$	< 5.0			< 5.0	< 5.0
243	$\rho^-e^+\mu^+$	< 3.3			< 3.3	< 3.3
244	$K^-e^+e^+$	< 1.0			< 1.0	< 1.0
245	$K^-\mu^+\mu^+$	< 1.8			< 1.8	< 1.8
246	$K^-e^+\mu^+$	< 2.0			< 2.0	< 2.0
247	$K^{*-}e^+e^+$	< 2.8			< 2.8	< 2.8
248	$K^{*-}\mu^+\mu^+$	< 8.3			< 8.3	< 8.3
249	$K^{*-}e^+\mu^+$	< 4.4			< 4.4	< 4.4

§ $M_{K\pi\pi} < 2.4$ GeV/c^2; ‡ Central values are not significant.

Table 39: Branching fractions of semileptonic and radiative B^0 decays (in units of 10^{-6}). Upper limits are at 90% CL. Values in red (blue) are new published (preliminary) result since PDG2004 [as of July 15, 2005].

RPP#	Mode	PDG2004 Avg.	BABAR	Belle	CLEO	New Avg.
162	$K^*(892)^0\gamma$	43 ± 4	$39.2 \pm 2.0 \pm 2.4$	$40.1 \pm 2.1 \pm 1.7$	$45.5^{+7.2}_{-6.8} \pm 3.4$	40.1 ± 2.0
163	$K^0\phi\gamma$	< 8.3		< 8.3		< 8.3
164	$K^+\pi^-\gamma$ †	4.6 ± 1.4		$4.6^{+1.3+0.5}_{-1.2-0.7}$		4.6 ± 1.4
–	$K^0\pi^+\pi^-\gamma$	New	$18.5 \pm 2.1 \pm 1.2$	$24 \pm 4 \pm 3$		19.5 ± 2.2
–	$K^+\pi^-\pi^0\gamma$	New	$40.7 \pm 2.2 \pm 3.1$			40.7 ± 3.8
165	$K^*(1410)^0\gamma$	< 130		< 130		< 130
166	$K^+\pi^-\gamma$ (N.R.) †	< 2.6		< 2.6		< 2.6
167	$K_1(1270)^0\gamma$	< 7000		< 58		< 58
168	$K_1(1400)^0\gamma$	< 4300		< 12		< 12
169	$K_2^*(1430)^0\gamma$	13 ± 5	$12.2 \pm 2.5 \pm 1.0$	$13 \pm 5 \pm 1$		12.4 ± 2.4
–	$K^0\eta\gamma$	New		$8.7^{+3.1+1.9}_{-2.7-1.6}$		$8.7^{+3.6}_{-3.1}$
173	$\rho^0\gamma$	< 1.2	$0.0 \pm 0.2 \pm 0.1$	$1.17^{+0.35+0.09}_{-0.31-0.08}$	< 17	0.38 ± 0.18
174	$\omega\gamma$	< 1.0	$0.5 \pm 0.3 \pm 0.1$	$0.58^{+0.35+0.07}_{-0.27-0.08}$	< 9.2	$0.54^{+0.23}_{-0.21}$
175	$\phi\gamma$	< 3.3	< 0.85		< 3.3	< 0.85
237	$K^0e^+e^-$	< 0.54	$0.14^{+0.16}_{-0.11} \pm 0.02$ ‡	$-0.070^{+0.129+0.014}_{-0.082-0.028}$ ‡	< 8.45	$0.045^{+0.090}_{-0.080}$
238	$K^0\mu^+\mu^-$	$0.56^{+0.29}_{-0.24}$	$0.60^{+0.34}_{-0.27} \pm 0.05$	$0.626^{+0.217+0.038}_{-0.181-0.041}$	< 6.64	$0.618^{+0.185}_{-0.155}$
239	$K^0l^+l^-$	< 0.68		$0.328^{+0.134+0.022}_{-0.113-0.026}$		$0.328^{+0.136}_{-0.116}$
240	$K^*(892)^0e^+e^-$	< 2.4	$1.03^{+0.33}_{-0.29} \pm 0.12$	$1.85^{+0.55}_{-0.49} \pm 0.19$		$1.28^{+0.30}_{-0.29}$
241	$K^*(892)^0\mu^+\mu^-$	1.3 ± 0.4	$0.89^{+0.39}_{-0.33} \pm 0.14$	$1.85^{+0.35}_{-0.31} \pm 0.10$		1.48 ± 0.26
243	$K^*(892)^0l^+l^-$	1.17 ± 0.30		$1.69^{+0.26}_{-0.24} \pm 0.11$		$1.69^{+0.28}_{-0.26}$

† $1.25\ \text{GeV}/c^2 < M_{K\pi} < 1.6\ \text{GeV}/c^2$; ‡ Central values are not significant.

Table 40: Branching fractions of semileptonic and radiative B decays (in units of 10^{-6}). Upper limits are at 90% CL. Values in red (blue) are new published (preliminary) result since PDG2004 [as of July 15, 2005].

RPP#	Mode	PDG2004 Avg.	BABAR	Belle	CLEO	New Avg.
60	$K_3^*(1780)\gamma$	< 3000		< 2.8		< 2.8
–	$s\gamma$ with baryons	New			< 38 †	< 38 †
71	$\rho\gamma$	< 1.9	$0.6 \pm 0.3 \pm 0.1$	$1.34^{+0.34+0.14}_{-0.31-0.10}$	< 14	0.96 ± 0.23
–	$K\eta\gamma$	New		$8.5^{+1.3}_{-1.2} \pm 0.9$		$8.5^{+1.6}_{-1.5}$
101	se^+e^- ‡	5.0 ± 2.6	$6.0 \pm 1.7 \pm 1.3$	$4.04 \pm 1.30^{+0.87}_{-0.83}$	< 57	$4.70^{+1.24}_{-1.23}$
102	$s\mu^+\mu^-$	$7.9^{+3.0}_{-2.6}$	$5.0 \pm 2.8 \pm 1.2$	$4.13 \pm 1.05^{+0.85}_{-0.81}$	< 58	$4.26^{+1.18}_{-1.16}$
103	$s\ell^+\ell^-$ ‡	$6.1^{+2.0}_{-1.8}$	$5.6 \pm 1.5 \pm 1.3$	$4.11 \pm 0.83^{+0.85}_{-0.81}$	< 42	$4.46^{+0.98}_{-0.96}$
104	Ke^+e^-	$0.48^{+0.15}_{-0.13}$	$0.33^{+0.09}_{-0.08} \pm 0.02$	$0.454^{+0.116+0.023}_{-0.104-0.025}$		$0.380^{+0.073}_{-0.067}$
105	$K^*(892)e^+e^-$	1.5 ± 0.5	$0.97^{+0.30}_{-0.27} \pm 0.15$	$1.84^{+0.48}_{-0.44} \pm 0.17$		$1.26^{+0.28}_{-0.27}$
106	$K\mu^+\mu^-$	0.48 ± 0.12	$0.35^{+0.13}_{-0.11} \pm 0.03$	$0.626^{+0.103+0.033}_{-0.064-0.034}$		$0.561^{+0.066}_{-0.061}$
107	$K^*(892)\mu^+\mu^-$	$1.17^{+0.37}_{-0.33}$	$0.90^{+0.35}_{-0.30} \pm 0.13$	$1.81^{+0.30}_{-0.28} \pm 0.11$		1.45 ± 0.23
108	$K\ell^+\ell^-$	0.54 ± 0.08	$0.34 \pm 0.07 \pm 0.03$	$0.550^{+0.075}_{-0.070} \pm 0.027$	< 1.7	0.446 ± 0.053
109	$K^*(892)\ell^+\ell^-$	1.05 ± 0.20	$0.78^{+0.19}_{-0.17} \pm 0.12$	$1.65^{+0.23}_{-0.22} \pm 0.11$	< 3.3	1.18 ± 0.17
111	$\pi e^\pm\mu^\mp$	< 1.6			< 1.6	< 1.6
112	$\rho e^\pm\mu^\mp$	< 3.2			< 3.2	< 3.2
113	$Ke^\pm\mu^\mp$	< 1.6			< 1.6	< 1.6
114	$K^*e^\pm\mu^\mp$	< 6.2			< 6.2	< 6.2

†$E_\gamma > 2.0$ GeV; ‡$M(\ell^+\ell^-) > 0.2\ \text{GeV}/c^2$

Table 41: Branching fractions of leptonic B decays (in units of 10^{-6}). Upper limits are at 90% CL. Values in red (blue) are new published (preliminary) result since PDG2004 [as of July 15, 2005].

RPP#	Mode	PDG2004 Avg.	BABAR	Belle	CLEO	CDF	D0	New Avg.
12	$e^+\nu$	< 15		< 5.4	< 15			< 5.4
13	$\mu^+\nu$	< 21	< 6.6	< 2.0	< 21			< 2.0
14	$\tau^+\nu$	< 570	130^{+100}_{-90}	81^{+58}_{-45}	< 840			92^{+51}_{-41}
15	$e^+\nu_e\gamma$	< 200		< 22	< 200			< 22
16	$\mu^+\nu_\mu\gamma$	< 52		< 23	< 52			< 23
234	$\gamma\gamma$	< 1.7	< 1.7	< 0.54				< 0.54
235	e^+e^-	< 0.19	< 0.061	< 0.19	< 0.83			< 0.061
236	$\mu^+\mu^-$	< 0.16	< 0.083	< 0.16	< 0.61	< 0.039		< 0.039
–	$\tau^+\tau^-$	New	< 3200					< 2700
244	$e^\pm\mu^\mp$	< 0.17	< 0.18	< 0.17	< 1.5			< 0.17
247	$e^\pm\tau^\mp$	< 530			< 110			< 110
248	$\mu^\pm\tau^\mp$	< 830			< 38			< 38
–	$\nu\overline{\nu}$	New	< 220					< 220
–	$\nu\overline{\nu}\gamma$	New	< 47					< 47

6.3 $B \to s\gamma$

The decay $b \to s\gamma$ proceeds through a process of flavor changing neutral current. Since the charged Higgs or SUSY particles may contribute in the penguin loop, the branching fraction is sensitive to physics beyond the Standard Model. Experimentally, the branching fraction is measured using either a semi-inclusive or an inclusive approach. A minimum photon energy requirement is applied in the analysis and the branching fraction is corrected based on the theoretical model for the photon energy spectrum (shape function). Although there are several experimental results available, only one measurement each for *BABAR*, Belle and CLEO is used in the HFAG average [3, 4] to avoid dealing with correlated errors for results reported from the same experiment. Furthermore, the model uncertainties from the shape function should be highly correlated but no proper action was made in our previous averages. To perform the average with better precision and good accuracy, it is important to use as many experimental results as possible and to handle the shape function issue in a proper way. In this note, we report the updated average of $b \to s\gamma$ branching fraction by implementing a common shape function.

Several shape function schemes are commonly used. Usually one is chosen to obtain the extrapolation factor, defined as the ratio of the $b \to s\gamma$ branching fractions with minimum photon energies above and at 1.6 GeV, and the difference between various schemes are treated as the model uncertainty. Recently O. Buchmüller and H. Flächer have calculated the extrapolation factors [259]. Table 42 lists the extrapolation factors with various photon energy cuts for three different schemes and the average. The appropriate approach to average the experimental results is to first convert them according to the average extrapolation factors and then perform the average, assuming that the errors of the extrapolation factors are 100% correlated.

Table 42: Extrapolation factor in various scheme with various minimum photon energy requirement (in GeV).

Scheme	$E_\gamma > 1.7$	$E_\gamma > 1.8$	$E_\gamma > 1.9$	$E_\gamma > 2.0$	$E_\gamma > 2.242$
Kinetic [260]	0.986 ± 0.001	0.968 ± 0.002	0.939 ± 0.005	0.903 ± 0.009	0.656 ± 0.031
Neubert SF [261]	0.982 ± 0.002	0.962 ± 0.004	0.930 ± 0.008	0.888 ± 0.014	0.665 ± 0.035
Kagan-Neubert [262]	0.988 ± 0.002	0.970 ± 0.005	0.940 ± 0.009	0.892 ± 0.014	0.643 ± 0.033
Average	0.985 ± 0.004	0.967 ± 0.006	0.936 ± 0.010	0.894 ± 0.016	0.655 ± 0.037

After surveying all available experimental results, we choose the most updated ones from each experiment for the average. Since the $b \to s\gamma$ branching fraction from $\Upsilon(4S)$ and Z pole decays are not equal footing, we drop the ALEPH measurement in this average [263]. Finally the five shown in Table 43 are selected. They have provided in their papers either the $b \to s\gamma$ branching fraction at a certain photon energy cut or the extrapolation factor used. Therefore we are able to convert them to the values at $E_{\rm min} = 1.6$ GeV using the information in Table 42. The errors are, in order, statistical, systematic and shape-function systematic, except for the *BABAR* inclusive where there is a second systematic error (third quoted error) due to theoretical uncertainties. Moreover, in the three inclusive analyses a possible $b \to d\gamma$ contamination has been considered according to the theoretical expectation of $(4.0 \pm 1.6)\%$. The uncertainty from the $b \to d\gamma$ fraction in the three inclusive measurements should not be considered independently. For those three measurements, a fourth uncertainty for the $b \to d\gamma$ fraction is included. We perform the average assuming that the systematic errors of the shape function and the $d\gamma$ fraction are correlated, and the other systematic errors and the statistical errors are Gaussian and uncorrelated. The obtained average is $\mathcal{B}(b \to s\gamma) = (355 \pm 24^{+9}_{-10} \pm 3) \times 10^{-6}$ with a $\chi^2/\text{DOF} = 0.74/4$, where the errors are combined statistical and systematic, systematic due to the shape function, and the $d\gamma$ fraction. The last two errors are estimated to be the difference of the average after simultaneously varying the central value of each experimental result by $\pm 1\sigma$. Although a small fraction of events was used in both the semi-inclusive and inclusive analyses in the same experiment, we neglect their statistical correlations. Some other correlated systematic errors, such as photon detection and the background suppression, are not considered in our new average. In the future it would be better if each collaboration would provide a single combined result so that the average can be performed more accurately and easily.

Table 43: Reported branching fraction, minimum photon energy, branching fraction at minimum photon energy and converted branching fraction for the decay $b \to s\gamma$. All the branching fractions are in units of 10^{-6}. See text for an explanation of the errors.

Mode	Reported $\mathcal{B}$	$E_{\rm min}$	$\mathcal{B}$ at $E_{\rm min}$	Modified $\mathcal{B}$ ($E_{\rm min} = 1.6$)
CLEO Inc. [264]	$321 \pm 43 \pm 27^{+18}_{-10}$	2.0	$306 \pm 41 \pm 26$	$329 \pm 44 \pm 28 \pm 6 \pm 6$
Belle Semi. [265]	$336 \pm 53 \pm 42^{+50}_{-54}$	2.24	–	$369 \pm 58 \pm 46^{+56}_{-60}$
Belle Inc. [266]	$355 \pm 32^{+30+11}_{-31-7}$	1.8	$351 \pm 32 \pm 29$	$350 \pm 32^{+30}_{-31} \pm 2 \pm 2$
BABAR Semi. [267]	$335 \pm 19^{+56+4}_{-41-9}$	1.9	$327 \pm 18^{+55+4}_{-43-9}$	$349 \pm 20^{+59+4}_{-46-3}$
BABAR Inc. [268]	–	1.9	$367 \pm 29 \pm 34 \pm 29$	$392 \pm 31 \pm 36 \pm 30 \pm 4 \pm 6$

6.4 Baryonic decays

Table 44: Branching fractions of baryonic B^+ decays (in units of 10^{-6}). Upper limits are at 90% CL. values in red (blue) are new published (preliminary) result since PDG2004 [as of July 15, 2005].

RPP#	Mode	PDG2004 Avg.	BABAR	Belle	CLEO	New Avg.
201	$p\overline{p}\pi^+$	< 3.7		$3.06^{+0.73}_{-0.62} \pm 0.37$‡	< 160	$3.06^{+0.82}_{-0.72}$
204	$p\overline{p}K^+$	$4.3^{+1.2}_{-1.0}$	$6.7 \pm 0.5 \pm 0.4$†	$5.30^{+0.45}_{-0.39} \pm 0.58$‡		6.10 ± 0.48
	$\Theta^{++}\overline{p}$ *	New	< 0.09	< 0.091		< 0.09
	$\mathcal{G}K^+$ *	New		< 0.41		< 0.41
–	$p\overline{p}K^{*+}$	New		$10.31^{+3.62+1.34}_{-2.77-1.65}$‡		$10.31^{+3.86}_{-3.22}$
206	$p\overline{\Lambda}$	< 1.5		< 0.49	< 1.5	< 0.49
–	$p\overline{\Lambda}(1520)$	New	< 1.5			< 1.5
–	$\Lambda\overline{\Lambda}K^+$	New		$2.91^{+0.90}_{-0.70} \pm 0.38$‡		$2.91^{+0.98}_{-0.80}$
–	$\Lambda\overline{\Lambda}\pi^+$	New		< 2.8‡		< 2.8‡

† Charmonium decays to $p\overline{p}$ have been statistically subtracted.
‡ The charmonium mass region has been vetoed.
* Product BF - daughter BF taken to be 100%:
$\Theta(1540)^{++} \to K^+p$ (pentaquark candidate);
$\mathcal{G}(2220) \to p\overline{p}$ (glueball candidate).

Table 45: Branching fractions of baryonic B^0 decays (in units of 10^{-6}). Upper limits are at 90% CL. values in red (blue) are new published (preliminary) result since PDG2004 [as of July 15, 2005].

RPP#	Mode	PDG2004 Avg.	BABAR	Belle	CLEO	New Avg.
212	$p\overline{p}$	< 1.2	< 0.27	< 0.41	< 1.4	< 0.27
214	$p\overline{p}K^0$	< 7.2		$1.20^{+0.32}_{-0.22} \pm 0.14$‡		$1.20^{+0.35}_{-0.26}$
	$\Theta^+\overline{p}$ ‡	New		< 0.23		< 0.23
–	$p\overline{p}K^{*0}$	New		< 7.6‡		< 7.6‡
215	$p\overline{\Lambda}\pi^-$	$4.0^{+1.1}_{-1.0}$		$3.27^{+0.62}_{-0.51} \pm 0.39$	< 13	$3.27^{+0.73}_{-0.64}$
216	$p\overline{\Lambda}K^-$	< 0.82		< 0.82		< 0.82
217	$p\overline{\Sigma}^0\pi^-$	< 3.8		< 3.8		< 3.8
218	$\Lambda\overline{\Lambda}$	< 1.0		< 0.69	< 1.2	< 0.69

† Product BF - daughter BF taken to be 100%: ‡ The charmonium mass region has been vetoed. $\Theta(1540)^+ \to pK^0_S$ (pentaquark candidate).

6.5 B_s decays

Table 46: B_s branching fractions (in units of 10^{-6}). Upper limits are at 90% CL. Values in red (blue) are new published (preliminary) result since PDG2004 [as of July 15, 2005].

RPP#	Mode	PDG2004 Avg.	CDF	D0	New Avg.
15	$\phi\phi$	< 1183	$14^{+6}_{-5} \pm 6$ †		14^{+8}_{-7}
24	$\mu^+\mu^-$	< 2.0	< 0.15	< 0.30	< 0.16
26	$e^\pm\mu^\mp$	< 6.1	< 6.1		< 6.1
27	$\mu^+\mu^-\phi$	< 47	< 47	< 3.2 †	< 3.2 †

†Relative BF converted to absolute BF

Table 47: B_s rare relative branching fractions. Values in red (blue) are new published (preliminary) result since PDG2004 [as of July 15, 2005].

RPP#	Mode	PDG2004 Avg.	CDF	D0	New Avg.
9	$\mathcal{B}(B_s^0 \to \pi^+\pi^-)/\mathcal{B}(B_s^0 \to K^+K^-)$		< 0.10		< 0.10
15	$\mathcal{B}(B_s^0 \to \phi\phi)/\mathcal{B}(B_s^0 \to J/\psi\phi)$		$(10^{+5}_{-4} \pm 1) \times 10^{-3}$		10^{+7}_{-6}
16	$f_s\mathcal{B}(B_s^0 \to K^+\pi^-)/f_d\mathcal{B}(B_d^0 \to K^+\pi^-)$		< 0.11		< 0.11
17	$f_s\mathcal{B}(B_s^0 \to K^+K^-)/f_d\mathcal{B}(B_d^0 \to K^+\pi^-)$		$0.50 \pm 0.08 \pm 0.07$		0.50 ± 0.11
27	$\mathcal{B}(B_s^0 \to \mu^+\mu^-\phi)/\mathcal{B}(B_s^0 \to J/\psi\phi)$			$< 3.5 \times 10^{-3}$	$< 3.5 \times 10^{-3}$

6.6 Charge asymmetries

Table 48: CP asymmetries for charmless hadronic charged B decays. Values in red (blue) are new published (preliminary) result since PDG2004 [as of July 15, 2005].

RPP#	Mode	PDG2004 Avg.	BABAR	Belle	CLEO	CDF	New Avg.
117	$K^0\pi^+$	0.03 ± 0.08	$-0.09 \pm 0.05 \pm 0.01$	$0.05 \pm 0.05 \pm 0.01$	$0.18 \pm 0.24 \pm 0.02$		-0.02 ± 0.04
118	$K^+\pi^0$	-0.10 ± 0.08	$0.06 \pm 0.06 \pm 0.01$	$0.04 \pm 0.04 \pm 0.02$	$-0.29 \pm 0.23 \pm 0.02$		0.04 ± 0.04
119	$\eta' K^+$	0.009 ± 0.035	$0.033 \pm 0.028 \pm 0.005$	$0.029 \pm 0.028 \pm 0.021$	$0.03 \pm 0.12 \pm 0.02$		0.031 ± 0.021
121	ηK^+	New	$-0.20 \pm 0.15 \pm 0.01$	$-0.55 \pm 0.19^{+0.04}_{-0.03}$			-0.33 ± 0.12
122	ηK^{*+}	New	$0.13 \pm 0.14 \pm 0.02$	$-0.09^{+0.16}_{-0.15} \pm 0.01$			$0.03^{+0.11}_{-0.10}$
123	ωK^+	$-0.21 \pm 0.28 \pm 0.03$	$-0.09 \pm 0.17 \pm 0.01$	$0.05 \pm 0.08 \pm 0.01$			0.02 ± 0.07
125	$K^{*0}\pi^+$	New	$0.07 \pm 0.08 \pm 0.07$	$-0.149 \pm 0.064 \pm 0.031$			-0.093 ± 0.060
126	$K^{*+}\pi^0$	New	$0.04 \pm 0.29 \pm 0.05$				0.04 ± 0.29
127	$K^+\pi^+\pi^-$	$0.01 \pm 0.07 \pm 0.03$	$-0.013 \pm 0.037 \pm 0.011$	$0.049 \pm 0.026 \pm 0.030$			0.022 ± 0.029
129	$K^+ f_0(980)$	New	$0.09 \pm 0.10^{+0.10}_{-0.06}$	$-0.077 \pm 0.065^{+0.051}_{-0.034}$			$-0.020^{+0.068}_{-0.065}$
130	$K^+\rho^0$	New	$0.32 \pm 0.13^{+0.10}_{-0.08}$	$0.30 \pm 0.11^{+0.11}_{-0.05}$			$0.31^{+0.12}_{-0.11}$
	$K_0^*(1430)^0\pi^+$	New	$-0.064 \pm 0.032^{+0.023}_{-0.026}$	$0.076 \pm 0.038^{+0.036}_{-0.031}$			0.019 ± 0.037
	$f_2(1270)K^+$	New		$-0.59 \pm 0.22 \pm 0.04$			-0.59 ± 0.22
–	$K^{*0}\rho^+$	New	$-0.14 \pm 0.17 \pm 0.4$				-0.14 ± 0.43
138	$K^{*+}\rho^0$	$0.20^{+0.32}_{-0.29} \pm 0.04$	$0.20^{+0.32}_{-0.29} \pm 0.04$				$0.20^{+0.32}_{-0.29}$
142	$K^+\overline{K^0}$	New	$0.15 \pm 0.33 \pm 0.03$				0.15 ± 0.33
144	$K^+K_SK_S$	New	$-0.04 \pm 0.11 \pm 0.02$				-0.04 ± 0.11
152	$K^+K^-K^+$	$0.02 \pm 0.07 \pm 0.03$	$0.02 \pm 0.07 \pm 0.03$				0.02 ± 0.08
153	ϕK^+	0.03 ± 0.07	$0.054 \pm 0.056 \pm 0.012$	$0.01 \pm 0.12 \pm 0.05$		$-0.07 \pm 0.17^{+0.03}_{-0.02}$	0.037 ± 0.050
156	ϕK^{*+}	0.09 ± 0.15	$0.16 \pm 0.17 \pm 0.03$	$-0.02 \pm 0.14 \pm 0.03$			0.05 ± 0.11
173	$\pi^+\pi^0$	0.05 ± 0.15	$-0.01 \pm 0.10 \pm 0.02$	$0.02 \pm 0.08 \pm 0.01$			0.01 ± 0.06
174	$\pi^+\pi^-\pi^+$	$-0.39 \pm 0.33 \pm 0.12$	$-0.01 \pm 0.08 \pm 0.03$				-0.01 ± 0.09
175	$\rho^0\pi^+$	New	$-0.07 \pm 0.12^{+0.03}_{-0.06}$				$-0.07^{+0.12}_{-0.13}$
176	$f_0(980)\pi^+$	New	$-0.50 \pm 0.54 \pm 0.61$				-0.50 ± 0.81
180	$\rho^+\pi^0$	New	$-0.01 \pm 0.13 \pm 0.02$	$0.06 \pm 0.19^{+0.04}_{-0.06}$			0.01 ± 0.11
182	$\rho^+\rho^0$	-0.09 ± 0.16	$-0.19 \pm 0.23 \pm 0.03$	$0.00 \pm 0.22 \pm 0.03$			-0.09 ± 0.16
185	$\omega\pi^+$	-0.21 ± 0.19	$0.03 \pm 0.16 \pm 0.01$	$-0.03 \pm 0.09 \pm 0.02$	$-0.34 \pm 0.25 \pm 0.02$		-0.04 ± 0.08
186	$\omega\rho^+$	New	$0.05 \pm 0.26 \pm 0.02$				0.05 ± 0.26
187	$\eta\pi^+$	New	$-0.13 \pm 0.12 \pm 0.01$	$-0.10 \pm 0.11 \pm 0.02$			-0.11 ± 0.08
188	$\eta'\pi^+$	New	$0.14 \pm 0.16 \pm 0.01$	$0.15 \pm 0.38^{+0.02}_{-0.06}$			0.14 ± 0.15
190	$\eta\rho^+$	New	$0.02 \pm 0.18 \pm 0.02$	$-0.17^{+0.33}_{-0.29} \pm 0.02$			-0.03 ± 0.16

Table 49: Charmless hadronic CP asymmetries for $B^{\pm}/B^0$ admixtures. Values in red (blue) are new published (preliminary) result since PDG2004 [as of July 15, 2005].

RPP#	Mode	PDG2004 Avg.	BABAR	Belle	CLEO	CDF	New Avg.
56	$K^*\gamma$	-0.01 ± 0.07	$-0.013 \pm 0.036 \pm 0.010$	$-0.015 \pm 0.044 \pm 0.012$	$0.08 \pm 0.13 \pm 0.03$		-0.010 ± 0.028
67	$s\gamma$	$-0.079 \pm 0.108 \pm 0.022$	$0.025 \pm 0.050 \pm 0.015$	$0.002 \pm 0.050 \pm 0.026$	$-0.079 \pm 0.108 \pm 0.022$		0.004 ± 0.036
103	$s\ell\ell$	New	$-0.22 \pm 0.26 \pm 0.02$				-0.22 ± 0.26

Table 50: CP asymmetries for charmless hadronic neutral B decays. Values in red (blue) are new published (preliminary) result since PDG2004 [as of July 15, 2005].

RPP#	Mode	PDG2004 Avg.	BABAR	Belle	CLEO	CDF	New Avg.
123	$K^+\pi^-$	-0.09 ± 0.04	$-0.133 \pm 0.030 \pm 0.009$	$-0.113 \pm 0.022 \pm 0.008$	$-0.04 \pm 0.16 \pm 0.02$	$-0.04 \pm 0.08 \pm 0.01$	-0.115 ± 0.018
124	$K^0\pi^0$ †						
127	ηK^{*0}	New	$0.02 \pm 0.11 \pm 0.02$	$-0.04^{+0.11}_{-0.10} \pm 0.01$			-0.01 ± 0.08
136	$K^+\rho^-$	0.28 ± 0.19	$0.13^{+0.14}_{-0.17} \pm 0.14$	$0.22^{+0.22+0.06}_{-0.23-0.02}$			$0.17^{+0.15}_{-0.16}$
–	$K_0^*(1430)^+\pi^-$	New	$-0.07 \pm 0.12 \pm 0.08$				-0.07 ± 0.14
–	$K_0^*(1430)^0\pi^0$	New	$-0.34 \pm 0.15 \pm 0.11$				-0.34 ± 0.19
140	$K^{*+}\pi^-$	0.26 ± 0.35	$-0.11 \pm 0.14 \pm 0.05$		$0.26^{+0.33+0.10}_{-0.34-0.08}$		-0.05 ± 0.14
–	$K^+\pi^-\pi^0$	New		$0.07 \pm 0.11 \pm 0.01$			0.07 ± 0.11
141	$K^{*0}\pi^0$	New	$-0.01^{+0.24}_{-0.22} \pm 0.13$				$-0.01^{+0.27}_{-0.26}$
154	ϕK^{*0}	0.05 ± 0.10	$-0.01 \pm 0.09 \pm 0.02$	$0.02 \pm 0.09 \pm 0.02$			0.00 ± 0.07
177	$\pi^0\pi^0$	New	$0.12 \pm 0.56 \pm 0.06$	$0.44^{+0.53}_{-0.52} \pm 0.17$			$0.28^{+0.40}_{-0.39}$
196	$\rho^0\pi^0$	New		$-0.49^{+0.67}_{-0.81} \pm 0.200.24$			$-0.49^{+0.70}_{-0.83}$
197	$\rho^+\pi^-$ †						

† Measurements of time-dependent CP asymmetries are listed on the Unitarity Triangle home page. (http://www.slac.stanford.edu/xorg/hfag/triangle/index.html)

6.7 Polarization measurements

Table 51: Longitudinal polarization fraction f_L for B^+ decays. Values in red (blue) are new published (preliminary) result since PDG2004 [as of July 15, 2005].

RPP#	Mode	PDG2004 Avg.	BABAR	Belle	New Avg.
–	$K^{*0}\rho^+$	New	$0.79 \pm 0.08 \pm 0.04$	$0.43 \pm 0.11^{+0.05}_{-0.02}$	0.66 ± 0.07
138	$K^{*+}\rho^0$	$0.96^{+0.04}_{-0.15} \pm 0.04$	$0.96^{+0.04}_{-0.15} \pm 0.04$		$0.96^{+0.06}_{-0.15}$
156	ϕK^{*+}	$0.46 \pm 0.12 \pm 0.03$	$0.46 \pm 0.12 \pm 0.03$	$0.52 \pm 0.08 \pm 0.03$	0.50 ± 0.07
182	$\rho^+\rho^0$	0.96 ± 0.06	$0.97^{+0.03}_{-0.07} \pm 0.04$	$0.95 \pm 0.11 \pm 0.02$	$0.97^{+0.05}_{-0.07}$
186	$\omega\rho^+$	New	$0.88^{+0.12}_{-0.15} \pm 0.03$		$0.88^{+0.12}_{-0.15}$

Table 52: Full angular analysis of $B^+ \to \phi K^{*+}$. Values in red (blue) are new published (preliminary) result since PDG2004 [as of July 15, 2005].

Parameter	PDG2004 Avg.	BABAR	Belle	New Avg.
$f_\perp$	New		$0.19 \pm 0.08 \pm 0.02$	0.19 ± 0.08
$\phi_\parallel$	New		$2.10 \pm 0.28 \pm 0.04$	2.10 ± 0.28
$\phi_\perp$	New		$2.31 \pm 0.30 \pm 0.07$	2.31 ± 0.31

BR, f_L and A_{CP} are tabulated separately.

Table 53: Longitudinal polarization fraction f_L for B^0 decays. Values in red (blue) are new published (preliminary) result since PDG2004 [as of July 15, 2005].

RPP#	Mode	PDG2004 Avg.	BABAR	Belle	New Avg.
154	ϕK^{*0}	0.57 ± 0.11	$0.52 \pm 0.05 \pm 0.02$	$0.45 \pm 0.05 \pm 0.02$	0.48 ± 0.04
203	$\rho^+\rho^-$	New	$0.99 \pm 0.03^{+0.04}_{-0.03}$	$0.941^{+0.034}_{-0.040} \pm 0.030$	$0.971^{+0.031}_{-0.030}$

Table 54: Full angular analysis of $B^0 \to \phi K^{*0}$. Values in red (blue) are new published (preliminary) result since PDG2004 [as of July 15, 2005].

Parameter	PDG2004 Avg.	BABAR	Belle	New Avg.
$f_\perp = \Lambda_{\perp\perp}$	New	$0.22 \pm 0.05 \pm 0.02$	$0.31^{+0.06}_{-0.05} \pm 0.02$	0.26 ± 0.04
$\phi_\parallel$	New	$2.34^{+0.23}_{-0.20} \pm 0.05$	$2.40^{+0.28}_{-0.24} \pm 0.07$	$2.36^{+0.18}_{-0.16}$
$\phi_\perp$	New	$2.47 \pm 0.25 \pm 0.05$	$2.51 \pm 0.25 \pm 0.06$	2.49 ± 0.18
A^0_{CP}	New	$-0.06 \pm 0.10 \pm 0.01$	$0.13 \pm 0.12 \pm 0.04$	0.01 ± 0.08
$A^\perp_{CP}$	New	$-0.10 \pm 0.24 \pm 0.05$	$-0.20 \pm 0.18 \pm 0.04$	-0.16 ± 0.15
$\Delta\phi_\parallel$	New	$0.27^{+0.20}_{-0.23} \pm 0.05$	$-0.32 \pm 0.27 \pm 0.07$	0.03 ± 0.18
$\Delta\phi_\perp$	New	$0.36 \pm 0.25 \pm 0.05$	$-0.30 \pm 0.25 \pm 0.06$	0.03 ± 0.18
$f_\parallel = \Lambda_{\parallel\parallel}$	New	$0.26 \pm 0.05 \pm 0.02$	$0.24 \pm 0.06 \pm 0.02$	0.25 ± 0.04
$\mathcal{A}^0_T = -0.5\Lambda_{\perp 0}$	New	$0.11 \pm 0.05 \pm 0.01$	$-0.08 \pm 0.08 \pm 0.02$	0.06 ± 0.04
$\mathcal{A}^\parallel_T = -0.5\Lambda_{\perp\parallel}$	New	$-0.02 \pm 0.04 \pm 0.01$	$-0.01 \pm 0.05 \pm 0.01$	-0.02 ± 0.03
$\Lambda_{\parallel 0}$	New	$-0.50 \pm 0.12 \pm 0.03$	$-0.45 \pm 0.11 \pm 0.02$	-0.47 ± 0.08
Σ_{00}	New	$0.03 \pm 0.05 \pm 0.01$	$-0.06 \pm 0.05 \pm 0.01$	-0.02 ± 0.04
$\Sigma_{\parallel\parallel}$	New	$-0.05 \pm 0.06 \pm 0.01$	$-0.01 \pm 0.06 \pm 0.01$	-0.03 ± 0.04
$\Sigma_{\perp\perp}$	New	$0.02^{+0.06}_{-0.05} \pm 0.01$	$0.06 \pm 0.06 \pm 0.01$	0.04 ± 0.04
$\Sigma_{\perp 0}$	New	$-0.41 \pm 0.14 \pm 0.03$	$-0.41^{+0.16}_{-0.14} \pm 0.04$	$-0.41^{+0.11}_{-0.10}$
$\Sigma_{\perp\parallel}$	New	$-0.06^{+0.09}_{-0.08} \pm 0.02$	$-0.06 \pm 0.10 \pm 0.01$	$-0.06^{+0.07}_{-0.06}$
$\Sigma_{\parallel 0}$	New	$0.18^{+0.11}_{-0.13} \pm 0.03$	$-0.11 \pm 0.11 \pm 0.02$	0.01 ± 0.09

Results below the line have been derived from the primary results. BR, f_L and A_{CP} are tabulated separately.

7 B Decays to open charm and charmonium final states

This section is the first contribution to the HFAG report from the "$B \to$ charm " group[17]. The mandate of the group is to compile measurements and perform averages of all available quantities related to B decays to charmed particles, excluding CP related quantities. To date the group has analyzed a total of 330 measurements reported in 124 papers, principally branching fractions. The group aims to organize and present the copious information on B decays to charmed particles obtained from a combined sample of more than one billion B mesons from the BABAR, Belle and CDF Collaborations.

Branching fractions for rare B-meson decays or decay chains of a few 10^{-7} are now being measured with statistical uncertainties typically below 30%. Results for more common decays, with branching fractions around 10^{-4}, are becoming precision measurements, with uncertainties typically at the 3% level. Some decays have been observed for the first time, for example $\overline{B}^0 \to D_s^- \pi^+$ or $B^- \to \psi(3770)K^-$, with a branching fraction of $(2.74^{+0.67}_{-0.74})\times 10^{-5}$ and $(4.4\pm 1.1)\times 10^{-4}$, respectively.

Among the many results, we highlight the great improvements that have been attained towards a deeper understanding of recently discovered new states with either hidden or open charm content. The new average for the branching fraction of the decay chain $B^- \to X(3870)K^-$, where $X(3870) \to J/\psi\pi^+\pi^-$ is $(1.16 \pm 0.19) \times 10^{-5}$; many more $X(3870)$ decay modes have been searched for and several measurements or upper limits are reported. With an inclusive approach, an upper limit on the branching fraction for $B^- \to X(3870)K^-$ has been derived of 3.2×10^{-4}, 90% C.L.. In addition, a new state at about 3940 MeV, $Y(3940)$, has been observed in B decays and the branching fraction for $B \to Y(3940)K, Y(3940) \to \omega J/\psi$ has been measured to be $(7.1 \pm 3.4) \times 10^{-5}$. Several B decays to $D_{sJ}^{*-}(2317)$ and $D_{sJ}^-(2460)$ have been observed for the first time and the branching fractions measured. The abundance of measurements with many different final states is of the greatest importance for quantum number assignments, and already some of the proposed theoretical interpretations have been ruled out.

The measurements are classified according to the decaying particle : Charged B, Neutral B or Miscellaneous; the decay products and the type of quantity : branching fraction, product of branching fractions, ratio of branching fractions or other quantities. For the decay product classification the below precedence order is used to ensure that each measurement appears in only one category.

- new particles
- strange D mesons
- baryons
- J/ψ
- charmonium other than J/ψ
- multiple D, D^* or D^{**} mesons
- a single D^* or D^{**} meson
- a single D meson

[17]The HFAG/Charm group was formed in the spring of 2005; it performs its work using an XML database backed web application.

Within each table the measurements are color coded according to the publication status and age. Table 55 provides a key to the color scheme and categories used. When viewing the tables with most pdf viewers every number, label and average provides hyperlinks to the corresponding reference and individual quantity web pages on the HFAG/Charm group website http://hfag.phys.ntu.edu.tw. The links provided in the captions of the table lead to the corresponding compilation pages. Both the individual and compilation webpages provide a graphical view of the results, in a variety of formats.

Tables 56 to 90 provide either limits at 90% confidence level or measurements with statistical and systematic uncertainties and in some cases a third error corresponding to correlated systematics. For details on the meanings of the uncertainties and access to the references click on the numbers to visit the corresponding web pages. Where there are multiple determinations of the same quantity by one experiment the table footnotes act to distinguish the methods or datasets used; such cases are visually highlighted in the table by presenting the measurements on the lines beneath the quantity label. Where both limits and measured values of a quantity are available the limits are presented in the tables but are not used in the determination of the average. Where only limits are available the most stringent is presented in the Average column of the tables. Where available the PDG 2004 result is also presented.

Table 55: Key to the colors used to classify the results presented in tables 56 to 90. When viewing these tables in a pdf viewer each number, label and average provides a hyperlink to the corresponding online version provided by the charm subgroup website http://hfag.phys.ntu.edu.tw. Where an experiment has multiple determinations of a single quantity they are distinguished by the table footnotes.

Class	Definition
waiting	Results without a preprint available
pubhot	Results published in 2005
prehot	Preprint released in 2005
pub	Results published after or during the last PDG year
pre	Preprint released after or during the last PDG year
pubold	Results published before the last PDG year
preold	Preprint released before the last PDG year
error	Incomplete information to classify
superceeded	Results superceeded by more recent measurements from the same experiment
inactive	Results in the process of being entered into the database
noquo	Results without quotes

Table 56: Branching fractions of charged B modes producing new particles in units of 10^{-4}, upper limits are at 90% CL. The latest version is available at: http://hfag.phys.ntu.edu.tw/hfagc/00101.html

Mode	PDG 2004	Belle	*BABAR*	CDF	Average
$X(3870)K^-$			< 3.2		< 3.2

Table 57: Product branching fractions of charged B modes producing new particles in units of 10^{-4}, upper limits are at 90% CL. The latest version is available at: http://hfag.phys.ntu.edu.tw/hfagc/00101.html

Mode	PDG 2004	Belle	*BABAR*	CDF	Average
$K^-X(3870)[\gamma J/\psi(1S)]$		$0.018 \pm 0.006 \pm 0.001$			0.018 ± 0.006
$K^-X(3870)[J/\psi(1S)\eta]$			< 0.077		< 0.077
$K^-X(3870)[\pi^+\pi^- J/\psi(1S)]$	0.136 ± 0.031	$0.131 \pm 0.024 \pm 0.013$	$0.101 \pm 0.025 \pm 0.010$		0.116 ± 0.019
$K^-Y(4260)[J/\psi(1S)\pi^+\pi^-]$			$0.200 \pm 0.070 \pm 0.020$		0.200 ± 0.073
$\overline{K}^0X^-(3870)[J/\psi(1S)\pi^-\pi^0]$			< 0.22		< 0.22
$K^-X(3870)[D^+D^-]$		< 0.40			< 0.40
$K^-X(3870)[D^0\overline{D}^0\pi^0]$		< 0.60			< 0.60
$K^-X(3870)[D^0\overline{D}^0]$		< 0.60			< 0.60
$D^0D_{sJ}^-(2460)[D_s^-\pi^+\pi^-]$		< 2.2			< 2.2
$D^0D_{sJ}^-(2460)[D_s^-\pi^0]$		< 2.7			< 2.7
$D^0D_{sJ}^-(2460)[D_s^-\gamma]$	5.6 ± 2.3	$5.6 \pm^{1.6}_{1.5} \pm 1.7$	$6.0 \pm 2.0 \pm 1.0 \pm^{2.0}_{1.0}$		$5.8 \pm^{1.7}_{1.9}$
$D^0D_{sJ}^*(2317)^-[D_s^{*-}\gamma]$		< 7.6			< 7.6
$D^{*0}(2007)D_{sJ}^*(2317)^-[D_s^-\pi^0]$			$9.0 \pm 6.0 \pm 2.0 \pm^{3.0}_{2.0}$		$9.0 \pm^{7.0}_{6.6}$
$D^0D_{sJ}^*(2317)^-[D_s^-\pi^0]$	8.1 ± 3.7	$8.1 \pm^{3.0}_{2.7} \pm 2.4$	$10.0 \pm 3.0 \pm 1.0 \pm^{4.0}_{2.0}$		$8.9 \pm^{2.7}_{3.2}$
$D^0D_{sJ}^-(2460)[D_s^{*-}\gamma]$		< 9.8			< 9.8
$D^{*0}(2007)D_{sJ}^-(2460)[D_s^-\gamma]$			$14.0 \pm 4.0 \pm 3.0 \pm^{5.0}_{3.0}$		$14.0 \pm^{7.1}_{5.8}$
$D^0D_{sJ}^-(2460)[D_s^{*-}\pi^0]$	11.9 ± 6.5	$11.9 \pm^{6.1}_{4.9} \pm 3.6$	$27 \pm 7 \pm 5 \pm^{9}_{6}$		$15.0 \pm^{5.3}_{5.8}$
$D^{*0}(2007)D_{sJ}^-(2460)[D_s^{*-}\pi^0]$			$76 \pm 17 \pm 18 \pm^{26}_{16}$		$76 \pm^{36}_{29}$

Table 58: Branching fractions of charged B modes producing strange D mesons in units of 10^{-5}, upper limits are at 90% CL. The latest version is available at: http://hfag.phys.ntu.edu.tw/hfagc/00102.html

Mode	PDG 2004	Belle	*BABAR*	CDF	Average
$D_s^-\phi(1020)$	< 32		< 0.190		< 0.190
$D_s^{*-}\phi(1020)$	< 40		< 1.20		< 1.20
$D_s^-\pi^0$	< 20		< 2.8		< 2.8

Table 59: Branching fractions of charged B modes producing baryons in units of 10^{-5}, upper limits are at 90% CL. The latest version is available at: http://hfag.phys.ntu.edu.tw/hfagc/00103.html

Mode	PDG 2004	Belle	*BABAR*	CDF	Average
$J/\psi(1S)\Lambda\overline{p}$	1.20 ± 0.80		$1.16 \pm^{0.74}_{0.53} \pm^{0.42}_{0.18}$		$1.16 \pm^{0.85}_{0.56}$
$D^{*+}(2010)p\overline{p}$		< 1.50			< 1.50
$D^{+}p\overline{p}$		< 1.50			< 1.50
$\Sigma_c^{*0}\overline{p}$	< 4.6	< 4.6			< 4.6
$\Sigma_c^{0}\overline{p}$	< 8.0	< 9.3			< 9.3
$\Lambda_c^{+}\overline{p}\pi^{-}$	21 ± 7	$18.7 \pm^{4.3}_{4.0} \pm 2.8 \pm 4.9$			$18.7 \pm^{7.1}_{6.9}$

Table 60: Branching fractions of charged B modes producing $J/\psi(1S)$ in units of 10^{-4}, upper limits are at 90% CL. The latest version is available at: http://hfag.phys.ntu.edu.tw/hfagc/00104.html

Mode	PDG 2004	Belle	*BABAR*	CDF	Average
$J/\psi(1S)D^0\pi^-$		< 0.25	< 0.52		< 0.25
$J/\psi(1S)\phi(1020)K^-$	0.52 ± 0.17		$0.44 \pm 0.14 \pm 0.05 \pm 0.01$		0.44 ± 0.15
$J/\psi(1S)\pi^-$	0.40 ± 0.05	$0.38 \pm 0.06 \pm 0.03$	$0.54 \pm 0.04 \pm 0.02$		0.48 ± 0.04
$J/\psi(1S)\eta K^-$			$1.08 \pm 0.23 \pm 0.24 \pm 0.03$		1.08 ± 0.33
$J/\psi(1S)D^-$			< 1.20		< 1.20
$J/\psi(1S)K^-$	10.0 ± 0.4				10.3 ± 0.4
		$10.1 \pm 0.2 \pm 0.7 \pm 0.2$	$10.6 \pm 0.2 \pm 0.4 \pm 0.2$ [1]		
			$10.1 \pm 0.9 \pm 0.6$ [2]		
			$8.1 \pm 1.3 \pm 0.7$ [3]		
$J/\psi(1S)K^-\pi^+\pi^-$	7.7 ± 2.0		$11.6 \pm 0.7 \pm 0.9$	$6.9 \pm 1.8 \pm 1.2$	10.6 ± 1.0
$J/\psi(1S)K^{*-}(892)$	13.5 ± 1.0	$12.8 \pm 0.7 \pm 1.4 \pm 0.2$	$14.5 \pm 0.5 \pm 0.9 \pm 0.2$	$15.8 \pm 4.7 \pm 2.7$	14.0 ± 0.9
$J/\psi(1S)K_1^-(1270)$	18.0 ± 5.2	$18.0 \pm 3.4 \pm 3.0 \pm 2.5$			18.0 ± 5.2

[1] MEASUREMENT OF BRANCHING FRACTIONS AND CHARGE ASYMMETRIES FOR EXCLUSIVE B DECAYS TO CHARMONIUM (124M $B\overline{B}$ pairs) ; $B^- \to J/\psi K^-$ with J/ψ to leptons
[2] MEASUREMENT OF THE $B^+ \to p\overline{p}K^+$ BRANCHING FRACTION AND STUDY OF THE DECAY DYNAMICS (232M $B\overline{B}$ pairs) ; $B^- \to J/\psi K^-$ with $J/\psi \to p\overline{p}$
[3] Measurements of the absolute branching fractions of $B^\pm \to K^\pm X_{c\overline{c}}$ (231.8M $B\overline{B}$ pairs) ; $B^- \to J/\psi K^-$ (inclusive)

Table 61: Product branching fractions of charged B modes producing $J/\psi(1S)$ in units of 10^{-4}, upper limits are at 90% CL. The latest version is available at: http://hfag.phys.ntu.edu.tw/hfagc/00104.html

Mode	PDG 2004	Belle	*BABAR*	CDF	Average
$K^- h_c(1P)[J/\psi(1S)\pi^+\pi^-]$			< 0.034		< 0.034

Table 62: Ratios of branching fractions of charged B modes producing $J/\psi(1S)$ in units of 10^0, upper limits are at 90% CL. The latest version is available at: http://hfag.phys.ntu.edu.tw/hfagc/00104.html

Mode	PDG 2004	Belle	*BABAR*	CDF	Average
$\frac{\mathcal{B}(B^-\to J/\psi(1S)\pi^-)}{\mathcal{B}(B^-\to J/\psi(1S)K^-)}$	0.040 ± 0.005		$0.054 \pm 0.004 \pm 0.001$	$0.050 \pm^{0.019}_{0.017} \pm 0.001$	0.053 ± 0.004
$\frac{\mathcal{B}(B^-\to J/\psi(1S)K_1^-(1400))}{\mathcal{B}(B^-\to J/\psi(1S)K_1^-(1270))}$	< 0.30	< 0.30			< 0.30
$\frac{\mathcal{B}(B^-\to \chi_{c0}(1P)K^-)}{\mathcal{B}(B^-\to J/\psi(1S)K^-)}$	0.60 ± 0.20	$0.60 \pm^{0.21}_{0.18} \pm 0.05 \pm 0.08$			$0.60 \pm^{0.23}_{0.20}$
$\frac{\mathcal{B}(B^-\to \eta_c(1S)K^-)}{\mathcal{B}(B^-\to J/\psi(1S)K^-)}$			$1.28 \pm 0.10 \pm 0.38$ [1]		1.12 ± 0.20
			$1.06 \pm 0.23 \pm 0.04$ [2]		
$\frac{\mathcal{B}(B^-\to J/\psi(1S)K^{*-}(892))}{\mathcal{B}(B^-\to J/\psi(1S)K^-)}$	1.40 ± 0.11		$1.37 \pm 0.05 \pm 0.08$	$1.92 \pm 0.60 \pm 0.17$	1.38 ± 0.09
$\frac{\mathcal{B}(B^-\to J/\psi(1S)K_1^-(1270))}{\mathcal{B}(B^-\to J/\psi(1S)K^-)}$		$1.80 \pm 0.34 \pm 0.34$			1.80 ± 0.48

[1] Branching Fraction Measurements of $B \to \eta_c K$ Decays (86.1M $B\overline{B}$ pairs) ; Ratio $B^- \to \eta_c K^-$ to $B^- \to J/\psi K^-$ with $\eta_c \to K\overline{K}\pi$
[2] Measurements of the absolute branching fractions of $B^\pm \to K^\pm X_{c\overline{c}}$ (231.8M $B\overline{B}$ pairs) ; Ratio $B^- \to \eta_c K^-$ to $B^- \to J/\psi K^-$ (inclusive analysis)

Table 63: Branching fractions of charged B modes producing charmonium other than $J/\psi(1S)$ in units of 10^{-3}, upper limits are at 90% CL. The latest version is available at: http://hfag.phys.ntu.edu.tw/hfagc/00105.html

Mode	PDG 2004	Belle	*BABAR*	CDF	Average
$\chi_{c2}(1P)K^{*-}(892)$			< 0.012		< 0.012
$\chi_{c2}(1P)K^-$					< 0.030
			< 0.030 [1]		
			< 0.200 [2a]		
$\chi_{c0}(1P)\pi^-$			< 0.061		< 0.061
$\chi_{c0}(1P)K^-$	0.60 ± 0.20				0.191 ± 0.040
		$0.60 \pm^{0.21}_{0.18} \pm 0.07 \pm 0.09$	0.27 ± 0.07 [3]		
			$0.134 \pm 0.045 \pm 0.015 \pm 0.014$ [4]		
			< 0.180 [2c]		
$\chi_{c1}(1P)K^{*-}(892)$	< 2.1		$0.29 \pm 0.10 \pm 0.09 \pm 0.03$		0.29 ± 0.14
$\eta_c(2S)K^-$			$0.34 \pm 0.18 \pm 0.03$		0.34 ± 0.18
$\psi(3770)K^-$		$0.48 \pm 0.11 \pm 0.07$	$0.35 \pm 0.25 \pm 0.03$		0.45 ± 0.12
$\chi_{c1}(1P)K^-$	0.68 ± 0.12				0.63 ± 0.06
			$0.58 \pm 0.03 \pm 0.06$ [5a]	$1.55 \pm 0.54 \pm 0.20$	
			$0.80 \pm 0.14 \pm 0.07$ [2b]		
$\psi(2S)K^-$	0.68 ± 0.04				0.63 ± 0.04
		0.69 ± 0.06	$0.62 \pm 0.03 \pm 0.04 \pm 0.02$ [5b]	$0.55 \pm 0.10 \pm 0.06$	
			$0.49 \pm 0.16 \pm 0.04$ [2e]		
$\psi(2S)K^{*-}(892)$	0.92 ± 0.22	$0.81 \pm 0.08 \pm 0.09$	$0.59 \pm 0.08 \pm 0.09 \pm 0.02$		0.71 ± 0.09
$\eta_c(1S)K^-$	0.90 ± 0.27				0.98 ± 0.13
		$1.25 \pm 0.14 \pm^{0.10}_{0.12} \pm 0.38$	$1.29 \pm 0.09 \pm 0.13 \pm 0.36$ [6]		
			$1.38 \pm^{0.23}_{0.15} \pm 0.15 \pm 0.42$ [7]		
			0.87 ± 0.15 [2d]		
$\chi_{c0}(1P)K^{*-}(892)$			< 2.9		< 2.9

[1] SEARCH FOR FACTORIZATION-SUPPRESSED $B \to \chi_c K^{(*)}$ DECAYS (124M $B\overline{B}$ pairs) ; $B^- \to \chi_{c2} K^-$ with $\chi_{c2} \to J/\psi\gamma$

[2] Measurements of the absolute branching fractions of $B^\pm \to K^\pm X_{c\overline{c}}$ (231.8M $B\overline{B}$ pairs) ; [2a] $B^- \to \chi_{c2} K^-$ (inclusive) ; [2b] $B^- \to \chi_{c1} K^-$ (inclusive) ; [2c] $B^- \to \chi_{c0} K^-$ (inclusive) ; [2d] $B^- \to \eta_c K^-$ (inclusive) ; [2e] $B^- \to \psi(2S) K^-$ (inclusive)

[3] MEASUREMENT OF THE BRANCHING FRACTION FOR $B^\pm \to \chi_{c0} K^\pm$. (88.9M $B\overline{B}$ pairs) ; $B^- \to \chi_{c0} K^-$ with $\chi_{c0} \to K^+K^-, \pi^+\pi^-$

[4] Dalitz-plot analysis of the decays $B^\pm \to K^\pm \pi^\mp \pi^\pm$ (226M $B\overline{B}$ pairs) ; $B^- \to \chi_{c0} K^-$ with $\chi_{c0} \to \pi^+\pi^-$ (Dalitz analysis)

[5] MEASUREMENT OF BRANCHING FRACTIONS AND CHARGE ASYMMETRIES FOR EXCLUSIVE B DECAYS TO CHARMONIUM (124M $B\overline{B}$ pairs) ; [5a] $B^- \to \chi_{c1} K^-$ with χ_{c1} to $J/\psi\gamma$; [5b] $B^- \to \psi(2S) K^-$ with $\psi(2S)$ to leptons

[6] Branching Fraction Measurements of $B \to \eta_c K$ Decays (86.1M $B\overline{B}$ pairs) ; $B^- \to \eta_c K^-$ with $\eta_c \to K\overline{K}\pi$

[7] MEASUREMENT OF THE $B^+ \to p\overline{p}K^+$ BRANCHING FRACTION AND STUDY OF THE DECAY DYNAMICS (232M $B\overline{B}$ pairs) ; $B^- \to \eta_c K^-$ with $\eta_c \to p\overline{p}$

Table 64: Ratios of branching fractions of charged B modes producing charmonium other than $J/\psi(1S)$ in units of 10^0, upper limits are at 90% CL. The latest version is available at: http://hfag.phys.ntu.edu.tw/hfagc/00105.html

Mode	PDG 2004	Belle	*BABAR*	CDF	Average
$\frac{\mathcal{B}(B^-\to\chi_{c1}(1P)K^{*-}(892))}{\mathcal{B}(B^-\to\chi_{c1}(1P)K^-)}$			$0.51 \pm 0.17 \pm 0.16$		0.51 ± 0.23
$\frac{\mathcal{B}(B^-\to\psi(2S)K^{*-}(892))}{\mathcal{B}(B^-\to\psi(2S)K^-)}$			$0.96 \pm 0.15 \pm 0.09$		0.96 ± 0.17

Table 65: Branching fractions of charged B modes producing multiple D, D^* or D^{**} mesons in units of 10^{-3}, upper limits are at 90% CL. The latest version is available at: http://hfag.phys.ntu.edu.tw/hfagc/00106.html

Mode	PDG 2004	Belle	*BABAR*	CDF	Average
$D^0D^{*-}(2010)$	< 13.0	$0.46 \pm 0.07 \pm 0.06$			0.46 ± 0.09
D^0D^-	< 6.7	$0.56 \pm 0.08 \pm 0.06$			0.56 ± 0.10
$D^+D^-K^-$	< 0.40	< 0.90	< 0.40		< 0.40
$D^+D^{*-}(2010)K^-$			< 0.70		< 0.70
$D^0\overline{D}^0K^-$	1.90 ± 0.40	$1.17 \pm 0.21 \pm 0.15$	$1.90 \pm 0.30 \pm 0.30$		1.37 ± 0.22
$D^{*+}(2010)D^-K^-$			$1.50 \pm 0.30 \pm 0.20$		1.50 ± 0.36
$D^{*-}(2010)D^{*+}(2010)K^-$	< 1.80		< 1.80		< 1.80
$D^0D^-\overline{K}^0$	< 2.8		< 2.8		< 2.8
$D^{*0}(2007)\overline{D}^0K^-$	< 3.8		< 3.8		< 3.8
$D^0\overline{D}^{*0}(2007)K^-$	4.7 ± 1.0		$4.7 \pm 0.7 \pm 0.7$		4.7 ± 1.0
$D^0D^{*-}(2010)\overline{K}^0$	5.2 ± 1.2		$5.2 \pm^{1.0}_{0.9} \pm 0.7$		$5.2 \pm^{1.2}_{1.1}$
$\overline{D}^{*0}(2007)D^{*0}(2007)K^-$			$5.3 \pm^{1.1}_{1.0} \pm 1.2$		5.3 ± 1.6
$D^{*0}(2007)D^-\overline{K}^0$	< 6.1		< 6.1		< 6.1
$D^{*0}(2007)D^{*-}(2010)\overline{K}^0$			$7.8 \pm^{2.3}_{2.1} \pm 1.4$		$7.8 \pm^{2.7}_{2.5}$

Table 66: Product branching fractions of charged B modes producing multiple D, D^* or D^{**} mesons in units of 10^{-4}, upper limits are at 90% CL. The latest version is available at: http://hfag.phys.ntu.edu.tw/hfagc/00106.html

Mode	PDG 2004	Belle	*BABAR*	CDF	Average
$\pi^- D_1^0(2420)[D^{*0}(2007)\pi^-\pi^+]$		< 0.060			< 0.060
$\pi^- D_2^{*0}(2460)[D^{*0}(2007)\pi^-\pi^+]$		< 0.22			< 0.22
$\pi^- D_2^{*0}(2460)[D^{*+}(2010)\pi^-]$		$1.80 \pm 0.30 \pm 0.30 \pm 0.20$	$1.80 \pm 0.30 \pm 0.50$		1.80 ± 0.36
$\pi^- D_1^0(2420)[D^0\pi^-\pi^+]$		$1.85 \pm 0.29 \pm 0.35 \pm^{0.00}_{0.46}$			$1.85 \pm^{0.45}_{0.65}$
$\pi^- D_2^{*0}(2460)[D^+\pi^-]$		$3.4 \pm 0.3 \pm 0.6 \pm 0.4$	$2.9 \pm 0.2 \pm 0.5$		3.1 ± 0.4
$\pi^- D_1^0(H)[D^{*+}(2010)\pi^-]$		$5.0 \pm 0.4 \pm 1.0 \pm 0.4$			5.0 ± 1.1
$\pi^- D_0^{*0}[D^+\pi^-]$		$6.1 \pm 0.6 \pm 0.9 \pm 1.6$			6.1 ± 1.9
$\pi^- D_1^0(2420)[D^{*+}(2010)\pi^-]$		$6.8 \pm 0.7 \pm 1.3 \pm 0.3$	$5.9 \pm 0.3 \pm 1.1$		6.2 ± 0.9

Table 67: Ratios of branching fractions of charged B modes producing multiple D, D^* or D^{**} mesons in units of 10^0, upper limits are at 90% CL. The latest version is available at: http://hfag.phys.ntu.edu.tw/hfagc/00106.html

Mode	PDG 2004	Belle	*BABAR*	CDF	Average
$\frac{\mathcal{B}(B^-\to D^{*0}(2007)K^-)}{\mathcal{B}(B^-\to D^{*0}(2007)\pi^-)}$	0.078 ± 0.021	$0.078 \pm 0.019 \pm 0.009$	$0.081 \pm 0.004 \pm^{0.004}_{0.003}$		0.081 ± 0.005
$\frac{\mathcal{B}(B^-\to D^0K^-)}{\mathcal{B}(B^-\to D^0\pi^-)}$	0.083 ± 0.010	$0.077 \pm 0.005 \pm 0.006$	$0.083 \pm 0.003 \pm 0.002$		0.082 ± 0.004
$\frac{\mathcal{B}(B^-\to D_2^{*0}(2460)\pi^-)}{\mathcal{B}(B^-\to D_1^0(2420)\pi^-)}$			$0.80 \pm 0.07 \pm 0.16$		0.80 ± 0.17
$\frac{\mathcal{B}(B^-\to D^0\pi^-)}{\mathcal{B}(\overline{B}^0\to D^+\pi^-)}$				$1.97 \pm 0.10 \pm 0.21$	1.97 ± 0.23

Table 68: Branching fractions of charged B modes producing a single D^* or D^{**} meson in units of 10^{-4}, upper limits are at 90% CL. The latest version is available at: http://hfag.phys.ntu.edu.tw/hfagc/00107.html

Mode	PDG 2004	Belle	*BABAR*	CDF	Average
$D^{*-}(2010)\overline{K}^0$	< 0.95		< 0.090		< 0.090
$D^{*0}(2007)K^-$	3.6 ± 1.0	$3.6 \pm 0.9 \pm 0.4 \pm 0.3$			3.6 ± 1.0
$D^{*0}(2007)K^{*-}(892)$	7.2 ± 3.4		$8.3 \pm 1.1 \pm 1.0 \pm 0.3$		8.3 ± 1.5
$D^{*0}(2007)K^-K^0$	< 10.6	< 10.6			< 10.6
$D^{*+}(2010)\pi^-\pi^-$	21 ± 6	$12.5 \pm 0.8 \pm 2.2$	$12.2 \pm 0.5 \pm 1.8$		12.3 ± 1.5
$D^{*0}(2007)K^-K^{*0}(892)$	15.0 ± 4.0	$15.3 \pm 3.1 \pm 2.9$			15.3 ± 4.2
$D^{*+}(2010)\pi^-\pi^+\pi^-\pi^-$	< 100	$26 \pm 3 \pm 3$			26 ± 4
$D^{*0}(2007)\pi^-\pi^+\pi^-\pi^+\pi^-$		$57 \pm 9 \pm 8$			57 ± 12
$D^{*0}(2007)\pi^-\pi^+\pi^-$	94 ± 26	$106 \pm 5 \pm 13$			106 ± 14

Table 69: Branching fractions of charged B modes producing a single D meson in units of 10^{-4}, upper limits are at 90% CL. The latest version is available at: http://hfag.phys.ntu.edu.tw/hfagc/00108.html

Mode	PDG 2004	Belle	*BABAR*	CDF	Average
$D^-\overline{K}^0$			< 0.050		< 0.050
D^0K^-	3.7 ± 0.6	$3.8 \pm 0.2 \pm 0.3 \pm 0.2$			3.8 ± 0.4
$D^0K^-K^0$	5.5 ± 1.6	$5.5 \pm 1.4 \pm 0.8$			5.5 ± 1.6
$D^0K^{*-}(892)$	6.1 ± 2.3		$6.3 \pm 0.7 \pm 0.5$		6.3 ± 0.9
$D^0K^-K^{*0}(892)$	7.5 ± 1.7	$7.5 \pm 1.3 \pm 1.1$			7.5 ± 1.7
$D^+\pi^-\pi^-$	< 14.0	$10.2 \pm 0.4 \pm 1.5$	$8.7 \pm 0.4 \pm 1.3$		9.4 ± 1.0

Table 70: Branching fractions of neutral B modes producing new particles in units of 10^{-4}, upper limits are at 90% CL. The latest version is available at: http://hfag.phys.ntu.edu.tw/hfagc/00201.html

Mode	PDG 2004	Belle	*BABAR*	CDF	Average
$X^+(3870)K^-$			< 5.0		< 5.0

Table 71: Product branching fractions of neutral B modes producing new particles in units of 10^{-4}, upper limits are at 90% CL. The latest version is available at: http://hfag.phys.ntu.edu.tw/hfagc/00201.html

Mode	PDG 2004	Belle	*BABAR*	CDF	Average
$\pi^+ D_{sJ}^-(2460)[D_s^-\gamma]$		< 0.040			< 0.040
$\overline{K}^0 X(3870)[J/\psi(1S)\pi^+\pi^-]$			$0.051 \pm 0.028 \pm 0.007$		0.051 ± 0.029
$K^- X^+(3870)[J/\psi(1S)\pi^+\pi^0]$			< 0.054		< 0.054
$K^- D_{sJ}^+(2460)[D_s^+\gamma]$					< 0.086
		< 0.086 [1a]			
		< 0.094 [2a]			
$\pi^+ D_{sJ}^*(2317)^-[D_s^-\pi^0]$		< 0.25			< 0.25
$K^- D_{sJ}^*(2317)^+[D_s^+\pi^0]$					0.44 ± 0.15
		$0.44 \pm 0.08 \pm 0.06 \pm 0.11$ [1b]			
		$0.53 \pm^{0.15}_{0.13} \pm 0.07 \pm 0.14$ [2b]			
$D^+ D_{sJ}^-(2460)[D_s^-\pi^+\pi^-]$		< 2.00			< 2.00
$D^+ D_{sJ}^-(2460)[D_s^-\pi^0]$		< 3.6			< 3.6
$D^+ D_{sJ}^-(2460)[D_s^{*-}\gamma]$		< 6.0			< 6.0
$D^+ D_{sJ}^-(2460)[D_s^-\gamma]$	8.2 ± 3.2	$8.2 \pm^{2.2}_{1.9} \pm 2.5$	$8.0 \pm 2.0 \pm 1.0 \pm^{3.0}_{2.0}$		$8.1 \pm^{2.2}_{2.5}$
$D^+ D_{sJ}^*(2317)^-[D_s^{*-}\gamma]$		< 9.5			< 9.5
$D^+ D_{sJ}^*(2317)^-[D_s^-\pi^0]$	8.6 ± 4.0	$8.6 \pm^{3.3}_{2.6} \pm 2.6$	$18.0 \pm 4.0 \pm 3.0 \pm^{6.0}_{4.0}$		$10.4 \pm^{3.2}_{3.5}$
$D^{*+}(2010) D_{sJ}^*(2317)^-[D_s^-\pi^0]$			$15.0 \pm 4.0 \pm 2.0 \pm^{5.0}_{3.0}$		$15.0 \pm^{6.7}_{5.4}$
$D^{*+}(2010) D_{sJ}^-(2460)[D_s^-\gamma]$			$23 \pm 3 \pm 3 \pm^{8}_{5}$		$23 \pm^{9}_{7}$
$D^+ D_{sJ}^-(2460)[D_s^{*-}\pi^0]$	23 ± 10	$23 \pm^{7}_{6} \pm 7$	$28 \pm 8 \pm 5 \pm^{10}_{6}$		$25 \pm^{7}_{8}$
$D^{*+}(2010) D_{sJ}^-(2460)[D_s^{*-}\pi^0]$			$55 \pm 12 \pm 10 \pm^{19}_{12}$		$55 \pm^{25}_{20}$

[1] Improved Measurements of $\overline{B}^0 \to D_{sJ}^+ K^-$ decays (386M $B\overline{B}$ pairs) ; [1a] improved limit ; [1b] improved measurement
[2] Observation of $\overline{B}^0 \to D_{sJ}^*(2317)^+ K^-$ decay (152M $B\overline{B}$ pairs) ; [2a] first measurement ; [2b] first measurement

Table 72: Ratios of branching fractions of neutral B modes producing new particles in units of 10^0, upper limits are at 90% CL. The latest version is available at: http://hfag.phys.ntu.edu.tw/hfagc/00201.html

Mode	PDG 2004	Belle	*BABAR*	CDF	Average
$\frac{\mathcal{B}(\overline{B}^0 \to X(3870)\overline{K}^0)}{\mathcal{B}(B^- \to X(3870)K^-)}$			$0.50 \pm 0.30 \pm 0.05$		0.50 ± 0.30

Table 73: Branching fractions of neutral B modes producing strange D mesons in units of 10^{-3}, upper limits are at 90% CL. The latest version is available at: http://hfag.phys.ntu.edu.tw/hfagc/00202.html

Mode	PDG 2004	Belle	*BABAR*	CDF	Average
$D_s^- a_0^+(1450)$			< 0.019		< 0.019
$D_s^- \rho^+(770)$	< 0.70		< 0.019		< 0.019
$D_s^{*+} K^-$	< 0.025		< 0.025		< 0.025
$D_s^- \pi^+$	0.027 ± 0.010	$0.024 \pm^{0.010}_{0.008} \pm 0.004 \pm 0.006$	$0.032 \pm 0.009 \pm 0.007 \pm 0.008$		0.027 ± 0.009
$D_s^{*-} a_0^+(1450)$			< 0.036		< 0.036
$D_s^+ K^-$	0.038 ± 0.013	$0.046 \pm^{0.012}_{0.011} \pm 0.006 \pm 0.012$	$0.032 \pm 0.010 \pm 0.007 \pm 0.008$		0.037 ± 0.011
$D_s^{*-} \pi^+$	< 0.041		< 0.041		< 0.041
$D_s^- D_s^{*+}$			< 0.130		< 0.130
$D_s^- D_s^+$		< 0.200	< 0.100		< 0.100
$D_s^- a_2^+(1320)$			< 0.190		< 0.190
$D_s^{*-} a_2^+(1320)$			< 0.200		< 0.200
$D_s^{*+} D_s^{*-}$			< 0.24		< 0.24
$D_s^- D^+$	8.0 ± 3.0	$7.4 \pm 0.2 \pm 1.4$			7.4 ± 1.4
$D_s^- D^{*+}(2010)$	10.7 ± 2.9		$10.3 \pm 1.4 \pm 1.3 \pm 2.6$		10.3 ± 3.2
$D_s^{*-} D^{*+}(2010)$	19.0 ± 5.0				18.9 ± 1.8
			$18.8 \pm 0.9 \pm 1.6 \pm 0.6$ [1]		
			$19.7 \pm 1.5 \pm 3.0 \pm 4.9$ [2]		

[1] Measurement of the $\overline{B}^0 \to D_s^{*-} D^+$ and $D_s^+ \to \phi\pi^+$ branching fractions (123M $B\overline{B}$ pairs) ; $\overline{B}^0 \to D_s^{*-} D^{*+}$

[2] Measurement of $\overline{B}^0 \to D_s^{(*)} D^*$ Branching Fractions and $D_s^* D^*$ Polarization with a Partial Reconstruction technique (22.7M $B\overline{B}$ pairs) ; $\overline{B}^0 \to D_s^{*-} D^{*+}$

Table 74: Product branching fractions of neutral B modes producing strange D mesons in units of 10^{-4}, upper limits are at 90% CL. The latest version is available at: http://hfag.phys.ntu.edu.tw/hfagc/00202.html

Mode	PDG 2004	Belle	*BABAR*	CDF	Average
$D^+ D_s^- [\pi^- \phi(1020)[K^+ K^-]]$	1.42 ± 0.40	$1.47 \pm 0.05 \pm 0.21$			1.47 ± 0.22

Table 75: Ratios of branching fractions of neutral B modes producing strange D mesons in units of 10^0, upper limits are at 90% CL. The latest version is available at: http://hfag.phys.ntu.edu.tw/hfagc/00202.html

Mode	PDG 2004	Belle	*BABAR*	CDF	Average
$\frac{\mathcal{B}(\overline{B}^0\to D_s^{*-}D^+)}{\mathcal{B}(\overline{B}^0\to D_s^-D^+)}$				$0.90\pm0.20\pm0.10$	0.90 ± 0.22
$\frac{\mathcal{B}(\overline{B}^0\to D_s^-D^{*+}(2010))}{\mathcal{B}(\overline{B}^0\to D_s^-D^+)}$				$1.50\pm0.50\pm0.10$	1.50 ± 0.51
$\frac{\mathcal{B}(\overline{B}^0\to D_s^-D^+)}{\mathcal{B}(\overline{B}^0\to D^+\pi^+\pi^-\pi^-)}$				$1.99\pm0.13\pm0.11\pm0.45$	1.99 ± 0.48
$\frac{\mathcal{B}(\overline{B}^0\to D_s^{*-}D^{*+}(2010))}{\mathcal{B}(\overline{B}^0\to D_s^-D^+)}$				$2.6\pm0.5\pm0.2$	2.6 ± 0.5

Table 76: Branching fractions of neutral B modes producing baryons in units of 10^{-5}, upper limits are at 90% CL. The latest version is available at: http://hfag.phys.ntu.edu.tw/hfagc/00203.html

Mode	PDG 2004	Belle	*BABAR*	CDF	Average
$J/\psi(1S)\overline{p}p$	<0.190		<0.190		<0.190
$\Lambda_c^+\overline{p}$	2.2 ± 0.8	$2.2\pm^{0.6}_{0.5}\pm0.3\pm0.6$			$2.2\pm^{0.9}_{0.8}$
$D^{*0}(2007)p\overline{p}$		$12.0\pm^{3.3}_{2.9}\pm2.1$	$6.7\pm2.1\pm0.8\pm0.4$		8.0 ± 2.0
$\Sigma_c^{*0}\overline{p}\pi^+$	<12.1	<12.1			<12.1
$D^0p\overline{p}$		$11.8\pm1.5\pm1.6$	$12.4\pm1.4\pm1.2\pm0.3$		12.2 ± 1.4
$\Sigma_c^0\overline{p}\pi^+$	10.0 ± 8.0	<15.9			<15.9
$\Sigma_c^{*++}\overline{p}\pi^-$	16.0 ± 7.0	$16.3\pm^{5.7}_{5.1}\pm2.8\pm4.2$			$16.3\pm^{7.6}_{7.2}$
$\Sigma_c^{++}\overline{p}\pi^-$	28 ± 9	$24\pm^{6}_{6}\pm4\pm6$			$24\pm^{10}_{9}$
$D^+p\overline{p}\pi^-$			$38\pm4\pm5\pm1$		38 ± 6
$D^{*+}(2010)p\overline{p}\pi^-$	65 ± 16		$56\pm6\pm6\pm4$		56 ± 9
$\Lambda_c^+\overline{p}\pi^+\pi^-$	130 ± 40	$110\pm^{12}_{12}\pm19\pm29$			110 ± 37

Table 77: Branching fractions of neutral B modes producing $J/\psi(1S)$ in units of 10^{-4}, upper limits are at 90% CL. The latest version is available at: http://hfag.phys.ntu.edu.tw/hfagc/00204.html

Mode	PDG 2004	Belle	*BABAR*	CDF	Average
$J/\psi(1S)\gamma$			< 0.016		< 0.016
$J/\psi(1S)\phi(1020)$	< 0.092		< 0.090		< 0.090
$J/\psi(1S)f_2(1270)$		$0.098 \pm 0.039 \pm 0.020$			0.098 ± 0.044
$J/\psi(1S)D^0$		< 0.200	< 0.130		< 0.130
$J/\psi(1S)\pi^0$	0.22 ± 0.04	$0.23 \pm 0.05 \pm 0.02$	$0.194 \pm 0.022 \pm 0.017$		0.20 ± 0.02
$J/\psi(1S)\rho^0(770)$	0.160 ± 0.070	$0.28 \pm 0.03 \pm 0.03$	$0.160 \pm 0.060 \pm 0.040$		0.25 ± 0.04
$J/\psi(1S)\eta$	< 0.27		< 0.27		< 0.27
$J/\psi(1S)\pi^+\pi^-$	0.46 ± 0.09	< 0.100	$0.46 \pm 0.07 \pm 0.06$		0.46 ± 0.09
$J/\psi(1S)\eta'(958)$	< 0.63		< 0.63		< 0.63
$J/\psi(1S)\eta K_S^0$			$0.84 \pm 0.26 \pm 0.27 \pm 0.02$		0.84 ± 0.38
$J/\psi(1S)\phi(1020)\overline{K}^0$	0.94 ± 0.26		$1.02 \pm 0.38 \pm 0.10 \pm 0.02$		1.02 ± 0.39
$J/\psi(1S)\overline{K}^0\rho^0(770)$	5.4 ± 3.0			$5.4 \pm 2.9 \pm 0.9$	5.4 ± 3.0
$J/\psi(1S)\overline{K}^{*0}(892)\pi^+\pi^-$	6.6 ± 2.2			$6.6 \pm 1.9 \pm 1.1$	6.6 ± 2.2
$J/\psi(1S)K^{*-}(892)\pi^+$	8.0 ± 4.0			$7.7 \pm 4.1 \pm 1.3$	7.7 ± 4.3
$J/\psi(1S)\overline{K}^0$	8.5 ± 0.5	$7.9 \pm 0.4 \pm 0.9 \pm 0.1$	$8.7 \pm 0.2 \pm 0.3 \pm 0.2$	$11.5 \pm 2.3 \pm 1.7$	8.6 ± 0.3
$J/\psi(1S)\overline{K}^0\pi^+\pi^-$	10.0 ± 4.0			$10.3 \pm 3.3 \pm 1.5$	10.3 ± 3.6
$J/\psi(1S)\overline{K}_1^0(1270)$	13.0 ± 4.7	$13.0 \pm 3.4 \pm 2.5 \pm 1.8$			13.0 ± 4.6
$J/\psi(1S)\overline{K}^{*0}(892)$	13.1 ± 0.7	$12.9 \pm 0.5 \pm 1.3 \pm 0.2$	$13.1 \pm 0.3 \pm 0.7 \pm 0.2$	$17.4 \pm 2.0 \pm 1.8$	13.3 ± 0.7

Table 78: Ratios of branching fractions of neutral B modes producing $J/\psi(1S)$ in units of 10^0, upper limits are at 90% CL. The latest version is available at: http://hfag.phys.ntu.edu.tw/hfagc/00204.html

Mode	PDG 2004	Belle	*BABAR*	CDF	Average
$\frac{\mathcal{B}(\overline{B}^0\to J/\psi(1S)\overline{K}_1^0(1270))}{\mathcal{B}(B^-\to J/\psi(1S)K^-)}$		$1.30 \pm 0.34 \pm 0.28$			1.30 ± 0.44
$\frac{\mathcal{B}(\overline{B}^0\to \eta_c(1S)\overline{K}^0)}{\mathcal{B}(\overline{B}^0\to J/\psi(1S)\overline{K}^0)}$			$1.34 \pm 0.19 \pm 0.13 \pm 0.38$		1.34 ± 0.44
$\frac{\mathcal{B}(\overline{B}^0\to J/\psi(1S)\overline{K}^{*0}(892))}{\mathcal{B}(\overline{B}^0\to J/\psi(1S)\overline{K}^0)}$	1.48 ± 0.12		$1.51 \pm 0.05 \pm 0.08$	$1.39 \pm 0.36 \pm 0.10$	1.50 ± 0.09

Table 79: Miscellaneous quantities of neutral B modes producing $J/\psi(1S)$ in units of 10^0, upper limits are at 90% CL. The latest version is available at: http://hfag.phys.ntu.edu.tw/hfagc/00204.html

Mode	PDG 2004	Belle	*BABAR*	CDF	Average
$\frac{\mathcal{A}(\overline{B}^0 \to J/\psi(1S)K^{*0}(892))}{\mathcal{A}(B^0 \to J/\psi(1S)K^{*0}(892))}$			< 0.26		< 0.26
$\frac{\mathcal{A}(B^0 \to J/\psi(1S)\overline{K}^{*0}(892))}{\mathcal{A}(\overline{B}^0 \to J/\psi(1S)\overline{K}^{*0}(892))}$			< 0.32		< 0.32

Table 80: Branching fractions of neutral B modes producing charmonium other than $J/\psi(1S)$ in units of 10^{-3}, upper limits are at 90% CL. The latest version is available at: http://hfag.phys.ntu.edu.tw/hfagc/00205.html

Mode	PDG 2004	Belle	*BABAR*	CDF	Average
$\chi_{c2}(1P)\overline{K}^{*0}(892)$			< 0.036		< 0.036
$\chi_{c2}(1P)\overline{K}^{0}$			< 0.041		< 0.041
$\chi_{c1}(1P)\overline{K}^{*0}(892)$	0.41 ± 0.15		$0.33 \pm 0.04 \pm 0.05 \pm 0.03$		0.33 ± 0.08
$\chi_{c1}(1P)\overline{K}^{0}$	0.40 ± 0.11		$0.45 \pm 0.04 \pm 0.02 \pm 0.05$		0.45 ± 0.07
$\psi(2S)\overline{K}^{0}$	0.62 ± 0.07	0.67 ± 0.11	$0.65 \pm 0.06 \pm 0.04 \pm 0.02$		0.65 ± 0.07
$\psi(2S)\overline{K}^{*0}(892)$	0.80 ± 0.13	$0.72 \pm 0.04 \pm 0.06$	$0.65 \pm 0.06 \pm 0.09 \pm 0.02$	$0.90 \pm 0.22 \pm 0.09$	0.71 ± 0.06
$\chi_{c0}(1P)\overline{K}^{*0}(892)$			< 0.77		< 0.77
$\eta_c(1S)\overline{K}^{0}$	1.20 ± 0.40	$1.23 \pm 0.23 \pm^{0.12}_{0.16} \pm 0.38$	$1.14 \pm 0.15 \pm 0.12 \pm 0.32$		1.18 ± 0.29
$\chi_{c0}(1P)\overline{K}^{0}$	< 0.50		< 1.24		< 1.24
$\eta_c(1S)\overline{K}^{*0}(892)$	1.60 ± 0.70	$1.62 \pm 0.32 \pm^{0.24}_{0.34} \pm 0.50$			$1.62 \pm^{0.64}_{0.68}$

Table 81: Ratios of branching fractions of neutral B modes producing charmonium other than $J/\psi(1S)$ in units of 10^{0}, upper limits are at 90% CL. The latest version is available at: http://hfag.phys.ntu.edu.tw/hfagc/00205.html

Mode	PDG 2004	Belle	*BABAR*	CDF	Average
$\frac{\mathcal{B}(\overline{B}^0\to\chi_{c1}(1P)\overline{K}^{*0}(892))}{\mathcal{B}(\overline{B}^0\to\chi_{c1}(1P)\overline{K}^{0})}$	0.89 ± 0.38		$0.72 \pm 0.11 \pm 0.12$		0.72 ± 0.16
$\frac{\mathcal{B}(\overline{B}^0\to\eta_c(1S)\overline{K}^{0})}{\mathcal{B}(B^-\to\eta_c(1S)K^-)}$			$0.87 \pm 0.13 \pm 0.07$		0.87 ± 0.15
$\frac{\mathcal{B}(\overline{B}^0\to\psi(2S)\overline{K}^{*0}(892))}{\mathcal{B}(\overline{B}^0\to\psi(2S)\overline{K}^{0})}$			$1.00 \pm 0.14 \pm 0.09$		1.00 ± 0.17
$\frac{\mathcal{B}(\overline{B}^0\to\eta_c(1S)\overline{K}^{*0}(892))}{\mathcal{B}(\overline{B}^0\to\eta_c(1S)\overline{K}^{0})}$	1.30 ± 0.40	$1.33 \pm 0.36 \pm^{0.24}_{0.33}$			$1.33 \pm^{0.43}_{0.49}$

Table 82: Branching fractions of neutral B modes producing multiple D, D^* or D^{**} mesons in units of 10^{-3}, upper limits are at 90% CL. The latest version is available at: http://hfag.phys.ntu.edu.tw/hfagc/00206.html

Mode	PDG 2004	Belle	*BABAR*	CDF	Average
D^-D^+	< 0.94	$0.32 \pm 0.06 \pm 0.05$			0.32 ± 0.07
$D^{*+}(2010)D^{*-}(2010)$	0.87 ± 0.18	$0.81 \pm 0.08 \pm 0.11$	$0.83 \pm 0.16 \pm 0.12$		0.82 ± 0.11
$D^{*+}(2010)D^-$	< 0.63		$0.88 \pm 0.10 \pm 0.11 \pm 0.06$		0.88 ± 0.16
$D^{*-}(2010)D^+$	< 0.63	$1.17 \pm 0.26 \pm^{0.20}_{0.24} \pm 0.08$			$1.17 \pm^{0.34}_{0.36}$
$D^0\overline{D}^0\overline{K}^0$	< 1.40		< 1.40		< 1.40
$D^+\overline{D}^0K^-$	1.70 ± 0.40		$1.70 \pm 0.30 \pm 0.30$		1.70 ± 0.42
$D^+D^-\overline{K}^0$	< 1.70		< 1.70		< 1.70
$D^{*+}(2010)\overline{D}^0K^-$	3.1 ± 0.6		$3.1 \pm^{0.4}_{0.3} \pm 0.4$		$3.1 \pm^{0.6}_{0.5}$
$D^0\overline{D}^{*0}(2007)\overline{K}^0$	< 3.7		< 3.7		< 3.7
$D^+\overline{D}^{*0}(2007)K^-$	4.6 ± 1.0		$4.6 \pm 0.7 \pm 0.7$		4.6 ± 1.0
$D^{*+}(2010)D^-\overline{K}^0$	6.5 ± 1.6		$6.5 \pm 1.2 \pm 1.0$		6.5 ± 1.6
$D^{*0}(2007)\overline{D}^{*0}(2007)\overline{K}^0$	< 6.6		< 6.6		< 6.6
$D^{*-}(2010)D^{*+}(2010)\overline{K}^0$	8.8 ± 1.9		$8.8 \pm^{1.5}_{1.4} \pm 1.3$		$8.8 \pm^{2.0}_{1.9}$
$D^{*+}(2010)\overline{D}^{*0}(2007)K^-$	11.8 ± 2.0		$11.8 \pm 1.0 \pm 1.7$		11.8 ± 2.0

Table 83: Product branching fractions of neutral B modes producing multiple D, D^* or D^{**} mesons in units of 10^{-4}, upper limits are at 90% CL. The latest version is available at: http://hfag.phys.ntu.edu.tw/hfagc/00206.html

Mode	PDG 2004	Belle	*BABAR*	CDF	Average
$K^-D_2^{*+}(2460)[D^0\pi^+]$			$0.183 \pm 0.040 \pm 0.031$		0.183 ± 0.051
$\pi^-D_2^{*+}(2460)[D^{*+}(2010)\pi^-\pi^+]$		< 0.24			< 0.24
$\pi^-D_1^+(2420)[D^{*+}(2010)\pi^-\pi^+]$		< 0.33			< 0.33
$\pi^-D_1^+(H)[D^{*0}(2007)\pi^+]$		< 0.70			< 0.70
$\pi^-D_1^+(2420)[D^+\pi^-\pi^+]$		$0.89 \pm 0.15 \pm 0.17 \pm^{0.00}_{0.26}$			$0.89 \pm^{0.23}_{0.34}$
$\pi^-D_0^{*+}[D^0\pi^+]$		< 1.20			< 1.20
$\pi^-D_2^{*+}(2460)[D^{*0}(2007)\pi^+]$		$2.4 \pm 0.4 \pm^{0.4}_{0.4} \pm^{0.4}_{0.2}$			$2.4 \pm^{0.7}_{0.6}$
$\pi^-D_2^{*+}(2460)[D^0\pi^+]$		$3.1 \pm 0.3 \pm 0.1 \pm^{0.2}_{0.0}$			$3.1 \pm^{0.4}_{0.3}$
$\pi^-D_1^+(2420)[D^{*0}(2007)\pi^+]$		$3.7 \pm 0.6 \pm^{0.7}_{0.4} \pm^{0.6}_{0.3}$			$3.7 \pm^{1.1}_{0.8}$

Table 84: Ratios of branching fractions of neutral B modes producing multiple D, D^* or D^{**} mesons in units of 10^0, upper limits are at 90% CL. The latest version is available at: http://hfag.phys.ntu.edu.tw/hfagc/00206.html

Mode	PDG 2004	Belle	*BABAR*	CDF	Average
$\frac{\mathcal{B}(\overline{B}^0 \to D^+ K^-)}{\mathcal{B}(\overline{B}^0 \to D^+ \pi^-)}$	0.068 ± 0.017	$0.068 \pm 0.015 \pm 0.007$			0.068 ± 0.017
$\frac{\mathcal{B}(\overline{B}^0 \to D^{*+}(2010) K^-)}{\mathcal{B}(\overline{B}^0 \to D^{*+}(2010) \pi^-)}$	0.074 ± 0.016	$0.074 \pm 0.015 \pm 0.006$	$0.078 \pm 0.003 \pm 0.003$		0.077 ± 0.004
$\frac{\mathcal{B}(\overline{B}^0 \to D^0 \rho^0(770))}{\mathcal{B}(\overline{B}^0 \to D^0 \omega(782))}$		1.60 ± 0.80			1.60 ± 0.80

Table 85: Branching fractions of neutral B modes producing a single D^* or D^{**} meson in units of 10^{-3}, upper limits are at 90% CL. The latest version is available at: http://hfag.phys.ntu.edu.tw/hfagc/00207.html

Mode	PDG 2004	Belle	*BABAR*	CDF	Average
$\overline{D}^{*0}(2007)\overline{K}^{*0}(892)$	< 0.040	< 0.040			< 0.040
$D^{*0}(2007)\overline{K}^{0}$	< 0.066	< 0.066	$0.045 \pm 0.019 \pm 0.005$		0.045 ± 0.020
$D^{*0}(2007)\overline{K}^{*0}(892)$	< 0.069	< 0.069			< 0.069
$D^{*0}(2007)\eta'(958)$	< 0.26	$0.121 \pm 0.034 \pm 0.022$	< 0.26		0.121 ± 0.040
$f_2(1270)D^{*0}(2007)$		$0.186 \pm 0.065 \pm 0.060 \pm^{0.080}_{0.052}$			0.186 ± 0.111
$D^{*+}(2010)K^-$	0.200 ± 0.050	$0.20 \pm 0.04 \pm 0.02 \pm 0.02$			0.20 ± 0.05
$D^{*0}(2007)\eta$	0.26 ± 0.06		$0.26 \pm 0.04 \pm 0.04 \pm 0.02$		0.26 ± 0.06
$D^{*0}(2007)\pi^0$	0.27 ± 0.05		$0.29 \pm 0.04 \pm 0.05 \pm 0.02$		0.29 ± 0.06
$D^{*+}(2010)K^0\pi^-$			$0.30 \pm 0.07 \pm 0.02 \pm 0.02$		0.30 ± 0.08
$D^{*+}(2010)K^{*-}(892)$	0.38 ± 0.15		$0.32 \pm 0.06 \pm 0.03 \pm 0.01$		0.32 ± 0.07
$D^{*0}(2007)\rho^0(770)$	< 0.51				0.37 ± 0.10
		$0.37 \pm 0.09 \pm 0.05 \pm^{0.02}_{0.01}$ [1]			
		< 0.51 [2]			
$D^{*0}(2007)\omega(782)$	0.42 ± 0.11		$0.42 \pm 0.07 \pm 0.09 \pm 0.03$		0.42 ± 0.11
$D^{*+}(2010)K^-K^0$	< 0.47	< 0.47			< 0.47
$D^{*0}(2007)\pi^+\pi^-$	0.62 ± 0.22				0.90 ± 0.14
		$0.62 \pm 0.12 \pm 0.18$ [2]			
		$1.09 \pm 0.08 \pm 0.16$ [1]			
$D^{*+}(2010)K^-K^{*0}(892)$	1.29 ± 0.33	$1.29 \pm 0.22 \pm 0.25$			1.29 ± 0.33
$D^{*+}(2010)\pi^-$		$2.3 \pm 0.1 \pm 0.2$			2.3 ± 0.2
$D^{*0}(2007)\pi^-\pi^+\pi^-\pi^+$	3.0 ± 0.9	$2.6 \pm 0.5 \pm 0.4$			2.6 ± 0.6
$D^{*+}(2010)\pi^-\pi^+\pi^-\pi^+\pi^-$		$4.7 \pm 0.6 \pm 0.7$			4.7 ± 0.9
$D^{*+}(2010)\pi^-\pi^+\pi^-$	7.6 ± 1.8	$6.8 \pm 0.2 \pm 0.7$			6.8 ± 0.8

[1] Study of $\overline{B}^0 \to D^{(*)0}\pi^+\pi^-$ decays ; Dalitz fit analysis (152M $B\overline{B}$ pairs)
[2] Study of $\overline{B^0} \to D^{(*)0}\pi^+\pi^-$ Decays (31.3M $B\overline{B}$ pairs)

Table 86: Branching fractions of neutral B modes producing a single D meson in units of 10^{-3}, upper limits are at 90% CL. The latest version is available at: http://hfag.phys.ntu.edu.tw/hfagc/00208.html

Mode	PDG 2004	Belle	*BABAR*	CDF	Average
$\overline{D}^0 K^- \pi^+$			< 0.019		< 0.019
$\overline{D}^0 \overline{K}^{*0}(892)$	< 0.018	< 0.018	< 0.041		< 0.018
$D^0 \overline{K}^{*0}(892)$	0.048 ± 0.012	$0.048 \pm^{0.011}_{0.010} \pm 0.005$	$0.062 \pm 0.014 \pm 0.006$		0.053 ± 0.009
$D^0 \overline{K}^0$	0.050 ± 0.014	$0.050 \pm^{0.013}_{0.012} \pm 0.006$	$0.062 \pm 0.012 \pm 0.004$		0.056 ± 0.009
$D^0 K^- \pi^+$			$0.088 \pm 0.015 \pm 0.009$		0.088 ± 0.017
$D^0 \eta'(958)$	0.170 ± 0.040	$0.114 \pm 0.020 \pm^{0.010}_{0.013}$	$0.170 \pm 0.040 \pm 0.018 \pm 0.010$		0.126 ± 0.021
$f_2(1270) D^0$		$0.195 \pm 0.034 \pm 0.038 \pm^{0.032}_{0.002}$			0.195 ± 0.056
$D^+ K^-$	0.200 ± 0.060	$0.20 \pm 0.05 \pm 0.02 \pm 0.03$			0.20 ± 0.06
$D^0 \eta$	0.22 ± 0.05		$0.25 \pm 0.02 \pm 0.03 \pm 0.01$		0.25 ± 0.04
$D^0 \pi^0$	0.29 ± 0.03		$0.29 \pm 0.02 \pm 0.03 \pm 0.01$		0.29 ± 0.04
$D^0 \rho^0(770)$	0.29 ± 0.11				0.29 ± 0.05
		$0.29 \pm 0.10 \pm 0.04$ [2]			
		$0.29 \pm 0.03 \pm 0.03 \pm^{0.01}_{0.05}$ [1]			
$D^0 \omega(782)$	0.25 ± 0.06		$0.30 \pm 0.03 \pm 0.04 \pm 0.01$		0.30 ± 0.05
$D^+ K^- K^0$	< 0.31	< 0.31			< 0.31
$D^+ K^{*-}(892)$	0.37 ± 0.18		$0.46 \pm 0.06 \pm 0.05 \pm 0.02$		0.46 ± 0.08
$D^+ K^0 \pi^-$			$0.49 \pm 0.07 \pm 0.04 \pm 0.03$		0.49 ± 0.09
$D^+ K^- K^{*0}(892)$	0.88 ± 0.19	$0.88 \pm 0.11 \pm 0.15$			0.88 ± 0.19
$D^0 \pi^+ \pi^-$	0.80 ± 0.16				0.98 ± 0.09
		$0.80 \pm 0.06 \pm 0.15$ [2]			
		$1.07 \pm 0.06 \pm 0.10$ [1]			

[1] Study of $\overline{B}^0 \to D^{(*)0}\pi^+\pi^-$ decays ; Dalitz fit analysis (152M $B\overline{B}$ pairs)
[2] Study of $\overline{B^0} \to D^{(*)0}\pi^+\pi^-$ Decays (31.3M $B\overline{B}$ pairs)

Table 87: Product branching fractions of neutral B modes producing a single D meson in units of 10^{-5}, upper limits are at 90% CL. The latest version is available at: http://hfag.phys.ntu.edu.tw/hfagc/00208.html

Mode	PDG 2004	Belle	*BABAR*	CDF	Average
$D^0 \overline{K}^{*0}(892)$			$3.8 \pm 0.6 \pm 0.4$		3.8 ± 0.7

Table 88: Branching fractions of miscellaneous modes producing charmed particles in units of 10^{-3}, upper limits are at 90% CL. The latest version is available at: http://hfag.phys.ntu.edu.tw/hfagc/00300.html

Mode	PDG 2004	Belle	*BABAR*	CDF	Average
$\mathcal{B}(\overline{\Lambda}_b^0 \to J/\psi(1S)\overline{\Lambda})$	0.47 ± 0.28			$0.47 \pm 0.21 \pm 0.19$	0.47 ± 0.28
$\mathcal{B}(\overline{B}_s^0 \to J/\psi(1S)\phi(1020))$	0.93 ± 0.33			$0.93 \pm 0.28 \pm 0.17$	0.93 ± 0.33

Table 89: Product branching fractions of miscellaneous modes producing charmed particles in units of 10^{-5}, upper limits are at 90% CL. The latest version is available at: http://hfag.phys.ntu.edu.tw/hfagc/00300.html

Mode	PDG 2004	Belle	*BABAR*	CDF	Average
$\mathcal{B}(B \to KY(3940)[\omega(782)J/\psi(1S)])$		$7.1 \pm 1.3 \pm 3.1$			7.1 ± 3.4

Table 90: Ratios of branching fractions of miscellaneous modes producing charmed particles in units of 10^{0}, upper limits are at 90% CL. The latest version is available at: http://hfag.phys.ntu.edu.tw/hfagc/00300.html

Mode	PDG 2004	Belle	*BABAR*	CDF	Average
$\frac{\mathcal{B}(\overline{B}_s^0 \to \psi(2S)\phi(1020))}{\mathcal{B}(\overline{B}_s^0 \to J/\psi(1S)\phi(1020))}$				$0.52 \pm 0.13 \pm 0.07$	0.52 ± 0.15
$\frac{\mathcal{B}(\overline{B}_s^0 \to D_s^+\pi^-)}{\mathcal{B}(\overline{B}^0 \to D^+\pi^-)}$				$1.02 \pm 0.07 \pm 0.03 \pm 0.15$	1.02 ± 0.17
$\frac{\mathcal{B}(\overline{B}_s^0 \to D_s^+\pi^+\pi^-\pi^-)}{\mathcal{B}(\overline{B}^0 \to D^+\pi^+\pi^-\pi^-)}$				$1.17 \pm 0.18 \pm 0.34$	1.17 ± 0.38
$\frac{\mathcal{B}(\overline{\Lambda}_b^0 \to \Lambda_c^-\pi^+)}{\mathcal{B}(\overline{B}^0 \to D^+\pi^-)}$				$3.3 \pm 0.3 \pm 0.4 \pm 1.1$	3.3 ± 1.2
$\frac{\mathcal{B}(\overline{\Lambda}_b^0 \to \Lambda_c^-\mu^+\nu_\mu)}{\mathcal{B}(\overline{\Lambda}_b^0 \to \Lambda_c^-\pi^+)}$				$20.0 \pm 3.0 \pm 1.2 \pm^{0.9}_{2.2}$	$20.0 \pm^{3.4}_{3.9}$

Table 91: Brief summary of the world averages as of at the end of 2005.

b-hadron lifetimes	
$\tau(B^0)$	1.527 ± 0.008 ps
$\tau(B^+)$	1.643 ± 0.010 ps
$\tau(B_s^0 \to$ flavour specific)	1.454 ± 0.040 ps
$\overline{\tau}(B_s^0) = 1/\Gamma_s$	$1.396^{+0.044}_{-0.046}$ ps
$\tau(B_c^+)$	0.469 ± 0.065 ps
$\tau(\Lambda_b^0)$	1.288 ± 0.065 ps
b-hadron fractions	
f^{+-}/f^{00} in $\Upsilon(4S)$ decays	1.020 ± 0.034
$f_d = f_u$ at high energy	0.398 ± 0.010
f_s at high energy	0.104 ± 0.014
$f_{\rm baryon}$ at high energy	0.099 ± 0.017
B^0 and B_s^0 mixing parameters	
Δm_d	0.507 ± 0.004 ps^{-1}
$\lvert q/p\rvert_d$	1.0015 ± 0.0039
Δm_s	> 16.6 ps^{-1} at 95% CL
$\Delta\Gamma_s/\Gamma_s = (\Gamma_{\rm L} - \Gamma_{\rm H})/\Gamma_s$	$+0.31^{+0.10}_{-0.11}$
Semileptonic B decay parameters	
$\mathcal{B}(\overline{B}^0 \to D^{*+}\ell^-\overline{\nu})$	$(5.34 \pm 0.20)\%$
$\mathcal{B}(\overline{B}^0 \to D^{+}\ell^-\overline{\nu})$	$(2.12 \pm 0.20)\%$
$\mathcal{B}(\overline{B} \to X\ell\overline{\nu})$	$(10.95 \pm 0.15)\%$
$\lvert V_{cb}\rvert F(1)$ $(\overline{B}^0 \to D^{*+}\ell^-\overline{\nu})$	$(37.7 \pm 0.9) \times 10^{-3}$
$\lvert V_{cb}\rvert G(1)$ $(\overline{B}^0 \to D^{+}\ell^-\overline{\nu})$	$(42.2 \pm 3.7) \times 10^{-3}$
$\lvert V_{ub}\rvert$ (inclusive)	$(4.39 \pm 0.33) \times 10^{-3}$
$\mathcal{B}(\overline{B} \to \pi\ell\overline{\nu})$	$(1.34 \pm 0.11) \times 10^{-4}$
Rare B decays	
$\mathcal{B}(b \to s\gamma)$	$(355 \pm 24^{+9}_{-10} \pm 3) \times 10^{-6}$

8 Summary

This article provides the updated world averages for b-hadron properties as of at the end of 2005. A small selection of highlights of the results described in sections 3-7 is given in Table 91.

Concerning the lifetime and mixing averages, the most significant changes since winter 2005 [4] are due to new measurements from the Tevatron experiments in the areas of heavy b-baryon lifetimes and B_s^0 mixing parameters (in particular, it is worth noting that the 95% CL lower limit on Δm_s has now increased to 16.6 ps^{-1}, after having stayed for several years between 14 and 15 ps^{-1}). In the near future, CDF and DØ are expected to contribute with increasing significance in these areas, while the B^+ and B^0 lifetime and mixing properties, dominated by the B factory results, have probably already reached close to their asymptotic precisions.

In the field of semileptonic B-meson decays, the advances reported in this update center on the CKM matrix element $|V_{ub}|$. For the first time the extraction of $|V_{ub}|$ has been performed on

a consistent basis (using BLNP [225]) for all available measurements of the partial branching fraction to inclusive charmless semileptonic B-meson decays. The leading uncertainty ($\sim 5\%$) depends on the precision on the determination of the b-quark mass. The overall uncertainty of $\sim 8\%$ is approaching the lower bound of 5%, which is the irreducible theoretical uncertainty typically quoted by theorists. However it will be important in future to not rely on just one theoretical framework. In exclusive decays, in contrast, our average of the branching fraction to $B \to \pi l \nu$ is an input into several approaches of extracting $|V_{ub}|$. They rely on light cone sum rule and unquenched lattice QCD calculations. The uncertainty in $|V_{ub}|$ is dominated by theoretical uncertainties that are at the level of 15-20%. In future the uncertainties will be reduced with use of the measured differential decay rate in q^2.

Measurements by *BABAR* and Belle of the time-dependent *CP* violation parameter $S_{b\to c\bar{c}s}$ in B decays to charmonium and a neutral kaon have established *CP* violation in B decays, and allow a precise extraction of the Unitarity Triangle parameter $\sin 2\beta / \sin 2\phi_1$. Recent studies of $B \to J/\psi K^*$ (Sec. 4.5) and $B \to D^{(*)}h^0$, where $h^0 = \pi^0$ *etc.*. (Sec. 4.6) allow to resolve the ambiguity in the solutions for β/ϕ_1 from the measurement of $\sin 2\beta / \sin 2\phi_1$. Measurements of time-dependent *CP* asymmetries in hadronic $b \to s$ penguin decays continue to provide insight into possible new physics. In this update, results from Belle have been updated with more statistics, and both *BABAR* and Belle have added more decay modes, including the mode $K^0_S\pi^0\pi^0$ from *BABAR* and charmless modes with K^0_L in the final state. Compared to the previous round of averages, the consistency with the Standard Model expectation is improved. An intriguing discrepancy still exists, although it is not presently a significant effect. Results from time-dependent analyses with the decays $B^0 \to \pi^+\pi^-, \rho^\pm\pi^\mp$ and $\rho^+\rho^-$ provide constraints on the Unitarity Triangle angle α/ϕ_2 (Sec. 4.10). The most constraining measurements are the results from *BABAR* and Belle in the $\rho\rho$ system. Constraints on the third Unitarity Triangle angle γ/ϕ_3 have been obtained by *BABAR* and Belle, using $B^- \to D^{(*)}K^-$ decays (Sec. 4.12). At present, the most constraining results arise from the Dalitz plot analysis of the subsequent $D \to K^0_S\pi^+\pi^-$ decay.

For the rare B decays, many new measurements on branching fractions and CP violating asymmetries are included and summarized in section 6. A special effort has been made to handle the correlated model uncertainties of shape function in averaging the $b \to s\gamma$ results. The obtained average is highlighted in Table 91. Results of ratios of branching fractions for charmless two-body B decays reported by CDF are also added for the first time.

Quantities related to B decays to charmed particles, other than CP-asymmetry parameters, have been dealt with by HFAG for the first time. The huge sample of B mesons available has enabled measurements of branching fractions for rare decays or decay chains of a few 10^{-7} with statistical uncertainties typically below 30%, while results for more common decays, with branching fractions around 10^{-4}, are becoming precision measurements, with uncertainties typically at the 3% level. We highlight the great improvements that have been attained toward a deeper understanding of recently discovered new states with either hidden or open charm content, such as $X(3870)$, $D^{*-}_{sJ}(2317)$ and $D^-_{sJ}(2460)$.

Acknowledgments

We would like to thank collaborators of *BABAR*, Belle, CDF, CLEO, DØ, LEP, and SLD experiments who provided fruitful results on b-hadron properties and cooperated with the

HFAG for averaging. These results are thanks to the excellent operations of the accelerators and collaborations with experimental groups by the accelerator groups of PEP-II, KEKB, CESR, Tevatron, LEP, and SLC.

References

[1] N. Cabibbo, Phys. Rev. Lett. 10, 531 (1963); M. Kobayashi and T. Maskawa, Prog. Theor. Phys. **49**, 652 (1973).

[2] ALEPH, CDF, DELPHI, L3, OPAL, and SLD collaborations, "Combined results on b-hadron production rates and decay properties", CERN-EP-2000-096, hep-ex/0009052 (2000); updated in CERN-EP-2001-050, hep-ex/0112028 (2001).

[3] Heavy Flavor Averaging Group (HFAG) "Averages of b-hadron Properties as of Summer 2004" hep-ex/0412073 (2004).

[4] Heavy Flavor Averaging Group (HFAG) "Averages of b-hadron Properties as of Winter 2005" hep-ex/0505100 (2005).

[5] S. Eidelman *et al.* (Particle Data Group Collaboration), Phys. Lett. B **592**, 1 (2004).

[6] J.P. Alexander *et al.* (CLEO Collaboration), Phys. Rev. Lett. **86**, 2737 (2001).

[7] B. Aubert *et al.* (*BABAR* Collaboration), Phys. Rev. D **65**, 032001 (2002).

[8] S.B. Athar *et al.* (CLEO Collaboration), Phys. Rev. D **66**, 052003 (2002).

[9] N.C. Hastings *et al.* (Belle Collaboration), Phys. Rev. D **67**, 052004 (2003).

[10] B. Aubert *et al.* (*BABAR* Collaboration), Phys. Rev. D **69**, 071101 (2004).

[11] B. Aubert *et al.* (*BABAR* Collaboration), Phys. Rev. Lett. **95**, 042001 (2005).

[12] K. Abe *et al.* (Belle Collaboration), BELLE-CONF-0510, hep-ex/0512034, submitted to summer 2005 conferences.

[13] B. Barish *et al.* (CLEO Collaboration), Phys. Rev. Lett. **76**, 1570 (1996).

[14] P. Abreu *et al.* (DELPHI Collaboration), Phys. Lett. B **289**, 199 (1992);
P.D. Acton *et al.* (OPAL Collaboration), Phys. Lett. B **295**, 357 (1992);
D. Buskulic *et al.* (ALEPH Collaboration), Phys. Lett. B **361**, 221 (1995).

[15] P. Abreu *et al.* (DELPHI Collaboration), Z. Phys. C **68**, 375 (1995).

[16] R. Barate *et al.* (ALEPH Collaboration), Eur. Phys. J. C **2**, 197 (1998).

[17] P. Abreu *et al.* (DELPHI Collaboration), Z. Phys. C **68**, 541 (1995).

[18] D. Buskulic *et al.* (ALEPH Collaboration), Phys. Lett. B **384**, 449 (1996).

[19] R. Barate *et al.* (ALEPH Collaboration), Eur. Phys. J. C **5**, 205 (1998).

[20] J. Abdallah *et al.* (DELPHI Collaboration), Phys. Lett. B **576**, 29 (2003).

[21] T. Affolder *et al.* (CDF Collaboration), Phys. Rev. Lett. **84**, 1663 (2000).

[22] F. Abe *et al.* (CDF Collaboration), Phys. Rev. D **60**, 092005 (1999).

[23] LEP collaborations ALEPH, CDF, DELPHI, L3, OPAL, LEP Electroweak Working Group, SLD Electroweak and Heavy Flavour Working Groups, "Precision electroweak measurements on the Z resonance", CERN-PH-EP/2005-041, SLAC-R-774, hep-ex/0509008, September 2005, to appear in Physics Reports; we use the average given in Eq. 5.39 of this paper, obtained from a 10-parameter global fit of all electroweak data where the asymmetry measurements have been excluded.

[24] D. Acosta *et al.* (CDF Collaboration), Phys. Rev. D **69**, 012002 (2004).

[25] M.A. Shifman and M.B. Voloshin, Sov. Phys. JETP **64**, 698 (1986);
J. Chay, H. Georgi and B. Grinstein, Phys. Lett. B **247**, 399 (1990);
I.I. Bigi, N.G. Uraltsev and A.I. Vainshtein, Phys. Lett. B **293**, 430 (1992), erratum ibid. B **297**, 477 (1993).

[26] I. Bigi, UND-HEP-95-BIG02 (1995);
G. Bellini, I. Bigi, and P. Dornan, Phys. Reports **289**, 1 (1997).

[27] M. Ciuchini, E. Franco, V. Lubicz, and F. Mescia, Nucl. Phys. B **625**, 211 (2002);
M. Beneke, G. Buchalla, C. Greub, A. Lenz and U. Nierste, Nucl. Phys. B **639**, 389 (2002);
E. Franco, V. Lubicz, F. Mescia, and C. Tarantino, Nucl. Phys. B **633**, 212 (2002).

[28] C. Tarantino, Eur. Phys. J. C **33**, S895 (2004), hep-ph/0310241;
F. Gabbiani, A. Onishchenko, and A. Petrov, Phys. Rev. D **68**, 114006 (2003).

[29] F. Gabbiani, A. Onischenko and A. Petrov, Phys. Rev. D **70**, 094031 (2004).

[30] L. Di Ciaccio *et al.*, internal note by former B lifetime working group (1996), `http://lepbosc.web.cern.ch/LEPBOSC/lifetimes/ps/final_blife.ps`

[31] D. Buskulic *et al.* (ALEPH Collaboration), Phys. Lett. B **314**, 459 (1993).

[32] P. Abreu *et al.* (DELPHI Collaboration), Z. Phys. C **63**, 3 (1994).

[33] P. Abreu *et al.* (DELPHI Collaboration), Phys. Lett. B **377**, 195 (1996).

[34] J. Abdallah *et al.* (DELPHI Collaboration), Eur. Phys. J. C **33**, 307 (2004).

[35] M. Acciarri *et al.* (L3 Collaboration), Phys. Lett. B **416**, 220 (1998).

[36] K. Ackerstaff *et al.* (OPAL Collaboration), Z. Phys. C **73**, 397 (1997).

[37] K. Abe *et al.* (SLD Collaboration), Phys. Rev. Lett. **75**, 3624 (1995).

[38] D. Buskulic *et al.* (ALEPH Collaboration), Phys. Lett. B **369**, 151 (1996).

[39] P.D. Acton *et al.* (OPAL Collaboration), Z. Phys. C **60**, 217 (1993).

[40] F. Abe *et al.* (CDF Collaboration), Phys. Rev. D **57**, 5382 (1998).

[41] R. Barate *et al.* (ALEPH Collaboration), Phys. Lett. B **492**, 275 (2000).

[42] D. Buskulic *et al.* (ALEPH Collaboration), Z. Phys. C **71**, 31 (1996).

[43] P. Abreu *et al.* (DELPHI Collaboration), Z. Phys. C **68**, 13 (1995).

[44] W. Adam *et al.* (DELPHI Collaboration), Z. Phys. C **68**, 363 (1995).

[45] P. Abreu *et al.* (DELPHI Collaboration), Z. Phys. C **74**, 19 (1997).

[46] M. Acciari *et al.* (L3 Collaboration), Phys. Lett. B **438**, 417 (1998).

[47] R. Akers *et al.* (OPAL Collaboration), Z. Phys. C **67**, 379 (1995).

[48] G. Abbiendi *et al.* (OPAL Collaboration), Eur. Phys. J. C **12**, 609 (2000).

[49] G. Abbiendi *et al.* (OPAL Collaboration), Phys. Lett. B **493**, 266 (2000).

[50] K. Abe *et al.* (SLD Collaboration), Phys. Rev. Lett. **79**, 590 (1997).

[51] F. Abe *et al.* (CDF Collaboration), Phys. Rev. D **58**, 092002 (1998).

[52] D. Acosta *et al.* (CDF Collaboration), Phys. Rev. D **65**, 092009 (2003).

[53] CDF Collaboration, CDF note 7409, 9 May 2004,
`http://www-cdf.fnal.gov/physics/new/bottom/040428.blessed-lft/`

[54] CDF Collaboration, CDF note 7514, 1 March 2005,
`http://www-cdf.fnal.gov/physics/new/bottom/050224.blessed-bsemi-life/`

[55] CDF Collaboration, CDF note 7386, 23 March 2005,
`http://www-cdf.fnal.gov/physics/new/bottom/050303.blessed-bhadlife/`

[56] CDF Collaboration, CDF note 7867, 22 November 2005,
`http://www-cdf.fnal.gov/physics/new/bottom/051020.blessed-lambdab-lifetime/`

[57] V.M. Abazov *et al.* (DØ Collaboration), Phys. Rev. Lett. **95**, 171801 (2005).

[58] V.M. Abazov *et al.* (DØ Collaboration), Phys. Rev. Lett. **94**, 042001 (2005).

[59] V.M. Abazov *et al.* (DØ Collaboration), Phys. Rev. Lett. **94**, 102001 (2005).

[60] B. Aubert *et al.* (*BABAR* Collaboration), Phys. Rev. Lett. **87**, 201803 (2001).

[61] B. Aubert *et al.* (*BABAR* Collaboration), Phys. Rev. Lett. **89**, 011802 (2002), erratum ibid. **89**, 169903 (2002).

[62] B. Aubert *et al.* (*BABAR* Collaboration), Phys. Rev. D **67**, 072002 (2003).

[63] B. Aubert *et al.* (*BABAR* Collaboration), Phys. Rev. D **67**, 091101 (2003).

[64] B. Aubert *et al.* (*BABAR* Collaboration), Phys. Rev. D **73**, 012004 (2006).

[65] K. Abe *et al.* (Belle Collaboration), Phys. Rev. D **71**, 072003 (2005).

[66] V.M. Abazov *et al.* (DØ Collaboration), Phys. Rev. Lett. **94**, 182001 (2005).

[67] A. Lenz, hep-ph/0412007;
M. Beneke *et al.*, Phys. Lett. B **459**, 631 (1999).

[68] K. Hartkorn and H.-G. Moser, Eur. Phys. J. C **8**, 381 (1999).

[69] D. Buskulic *et al.* (ALEPH Collaboration), Phys. Lett. B **377**, 205 (1996).

[70] F. Abe *et al.* (CDF Collaboration), Phys. Rev. D **59**, 032004 (1999).

[71] P. Abreu *et al.* (DELPHI Collaboration), Eur. Phys. J. C **16**, 555 (2000).

[72] K. Ackerstaff *et al.* (OPAL Collaboration), Phys. Lett. B **426**, 161 (1998).

[73] V.M. Abazov *et al.* (DØ Collaboration), DØ Note 4729-CONF, 3 March 2005, submitted to Moriond 2005.

[74] CDF Collaboration, CDF note 7386, 23 March 2005, submitted to Moriond 2005.

[75] CDF Collaboration, CDF note 7757, 13 August 2005.

[76] D. Buskulic *et al.* (ALEPH Collaboration), Eur. Phys. J. C **4**, 367 (1998).

[77] P. Abreu *et al.* (DELPHI Collaboration), Eur. Phys. J. C **18**, 229 (2000).

[78] K. Ackerstaff *et al.* (OPAL Collaboration), Eur. Phys. J. C **2**, 407 (1998).

[79] F. Abe *et al.* (CDF Collaboration), Phys. Rev. Lett. **81**, 2432 (1998).

[80] CDF Collaboration, CDF note 7926, 14 November 2005.

[81] V.M. Abazov *et al.* (DØ Collaboration), DØ Note 4539, contribution 11-0559 to ICHEP04, August 2004.

[82] A preliminary result of 5620 ± 1.6 (stat) ± 1.2 (sys) MeV/c^2 exists from CDF, CDF Note 6557, 15 July 2003, consistent with the world average. The PDG value is used for scaling, and its precision is not the dominant common systematic uncertainty.

[83] D. Buskulic *et al.* (ALEPH Collaboration), Phys. Lett. B **365**, 437 (1996).

[84] F. Abe *et al.* (CDF Collaboration), Phys. Rev. Lett. **77**, 1439 (1996).

[85] P. Abreu *et al.* (DELPHI Collaboration), Eur. Phys. J. C **10**, 185 (1999).

[86] P. Abreu *et al.* (DELPHI Collaboration), Z. Phys. C **71**, 199 (1996).

[87] R. Akers *et al.* (OPAL Collaboration), Z. Phys. C **69**, 195 (1996).

[88] M. Beneke, G. Buchalla, and I. Dunietz, Phys. Rev. D **54**, 4419 (1996); Y. Keum and U. Nierste, Phys. Rev. D **57**, 4282 (1998).

[89] M.B. Voloshin, Phys. Rep. **320**, 275 (1999); B. Guberina, B. Melic, and H. Stefancic, Phys. Lett. B **469**, 253 (1999); M. Neubert, and C.T. Sachrajda, Nucl. Phys. B **483**, 339 (1997).

[90] J. Bartelt *et al.* (CLEO Collaboration), Phys. Rev. Lett. **71**, 1680 (1993).

[91] B.H. Behrens *et al.* (CLEO Collaboration), Phys. Lett. B **490**, 36 (2000).

[92] D.E. Jaffe *et al.* (CLEO Collaboration), Phys. Rev. Lett. **86**, 5000 (2001).

[93] F. Abe *et al.* (CDF Collaboration), Phys. Rev. D **55**, 2546 (1997).

[94] K. Ackerstaff *et al.* (OPAL Collaboration), Z. Phys. C **76**, 401 (1997).

[95] R. Barate *et al.* (ALEPH Collaboration), Eur. Phys. J. C **20**, 431 (2001).

[96] B. Aubert *et al.* (*BABAR* Collaboration), Phys. Rev. Lett. **92**, 181801 (2004).

[97] B. Aubert *et al.* (*BABAR* Collaboration), Phys. Rev. Lett. **88**, 231801 (2002).

[98] E. Nakano *et al.* (Belle Collaboration), hep-ex/0505017, submitted to Phys. Rev. D.

[99] G. Abbiendi *et al.* (OPAL Collaboration), Eur. Phys. J. C **12**, 609 (2000).

[100] M. Beneke, G. Buchalla and I. Dunietz, Phys. Lett. B **393**, 132 (1997); I. Dunietz, Eur. Phys. J. C **7**, 197 (1999).

[101] D. Buskulic *et al.* (ALEPH Collaboration), Z. Phys. C **75**, 397 (1997).

[102] P. Abreu *et al.* (DELPHI Collaboration), Z. Phys. C **76**, 579 (1997).

[103] J. Abdallah *et al.* (DELPHI Collaboration), Eur. Phys. J. C **28**, 155 (2003).

[104] M. Acciarri *et al.* (L3 Collaboration), Eur. Phys. J. C **5**, 195 (1998).

[105] K. Ackerstaff *et al.* (OPAL Collaboration), Z. Phys. C **76**, 417 (1997).

[106] K. Ackerstaff *et al.* (OPAL Collaboration), Z. Phys. C **76**, 401 (1997).

[107] G. Alexander *et al.* (OPAL Collaboration), Z. Phys. C **72**, 377 (1996).

[108] G. Abbiendi *et al.* (OPAL Collaboration), Phys. Lett. B **493**, 266 (2000).

[109] F. Abe *et al.* (CDF Collaboration), Phys. Rev. Lett. **80**, 2057 (1998) and Phys. Rev. D **59**, 032001 (1999).

[110] F. Abe *et al.* (CDF Collaboration), Phys. Rev. D **60**, 051101 (1999).

[111] F. Abe *et al.* (CDF Collaboration), Phys. Rev. D **60**, 072003 (1999).

[112] T. Affolder *et al.* (CDF Collaboration), Phys. Rev. D **60**, 112004 (1999).

[113] CDF Collaboration, CDF note 7910, October 24, 2005,
http://www-cdf.fnal.gov/physics/new/bottom/050915.semi_B0mix/

[114] CDF Collaboration, CDF note 7920, November 15, 2005,
http://www-cdf.fnal.gov/physics/new/bottom/050804.hadr_B0mix/

[115] DØ Collaboration, DØ Note 4875, July 19, 2005, submitted to summer 2005 conferences.

[116] B. Aubert *et al.* (*BABAR* Collaboration), Phys. Rev. Lett. **88**, 221802 (2002) and Phys. Rev. D **66**, 032003 (2002).

[117] B. Aubert *et al.* (*BABAR* Collaboration), Phys. Rev. Lett. **88**, 221803 (2002).

[118] Y. Zheng *et al.* (Belle Collaboration), Phys. Rev. D **67**, 092004 (2003).

[119] H. Albrecht *et al.* (ARGUS Collaboration), Z. Phys. C **55**, 357 (1992); Phys. Lett. B **324**, 249 (1994).

[120] H.-G. Moser and A. Roussarie, Nucl. Instrum. Methods A **384**, 491 (1997).

[121] A. Heister *et al.* (ALEPH Collaboration), Eur. Phys. J. C **29**, 143 (2003).

[122] F. Abe *et al.* (CDF Collaboration), Phys. Rev. Lett. **82**, 3576 (1999).

[123] CDF Collaboration, CDF note 7907, October 24, 2005, submitted to fall 2005 conferences.

[124] CDF Collaboration, CDF note 7941, November 16, 2005, submitted to fall 2005 conferences.

[125] DØ Collaboration, DØ notes 4878 and 4881, July 2005, submitted to summer 2005 conferences.

[126] P. Abreu *et al.* (DELPHI Collaboration), Eur. Phys. J. C **16**, 555 (2000).

[127] J. Abdallah *et al.* (DELPHI Collaboration), Eur. Phys. J. C **35**, 35 (2004).

[128] G. Abbiendi *et al.* (OPAL Collaboration), Eur. Phys. J. C **11**, 587 (1999).

[129] G. Abbiendi *et al.* (OPAL Collaboration), Eur. Phys. J. C **19**, 241 (2001).

[130] K. Abe *et al.* (SLD Collaboration), Phys. Rev. D **67**, 012006 (2003).

[131] K. Abe *et al.* (SLD Collaboration), Phys. Rev. D **66**, 032009 (2002).

[132] SLD Collaboration, SLAC-PUB-8568, contrib. to 30th Int. Conf. on High-Energy Physics, Osaka, Japan (2000).

[133] R. Barate *et al.* (ALEPH Collaboration), Phys. Lett. B **486**, 286 (2000).

[134] R. Aleksan, Phys. Lett. B **316**, 567 (1993).

[135] D. Acosta *et al.* (CDF Collaboration), Phys. Rev. Lett. **94**, 101803 (2005).

[136] L.L. Chau and W.Y. Keung, Phys. Rev. Lett. **53**, 1802 (1984).

[137] L. Wolfenstein, Phys. Rev. Lett. **51**, 1945 (1983).

[138] A.J. Buras, M.E. Lautenbacher and G. Ostermaier, Phys. Rev. D **50**, 3433 (1994).

[139] D. Atwood, M. Gronau and A. Soni, Phys. Rev. Lett **79**, 185 (1997).

[140] D. Atwood, T. Gershon, M. Hazumi and A. Soni, Phys. Rev. D **71**, 076003 (2005).

[141] I.I. Bigi and A.I. Sanda, Phys. Lett. B **211**, 213 (1988).

[142] M. Gronau and D. London, Phys. Lett. B **253**, 483 (1991), M. Gronau and D. Wyler, Phys. Lett. B **265**, 172 (1991).

[143] D. Atwood, I. Dunietz, and A. Soni, Phys. Rev. Lett. **78**, 3257 (1997), Phys. Rev. D **63**, 036005 (2001).

[144] A. Giri, Y. Grossman, A. Soffer and J. Zupan, Phys. Rev. D **68**, 054018 (2003); A. Poluektov *et al.* (Belle Collaboration), Phys. Rev. D **70**, 072003 (2004).

[145] A. Bondar and T. Gershon, Phys. Rev. D **70**, 091503(R) (2004).

[146] B. Aubert *et al.* (*BABAR* Collaboration), Phys. Rev. D **71**, 032005 (2005).

[147] R. Itoh, Y. Onuki, *et al.* (Belle Collaboration), Phys. Rev. Lett. **95**, 091601 (2005).

[148] B. Aubert *et al.* (*BABAR* Collaboration), Phys. Rev. Lett. **94**, 161803 (2005)

[149] K. Abe *et al.* (Belle Collaboration), BELLE-CONF-0569 (hep-ex/0507037).

[150] R. Barate *et al.* (ALEPH Collaboration), Phys. Lett. B **492**, 259 (2000).

[151] K. Ackerstaff *et al.* (OPAL Collaboration), Eur. Phys. J C **5**, 379 (1998).

[152] T. Affolder *et al.* (CDF Collaboration), Phys. Rev. D **61**, 072005 (2000).

[153] CKMfitter Group (J. Charles *et al.*), Eur. Phys. J. C **41**, 1 (2005). Updated results available at `http://www.slac.stanford.edu/xorg/ckmfitter/`

[154] UTfit Collaboration (M. Bona *et al.*) JHEP **0507**, 028 (2005). Updated results available at `http://www.utfit.org/`

[155] I. Dunietz, H. Quinn, A. Snyder, W. Toki, H.J. Lipkin, Phys. Rev. D **43**, 2193 (1991).

[156] D. Aston *et al.* (LASS Collaboration), Nucl. Phys. B **296**, 493 (1988).

[157] M. Suzuki, Phys. Rev. D **64**, 117503 (2001).

[158] Yu. Grossman, M.P. Worah, Phys. Lett. B **395**, 241 (1997).

[159] R. Fleischer, Phys. Lett. B **562**, 234 (2003); Nucl. Phys. B **659**, 321 (2003).

[160] A. Bondar, T. Gershon, P. Krokovny, Phys. Lett. B **624**, 1 (2005).

[161] K. Abe *et al.* (Belle Collaboration), BELLE-CONF-0546 (hep-ex/0507065).

[162] See, for example, Y. Grossman, Z. Ligeti, Y. Nir, H. Quinn, Phys. Rev. D **68**, 015004 (2003), M. Gronau, Y. Grossman, J. Rosner, Phys. Lett. B **579**, 331 (2004), M. Gronau, J. Rosner, J. Zupan, Phys. Lett. B **596**, 107 (2004), H.Y. Cheng, C.K. Chua, A. Soni, Phys. Rev. D **72**, 014006 (2005), M. Gronau, J. Rosner, Phys. Rev. D **71**, 074019 (2005), M. Beneke, Phys. Lett. B **620**, 143 (2005), G. Engelhard, Y. Nir, G. Raz, Phys. Rev. D **72**, 075013 (2005), H.Y. Cheng, A. Soni, Phys. Rev. D **72**, 094003 (2005), A. R. Williamson, J. Zupan, hep-ph/0601214, and references therein.

[163] B. Aubert *et al.* (*BABAR* Collaboration), Phys. Rev. D **71**, 091102(R) (2005).

[164] K. Abe *et al.* (Belle Collaboration), BELLE-CONF-0569 (hep-ex/0507037).

[165] B. Aubert *et al.* (*BABAR* Collaboration), BABAR-CONF-05/014 (hep-ex/0507087).

[166] B. Aubert *et al.* (*BABAR* Collaboration), BABAR-CONF-04/019 (hep-ex/0408095).

[167] B. Aubert *et al.* (*BABAR* Collaboration), Phys. Rev. D **71**, 111102 (2005).

[168] B. Aubert *et al.* (*BABAR* Collaboration), BABAR-CONF-05/020 (hep-ex/0508017).

[169] B. Aubert *et al.* (*BABAR* Collaboration), BABAR-CONF-05/001 (hep-ex/0503018).

[170] B. Aubert *et al.* (*BABAR* Collaboration), BABAR-CONF-05/002 (hep-ex/0507016).

[171] B. Aubert *et al.* (*BABAR* Collaboration), BABAR-CONF-05/012 (hep-ex/0507052).

[172] B. Aubert *et al.* (*BABAR* Collaboration), BABAR-CONF-05/016 (hep-ex/0507074).

[173] S.U. Kataoka *et al.* (Belle Collaboration), Phys. Rev. Lett. **93**, 261801 (2004).

[174] B. Aubert *et al.* (*BABAR* Collaboration), Phys. Rev. Lett. **95**, 131802 (2005).

[175] B. Aubert *et al.* (*BABAR* Collaboration), Phys. Rev. Lett. **95**, 151804 (2005).

[176] H. Miyake, M. Hazumi, *et al.* (Belle Collaboration), Phys. Lett. B **618**, 34 (2005).

[177] T. Aushev, Y. Iwasaki *et al.* (Belle Collaboration), Phys. Rev. Lett. **93**, 201802 (2004).

[178] B. Aubert *et al.* (*BABAR* Collaboration), Phys. Rev. D **72**, 051103 (2005).

[179] K. Abe *et al.* (Belle Collaboration), BELLE-CONF-0570 (hep-ex/0507059).

[180] A.E. Snyder and H.R. Quinn, Phys. Rev. D **48**, 2139 (1993).

[181] B. Aubert *et al.* (*BABAR* Collaboration), Phys. Rev. Lett. **95**, 151803 (2005).

[182] H. Ishino, A. Kusaka, H. Kakuno, A. Kibayashi *et al.*, (Belle Collaboration), Phys. Rev. Lett. **95**, 101801 (2005).

[183] B. Aubert *et al.* (*BABAR* Collaboration), Phys. Rev. Lett. **95**, 041805 (2005).

[184] K. Abe *et al.* (Belle Collaboration), BELLE-CONF-0545 (hep-ex/0507039).

[185] B. Aubert *et al.* (*BABAR* Collaboration), Phys. Rev. Lett. **91**, 201802 (2003).

[186] C.C. Wang *et al.* (Belle Collaboration), Phys. Rev. Lett **94**, 121801 (2005).

[187] B. Aubert *et al.* (*BABAR* Collaboration), BABAR-CONF-04/038 (hep-ex/0408099).

[188] M. Gronau and J.L. Rosner, Phys. Rev. D **65**, 093012 (2002).

[189] B. Aubert *et al.* (*BABAR* Collaboration), Phys. Rev. Lett. **94**, 131801 (2005).

[190] M. Gronau and D. London, Phys. Rev. Lett. **65**, 3381 (1990).

[191] B. Aubert *et al.* (*BABAR* Collaboration), BABAR-CONF-05/015 (hep-ex/0507075).

[192] T. Sarangi, K. Abe *et al.* (Belle Collaboration), Phys. Rev. Lett. **93**, 031802 (2004); Erratum-ibid. **93**, 059901 (2004).

[193] B. Aubert *et al.* (*BABAR* Collaboration), Phys. Rev. D **71**, 112003 (2005).

[194] T. Gershon *et al.* (Belle Collaboration), Phys. Lett. B **624** 11 (2005).

[195] O. Long, M. Baak, R.N. Cahn, D. Kirkby, Phys.Rev. D **68**, 034010 (2003).

[196] R. Fleischer, Nucl. Phys. B **671**, 459 (2003).

[197] B. Aubert *et al.* (*BABAR* Collaboration), BABAR-PUB-05/051 (hep-ex/0512067).

[198] K. Abe *et al.* (Belle Collaboration), Belle Preprint 2006-1 (hep-ex/0601032).

[199] B. Aubert *et al.* (*BABAR* Collaboration), Phys. Rev. D **71**, 031102 (2005).

[200] B. Aubert *et al.* (*BABAR* Collaboration), Phys. Rev. D **72**, 071103(R) (2005).

[201] K. Abe *et al.* (Belle Collaboration), BELLE-CONF-0316 (hep-ex/0307074).

[202] B. Aubert *et al.* (*BABAR* Collaboration), Phys. Rev. D **72**, 032004 (2005).

[203] K. Abe *et al.* (Belle Collaboration), BELLE-CONF-0552 (hep-ex/0508048).

[204] B. Aubert *et al.* (*BABAR* Collaboration), BABAR-PUB-05/039 (hep-ex/0508001).

[205] M. Gronau, Phys. Lett. B **557**, 198 (2003).

[206] B. Aubert *et al.* (*BABAR* Collaboration), Phys. Rev. Lett. **95**, 121802 (2005); BABAR-CONF-05/018 (hep-ex/0507101).

[207] K. Abe *et al.* (Belle Collaboration), BELLE-CONF-0476 (hep-ex/0411049).

[208] K. Abe *et al.* (Belle Collaboration), BELLE-CONF-0502 (hep-ex/0504013).

[209] See, for example, I. I. Y. Bigi, M. A. Shifman and N. Uraltsev, Ann. Rev. Nucl. Part. Sci. **47**, 591 (1997); M. Neubert, Nucl. Phys. Proc. Suppl. **59**, 101 (1997); A. H. Hoang, Z. Ligeti and A. V. Manohar, Phys. Rev. D **59**, 074017 (1999), and references therein.

[210] S. E. Csorna *et al.* (CLEO Collab.), Phys. Rev. **D70**:032002 (2004).

[211] A. H. Mahmood *et al.* (CLEO Collab.), Phys. Rev. **D70**:032003 (2004).

[212] B. Aubert *et al.* (BABAR Collab.), Phys. Rev. **D69**:111103 (2004).

[213] B. Aubert *et al.* (BABAR Collab.), Phys. Rev. **D69**:111104 (2004).

[214] B. Aubert *et al.* (BABAR Collab.), Phys. Rev. Lett. **93**:011803 (2004).

[215] BELLE Collab., hep-ex/0408139 (2004).

[216] BELLE Collab., hep-ex/0409015 (2004).

[217] DELPHI Collab., CERN-PH-EP/2005-015 (2005).

[218] D. Acosta *et al.* (CDF Collab.), Phys. Rev. **D71**:051103 (2005).

[219] S. Chen *et al.* (CLEO Collab.), Phys. Rev. Lett. **87**:251807 (2001).

[220] P. Koppenburg *et al.* (BELLE Collab.), Phys. Rev. Lett. **93**:061803 (2004). Updated fits are available in hep-ex/0506057.

[221] B. Aubert *et al.* (BABAR Collab.), Phys. Rev. **D72**:052004 (2005).

[222] B. Aubert *et al.* (BABAR Collab.), hep-ex/0507001.

[223] O. Buchmüller and H. Flächer, hep-ph/0507253 (2005).

[224] M. Neubert, Phys. Lett. **B612**:13-20 (2005).

[225] B.O. Lange, M. Neubert and G. Paz, Phys. Rev. **D72**:073006 (2005).

[226] C. W. Bauer, Z. Ligeti, M. Luke, A. V. Manohar and M. Trott, Phys. Rev. **D70**, 094017 (2004).

[227] M. Battaglia *et al.*, Phys. Lett. B **556**, 41 (2003).

[228] A. H. Mahmood *et al.* (CLEO Collaboration), Phys. Rev. D **70**, 032003 (2004).

[229] B. Aubert *et al.* (*BABAR* Collaboration), Phys. Rev. Lett. **93**, 011803 (2004).

[230] S. B. Athar *et al.* (CLEO Collab.), Phys. Rev. **D68**:072003 (2003).

[231] BABAR Collab., Phys. Rev. **D72**: 051102 (2005).

[232] BELLE Collab., hep-ex/0508018.

[233] BABAR Collab., hep-ex/0506064.

[234] BABAR Collab., hep-ex/0506065.

[235] BABAR Collab., ICHEP 2004 conference contribution, hep-ex/0408068.

[236] P. Ball and R. Zwicky, Phys. Rev. **D71** (2005) 014015

[237] J. Shigemitsu *et al.* (HPQCD), Nucl. Phys. Proc. Suppl. **140**, 464 (2005)

[238] M. Okamoto *et al.* (Fermilab/MILC), Nucl. Phys. Proc. Suppl. **140**, 461 (2005)

[239] B. H. Behrens *et al.* (CLEO Collab.), Phys. Rev. **D61**:052001 (2000).

[240] B. Aubert *et al.* (BABAR Collab.), Phys. Rev. Lett. **90**:181801 (2003).

[241] K. Abe *et al.* (BELLE Collab.), Phys. Rev. Lett. **93**:131803 (2004).

[242] M.B. Voloshin, Phys. Lett. **B515**:74 (2001).

[243] S.W. Bosch, B.O. Lange, M. Neubert and G. Paz, Nucl. Phys. **B699**:335 (2004).

[244] S.W. Bosch, M. Neubert and G. Paz, JHEP **0411**:073 (2004).

[245] M. Neubert, hep-ph/0411027 (2004).

[246] M. Neubert, Phys. Lett. **B612**:13 (2005).

[247] R. Barate *et al.* (ALEPH Collab.), Eur. Phys. J. **C6**:555 (1999).

[248] M. Acciarri *et al.* (L3 Collab.), Phys. Lett. **B436**:174 (1998).

[249] G. Abbiendi *et al.* (OPAL Collab.), Eur. Phys. J. **C21**:399 (2001).

[250] P. Abreu *et al.* (DELPHI Collab.), Phys. Lett. **B478**:14 (2000).

[251] A. Bornheim *et al.* (CLEO Collab.), Phys. Rev. Lett. **88**:231803 (2002).

[252] B. Aubert *et al.* (BABAR Collab.) Phys. Rev. Lett. **95**, 111801 (2005).

[253] R. Kowalewski and S. Menke, Phys. Lett. **B541**:29 (2002).

[254] BABAR Collab., ICHEP 2004 conference contribution, hep-ex/0408075.

[255] A. Limosani *et al.* (BELLE Collab.) Phys. Lett. **B621**, 28 (2005).

[256] BABAR Collab., hep-ex/0507017. This is an update of B. Aubert *et al.* (BABAR Collab.), Phys. Rev. Lett. **92**:071802 (2004).

[257] H. Kakuno *et al.* (BELLE Collab.), Phys. Rev. Lett. **92**:101801 (2004).

[258] I. Bizjak *et al.* (BELLE Collab.), Phys. Rev. Lett. **95**:241801 (2005). hep-ex/0505088

[259] O. Buchmüller and H. Flächer, hep-ph/0507253.

[260] D. Benson, I.I. Bigi, and N. Uraltsev, Nucl. Phys. **B710**, 371 (2005); hep-ph/0410080.

[261] S.W. Bosch, B.O. Lange, M. Neubert, and G. Paz, Nucl. Phys. **B699**, 335 (2004); hep-ph/0402094.

[262] A.L. Kagan amd M. Neubert, Eur. Phys. Jour. **C7**, 5 (1999); hep-ph/9805303.

[263] ALEPH Collaboration (M.S. Alam *et al.*), Phys. Lett. B **429**, 169 (1998).

[264] CLEO Collaboration (S. Chen *et al.*), Phys. Rev. Lett. **87**, 251807 (2001).

[265] Belle Collaboration (K. Abe *et al.*), Phys. Lett. B **511**, 151 (2001).

[266] Belle Collaboration (P. Koppunberg *et al.*), Phys. Rev. Lett. **93**, 061803 (2004).

[267] *BABAR* Collaboration (B. Aubert *et al.*), Phys. Rev. D **72**, 052004 (2005).

[268] *BABAR* Collaboration (B. Aubert *et al.*), hep-ex/0507001.